

University of Alberta

**Electroosmotic Flow Modification and Prevention of Protein Adsorption in
Capillary Electrophoresis**

by

Amy Michelle MacDonald ©

A thesis submitted to the Faculty of Graduate Studies and Research
in partial fulfillment of the requirements for the degree of

Doctor of Philosophy

Department of Chemistry

Edmonton, Alberta
Fall 2008



Library and
Archives Canada

Published Heritage
Branch

395 Wellington Street
Ottawa ON K1A 0N4
Canada

Bibliothèque et
Archives Canada

Direction du
Patrimoine de l'édition

395, rue Wellington
Ottawa ON K1A 0N4
Canada

Your file *Votre référence*
ISBN: 978-0-494-46370-3
Our file *Notre référence*
ISBN: 978-0-494-46370-3

NOTICE:

The author has granted a non-exclusive license allowing Library and Archives Canada to reproduce, publish, archive, preserve, conserve, communicate to the public by telecommunication or on the Internet, loan, distribute and sell theses worldwide, for commercial or non-commercial purposes, in microform, paper, electronic and/or any other formats.

The author retains copyright ownership and moral rights in this thesis. Neither the thesis nor substantial extracts from it may be printed or otherwise reproduced without the author's permission.

AVIS:

L'auteur a accordé une licence non exclusive permettant à la Bibliothèque et Archives Canada de reproduire, publier, archiver, sauvegarder, conserver, transmettre au public par télécommunication ou par l'Internet, prêter, distribuer et vendre des thèses partout dans le monde, à des fins commerciales ou autres, sur support microforme, papier, électronique et/ou autres formats.

L'auteur conserve la propriété du droit d'auteur et des droits moraux qui protègent cette thèse. Ni la thèse ni des extraits substantiels de celle-ci ne doivent être imprimés ou autrement reproduits sans son autorisation.

In compliance with the Canadian Privacy Act some supporting forms may have been removed from this thesis.

Conformément à la loi canadienne sur la protection de la vie privée, quelques formulaires secondaires ont été enlevés de cette thèse.

While these forms may be included in the document page count, their removal does not represent any loss of content from the thesis.

Bien que ces formulaires aient inclus dans la pagination, il n'y aura aucun contenu manquant.

■ ■ ■
Canada

~ Dedicated to My Family ~

Abstract

Capillary electrophoresis is a technique capable of high separation efficiency, good resolution, and fast migration times due in part to the electroosmotic flow (EOF). However, separations can be hampered by adsorption of analytes to the capillary wall especially in the case of biomolecules. This thesis examines means of enhancing and suppressing the EOF, and of preventing protein adsorption.

The effect of a series of zwitterionic additives on the EOF is studied. The structures of the additives are found to have an effect on the overall EOF enhancement with the order of the amine headgroup and intercharge distance between the ionic functionalities having the largest influence. An EOF enhancement of 63% is noted with the highest order amine, Z1-Methyl, while a 70% enhancement is noted with the longest carbon chain additive, 8-aminocaprylic acid.

As these additives are not overly effective at preventing protein adsorption, a novel coating was developed for this purpose. The coating consists of a double-chain cationic surfactant bilayer of dioctadecyldimethylammonium bromide (DODAB) in direct contact with the capillary wall and an intercalated diblock copolymer, polyoxyethylene (POE) stearate. The POE moieties protrude into the surrounding solution resulting in a neutral hydrophilic surface. Efficiencies up to 1.3 million plates/m are achieved using this coating with protein recoveries of 84 – 97 % for basic and acidic proteins.

A modified coating method imparts greater stability with RSDs of migration times $\leq 0.5\%$ over 28 consecutive runs with no recoating between runs. Polymer concentration and chain length are varied to produce a tunable coating. The EOF can

also be tuned from $-1.2 \times 10^{-4} \text{cm}^2/\text{Vs}$ to $-0.4 \times 10^{-4} \text{cm}^2/\text{Vs}$ using mixtures of POE 40 stearate and POE 8 stearate on a DODAB coated capillary.

Band broadening sources other than adsorption are studied using the DODAB/POE stearate coating. Protein peak efficiencies and asymmetries improve with increasing buffer concentration. Buffer co-ion and low protein concentration also enhance these parameters in a manner consistent with a decrease in electromigration dispersion. Similar observations are noted on a commercially available polyvinyl alcohol (PVA) coating.

Acknowledgements

I would like to take this opportunity to thank my supervisor, Dr. Charles Lucy, first and foremost for his guidance, wisdom, and patience throughout my graduate career. His advice, both scientific and practical, has had a beneficial impact on my way of thinking and for this I am grateful.

The Lucy group members both past and present have enriched my graduate experience. I am especially thankful for the informative conversations with Dr. Mahmoud Yassine. The numerous discussions with Donna Gulcev on a variety of research topics as well as her friendship are highly valued. I am appreciative of the support and helpful comments from all of the group members, especially Richard Paproski, Patricia Arboleda, Stuart Chambers, Ting Zhou, and Karen Glenn.

I would also like to thank Kim Do, Al Chilton and Ed Feschuk from the Electronics Shop for their invaluable help when instrument or computer problems arose.

Dr. Chris Backhouse, Dr. Alex Brown, Dr. Chris Le, Dr. Mark McDermott, and Dr. Shaorong Liu are gratefully acknowledged for sitting on my thesis committee, as well as for their helpful comments and critique of this thesis.

I would like to thank the Department of Chemistry for the opportunity to teach undergraduate students, as well as for financial help. The financial support provided by the Natural Sciences and Engineering Research Council of Canada (NSERC) and the Alberta Ingenuity Fund throughout my graduate career is greatly appreciated, as well as funding from the Faculty of Graduate Studies and Research and the Graduate Students' Association.

Last but certainly not least a very heartfelt thank you is extended to my mom, Arlene; dad, Brian; and brother, Jonathan. Without their unwavering support and belief in my abilities, this would not have been possible. A special thanks to my grandmother, Isabel, for her gentle encouragement and kind words throughout my graduate work. I am very fortunate to have such wonderful people in my life.

Table of Contents

Chapter One: Introduction

1.1 History of Electrophoresis.....	1
1.2 Fundamentals of CE.....	3
1.2.1 Instrumentation.....	3
1.2.2 Electroosmotic Flow.....	6
1.2.3 Electrophoretic Mobility.....	12
1.2.3.1 Apparent vs. Electrophoretic Mobility.....	14
1.3 Band broadening.....	15
1.3.1 Longitudinal Diffusion.....	17
1.3.2 Injector Broadening.....	20
1.3.3 Thermal Broadening and Joule Heating.....	21
1.3.4 Detector Broadening.....	23
1.3.5 Electromigration Dispersion.....	25
1.3.6 Solute-Wall Interactions.....	28
1.4 Protein Adsorption.....	30
1.4.1 Theory.....	30
1.4.2 Measuring Protein Adsorption.....	34
1.4.2.1 Peak Efficiency.....	34
1.4.2.2 Protein Recovery.....	35
1.4.2.2.1 Towns and Regnier.....	35
1.4.2.2.2 Fluorescein Isothiocyanate-Myoglobin Saturation Method.....	36
1.4.2.3 EOF.....	36
1.4.2.4 Migration Time.....	37
1.5 Buffer Additives and Wall Coatings.....	38
1.5.1 Small Molecule Additives.....	38
1.5.2 Covalent Coatings.....	40
1.5.3 Surfactant Coatings.....	41
1.5.4 Physically Adsorbed Polymer Coatings.....	46
1.6 Thesis Outline.....	49
1.7 References.....	50
Chapter Two: Enhancement of Electroosmotic Flow in Capillary Electrophoresis Using Zwitterionic Additives	
2.1 Introduction.....	59

2.2 Experimental.....	62
2.2.1 Apparatus.....	62
2.2.2 Chemicals.....	62
2.2.3 EOF Measurement.....	63
2.2.4 Relative Viscosity Measurements.....	65
2.3 Results.....	67
2.3.1 Z1-Methyl.....	67
2.3.2 Effect of Charge Separation.....	69
2.3.3 Effect of Functional Group.....	76
2.3.4 pH and Buffer Cation.....	78
2.4 Discussion.....	79
2.4.1 Dielectric Constant.....	80
2.4.2 Zeta Potential.....	87
2.5 Concluding Remarks.....	88
2.6 References.....	89

Chapter Three: Highly Efficient Protein Separations in Capillary Electrophoresis Using a Supported Bilayer/Diblock Copolymer Coating

3.1 Introduction.....	92
3.2 Experimental.....	94
3.2.1 Apparatus.....	94
3.2.2 Chemicals.....	96
3.2.3 Preparation of the Surfactant/Polymer Coating.....	97
3.2.4 EOF Measurements.....	97
3.2.5 Coating Stability.....	99
3.2.6 Protein Separations.....	99
3.3 Results and Discussion.....	103
3.3.1 Coating Stability.....	105
3.3.2 Protein Separations Using the DODAB/POE 40 Stearate Coating.....	108
3.4 Concluding Remarks.....	117
3.5 References.....	118

Chapter Four: A Modified Supported Bilayer/Diblock Copolymer -Working Towards a Tunable Coating for Capillary Electrophoresis

4.1 Introduction.....	122
-----------------------	-----

4.2 Experimental.....	126
4.2.1 Apparatus.....	126
4.2.2 Chemicals.....	126
4.2.3 Preparation and Coating of the Surfactant/Polymer Solutions.....	127
4.2.4 EOF Measurements.....	129
4.2.5 Protein Separations.....	130
4.3 Results and Discussion.....	131
4.3.1 Mixed DODAB/POE Stearate.....	131
4.3.1.1 Tunability of EOF.....	131
4.3.1.2 Coat Time Study.....	135
4.3.1.3 Protein Separations with Mixed DODAB/POE 40 Stearate.....	137
4.3.1.4 Adjustment of Polymer Chain Length with Mixed DODAB/POE Stearate.....	142
4.3.1.4.1 EOF Modification.....	142
4.3.1.4.2 Protein Separation with Mixed DODAB/POE 8 Stearate.....	144
4.3.1.5 Capillary Age.....	146
4.3.1.6 Coating Stability.....	148
4.3.2 Sequential Coating Method.....	149
4.3.2.1 Temporal Coating Studies.....	150
4.3.2.2 EOF Studies.....	157
4.3.2.2.1 EOF with DODAB/POE Stearate Coatings.....	157
4.3.2.2.2 Adjustable EOF with DODAB/POE Stearate Coatings.....	157
4.3.3 Protein Separations.....	161
4.3.4 Histone Separations.....	163
4.4 Concluding Remarks.....	166
4.5 References.....	167

Chapter Five: Factors other than Adsorption Affecting Peak Efficiencies in Capillary Electrophoretic Separations of Proteins

5.1 Introduction.....	171
5.2 Experimental.....	173
5.2.1 Apparatus.....	173
5.2.2 Chemicals.....	174
5.2.3 Preparation and Coating of the Surfactant/Polymer Solutions.....	175
5.2.4 Protein Separations.....	175
5.3 Results and Discussion.....	176
5.3.1 Measurement of N.....	176
5.3.2 Band broadening with DODAB/POE 40 Stearate Coated Capillaries.....	180

5.3.2.1 Effect of Voltage on Protein Separations.....	180
5.3.2.2 Effect of Buffer Concentration.....	183
5.3.2.3 Effect of Buffer Co-ion.....	194
5.3.2.4 Effect of Protein Concentration.....	198
5.3.3 Protein Separations with Commercial Coatings.....	204
5.4 Concluding Remarks.....	213
5.5 References.....	214

Chapter Six: Summary and Future Work

6.1 Summary.....	217
6.1.1 Chapter 2.....	217
6.1.2 Chapter 3.....	218
6.1.3 Chapter 4.....	219
6.1.3.1 Mixed DODAB/POE Stearate Coating.....	219
6.1.3.2 Sequential DODAB/POE Stearate Coating.....	220
6.1.4 Chapter 5.....	221
6.1.5 Conclusions.....	222
6.2 Future Work.....	223
6.2.1 Cellulose Modified DODAB Bilayer Coating.....	223
6.2.2 Drug Separations.....	225
6.2.3 Drug Delivery Vehicles.....	227
6.2.4 Covalent Coating Comparison.....	229
6.3 References.....	230

List of Tables

Table 2.1	EOF Enhancement Factor, $\mu'_{eof, buf}$ in Pure Phosphate Buffer, Correlation Coefficient, and Dielectric Increment for Zwitterionic Additives from μ'_{eof} vs. Additive Concentration Plots ^a	73
Table 2.2	Effect of pH on EOF Enhancement.....	78
Table 2.3	Effect of Cation on the EOF Increase with Z1-Methyl.....	79
Table 3.1	Physical Properties of Proteins.....	98
Table 3.2	Separation Characteristics of Basic Proteins Using a 0.1 mM DODAB/0.1% POE 40 Stearate Coated Capillary 0.2 with 50 mM Sodium Phosphate Buffer, pH 3.0.....	109
Table 3.3	Efficiency and Migration Time Reproducibility of Acidic Proteins Using a 0.1 mM DODAB/0.1% POE 40 Stearate Coated Capillary with 75 mM Tris-acetate Buffer, pH 7.4 with and without Re-coating between Runs.....	111
Table 3.4	Efficiency and Migration Time Reproducibility of Basic Proteins Using a 0.1 mM DODAB/0.1% POE 40 Stearate Coated Capillary with 75 mM Tris-acetate Buffer, pH 7.4.....	113
Table 3.5	Efficiency, Migration Time Reproducibility, and Percent Recoveries of Acidic Proteins Using a 0.1 mM DODAB/0.1% POE 40 Stearate Coated Capillary with 50 mM CHES Buffer, pH 10.0.....	114
Table 4.1	EOF Values and Efficiencies for Mixed 0.1 mM DODAB/POE 40 Stearate Coatings with 0.1 mg/mL Basic Proteins, unless otherwise Noted.....	139
Table 4.2	EOF Values for the 0.01% POE 8, 40, and 100 Stearate Coatings.....	143
Table 4.3	Efficiency Range and % RSD of Basic Protein Migration Times for Mixed and Sequential Coating Methods Using 0.1 mM DODAB and 0.075% POE 40 Stearate	149
Table 4.4	EOF Mobility, Rate Constant and Correlation Coefficient for Sequential DODAB then POE Stearate Coatings.....	155
Table 4.5	EOF Values for the 0.01% POE 8, 40, and 100 Stearate Sequential Coatings.....	158

Table 4.6	Efficiency Ranges and EOF Values for Basic Proteins Separated on Sequential 0.1 mM DODAB then POE 40 Stearate Coatings.....	163
Table 5.1	Mobilities of Buffer Co-ions and Proteins in 75 mM Phosphate Buffer, pH 3.0.....	183
Table 5.2	Peak Efficiencies and Asymmetry Factors for Acidic Proteins Separated on a 0.1 mM DODAB/0.1% POE 40 Stearate at pH 7.4.....	195
Table 5.3	Mobility of Buffer Co-ions in 50 mM Tris Buffer, pH 7.4	198

List of Figures

Figure 1.1	Schematic of a Capillary Electrophoresis System.....	4
Figure 1.2	Schematic of the Electrical Double Layer.....	7
Figure 1.3	Schematic of the EOF Flow Profile within a Capillary.....	10
Figure 1.4	Comparison of Flow Profiles Generated by EOF and Pressure-Driven Systems and the Corresponding Analyte Zone.....	11
Figure 1.5	Migration Order within a Capillary under an Applied Electric Field and the Resultant Electropherogram.....	13
Figure 1.6	Schematic of the Parameters Used to Calculate Resolution.....	16
Figure 1.7	Schematic of Analyte Zone on the Capillary and the Corresponding Zone Profile.....	19
Figure 1.8	Temperature Profile within a Capillary.....	22
Figure 1.9	Schematic of Electromigration Dispersion (EMD) Resulting from Mismatched Sample and Buffer Co-ion Mobilities.....	26
Figure 1.10	Schematic of Protein Adsorption onto a Solid, Non-Porous Surface.....	31
Figure 1.11	Common Aggregate Structures of (A) Single-chain Surfactants and (B) Double-chain Surfactants.....	43
Figure 2.1	Structures of Zwitterions.....	61
Figure 2.2	Current through the Capillary vs. Additive Concentration in 10 mM Phosphate Buffer, pH 7.2 for glycine, 3-amino-1-propane sulfonic acid, Z1-Methyl, CAPS, 4-aminobutyric acid, 6-aminocaproic acid, and 8-aminocaprylic acid.....	64
Figure 2.3	Average Relative Viscosity of 10 mM Phosphate Buffers, pH 7.2 Containing Zwitterionic Additive vs. Zwitterion Concentration for glycine, 3-amino-1-propane sulfonic acid, Z1-Methyl, CAPS, 4-aminobutyric acid, 6-aminocaproic acid, and 8-aminocaprylic acid.....	66
Figure 2.4	(Fig. 3.8 from Mary Woodland's Thesis) Protein Separation Using 100 mM Phosphate Buffer at pH 7.21 with 1.0 M Z1-Methyl.....	68

Figure 2.5	Viscosity Corrected EOF vs. Concentration of Z1-Methyl, 3-amino-1-propane sulfonic acid, 4-aminobutyric acid, and CAPS.....	70
Figure 2.6	Viscosity Corrected EOF vs. Concentration of glycine, 4-aminobutyric acid, 6-aminocaproic acid, and 8-aminocaprylic acid.....	72
Figure 2.7	Slope of the Viscosity Corrected EOF Plots vs. Carbon Number for the Aminocarboxylic Acid Additives (Δ), Z1-Methyl, 3-amino-1-propane sulfonic acid, and CAPS.....	74
Figure 2.8	Plot of Streaming Potential Enhancement vs. Carbon Number for a Homologous Series of Cyclohexylamino alkyl sulfonates (CHES, CAPS, CABS).....	75
Figure 2.9	Plot of Enhancement Factor vs. Amine Order for Additives containing Primary, Secondary, and Quaternary) Amino Groups.....	77
Figure 2.10	Dielectric Increment of the Zwitterionic Additives Aminocarboxylic Acids, 3-Aminopropane sulfonic acid, Triethylammoniumpropane sulfonate, vs. Carbon Number in the Additive Chain.....	82
Figure 2.11	Enhancement Factors of the Aminocarboxylic Acid Additive Series vs. Literature Dielectric Increments.....	84
Figure 2.12	Observed Viscosity Corrected EOF Mobility vs. Viscosity Corrected EOF Mobility Predicted from Literature Dielectric Increment Measurements for Aminocarboxylic Acid Additives.....	85
Figure 3.1	Schematic of the DDAB/POE 100 Stearate Coating.....	95
Figure 3.2	Surfactant and Polymer Structures.....	98
Figure 3.3	Ohm's Plot for the 50 mM Ammonium Formate pH 3.5 Buffer System with a 0.1 mM DODAB/0.1% POE 40 Stearate Coated Capillary.....	101
Figure 3.4	Peak Asymmetry Measure (B/A) at 10% of the Peak Height.....	102
Figure 3.5	Coating Stability of Various DODAB/POE Stearate Concentrations.....	106
Figure 3.6	pH Stability of the DODAB/0.1% POE 40 Stearate Coating.....	107

Figure 3.7	Separation of Basic Proteins on a 0.1 mM DODAB/0.1% POE 40 Stearate Coating, pH 3.0.....	109
Figure 3.8	Separation of Acidic Proteins on a 0.1 mM DODAB/0.1% POE 40 Stearate Coating, pH 7.4.....	111
Figure 3.9	Separation of Basic Proteins on a 0.1 mM DODAB/0.1% POE 40 Stearate Coating, pH 7.4.....	113
Figure 3.10	Separation of Acidic Proteins on a 0.1 mM DODAB/0.1% POE 40 Stearate Coating, pH 10.0.....	114
Figure 3.11	Separation of Equine and Bovine Cytochrome <i>c</i> on a 0.1 mM DODAB/0.1% POE 40 Stearate Coating.....	116
Figure 4.1	Schematic of the Mixed and Sequential Coating Methods.....	128
Figure 4.2	EOF at Various Percentages of POE 40 Stearate.....	133
Figure 4.3a	Schematic of Vesicle Formation at Low and High Concentrations of POE 100 Stearate.....	136
Figure 4.3b	Representation of the Surfactant Bilayer/Polymer Structure at Low and High Concentrations of POE 100 Stearate.....	136
Figure 4.4	Coat Time Study for 0.1 mM DODAB/0.01% POE 40 Stearate.....	138
Figure 4.5	Separation of Basic Proteins on a 0.1 mM DODAB Coated Capillary.....	140
Figure 4.6	Separation of Basic Proteins on a 0.1 mM DODAB/0.5% POE 40 Stearate Coated Capillary.....	141
Figure 4.7	Separation of Three Acidic and Two Basic Proteins on a 0.1 mM DODAB/0.01% POE 8 Stearate Coated Capillary.....	145
Figure 4.8	Separation of Basic Proteins on a New and Previously Coated Stripped Capillary Freshly Coated with 0.1 mM DODAB/0.5% POE 40 Stearate.....	147
Figure 4.9	Effect of POE 8 Stearate Concentration on Intercalation Rate into the DODAB Bilayer.....	151
Figure 4.10	Effect of POE 40 Stearate Concentration on Intercalation Rate into the DODAB Bilayer.....	152

Figure 4.11	Effect of POE 100 Stearate Concentration on Intercalation Rate into the DODAB Bilayer.....	153
Figure 4.12	Rate Constant vs. POE 40 Stearate Concentration Rinsed through the DODAB Coated Capillary.....	156
Figure 4.13	EOF stability for Mixed and Sequential Coating Methods Using POE 40 Stearate.....	159
Figure 4.14	EOF vs. POE 40 Stearate Concentration on a Capillary First Coated with 0.1 mM DODAB Followed by Coating with a Mixture of 0.01% POE 8 Stearate and POE 40 Stearate.....	160
Figure 4.15	First and Twenty-eighth Separation of Basic Proteins on a Sequential 0.1 mM DODAB then 0.075% POE 40 Stearate Coating with no Recoating between Runs.....	162
Figure 4.16	Histone type III-S Separation on a 0.1 mM DODAB then 0.075% POE 40 Stearate Sequentially Coated Capillary.....	165
Figure 5.1a	Width-at-Half-Height Efficiencies ($N_{1/2}$) vs. Foley-Dorsey Efficiencies (N_{FD}) for Lysozyme and Ribonuclease A, on a 0.1 mM DODAB/0.1% POE 40 Stearate Coated Capillary.....	178
Figure 5.1b	% Bias of Peak Efficiencies as a Result of Calculation Method vs. Peak Asymmetry (B/A) for Lysozyme and Ribonuclease A on a 0.1 mM DODAB/0.1% POE 40 Stearate Coated Capillary.....	179
Figure 5.2	Ohm's Plot for 100 mM Sodium Phosphate on a 0.1 mM DODAB/0.1% POE 40 Stearate Coated Capillary.....	182
Figure 5.3a	Efficiency vs. Applied Voltage on a 0.1 mM DODAB/0.1% POE 40 Stearate Coated Capillary with 100 mM Sodium Phosphate Buffer.....	184
Figure 5.3b	Efficiency vs. Applied Voltage on a 0.1 mM DODAB/0.1% POE 40 Stearate Coated Capillary with 100 mM Lithium Phosphate Buffer.....	185
Figure 5.4a	Efficiency of Cytochrome <i>c</i> vs. Buffer Concentration on a 0.1 mM DODAB/0.1% POE 40 Stearate Coated Capillary.....	188
Figure 5.4b	Efficiency of Lysozyme vs. Buffer Concentration on a 0.1 mM DODAB/0.1% POE 40 Stearate Coated Capillary.....	189

Figure 5.4c	Efficiency of Ribonuclease A vs. Buffer Concentration on a 0.1 mM DODAB/0.1% POE 40 Stearate Coated Capillary.....	190
Figure 5.4d	Efficiency of α -chymotrypsinogen A vs. Buffer Concentration on a 0.1 mM DODAB/0.1% POE 40 Stearate Coated Capillary.....	191
Figure 5.5a	Peak Asymmetry vs. Buffer Concentration for Lysozyme on a 0.1 mM DODAB/0.1% POE 40 Stearate Coated Capillary.....	192
Figure 5.5b	Peak Asymmetry vs. Buffer Concentration for Ribonuclease A on a 0.1 mM DODAB/0.1% POE 40 Stearate Coated Capillary.....	193
Figure 5.6a	Efficiencies vs. Ribonuclease A Concentration for Separations in 50 mM Sodium Phosphate Buffer on a 0.1 mM DODAB/0.075% POE 40 Stearate Coated Capillary.....	200
Figure 5.6b	Efficiencies vs. Ribonuclease A Concentration for Separations in Sodium Phosphate, Lithium Phosphate, and Bis-tris Phosphate Buffers on a Sequential 0.1 mM DODAB then 0.075% POE 40 Stearate Coating.....	201
Figure 5.7	Ribonuclease A at Various Concentrations on a Sequential Coating of 0.1 mM DODAB then 0.075% POE 40 Stearate in 50 mM Lithium Phosphate.....	202
Figure 5.8	Peak Asymmetry vs. Ribonuclease A Concentration for Separations on a Sequential Coating of 0.1 mM DODAB then 0.075% POE 40 Stearate in 50 mM Lithium Phosphate.....	203
Figure 5.9	Commercial Polymer Coating Structures.....	205
Figure 5.10	Basic Protein Separation on LPA, PVA, and 0.1 mM DODAB/0.1% POE 40 Stearate with 75 mM Lithium Phosphate.....	206
Figure 5.11a	Efficiency of Cytochrome <i>c</i> vs. Buffer Concentration in Various Buffers on a PVA Coated Capillary.....	207
Figure 5.11b	Efficiency of Lysozyme vs. Buffer Concentration in Various Buffers on a PVA Coated Capillary.....	208
Figure 5.11c	Efficiency of Ribonuclease A vs. Buffer Concentration in Various Buffers on a PVA Coated Capillary.....	209

Figure 5.11d	Efficiency of α -chymotrypsinogen A vs. Buffer Concentration in Various Buffers on a PVA Coated Capillary.....	210
Figure 5.12	Peak Asymmetry vs. Buffer Concentration for Ribonuclease A on a PVA Coated Capillary.....	212
Figure 6.1	Structure of Epoxyalkyl Modified Hydroxypropylcellulose (HPC).....	225

List of Abbreviations

Abbreviation	Full Name
2C ₁₄ DAB	dimethylditetradecylammonium bromide
3C ₁₂ MAI	tridodecylmethylammonium iodide
cmc	critical micelle concentration
cyt <i>c</i>	cytochrome <i>c</i>
ins	insulin chain A
lys	lysozyme
mAu	milli absorbance units
rNase A	ribonuclease A
tryp	trypsin inhibitor
AFM	atomic force microscopy
Bis-tris	bis(2-hydroxyethyl)imino-tris(hydroxymethyl)methane
BSA	bovine serum albumin
CABS	4-(cyclohexylamino)-1-butanesulfonic acid
CAPS	3-(cyclohexylamino)-1-propanesulfonic acid
CAS U	coco amidopropylhydroxydimethylsulfobetaine
CE	capillary electrophoresis
CHES	2-(N-cyclohexylamino)ethane sulfonic acid
CIEF	capillary isoelectric focusing
CPA	cross-linked polyacrylamide
CTAB	cetyltrimethylammonium bromide
CZE	capillary zone electrophoresis

DDAB	didodecyldimethylammonium bromide
DLPC	1,2-dilauroyl- <i>sn</i> -phosphatidylcholine
DNA	deoxyribonucleic acid
DODAB	dioctadecyldimethylammonium bromide
DS	dextran sulfate
EMD	electromigration dispersion
EMG	exponentially modified Gaussian
EOF	electroosmotic flow
FITC	fluorescein isothiocyanate
HPC	hydroxypropylcellulose
HPLC	high performance liquid chromatography
HPMC	hydroxypropylmethylcellulose
HSA	human serum albumin
I.D.	inner diameter
IgG	immunoglobulin
IHP	inner Helmholtz plane
LPA	linear polyacrylamide
MEKC	micellar electrokinetic chromatography
NACE	non-aqueous capillary electrophoresis
O.D.	outer diameter
OHP	outer Helmholtz plane
PB	polybrene
PDADMAC	polydiallyldimethylammonium chloride

PDMA	polydimethylacrylamide
PEG	polyethylene glycol
PEI	polyethylene imine
PMOTAC	polymethacryl oxyethyl trimethylammonium chloride
POE	polyoxyethylene
PPO	polypropylene oxide
PSS	polystyrene sulfonate
PVA	polyvinyl alcohol
PVP	polyvinyl pyrrolidine
PVS	polyvinyl sulfonate
RSD	relative standard deviation
SD	standard deviation
SDS	sodium dodecyl sulfate
SMIL	successive multiple ionic layer
Tris	tris(hydroxymethyl)aminomethane
TTAB	tetradecyltrimethylammonium bromide
UV	ultraviolet
Z1-methyl	trimethylammoniumpropane sulfonate
α -chym A	alpha-chymotrypsinogen A
α -lact	alpha-lactalbumin

List of Symbols

Symbol	Parameter
a_h	cross-sectional area of surfactant headgroup
b	detection pathlength
d	capillary inner diameter
e	electron charge
k	coating formation constant
k'	retention factor
k_a	adsorption rate constant
k_b	Boltzmann constant
k_d	desorption rate constant
k_{emd}	electromigration dispersion factor
l_c	hydrocarbon chain length
l_{det}	detection window length
l_{inj}	injection plug length
$n_{additive}$	adsorption capacity of a capillary in the presence of an additive
$n_{capacity}$	adsorption capacity of a bare capillary
p	packing factor
pI	isoelectric point
pKa	negative logarithm of the acid dissociation constant
q	charge
r	radius
t_0	retention time of unretained compound

t_{buf}	migration time in buffer containing no additives
t_{eof}	neutral marker migration time
t_{inj}	injection time
t_m	migration time
t_{m1}	migration time of first sample peak
t_{m2}	migration time of second sample peak
t_r	analyte retention time
$t_{rise, max}$	maximum detector rise time
t_{zwit}	migration time in the presence of zwitterionic additives
v	velocity
v_{eof}	electroosmotic flow velocity
$w_{1/2}$	width of peak at half height
w_1	baseline width of first sample peak
w_2	baseline width of second sample peak
w_b	baseline width of peak
w_{inj}	width of injected sample zone
A	absorbance
B/A	asymmetry factor
C	analyte concentration
C_b	buffer concentration
$C_{s,0}$	initial sample concentration
D	diffusion coefficient
E	applied electric field

F_E	electric force
F_F	frictional force
H	plate height
I	current
I_s	ionic strength
K_d	equilibrium distribution coefficient
L_d	capillary length to detector
L_t	total capillary length
N	plate number
$N_{1/2}$	plate number calculated using width-at-half-height method
N_{max}	maximum plate number
N_{AV}	Avogadro's number
N_{FD}	plate number calculated using Foley-Dorsey method
P	power
P_t	intensity of transmitted light
P_0	intensity of transmitted light in the absence of absorption
R	resistance
R_s	resolution
S	electroosmotic flow enhancement factor
T	temperature
V	voltage
V_a	volume of the capillary
V_c	hydrocarbon chain volume

V_{inj}	injection volume
$W_{0.1}$	width at 10% peak height
δ	dielectric increment
ε	dielectric constant
ε_w	dielectric constant of water at 25°C
ε_λ	molar absorptivity
η	viscosity
η_{rel}	relative viscosity
κ	electrical conductivity
κ^{-1}	thickness of the diffuse double layer
μ_a	buffer co-ion mobility
μ_b	buffer counter-ion mobility
μ_{app}	apparent mobility
μ_e	electrophoretic mobility
$\mu_{e,0}$	electrophoretic mobility in the absence of adsorption
$\mu_{e,ads}$	electrophoretic mobility in the presence of adsorption
$\mu_e(T)$	electrophoretic mobility at temperature T
$\mu_e(T_1)$	electrophoretic mobility at temperature T_1
μ_{eof}	electroosmotic flow mobility
$\mu_{eof, buf}$	electroosmotic flow mobility in buffer containing no additive
$\mu_{eof, DODAB}$	electroosmotic flow mobility in DODAB coated capillary
$\mu_{eof, DODAB+POE\ stearate}$	electroosmotic flow mobility in DODAB POE stearate coated capillary

μ_s	sample ion mobility
μ'_{eof}	viscosity corrected electroosmotic flow mobility
$\mu'_{eof, obs}$	viscosity corrected electroosmotic flow mobility observed
$\mu'_{eof, pred}$	viscosity corrected electroosmotic flow mobility predicted
σ	standard deviation
σ^2	variance
ζ	zeta potential
ΔP	pressure difference
Ω_T	temperature coefficient of electrophoretic mobility
Ψ_0	potential at the capillary wall
Ψ_{OHP}	potential at the outer Helmholtz plane

Chapter One: Introduction *

Capillary electrophoresis (CE) is a powerful separation tool for a variety of analytes such as proteins, peptides, inorganic anions, carbohydrates, pharmaceuticals and enantiomers. It provides high separation efficiency, good resolution, fast analysis times and small sample loading. A concrete knowledge of the phenomena involved is required to use this technique to its full potential. Electroosmotic flow (EOF) is a fundamental property in CE and the various factors affecting it have consequences on the separation. Manipulation of the EOF is a simple method for modifying separations. A major problem with the separation of biomolecules such as proteins is adsorption, which leads to loss of efficiency, low sample recovery, and band broadening. A variety of methods have been used to prevent adsorption, the most common being coating the capillary wall. This thesis investigates the development and characterization of a novel coating to prevent adsorption of proteins as well as the role of EOF and other properties on the separation of proteins.

1.1 History of Electrophoresis

Electrophoresis is the differential movement of charged analytes as a result of the application of an electric field. It was first used as a separation technique by Tiselius in 1937.¹ He separated proteins in solution using a quartz U-tube. This marked the development of the moving boundary method of electrophoresis. He was awarded the Nobel Prize in chemistry in 1948 for this work. Electrophoresis in this format was hampered, however, by thermal convection, as the boundaries became blurred due to the

* A version of Sections 1.4 and 1.5 has been published as: Lucy, C.A., MacDonald, A.M., Gulcev, M.D., "Non-covalent capillary coatings for protein separations in capillary electrophoresis", *J. Chromatogr. A.*, **2008**, 1184, 81-105.

heating caused by the current passing through the solution.² For this reason, electrophoresis is regularly carried out in non-convective media, such as a polyacrylamide or agarose gel. The first account of the use of polyacrylamide gels for separating proteins was given by Raymond and Weintraub in 1959.³ Thermal convection was greatly reduced in the gel as compared to free solution. However, even with anti-convective gels, only hundreds of volts could be applied, which means that several hours are required to perform a separation. Therefore, gel electrophoresis was limited to separating large molecules.

In 1967, Hjerten developed an alternative method to slab gel electrophoresis to circumvent these limitations.⁴ In this paper, he described the use of a 3 mm diameter quartz tube to separate inorganic ions. The tube was rotated to reduce thermal convection. This was the first use of such a device for free zone electrophoresis. The potential of this method was fully realized when narrower (75 μm) diameter capillaries were introduced by Jorgenson and Lukacs in 1981.⁵ The high surface to volume ratio of the narrow capillaries enables rapid heat dissipation, allowing high voltages (10-30 kV) to be applied. This results in fast analysis times and high separation efficiencies.

Since the use of CE in the completion of the human genome project,^{6,7} it has carved out a niche in separation science. As a technique, CE continues to grow and expand, and is used in a variety of applications from proteomics and metabolomics to forensics and food science.⁸⁻¹¹

1.2 Fundamentals of CE

1.2.1 Instrumentation

The basic setup of a CE system is shown in Figure 1.1. A CE instrument consists of a capillary, most often fabricated from fused silica and coated on the exterior with polyimide, two reservoirs containing buffer solution into which the two capillary ends are placed, a high voltage power supply capable of applying voltages from 1-30 kV across the capillary, and a detection system for monitoring the analytes at a specific point along the capillary.

To perform a separation, the inlet end of the buffer-filled capillary is placed into the sample reservoir and a small plug of sample is injected into the capillary either by applying a voltage (electrokinetic) or pressure (hydrodynamic). For electrokinetic injection, the sample is introduced into the capillary by the EOF as well as the electrophoretic migration of the ion (Section 1.2.2). The dependence on the analyte mobility (Section 1.2.3) results in biasing of the amount of each analyte injected. Electrokinetic injection is generally not as reproducible as hydrodynamic injection, as the EOF is responsible for pumping the analytes onto the capillary. The EOF on a bare capillary can be variable, especially at low pH.¹² Hydrodynamic injections do not have this EOF dependence. In my work, all injections were performed hydrodynamically. Hydrodynamic injection is performed by applying a pressure at the injection end of the capillary or a vacuum at the detection end. The injected sample volume can be calculated using the Poiseuille equation:

$$Volume = \frac{\Delta P d^4 \pi t_{inj}}{128 \eta L_t} \quad (1.1)$$

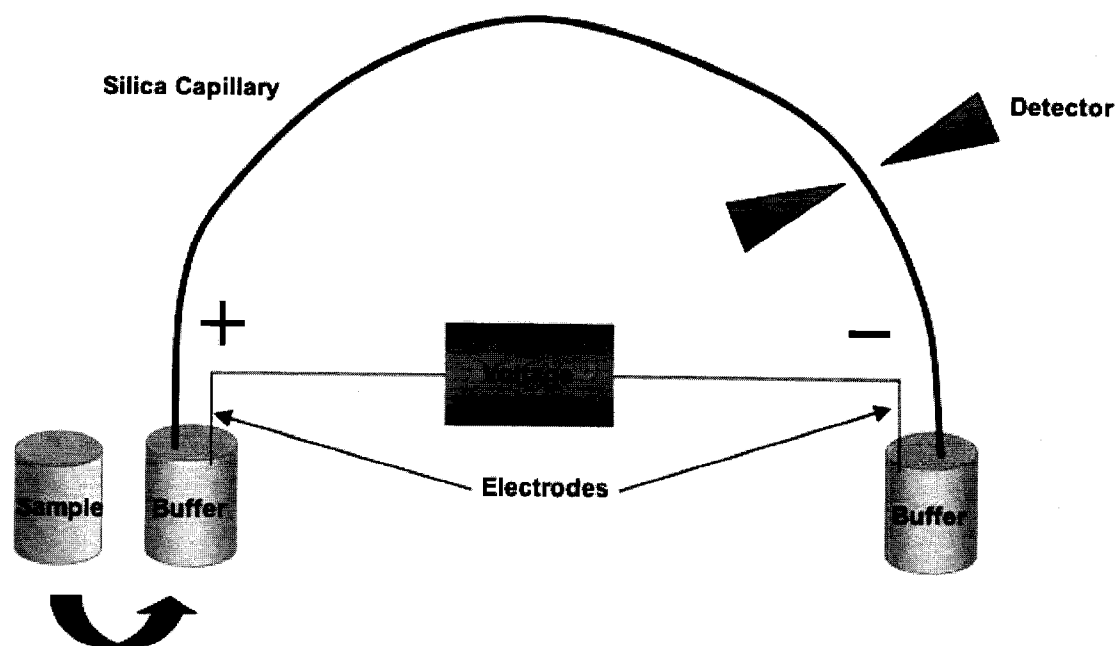


Figure 1.1: Schematic of a Capillary Electrophoresis System

where ΔP is the pressure drop across the capillary, d is the inner diameter of the capillary, t_{inj} is the injection time, η is the viscosity of the buffer, and L_t is the total length of the capillary. Typical injection volumes on a 50 μm inner diameter capillary range from 0.5 – 3.0 nL.¹³

Following injection, the inlet end of the capillary is placed back into the buffer reservoir. There are two platinum electrodes, one in each buffer reservoir, connected to the high voltage power supply. Once the sample has been injected into the capillary, a high voltage is applied across the electrodes to facilitate differential migration of the analytes through the capillary according to their charge to size ratios (Section 1.2.3). The analytes are typically detected on column by burning off a section of the polyimide coating to create a detection window. The output from the detector is then sent to a computer for processing.

Detection in CE can be performed using a variety of methods, the most common are UV-visible absorbance and fluorescence, and more recently mass spectrometry.¹⁴ UV-visible absorbance is the mode of detection used in all of my work due to its near universal nature. Absorbance detection is performed online, through a window burned on the polyimide coated capillary. A UV light source, often a deuterium lamp, is focused on the window after passing through a filter that selects the desired wavelength. The transmitted light then strikes a photodetector, which converts the photon flux into an electrical signal. The Beckman P/ACE 2100 instrument uses a photomultiplier tube while the Agilent HP^{3D} CE system uses a photodiode array to collect this light. The electrical signal is then converted from an analog to a digital signal which can then be handled by the computer.¹⁵

When the analyte passes through the detection window, light emitted from the lamp source excites electrons within the analyte into an excited electronic state. This decreases the amount of light transmitted by the solution. The decrease depends on the concentration of the analyte, as expressed in the Beer-Lambert law:¹⁶

$$\log\left(\frac{P_0}{P_t}\right) = A = \epsilon_\lambda b C \quad (1.2)$$

where P_0 is the intensity of the light in the absence of absorption, P_t is the intensity of light transmitted by the solution, A is the absorbance of the analyte, ϵ_λ is the molar absorptivity of the analyte, b is the detection pathlength, and C is the concentration of the analyte. The pathlength for a capillary is defined by the inner diameter (I.D.) and is smaller than the I.D. since the capillary is curved. This short pathlength is the limiting factor for sensitivity in CE using absorbance detection. Methods to increase sensitivity by increasing the pathlength have been developed.^{17,18} However, these modifications have not been integrated into mainstream CE systems as they increase band broadening, which limits the improvement in sensitivity.¹⁹ Limits of detection using absorbance detection usually range from 10^{-5} – 10^{-8} M.²⁰

1.2.2 Electroosmotic Flow

Electroosmotic flow (EOF) is a fundamental phenomenon in CE. It is the bulk flow of solution in the capillary upon application of an electric field. EOF results from the charge on the wall of the capillary. Silanol groups (-SiOH) on the surface of the capillary have a pKa of approximately 5.3. Thus the silanol groups readily dissociate under most pH conditions to give a negatively charged surface (-SiO⁻) with a surface potential of Ψ_0 (Figure 1.2).²¹ To maintain a balance of charge, positively charged ions

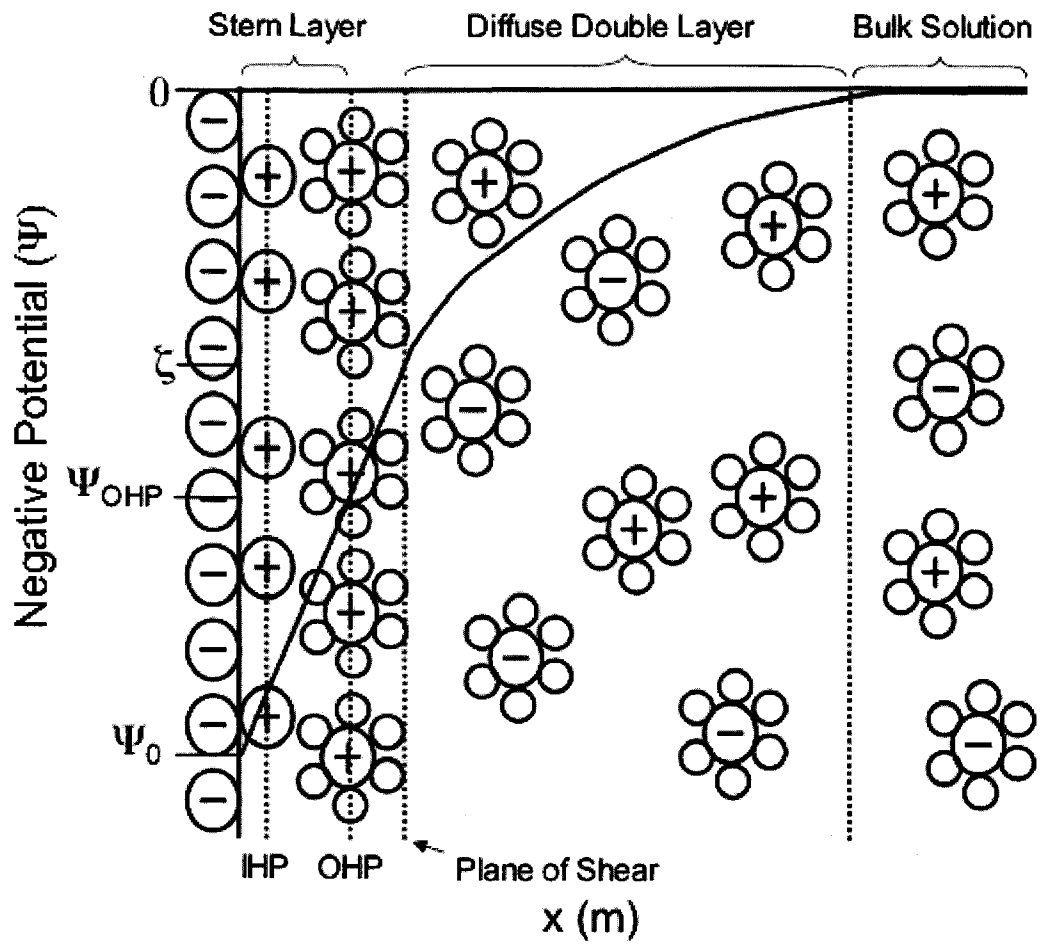


Figure 1.2: Schematic of the Electrical Double Layer

from the buffer gather at the wall, creating what is known as the electrical double layer. This is shown in Figure 1.2. The electrical double layer is considered to consist of a number of layers.²² The portion of the counter-ions and solvent molecules closest to the capillary wall are adsorbed to the wall, forming an immobilized compact layer known as the Helmholtz layer (Figure 1.2). This consists of two distinct planes. The inner Helmholtz plane (IHP) extends from the capillary wall to the center of the adsorbed ions. Further from the wall lies a layer of solvated ions electrostatically adsorbed to the surface. The distance from the centers of the unsolvated ions to the solvated ions is bounded by the outer Helmholtz plane (OHP).²³ This compact layer between the wall and the OHP is often referred to as the Stern layer. Just beyond the OHP lies the plane of shear. Any ions within the plane of shear are stationary. Beyond the plane of shear is the diffuse double layer.

Figure 1.2 shows the variation in potential in each of these layers. At the wall, the potential is negative as a result of the deprotonated silanol groups. The potential becomes less negative through the Stern layer due to the presence of the positive ions to a value symbolized by Ψ_{OHP} . Past the OHP, the potential decreases in magnitude exponentially through the diffuse layer until it becomes zero in the bulk solution. At the plane of shear, the potential is called the zeta potential (ζ). The thickness of the diffuse double layer (κ^{-1}) is given by equation 1.3:

$$\kappa^{-1} = \sqrt{\frac{\epsilon k_b T}{2000 e^2 N_{Av} I_s}} \quad (1.3)$$

where ϵ is the dielectric constant of the solvent, k_b is the Boltzmann constant, T is the temperature in Kelvin, e is the charge on an electron, N_{Av} is Avogadro's number, and I_s is the ionic strength of the bulk solution.²⁴ Therefore, the thickness of the double layer is

inversely proportional to the square root of the ionic strength of the bulk solution.

Typical values of double layer thickness for an aqueous solution of a uni-univalent electrolyte range from approximately 100 nm for a dilute bulk solution concentration of electrolyte (0.01 mM) to 1 nm for a more concentrated electrolyte solution (100 mM).²⁵

When an electric field is applied across the capillary the cations within the diffuse double layer are drawn towards the cathode. As these cations are solvated, this results in the bulk solution being dragged along with them,²⁴ as shown schematically in Figure 1.3. The magnitude of the EOF can be described by the von Smoluchowski equation:²⁶

$$\mu_{eof} = -\frac{\epsilon\zeta}{\eta} \quad (1.4)$$

where μ_{eof} is the EOF mobility and ζ is the zeta potential. Since the zeta potential depends on the charge at the surface of the capillary, the EOF varies with pH. At high pH the silanols are mostly deprotonated, resulting in a higher negative charge and thus a stronger EOF. At low pH, the silanols are largely protonated and a weaker EOF is observed. As the EOF mobility is inversely dependent on viscosity, an increase in temperature results in increased EOF due to the decrease in viscosity.

As shown in Figure 1.3, the EOF has essentially a flat flow profile. The driving force behind the EOF is the charge at the walls, which is distributed uniformly along the length of the capillary. Therefore, any change to the capillary wall charge results in a change in EOF. There is no pressure drop across the capillary as there is with a pressure-driven system,²⁷ such as high performance liquid chromatography (HPLC). A parabolic flow profile is normally observed for pressure driven flow as a result of shear force at the walls, as in Figure 1.4. The flat flow profile of the EOF does not directly contribute to broadening of the analyte zones, in contrast to the laminar profile generated in HPLC

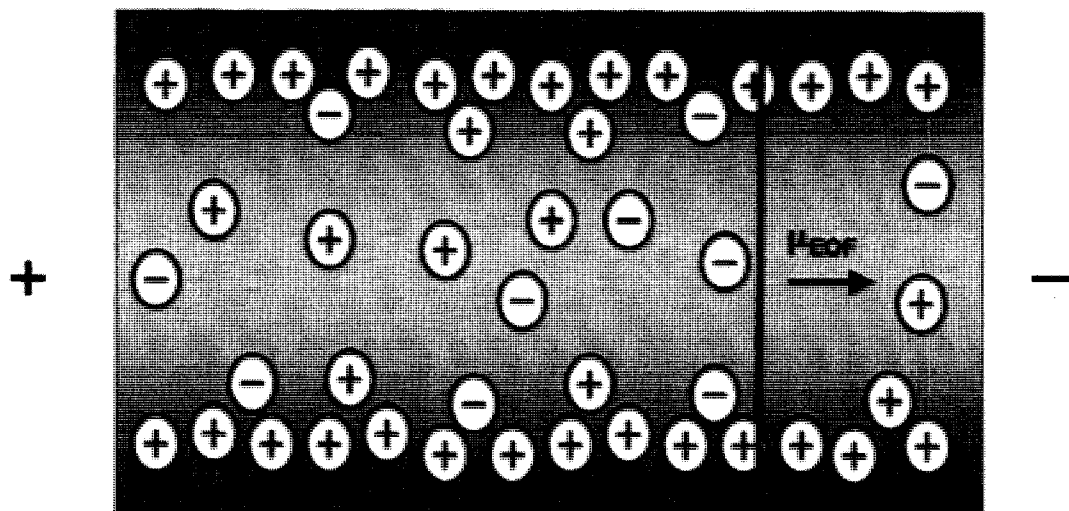


Figure 1.3: Schematic of the EOF Flow Profile within a Capillary

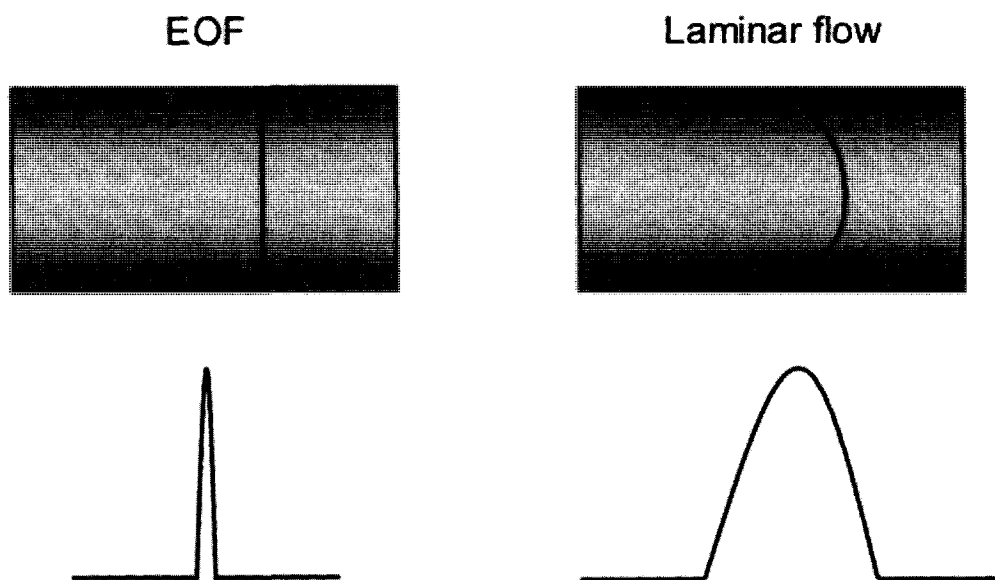


Figure 1.4: Comparison of Flow Profiles Generated by EOF and Pressure-Driven Systems and the Corresponding Analyte Zone

(Figure 1.4). This is true as long as the double layer thickness is small relative to the capillary diameter and the capillary diameter is small (typically $< 200 \mu\text{m}$).

Another advantage of the EOF is that so long as the flow is greater in magnitude than the mobility of the anionic species present, all species within the capillary have a net migration in the same direction.²⁷ In a bare capillary, the direction of this migration is toward the cathode (Figure 1.5). Therefore, cationic, neutral and anionic species can all be separated within a single run. Cations migrate ahead of the EOF as they are also electrophoretically attracted to the cathode, with smaller cations migrating the fastest. These species appear before the neutral species in an electropherogram. The neutral species are carried by the EOF, but are not separated from each other. Anions are attracted to the anode, but are swept towards the cathode by the greater mobility of the EOF, and therefore appear after the neutral species, as depicted in Figure 1.5.

1.2.3 Electrophoretic Mobility

As shown in Figure 1.5, the differential migration of charged analytes within a capillary is dependent not only on EOF, but also on how the ions behave under an applied electric field. The velocity of a charged particle is dependent upon the electric field as well as its mobility, an inherent property of the ion in a given medium. This can be described by equation 1.5:

$$v = \mu_e E \quad (1.5)$$

where v is the velocity of the ion in solution, μ_e is the electrophoretic mobility, and E is the applied electric field. When an ion is under the influence of an external electric field, it experiences an electric force, F_E , described by equation 1.6:

$$F_E = qE \quad (1.6)$$

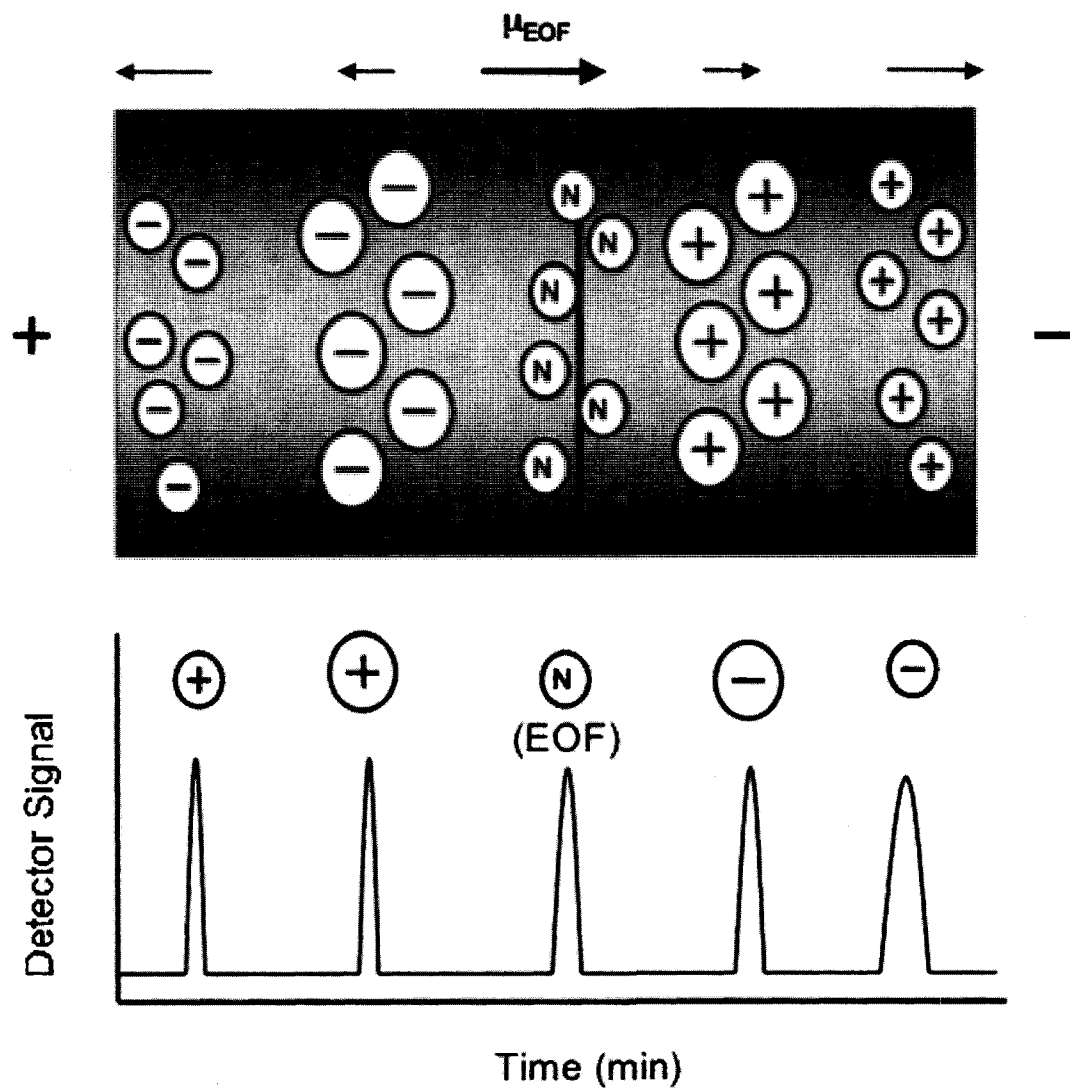


Figure 1.5: Migration Order within a Capillary under an Applied Electric Field and the Resultant Electropherogram. The arrows depict the direction and magnitude of the EOF (μ_{eof}) and the electrophoretic mobility of the ions.

where q is the charge on the ion. As the ion begins to move under the influence of this force, it experiences a frictional force in the opposite direction to its motion. This frictional force, F_F , can be described for a spherical ion by Stokes' law as:

$$F_F = -6\pi\eta r v \quad (1.7)$$

where η is the solution viscosity and r is the hydrated radius of the particle.²⁴ During electrophoresis the electric force is counterbalanced by the frictional force and a steady state velocity is reached. Equations 1.6 and 1.7 can be equated as follows:

$$qE = 6\pi\eta r v \quad (1.8)$$

Substituting this equation into equation 1.3 gives the Hückel equation, for the electrophoretic mobility of a spherical ion:

$$\mu_e = \frac{q}{6\pi\eta r} \quad (1.9)$$

Based on this equation, ions with a high charge and a small hydrodynamic radius will have high mobilities.

1.2.3.1 Apparent vs. Electrophoretic Mobility

As shown in Figure 1.5, the EOF moves all analytes in the same direction. Their movement within the capillary is described by the following equation:

$$\mu_{app} = \frac{L_d L_t}{V t_m} \quad (1.10)$$

where μ_{app} is the apparent mobility of the analyte, L_d is the length of the capillary to the detector, V is the applied voltage across the capillary, and t_m is the migration time of the analyte. The apparent mobility is measured in the presence of the EOF and includes both an electroosmotic contribution and an electrophoretic contribution.²⁸

$$\mu_{app} = \mu_e + \mu_{eof} \quad (1.11)$$

The electrophoretic mobility does not include an electroosmotic contribution. It can be determined experimentally by measurement of the apparent mobility and μ_{eof} . The mobility of a neutral marker, which will migrate with the EOF (Figure 1.5), can be measured to determine the electroosmotic mobility. The electroosmotic mobility can then be subtracted from the apparent mobility to obtain the electrophoretic mobility of the analyte. The neutral markers used in this work are mesityl oxide and benzyl alcohol.

1.3 Band broadening

As discussed in Section 1.2.3, analytes are separated in CE based on their mobility. The distance between analyte peaks divided by the width at baseline of the peaks is known as resolution, and is a measure of separation performance. The resolution between two analyte peaks is expressed by:

$$R_s = \frac{2(t_{m2} - t_{m1})}{w_1 + w_2} \quad (1.12)$$

where t_{m1} and t_{m2} are the migration times of the first and second sample peaks, respectively, and w_1 and w_2 are the baseline widths of the first and second sample peaks as shown in Figure 1.6. Two peaks are considered to be baseline resolved when $Res=1.5$, when the peaks are Gaussian and of comparable width.²⁴

The resolution between peaks is affected by *dispersion* or *band broadening*. Dispersive effects increase the width of the analyte peaks, which decreases resolution (eq. 1.12). Ideally in electrophoresis, peaks are Gaussian. The width of a Gaussian peak can be defined as follows:

$$w_b = 4\sigma \quad (1.13)$$

where w_b is the width of the peak at the baseline (Figure 1.6) and σ is the standard deviation of the peak.

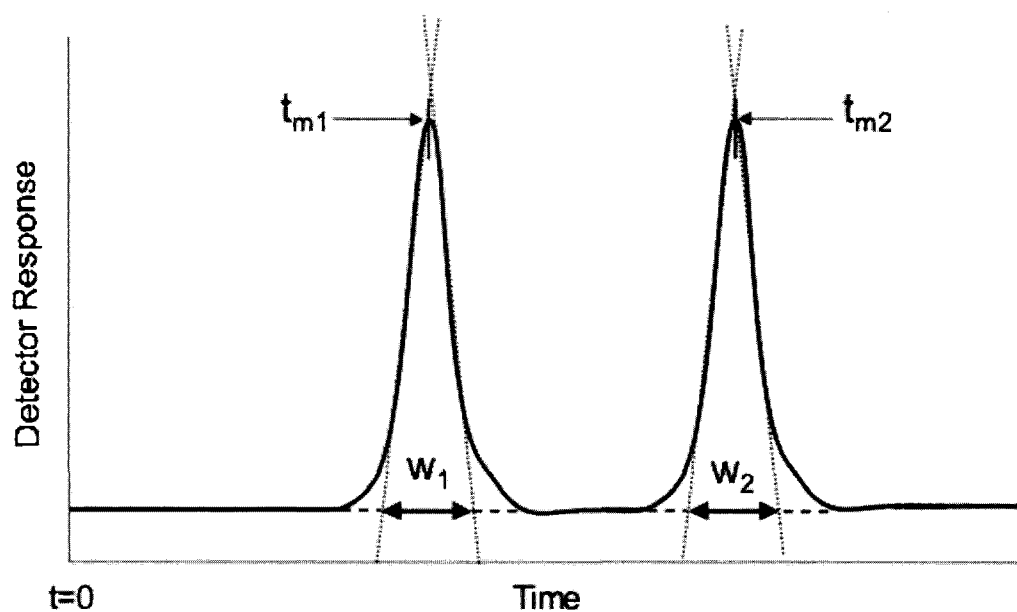


Figure 1.6: Schematic of the Parameters Used to Calculate Resolution. t_m is the migration time since application of voltage, and w is the width at baseline determined by drawing tangents to the sides of the peak.

Peak efficiency is another parameter important in determining separation performance. Efficiency can be expressed in terms of the plate number, N , as follows:

$$N = \left(\frac{L_d}{\sigma} \right)^2 \quad (1.14)$$

where σ^2 is the variance of the analyte zone. For Gaussian peaks the plate number can also be calculated using the width of the peak at half height, $w_{1/2}$:

$$N = 5.54 \left(\frac{t_m}{w_{1/2}} \right)^2 \quad (1.15)$$

Multiple phenomena contribute to the peak broadening. The plate height, H , is used to describe the contribution of various sources of band broadening. The plate height is defined as ²⁴:

$$H = \frac{L_d}{N} = \frac{\sigma^2}{L_d} \quad (1.16)$$

The variance includes all factors that contribute to dispersion of the zones. Ideally, only longitudinal diffusion (σ_{dif}^2) causes band broadening in CE. However, other factors contributing to dispersion include injection broadening, temperature gradients, detector broadening, electrodispersion, and adsorption onto the capillary wall. Assuming all variances act independently of one another, they can be summed as follows:

$$\sigma_{tot}^2 = \sigma_{dif}^2 + \sigma_{inj}^2 + \sigma_{temp}^2 + \sigma_{det}^2 + \sigma_{emd}^2 + \sigma_{ads}^2 \quad (1.17)$$

The following sections discuss the origin and characteristics of each of these sources of band broadening.

1.3.1 Longitudinal Diffusion

Under ideal separation conditions, longitudinal diffusion is the only contributor to band broadening in CE. Longitudinal diffusion is the spreading of the analyte along the

axis of the capillary as a result of a concentration gradient. The analyte is injected as a plug (top schematic in Figure 1.7). With time the analyte molecules begin to diffuse away from the area of highest concentration, which is the center of the plug, resulting in a broadened concentration profile. As diffusion occurs symmetrically along the axis of the capillary the peak has a Gaussian shape,²⁹ as in the lower schematics in Figure 1.7.

The variance caused by molecular diffusion can be described by the Stokes-Einstein equation:

$$\sigma^2_{dif} = 2Dt_m \quad (1.18)$$

where D is the diffusion coefficient of the analyte. Large molecules have small diffusion coefficients, and so undergo less longitudinal diffusion than small molecules, which have large diffusion coefficients. The longer the analyte remains in the capillary, the broader the peak becomes, as depicted by the sequence of schematics in Figure 1.7. This expression can be related back to the plate number, N , by first substituting equation 1.10 into equation 1.18 as follows:

$$\sigma^2_{dif} = \frac{2DL_dL_t}{\mu_{app}V} \quad (1.19)$$

Equation 1.19 can be substituted into equation 1.14 to give the following relationship for plate number:⁵

$$N = \frac{\mu_{app}VL_d}{2DL_t} = \frac{\mu_{app}EL_d}{2D} \quad (1.20)$$

Upon examination of equation 1.20, increasing the electric field will increase the separation efficiency. However, this can be limited by Joule heating (Section 1.3.3).

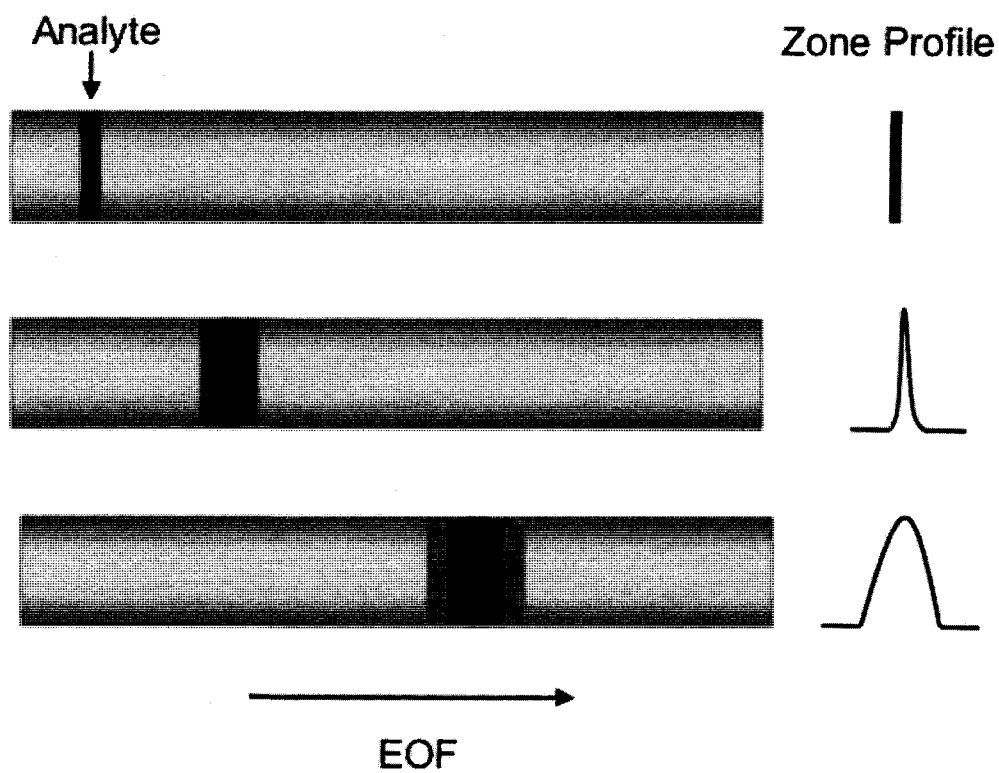


Figure 1.7: Schematic of Analyte Zone on the Capillary and the Corresponding Zone Profile. The time the analyte spends on the capillary increases from the top to the bottom schematic.

1.3.2 Injector Broadening

CE systems are easily overloaded by large sample volumes. The capillaries typically used in these systems have volumes of a few microliters. Therefore, even nanoliters of sample can lead to band broadening.³⁰ It is important to minimize the length of the sample plug during injection. The contribution to total system variance can be expressed in terms of volume (cm³) or sample zone width (mm) as follows:^{31,32}

$$\sigma_{inj}^2 = \frac{V_{inj}^2}{12} = \frac{w_{inj}^2}{12} \quad (1.21)$$

where V_{inj} is the volume injected and w_{inj} is the width of the injected sample zone. By substituting this into equation 1.14, an expression for the maximum plate number for the system can be given as:³¹

$$N_{max} = 12 \left(\frac{V_a}{V_{inj}} \right)^2 \quad (1.22)$$

where V_a is the volume of the capillary. This equation is true in the absence of stacking effects, which will be discussed in Section 1.3.5. Thus, the maximum plate number for the system under these conditions is limited to a value proportional to the square of the ratio between the capillary volume and the volume of the sample zone length.

Assuming that injection should not decrease efficiency by more than 10%, the maximum length of the sample plug is:^{30,33,34}

$$l_{inj} = \sqrt{2.4Dt_m} \quad (1.23)$$

A protein with a diffusion coefficient of 1×10^{-6} cm²/s and a migration time of 10 min should have an injection plug length of less than 380 μm for an efficiency decrease of less than 10%. For a smaller, faster molecule with a diffusion coefficient of 1×10^{-5} cm²/s, the injection plug length should be less than 1.2 mm.³³

1.3.3 Thermal Broadening and Joule Heating

An advantage of capillary electrophoresis over slab electrophoresis is the reduction of heating effects that have limited voltages in the slab technique. The large surface to volume ratio of the capillaries allows rapid heat dissipation. Therefore, very small temperature gradients can be achieved in CE. However, even for small diameter capillaries these gradients still exist and can contribute to sample zone broadening. The temperature profile within a 25 μm I.D., 375 μm O.D. capillary is shown in Figure 1.8. This thermal gradient within the capillary has a parabolic profile³⁵ and is dependent on the inner and outer diameter of the capillary, the thickness of the polyimide coating, and the heat transfer coefficient to the surroundings.

These heating effects are a result of the current passing through the buffer solution in the capillary and are referred to as *Joule heating*.³⁵ Joule heating can be explained using Ohm's law:

$$V = IR \quad (1.24a)$$

which can also be expressed as:

$$P = I^2R \quad (1.24b)$$

where V is the voltage applied across the capillary, I is the current through the capillary, and R is the resistance to current flow, and P is the applied power. If the voltage is increased, the current should increase proportionally. However, if heat generated by the passage of current through the capillary is not effectively removed from the capillary surface, the temperature within the capillary increases. As the conductivity of the capillary changes with temperature, increasing the applied power can cause a deviation in the linear relationship between voltage and current.³⁶ Joule heating can be detected by

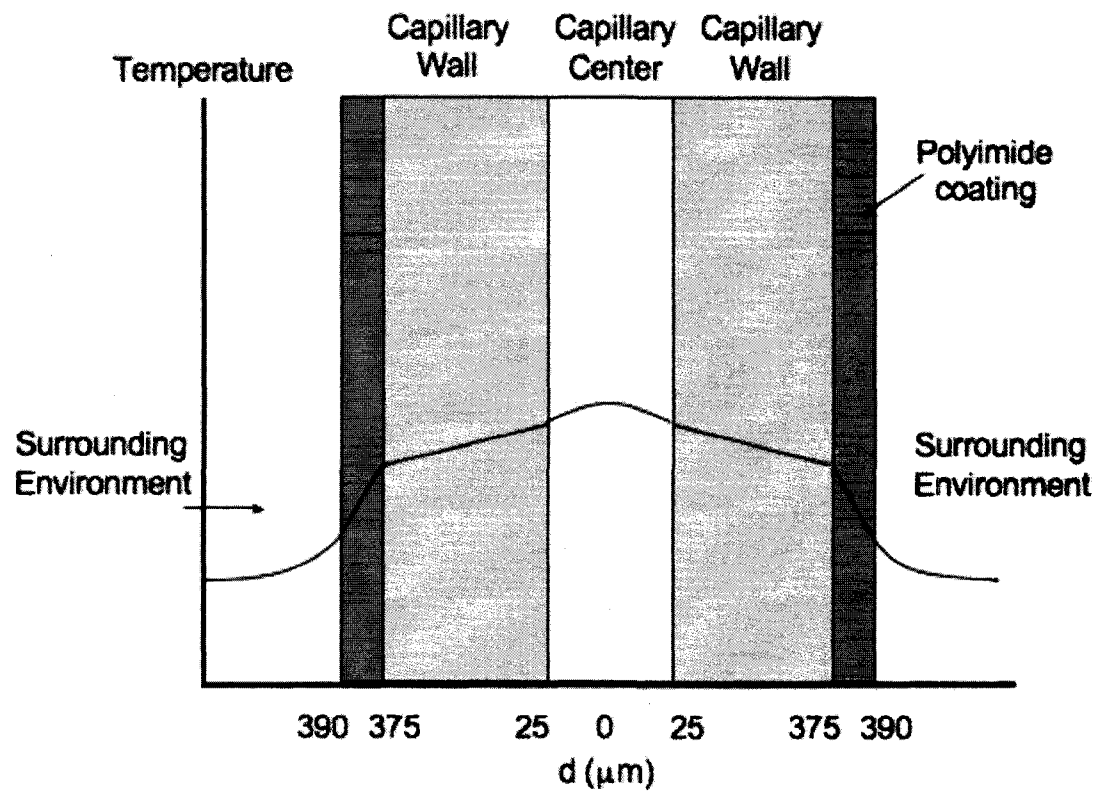


Figure 1.8: Temperature Profile within a Capillary (adapted from ¹³)

plotting current versus applied voltage for a given buffer system. Joule heating is occurring if the plot deviates from linearity. The applied voltage used in the experiment should remain in the linear portion of the plot.

The contribution to the overall variance by thermal gradients can be expressed as:²⁴

$$\sigma_{temp}^2 = \frac{r^6 E^6 \kappa^2 \Omega_T^2 \mu_{app}^2}{1536 D k_b^2} t_m \quad (1.25)$$

where r is the capillary radius, E is the applied electric field, κ is the electrical conductivity of the background electrolyte solution, and Ω_T is a temperature coefficient of the electrophoretic mobility. The temperature coefficient can be expressed as:

$$\Omega_T = \frac{\mu_e(T) - \mu_e(T_1)}{\mu_e(T_1)(T - T_1)} \quad (1.26)$$

where $\mu_e(T)$ and $\mu_e(T_1)$ are the electrophoretic mobilities at temperatures T and T_1 , respectively.²⁴ From equation 1.25, there is a strong dependence of the variance on both the radius of the capillary and the electric field. In addition to reducing the capillary diameter, decreasing the applied voltage can also reduce temperature broadening. However, reducing the capillary diameter decreases the sensitivity. Decreasing the voltage leads to decreased efficiency and resolution.³⁷ From equation 1.25, decreasing the conductivity of the buffer (i.e., buffer concentration) can also reduce Joule heating. An alternative to this is using zwitterionic additives in the buffer, which do not increase the conductivity appreciably with increasing ionic strength³⁸ (Section 1.5.1).

1.3.4 Detector Broadening

For UV-visible absorbance, detection is performed online (Section 1.2.1). With this type of detection scheme, a finite length of the capillary is monitored through the

detection window burned in the polyimide coating. The length of the detection window determines the amount of broadening introduced, in a similar manner as injection broadening. The variance resulting from the detector broadening can therefore be expressed as:

$$\sigma_{\text{det}}^2 = \frac{l_{\text{det}}^2}{12} \quad (1.27)$$

where l_{det} is the length of the detection window. In most cases, the contribution from detector broadening is minimal.²⁴ However, if the length of the detection window is comparable to the width of the sample zone, broadening can occur.³⁰ If detector broadening is to decrease efficiency by 10% or less, the maximum width of the detection window is:

$$l_{\text{det}} = \sqrt{2.4Dt_m} \quad (1.28)$$

Typical values for the maximum detection window length are 380 μm for larger molecules and 1.2 mm for smaller molecules (Section 1.3.2). All work in this thesis was carried out using a detection length of 200 μm .

Another cause of detector broadening is slow detector electronics. There is a finite response time associated with the detector, referred to as the rise time. This is the time required for the detector output to increase from 10% to 90% of its final value.³⁰ Broadening can be significantly reduced by selecting a short rise time. However, shortening the rise time can lead to increased baseline noise. Assuming a decrease in efficiency from this type of broadening should be no more than 10%, the maximum detector rise time is:

$$t_{\text{rise,max}} = \sqrt{\frac{0.2Dt_m^3}{L_d^2}} \quad (1.29)$$

1.3.5 Electromigration Dispersion

Electromigration dispersion (EMD) occurs when there is a mismatch between the conductance of the sample zone and the buffer. Usually, the concentration of the sample is kept low relative to the buffer concentration in order to reduce the conductance difference between the two.²⁴ This keeps the field strength constant along the length of the capillary. If the sample ions carry a larger or smaller amount of the current through the capillary, the field strength will be different in the sample zone than in the buffer. This results in the sample ions moving at different velocities through the zone, resulting in broadening of the zone.

Figure 1.9 demonstrates what happens to the sample within the capillary as well as the resultant peak when EMD occurs. When the sample zone has a lower mobility than the buffer zone (left-hand side of Figure 1.9), the leading edge of the sample zone will be sharp and the trailing edge will be diffuse. Lower sample mobility translates into a lower localized conductance and thus a higher field strength in the sample zone than the surrounding buffer zone. Thus within the sample zone the sample ions migrate with a high velocity. However, when the sample ions migrate out of the sample zone towards the cathode, they encounter a lower field strength in the buffer zone. As a result, the sample ions that have just entered the buffer zone will move more slowly than they did in the sample zone. This results in a sharpening of the leading edge of the sample zone as the rest of the sample ions in the zone overtake those reaching the sample/buffer interface first.

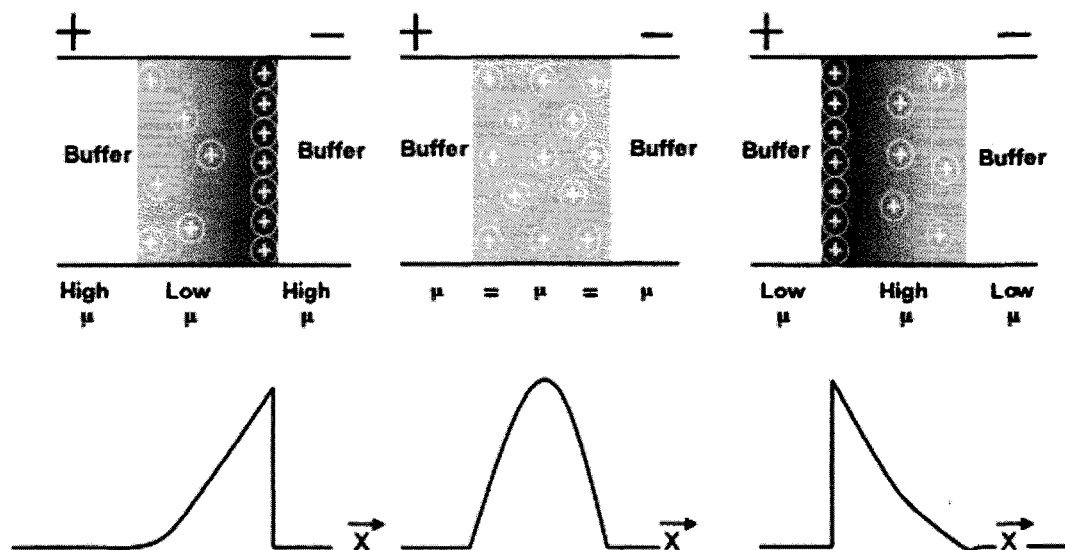


Figure 1.9: Schematic of Electromigration Dispersion (EMD) Resulting from Mismatched Sample and Buffer Co-ion Mobilities

Alternately, if the sample zone has a higher mobility than the buffer zone, the sample ions encounter a higher field strength in the buffer zone resulting in a sharp tailing edge, as in the rightmost portion of Figure 1.9. If both sample and buffer ion mobility are matched (center panel of Figure 1.9), no fronting or tailing will occur from conductance differences.³⁹

The peak variance resulting from EMD can be expressed as:

$$\sigma^2_{emd} = \frac{2El_{inj}C_{s,0}|k_{emd}|}{9C_Bv} \quad (1.30)$$

where l_{inj} is the injection length, $C_{s,0}$ is the initial sample concentration, k_{emd} is the EMD factor, C_B is the buffer concentration, and v is the apparent velocity of the sample ions.^{40,41} The EMD factor can be calculated by:

$$k_{emd} = \frac{(\mu_a - \mu_s)(\mu_b - \mu_s)}{(-\mu_a + \mu_b)\mu_s} \quad (1.31)$$

where μ_a , μ_b , and μ_s are the mobilities of the buffer co-ion, buffer counter-ion, and sample, respectively.^{39,40,42} This factor describes how sensitive the sample/buffer combination is to EMD. From equations 1.30 and 1.31, the variance introduced by EMD can be minimized by decreasing the field strength, injection length, sample concentration, and mobility difference between sample and buffer co-ions, or by increasing buffer concentration and sample ion velocity. Decreasing the applied voltage increases longitudinal band broadening (Section 1.3.3), as well as analysis time. Reducing EMD through sample and buffer properties, such as concentration and mobility will be discussed in detail in Chapter 5.

The principles behind EMD can be used to perform sample *stacking*, which is a method of sample preconcentration. Burgi and Chen performed detailed studies on this

optimization method for free zone capillary electrophoresis.⁴³⁻⁴⁶ A plug of sample is injected into the capillary in dilute buffer. Keeping the buffer concentration in the sample zone low compared to the remainder of the capillary results in sample stacking. Upon application of a high voltage, the sample ions migrate to the boundary between sample and buffer zones where they experience a lower electric field and slow down.⁴⁴ This causes the ions to form narrow zones within the sample plug, with the positive ions stacking at the front of the plug and negative ions stacking at the back. These zones then migrate through the rest of the capillary. As in equation 1.30, the zones will be narrowest when the ratio of sample to buffer concentration is small.

1.3.6 Solute-Wall Interactions

Under almost all buffer conditions the capillary wall in CE is charged. Thus the capillary can potentially interact electrostatically with sample ions.⁴⁷ Hydrophobic and hydrogen bond interactions can also occur. All of these can have detrimental effects on the separation performance. As discussed in Section 1.2.3, sample ions migrate through the capillary based on differences in mobility. However, if these ions are interacting with the capillary wall chromatographic retention will also contribute to the overall migration time,⁴⁸ and more importantly additional chromatographic sources of band broadening will be introduced. These interactions are particularly a problem with proteins as they possess a large number of charges and hydrophobic moieties. As a large portion of this thesis is devoted to preventing protein adsorption, Section 1.4 deals with protein-wall adsorption specifically.

The variance due to adsorption onto the capillary wall is given by:

$$\sigma^2_{ads} = \frac{k'v_{eof}}{(1+k')^2} \left(\frac{r^2k'}{4D} + \frac{2}{K_d} \right) \quad (1.32)$$

where k' is the retention factor of the analyte, v_{eof} is the velocity of the EOF, and K_d is the equilibrium distribution coefficient.⁴⁹ The retention factor is defined as:

$$k' = \frac{t_r - t_0}{t_0} \quad (1.33)$$

where t_r is the retention time of the analyte and t_0 is the retention time of an unretained solute.⁵⁰ The left term in the brackets of equation 1.32 takes into account the radial diffusion of the solute to the capillary wall. The right-hand term in the brackets accounts for adsorption-desorption kinetics as K_d relates the adsorption, k_a , and desorption, k_d , rate constants as follows:⁴⁹

$$K_d = \frac{k_a}{k_d} \quad (1.34)$$

From equation 1.32 and 1.34, slow desorption from the capillary wall results in a larger contribution to peak variance from adsorption. This contribution is highly dependent upon the retention factor (equation 1.32). Reducing interactions between the solute and capillary wall will reduce this factor.

A number of methods have been employed to reduce protein-capillary interactions, including using extreme pH,^{51,52} additives in the buffer,^{38,50} and coating the capillary wall.⁵³⁻⁵⁵ Coating the capillary is the most frequently used method for preventing solute adsorption. Chapters 3, 4, and 5 of this thesis are devoted to developing and characterizing a novel coating for this purpose. Section 1.5 is devoted to a discussion of various types of wall coatings.

1.4 Protein Adsorption

1.4.1 Theory

Proteins are biomolecules consisting of amino acids linked through peptide bonds.⁵⁶ They contain charged groups and possess a pI at which they are uncharged. Basic proteins have a pI greater than 7.0 while acidic proteins have a pI less than 7.0. The pI of a protein depends on the amino acids of which it consists. The amino acids also dictate the hydrophobicity of the protein. The main driving forces for protein adsorption onto a surface are electrostatic and hydrophobic interactions, as well as changes in protein structure.⁵⁷ Electrostatic interactions depend on the protein charge and thus the polar residues within a protein. Hydrophobic interactions stem from the non-polar residues within the protein. Protein adsorption in CE can have serious deleterious effects on separations. It can lead to band broadening (Section 1.3.5), peak tailing,⁴⁹ poor reproducibility,⁵² and low sample recovery.⁵⁸

A simple model for protein adsorption onto a non-porous surface is shown in Figure 1.10.⁵⁹⁻⁶¹ A protein is first transported from the bulk solution to the interfacial region through diffusion. Once in the interfacial region, the protein interacts with and attaches to the surface. This attachment may involve changes to the protein structure. The protein in this form may then desorb from the surface (reversible adsorption) or undergo further structural changes to its steady state structure and remain adsorbed on the surface (irreversible adsorption). As the residence time of the protein on a surface increases, the protein becomes irreversibly bound. For example, 200 mM sodium dodecyl sulfate (SDS) could remove myoglobin that had been freshly adsorbed.⁶²

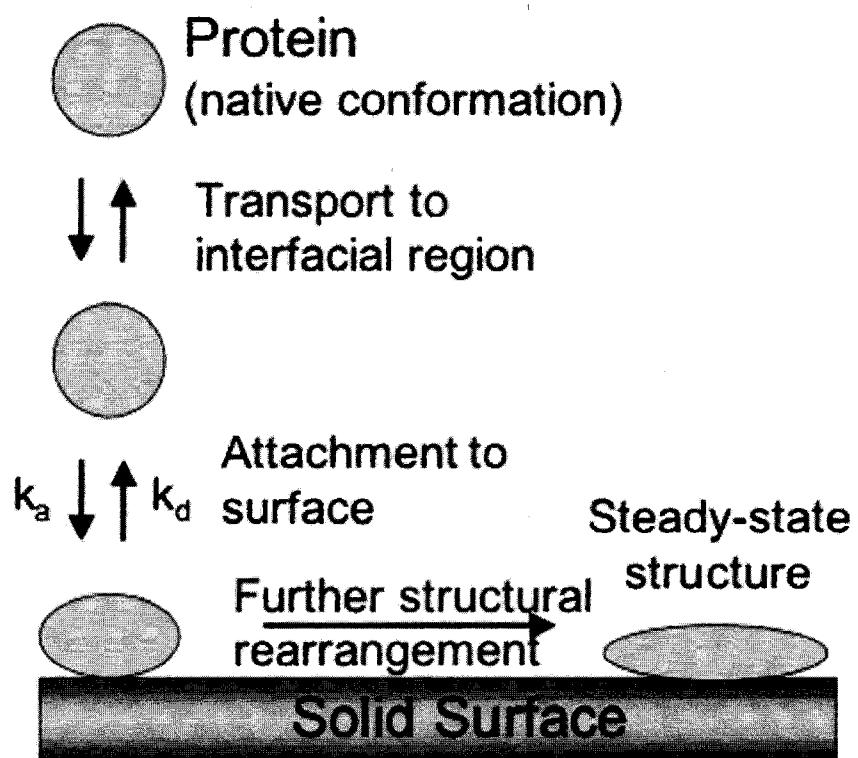


Figure 1.10: Schematic of Protein Adsorption onto a Solid, Non-Porous Surface. Adapted from reference⁵⁷

However, after 24 hours 200 mM SDS was not able to remove the adsorbed myoglobin as it had become irreversibly adsorbed. Both types of adsorption can occur during protein separations in CE. Therefore, it is important to be able to identify and quantify both types of adsorption (Section 1.4.2).

Electrostatic and hydrophobic interactions drive protein adsorption. Electrostatic interactions depend upon the distribution of hydrophilic amino acids within the protein. These residues tend to be present on the periphery of the protein, as they interact with the aqueous environment surrounding the protein. However, if these hydrophilic residues are within the interior of the protein they tend to be present as ion pairs.⁶³ Near the pI of the protein an attractive electrostatic interaction dominates within the protein as a result of discretely distributed positive and negative charges while there is a repulsive force at more extreme pH. Therefore, a more compact structure will be attained near the pI whereas at extreme pH the protein will adopt a more expanded conformation. Hydration or ionization of these ion pairs in the interior of the protein can lead to protein unfolding, also affecting the overall structure of the protein.⁶³

The charge on the exterior of the protein has been shown to greatly affect its adsorption onto a surface. Towns and Regnier⁵⁸ demonstrated proteins with high pI values (positive charge) adsorbed quantitatively onto the surface of a capillary at pH 7.0. Proteins with a near neutral pI showed only partial adsorption. Finally, proteins possessing a pI well below 7.0 showed less adsorption and thus better recovery due to the electrostatic repulsion between the negatively charged protein and the negatively charged wall. However, the majority of the low pI proteins still showed non-quantitative recoveries, suggesting electrostatic interactions are not the only factors at play. Charge

localization on the protein is also important when investigating protein-surface interactions.^{64,65} Configurations in which a large number of positive charges are near the protein surface result in the most favourable binding to the adsorbent.⁶⁴ Therefore, the conformational flexibility of the protein affects the strength of its electrostatic interaction with a surface.

Kauzmann recognized hydrophobic dehydration to be another driving force behind protein adsorption.⁶⁶ Hydrophobic dehydration occurs when the hydrophobic patches of a protein interact and bind with hydrophobic surfaces. This is a relatively unimportant force for very hydrophilic proteins and surfaces. Dehydration of non-polar residues in an aqueous environment leads to an increase in the entropy of the water molecules surrounding these residues. This energetically favourable dehydration leads to aggregation of the non-polar residues. The contribution from this hydrophobic interaction to the overall stabilization of the protein depends on the hydrophobic residues present in the amino acids. If these interactions are reduced a decrease in the stabilization of the secondary structure of the protein occurs. Therefore, protein adsorption onto a surface increases if the hydrophobicity of both the protein and the surface are increased.^{60,63}

The amount of protein adsorbed on a surface is affected by various factors including stability of the protein structure, size, charge, composition of amino acids, and steric conformation.⁶⁷ Proteins can be placed into two broad classes depending on their internal stability: “hard” or “soft”. Globular proteins (lysozyme, α -chymotrypsinogen, ribonuclease, and β -lactoglobulin) have high internal stability and are referred to as hard proteins.^{60,68,69} Hard proteins interact with surfaces mainly through electrostatic

interactions. Therefore, very little of these proteins adsorb onto surfaces unless these interactions are present. Soft proteins (bovine serum albumin (BSA), human serum albumin (HSA), immunoglobulin (IgG), α -lactalbumin, β -casein, and hemoglobin) have low internal stability and tend to adsorb onto surfaces whether or not there are electrostatic interactions with the surface.

1.4.2 Measuring Protein Adsorption

As discussed in Section 1.3.1, both reversible and irreversible protein adsorption can occur within a capillary so it is important to be able to quantify both. Techniques for the measurement of adsorption will be discussed in the following sections.

1.4.2.1 Peak Efficiency

Peak efficiency (also referred to simply as efficiency) was discussed in detail in Section 1.3 as an important measure of separation performance. Equation 1.32 describes the variance of a peak when adsorption is a contributing factor to the overall system variance. The rate constants in equation 1.34 are the same as those shown in Figure 1.11 for adsorption of a protein onto a surface. If the diffusion across the capillary or the kinetics is slow, there will be an increase in variance and thus a decrease in efficiency. Peak efficiency is generally an indicator for reversible adsorption, but may also indicate irreversible adsorption.

A model taking into account the various factors (adsorption/desorption rate constants, capillary length, wall binding capacity, initial sample concentration) affecting peak shape was developed by Ermakov et al.⁴⁷ This model is based on non-linear equilibrium chromatography (i.e., the concentration of a solute on the surface is not proportional to its concentration in the bulk solution) and sample desorption from the

wall based on diffusion. Computer simulations of peaks were performed for various values of the desorption rate constant and the profiles were examined. As the desorption rate decreased ($K_d < 1$, eq. 1.33), plate number also decreased until a value of $k_d = 0.05$ where significant peak tailing was evident and the tail never returned to baseline. The peak tail never returning to baseline is indicative of irreversible adsorption.

If tailing is present, peak efficiencies should not be determined using equation 1.21 as it assumes that the peak is Gaussian. Other methods are available for calculating efficiencies of non-Gaussian peaks.⁷⁰ A common method known as the Foley-Dorsey method will be discussed in detail in Section 3.2.6.

1.4.2.2 Protein Recovery

Irreversible adsorption within a capillary can be quantified by measuring the loss of protein using the methods detailed in the following sections.

1.4.2.2.1 Towns and Regnier

The first method for determining protein recovery was developed by Towns and Regnier⁷¹ whereby two on-capillary detectors were positioned 50 cm apart. Peak areas were measured for the migrating peaks at both detectors. The decrease in peak area from the first to the second detector yields a measure of the irreversible adsorption on the capillary. This method was used for the studies discussed in Section 1.4.1 that examined the effect of pI on protein adsorption.⁵⁸ One drawback of this method is that a custom instrument is required.

Yeung and Lucy⁷² modified the Towns-Regnier technique for a one detector system. A sample containing proteins and an internal marker was injected and separated three times on a 47 cm (40 cm to the detector) capillary. The capillary was then cut to a

length of 27 cm (20 cm to the detector) and the sample run three more times. The decrease in peak area from the long to short capillary gave a measure of the percent recovery. The injection time, applied voltage and rinse times were scaled in accordance with the reduced capillary length. The internal standard accounted for any residual changes in injection volume. This technique can be used with commercial instruments and has been used in past studies of surfactant based capillary coatings.^{55,72-74}

1.4.2.2.2 Fluorescein isothiocyanate-myoglobin saturation method

A protein recovery method was developed by Righetti and coworkers^{75,76} whereby a bare uncoated capillary was equilibrated with fluorescein isothiocyanate (FITC) labeled myoglobin at pH 5.0 (the pI of myoglobin is 7.6) with no buffer additive present. When all adsorption sites on the capillary were saturated, the capillary was flushed with buffer to remove any unretained protein. SDS was used to elute the adsorbed myoglobin, which was collected for later quantification. This amount of protein was considered to be the adsorption capacity of the bare capillary ($n_{capacity}$). The same procedure was carried out in the presence of an additive to determine the additive's effectiveness at inhibiting protein adsorption. The percent inhibition can then be determined using the following equation:

$$\%Inhibition = 100\% \left(\frac{n_{additive}}{n_{capacity}} \right) \quad (1.35)$$

Past studies⁷⁷ demonstrated the Towns-Regnier method was a more sensitive measure of irreversible protein adsorption than the saturation method. Therefore, the modified Towns-Regnier method is used in this thesis to measure protein recovery.

1.4.2.3 EOF

The EOF changes when protein is adsorbed onto the capillary as the adsorbed proteins will change the zeta potential within the capillary.⁵⁸ Therefore, protein

adsorption can be detected by monitoring the EOF during a series of protein injections. Graf et al. performed consecutive injections of an EOF marker to determine the EOF reproducibility in the absence of protein.⁶² Then a protein sample was injected onto a bare silica capillary and the EOF was observed following each injection. The EOF changed significantly (decreased by approximately 55%) in the presence of the protein. Once the protein was removed from the sample and a neutral EOF marker was injected by itself, the EOF did not return to its original value in the absence of protein, indicating that protein had irreversibly adsorbed onto the surface.

1.4.2.4 Migration Time

The migration time of an analyte will change if the EOF varies. Also, the migration time of a protein increases in the presence of reversible adsorption.⁵⁰ A CE simulation model was developed by Fang et al.⁷⁸ to describe adsorption quantitatively. They observed a Gaussian peak when there was no adsorption onto the wall. If reversible adsorption is introduced into the simulation, the migration time of the peak shifts to a later time. This effect is greatest at low analyte concentrations (0.005 mol/m^3) as the amount of analyte is small compared to the number of binding sites on the wall.⁷⁹ A broader Gaussian peak with a later migration time than observed in the absence of wall adsorption is noted. The broadening is due to slow adsorption/desorption kinetics described by equations 1.32 and 1.34. The migration time shift is a result of chromatographic retention as discussed in Section 1.3.6. The retention factor can be expressed in this case as:

$$k' = \frac{1 - (\mu_{e,0} / \mu_{e,ads})}{\mu_{e,0} / \mu_{e,ads}} \quad (1.36)$$

where $\mu_{e,0}$ is the electrophoretic mobility of the protein in the absence of adsorption and $\mu_{e,ads}$ is the electrophoretic mobility of the protein in the presence of adsorption. Fang et al. also observed that as the analyte concentration increased, more of these adsorption sites become occupied and the migration time shifted.⁷⁹ This results in increased peak asymmetry, which decreases the efficiency. Thus migration time changes can indicate reversible adsorption.

The measures discussed in the above section are applied in determining the efficacy of coatings in CE. The following section will examine methods of preventing protein adsorption in CE and their effectiveness based on these measures.

1.5 Buffer Additives and Wall Coatings

1.5.1 Small Molecule Additives

The addition of small molecules to the run buffer in CE is one method for reducing protein adsorption. These molecules either compete with the proteins for association with the negatively charged wall, or provide electrostatic screening between the protein and capillary wall. Green and Jorgenson demonstrated high concentrations of potassium sulfate provided electrostatic screening that allowed separation of a mixture of five proteins.⁵⁰ However, one drawback to this method is the high additive concentrations lead to Joule heating.

Bushey and Jorgenson followed this up by investigating zwitterionic additives.³⁸ Zwitterions are molecules containing both a positively and negatively charged moiety. They are electrically neutral at pH values where the two charged groups are equally but oppositely charged. This property makes them particularly useful in CE whereby they can be added to the running buffer, without increasing conductivity. Therefore, high

concentrations can be added with no increase in Joule heating (Section 1.3.3). According to Bushey and Jorgenson, the association of the zwitterions with the proteins and capillary wall should prevent adsorption and diminish interactions between proteins.³⁸ Bushey and Jorgenson added betaine to the buffer, but poor efficiencies were obtained unless other ionic additives were also present (i.e., potassium sulfate). Other work has since been done whereby the effect of zwitterions on protein separations has been investigated⁸⁰⁻⁸⁵ and will be outlined in Chapter 2. In addition to their effect on protein separations, zwitterions enhance the EOF, which is the primary subject of Chapter 2.

Amines are the most common small molecule additive as a result of their use in preventing peak tailing for basic compounds in HPLC.^{86,87} In CE, adsorption of amines onto the wall is used to slow the EOF^{88,89} or to prevent protein adsorption.^{75,90} The FITC-myoglobin saturation method detailed in Section 1.4.2.2.2 was used by Verzola et al. to determine if amines were effective at preventing protein adsorption.⁷⁵ These studies determined that polyamines were better able to prevent adsorption (90% binding inhibition), even at low millimolar concentrations, than mono-, di-, and triamines.^{75,76,91} One drawback to using polyamines for preventing protein adsorption is the amines must be protonated to be effective, which limits their usefulness to high pH buffers. A second disadvantage is these additives must be present in the run buffer. This can lead to signal suppression if electrospray ionization mass spectrometric detection is used.^{15,92,93} This suppression results from Coulombic interactions between the oppositely charged solute and surfactant ions in the droplets. The greater the surface activity of the surfactant, the larger the suppression of the analyte signal.⁹² Righetti et al. developed a new type of additive called the “Skorpis” reagents, which are trifunctional as they possess a

quaternary amine, a tertiary amine and an ω -alkyl iodine functionality.⁷⁶ When rinsed through the capillary, a reversed EOF is achieved. However, if the Skorprios reagent is removed from the running buffer the EOF becomes significantly less reversed over just ten runs.

1.5.2 Covalent Coatings

Covalent polymer coatings are typically formed on capillary walls by first derivatizing the surface silanols with a reagent, such as an alkylsilane.^{94,95} One portion of the reagent bonds with the silanols on the capillary wall to form an anchor (siloxane bond). The other portion reacts with the monomers to form a polymer on the capillary wall. Hjerten reported the first use of a covalently bound polymer coating for protein separations in CE in 1985.⁵³ However such linear polyacrylamide (LPA) coatings do not completely cover the capillary wall. This can result in non-uniform EOF and proteins adsorbing onto the uncovered areas.⁹⁶ Cross-linking the acrylamide monomers on the surface increases the coverage and thus the stability and overall performance of polyacrylamide coatings. Gao and Liu show that the crosslinked polyacrylamide blocks off nano-cavities known to be present on silica surfaces from attack by nucleophiles.⁹⁶ Gao and Liu also demonstrated that a crosslinked polyacrylamide (CPA) coating consistently generated a 20-fold lower EOF than on a LPA coating.⁹⁶ They showed that a CPA coating soaked in a basic, amino acid containing solution for two hours retained the same resolution as its original condition. After the same treatment, the resolution on the LPA coating deteriorated significantly. Covalent coatings can also be formed without using a silylating reagent.⁹⁷ Other common covalent coatings that have been used for the separation of proteins include polyoxyethylene (POE) or polyethylene glycol

(PEG),^{54,98,99} and polyvinyl pyrrolidone (PVP).^{51,100} POE and PEG have the same chemical structure, but PEG generally refers to smaller molecular weight polymers (< 40 000 g/mol) while POE refers to higher molecular weight polymers (> 100 000 g/mol).¹⁰¹ These are all neutral hydrophilic coatings. Therefore, electrostatic interactions between the proteins and the coating are virtually eliminated. Charged covalent coatings are also used for protein separations, but may result in irreversible adsorption of anionic proteins.¹⁰²

Covalent coatings are commonly used for protein separations as they are effective at preventing adsorption and can have high stability and peak efficiencies. They are typically stable for a large number of runs.^{94,96} Moderate to high efficiencies (> 200 000 plates/m) are often achieved.^{103,104} However, the drawbacks associated with this type of coating include long preparation times, no regeneration possible, higher cost, and limited pH stability.

In contrast, non-covalent coatings can be regenerated on the capillary, have fast preparation times, and are more cost effective than their covalent counterparts. Disadvantages of non-covalent coatings include the possibility that recoating between runs is necessary for optimal performance and lower stability than covalent coatings.. However, non-covalent coatings still offer a fast, simple, and efficient form of capillary coating and will be the main focus of the following sections, and of this thesis. Coating stability is a key parameter that will be monitored in these studies.

1.5.3 Surfactant Coatings

Surfactants are amphiphilic molecules consisting of a hydrophilic headgroup and at least one hydrophobic tail or chain. They are classified as cationic, anionic, nonionic

or zwitterionic, depending on the nature of the headgroup. When the concentration of the surfactant reaches the critical micelle concentration (cmc), free surfactant monomers aggregate to minimize the energetically unfavourable interaction of the hydrocarbon chains with the water. These aggregates may be in the form of spherical micelles or bilayers.⁵⁵ The type of aggregate formed depends on the shape of the monomers, as in Figure 1.11, and can be predicted using the packing factor:^{105,106}

$$p = \frac{V_c}{l_c a_h} \quad (1.37)$$

where V_c and l_c are the volume and length of the hydrocarbon chain, respectively, and a_h is the electrostatic cross-sectional area (i.e., accounts for electrostatic repulsion) of the headgroup. If the packing factor is less than 1/3, the surfactant molecule is conical and packs as a spherical micelle (Figure 1.11A). The packing factor can be increased by decreasing the electrostatic repulsion between the headgroups (eq. 1.37), for example by increasing the ionic strength. Vinson et al. demonstrated that cetyltrimethylammonium bromide (CTAB) micelles undergo a transition from spherical to cylindrical to wormlike micelles when the ionic strength is increased by addition of NaBr.¹⁰⁷ The packing factor can also be increased by increasing the volume of the hydrocarbon chain while keeping the length constant, for instance by using a surfactant with multiple tails. Multiply tailed surfactants tend to possess packing factors of $\frac{1}{2} - 1$ and a cylindrical geometry, and pack as a bilayer^{105,106} (Figure 1.11B). In solution these bilayer aggregates form vesicles, which are spherical or ellipsoidal particles formed by the bilayer wrapping around and enclosing a volume of solution.

The adsorption of surfactants onto a charged surface occurs in a series of stages.¹⁰⁸ At low surfactant concentrations, electrostatic forces between the surfactant

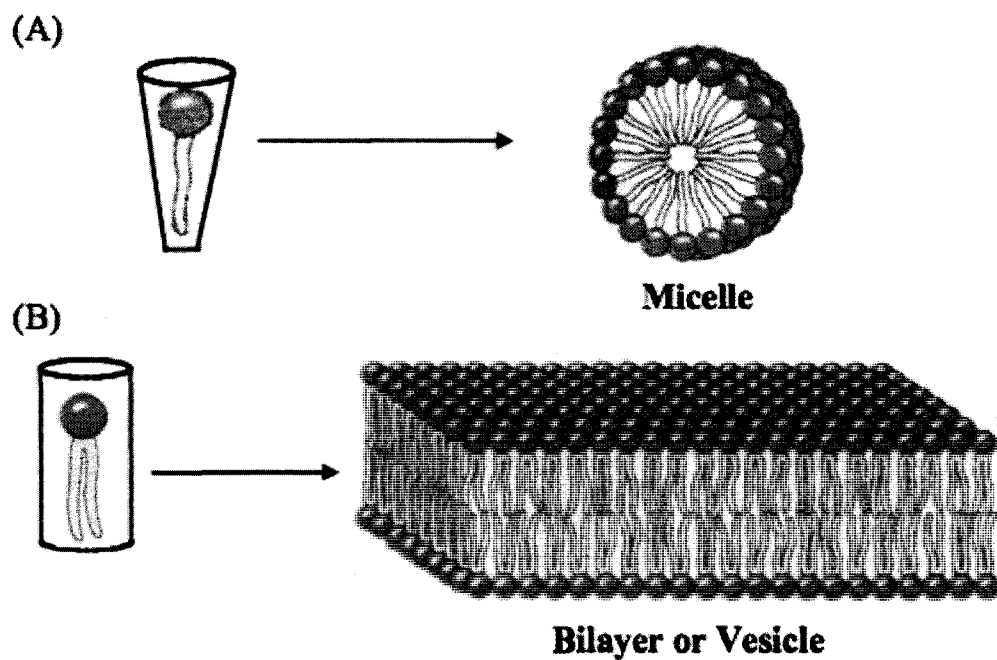


Figure 1.11: Common Aggregate Structures of (A) Single-Chain Surfactants and (B) Double-Chain Surfactants. Reprinted with permission from reference⁵⁵.

monomers and the wall dominate the adsorption. At slightly higher concentration, there is lateral association of the hydrocarbon chains and the monomers begin to form aggregates, based on their packing factor (eq. 1.37). This force, in addition to electrostatic interactions, causes an increase in adsorption density onto the wall. Once the surface charge is neutralized by the adsorbed surfactant, electrostatic interactions are no longer in effect and only the lateral interaction causes further adsorption. At the cmc, any further increase in surfactant concentration results in micellization of the free monomers, but does not change the adsorption density. The aggregate structures on the surface can be examined using atomic force microscopy (AFM).¹⁰⁹⁻¹¹¹ Our lab has previously studied two common surfactants, CTAB and didodecyldimethylammonium bromide (DDAB), under typical CE conditions.⁷³ The image of CTAB (single-chain surfactant) on fused silica shows spherical aggregates, or hemimicelles, while the image of DDAB (double-chain surfactant) shows a flat image. This flat image indicates a bilayer on the surface.

The structure of the aggregates on the surface is important when developing coatings for CE separations. Single-chain surfactants usually must be present in the run buffer during a separation in order for them to effectively prevent adsorption.¹¹² These types of coatings are termed “dynamic” coatings. If the surfactant is removed from the buffer during the separation, the system is pushed away from equilibrium and the surfactant adsorbed to the wall will desorb in order to restore equilibrium. This results in incomplete surface coverage.⁵⁵

Double-chain surfactants, which contain two hydrocarbon tails, do not need to be in the separation buffer in order to form a stable coating due to their bilayer structure

which results in increased surface coverage of the capillary wall.⁵⁵ These are referred to as “semi-permanent” coatings. A head to head comparison of CTAB and DDAB was performed previously in our lab whereby five proteins were injected onto a capillary coated with CTAB and one coated with DDAB. Only three of the five proteins migrated off the CTAB coated capillary, while all five were observed on the DDAB coated capillary.⁵⁵ Efficiencies were similar for the observed proteins, but recoveries were better with the DDAB coating, indicative of higher surface coverage. Therefore, the structure of the surfactant aggregates dictates their ultimate usefulness as coatings. Surfactants forming spherical aggregates on the capillary wall (single-chain) tend to be less stable and therefore less desirable as a coating material than those forming a bilayer structure (double-chain). As double-chain surfactants have been shown to result in better coatings overall, these are used in Chapters 3-5 herein. Thus, given the importance of double-chain surfactants in my research, they will be the focus of the remainder of this section.

The main reason for the better performance of coatings formed with double-chain surfactants is the formation of the bilayer on the capillary wall. This imparts greater stability to the coating. A study of DDAB determined that this bilayer coating was stable for up to 540 minutes of electrophoresis with no recoating between runs.¹¹³ Any factor that decreases the cmc of DDAB increases the stability of the coating.¹¹⁴ For example, when the ionic strength of the buffer solution is increased, the headgroups pack more tightly. This is a result of increased electrostatic screening of the charges on the headgroups by the buffer ions.¹¹⁵ It was also observed that DDAB is more stable in phosphate buffer than acetate buffer, due to the stronger ion association of the phosphate

leading to a lower cmc.¹¹⁴ pH, capillary diameter,¹¹³ and aging time of the coating¹¹⁴ were all observed to affect the stability of the DDAB coating.

Another method of decreasing the cmc is to increase the hydrophobicity of the carbon chain.¹¹⁶ Previous work in our lab examined the ability of longer hydrocarbon chain analogs of DDAB (2C₁₄, 2C₁₆, 2C₁₈DAB, and a triple-chain surfactant (containing three hydrocarbon chains), tridodecylmethylammonium iodide, 3C₁₂MAI) to form stable coatings.¹¹⁷ 2C₁₈DAB or DODAB (dioctadecyldimethylammonium bromide) was observed to be the most stable of the surfactants studied, as it was used for over 60 successive electrophoretic runs over twelve days. Other types of surfactants showing usefulness as coatings include zwitterionic phospholipids,¹¹⁸⁻¹²¹ zwitterionic phospholipid and cationic surfactant mixtures,^{77,122-124} cationic surfactants,¹²⁵ and polymerized surfactants.^{126,127} However, the dialkylammonium bromide type surfactants had been shown to allow for intercalation (i.e., inclusion) of the hydrophobic portion of the polyoxyethylene stearate polymer into the bilayer,¹²⁸ which will be discussed in more detail in Chapter 3. Therefore, the DODAB was chosen as the surfactant portion of the coating developed and characterized in Chapters 3-5.

1.5.4 Physically Adsorbed Polymer Coatings

Polymers can be used to prepare both dynamic and semi-permanent coatings. They can be categorized as neutral, cationic, or successive multiple ionic layer (SMIL) coatings. Neutral hydrophilic polymers interact with the silica surface predominately through hydrogen bonds between the polymer and the protonated silanols on the wall.¹²⁹ Therefore, pretreatment of the surface to obtain protonated silanols is an important step in forming these coatings. Polyoxyethylene (POE) has been used as both dynamic^{130,131} and

semi-permanent¹²⁹ coatings. POE is well known to resist protein adsorption^{129,132,133} and forms a neutral, hydrophilic coating. For these reasons POE was chosen as the polymer portion of the coating developed and discussed in Chapters 3-5.

Polyvinyl alcohol (PVA) is a neutral polymer that has also been used to prepare both dynamic^{134,135} and non-covalent (permanent)^{134,136} coatings. However, dynamic PVA coatings weakly interact with the silica surface resulting in peak tailing and low protein recoveries.^{134,137} They are also ineffective at separating proteins at neutral pH.¹³⁸ Thermally treated PVA¹³⁴ and cross-linked PVA¹³⁶ have demonstrated much better separation ability, resulting in high efficiencies for protein separations at low pH and low migration time relative standard deviations (RSDs) ($\leq 2.1\%$ over 60 injections¹³⁴ and $\leq 1.2\%$ over 900 runs,¹³⁶ respectively). A permanent PVA coating is investigated in Chapter 5 and is used as a comparison standard for the coating developed in Chapter 3. Other neutral polymers useful as physically adsorbed coatings for protein separations include pluronics (PEO-polypropylene oxide (PPO)-PEO),¹³⁹ more hydrophilic polyacrylamides,^{140,141} polyamine-ester,¹⁴² and cellulose acetate.¹⁴³

Cationic polymers can also be used to form useful dynamic¹⁴⁴⁻¹⁴⁶ and semi-permanent coatings. To form a cationic adsorbed coating, the surface of the capillary is typically pretreated with sodium hydroxide to deprotonate the silanols. The capillary is then flushed with a solution of the polymer, which adheres strongly to the negatively charged surface as a result of electrostatic interactions between the polymer and the surface. The polymer solution is allowed to sit within the capillary afterwards to ensure full coverage. The resulting positively charged surface generates a reversed EOF (i.e., towards the anode). Effective protein separations have been performed using adsorbed

coatings of polyethylene imine (PEI),¹⁴⁷ polybrene,¹⁴⁸ polydiallyldimethylammonium chloride (PDADMAC),¹⁴⁹ PolyE-323,¹⁵⁰ Poly-LA 313,¹⁵¹ chitosan,^{146,152} and quaternary ammonium substituted agarose.¹⁵³ However, cationic coatings are not useful for separating anionic proteins, which will strongly interact with the coating through electrostatic interactions.

The final category of adsorbed polymer coatings is the SMIL coatings. These consist of alternating layers of polycationic and polyanionic polymers. Following a pretreatment step, a polycationic polymer is rinsed through the capillary, as above. This is then followed by a rinse with a polyanionic polymer to create a negatively charged surface that generates a normal (i.e., cathodic) EOF. Further rinses with polycationic and polyanionic polymer solutions may be performed. The composition of a SMIL coating is typically abbreviated as SMIL-X(#) where X is the layer exposed to the solution and # is the number of layers. With two layer SMILs the # is often omitted. Examples of SMIL coatings that have demonstrated usefulness for protein separations include SMIL-dextran sulfate (DS),¹⁵⁴ SMIL-polybrene (PB) (3),¹⁵⁵ SMIL-polyvinyl sulfonate (PVS),^{156,157} PDADMAC-polystyrene sulfonate (PSS),¹⁴⁹ and CEofix.¹⁵⁶ SMIL coatings show excellent stability. For instance, the SMIL-PB(3) coating is useful for 600 runs with no recoating.¹⁵⁵ This stability has been attributed to the strong electrostatic interactions between the polymer layers.¹⁵⁴ However, not all SMIL coatings show complete suppression of protein adsorption. The SMIL-PVS required a NaOH rinse after HSA injections, and a high concentration buffer for high efficiencies to be achieved.^{156,157}

1.6 Thesis Outline

Understanding the fundamental aspects of a field is important for progressing further. The EOF is an important phenomenon in CE. Manipulating the EOF through additives or modifying the capillary wall can lead to interesting effects. Modification of the capillary wall can also prevent protein adsorption, which is a major concern in CE. Coatings are the most effective way of achieving this. Protein separations are a significant application as they are necessary in a number of growing fields, such as proteomics and metabolomics.^{8,9} Knowledge of other effects besides adsorption that can affect separation performance is also important for developing the best possible separation conditions.

Chapter 2 of this thesis examines the effect of zwitterionic additives on the EOF within the capillary. The properties of the additives giving the greatest enhancement are highlighted. As these additives proved to be ineffective for preventing adsorption of proteins, a novel self-assembled bilayer/diblock copolymer coating is developed in Chapter 3. Chapter 4 investigates various analogs of this coating and their ability to modify the EOF. The ability of these coatings to perform protein separations is also examined. Chapter 5 looks at other underlying effects besides adsorption that can lead to poor separation performance in CE. Chapter 6 summarizes the studies within the thesis and suggests further areas of investigation.

1.7 References

- (1) Tiselius, A., *Trans. Faraday Soc.* **1937**, *33*, 0524-0530.
- (2) Hjerten, S., *Electrophoresis* **1988**, *9*, 3-15.
- (3) Raymond, S.; Weintraub, L., *Science* **1959**, *130*, 711-711.
- (4) Hjerten, S., *Chromatograph. Rev.* **1967**, *9*, 122-219.
- (5) Jorgenson, J. W.; Lukacs, K. D., *Anal. Chem.* **1981**, *53*, 1298-1302.
- (6) Dovichi, N. J.; Zhang, J. Z., *Angew. Chem. Int. Ed.* **2000**, *39*, 4463.
- (7) DePalma, A., *Gen. Eng. News* **2001**, *21*, 21.
- (8) Shen, Y. F.; Smith, R. D., *Electrophoresis* **2002**, *23*, 3106-3124.
- (9) Ramautar, R.; Demirci, A.; de Jong, G. J., *TRAC-Trend. Anal. Chem.* **2006**, *25*, 455-466.
- (10) Tagliaro, F.; Bortolotti, F., *Electrophoresis* **2006**, *27*, 231-243.
- (11) Garcia-Canas, V.; Cifuentes, A., *Electrophoresis* **2008**, *29*, 294-309.
- (12) Ciccone, B., *Am. Lab.* **2001**, *33*, 30-33.
- (13) Heiger, D., *An Introduction High Performance Capillary Electrophoresis*, Agilent Technologies, Germany, 2000.
- (14) Gaspar, A.; Englmann, M.; Fekete, A.; Harir, M.; Schmitt-Kopplin, P., *Electrophoresis* **2008**, *29*, 66-79.
- (15) Landers, J. P., *Handbook of Capillary Electrophoresis*, CRC Press, Boca Raton, 1994.
- (16) Harris, D., C., *Quantitative Chemical Analysis*, Fifth edn., W.H. Freeman and Company, New York, 1998.
- (17) Xue, Y. J.; Yeung, E. S., *Anal. Chem.* **1994**, *66*, 3575-3580.
- (18) Chervet, J. P.; Vansoest, R. E. J.; Ursem, M., *J. Chromatogr.* **1991**, *543*, 439-449.
- (19) Xu, X. M.; Li, L.; Weber, S. G., *TRAC-Trend. Anal. Chem.* **2007**, *26*, 68-79.

- (20) Ewing, A. G.; Wallingford, R. A.; Olefirowicz, T. M., *Anal. Chem.* **1989**, *61*, A292.
- (21) Schwer, C.; Kenndler, E., *Anal. Chem.* **1991**, *63*, 1801-1807.
- (22) Bard, A. J.; Faulkner, L. R., *Electrochemical Methods Fundamentals and Applications*, John Wiley & Sons, Toronto, 1980.
- (23) Hunter, R. J., *Zeta Potential in Colloid Science Principles and Applications*, Academic Press, Toronto, 1981.
- (24) Grossman, P. D.; Colburn, J. C., *Capillary Electrophoresis Theory and Practice*, Academic Press, Inc., Toronto, 1992.
- (25) Gas, B.; Stedry, M.; Kenndler, E., *J. Chromatogr. A* **1995**, *709*, 63-68.
- (26) Shaw, D. H., *Colloid & Surface Chemistry*, Fourth edn., Butterworth-Heinemann, Oxford, 1992.
- (27) Li, S. F. Y., *Capillary Electrophoresis Principles Practice and Applications*, Elsevier Science Publishers, Amsterdam, 1992.
- (28) Winefordner, J. D., *Chemical Analysis*, John Wiley & Sons, Inc., Toronto, 1998.
- (29) Huang, X. H.; Coleman, W. F.; Zare, R. N., *J. Chromatogr.* **1989**, *480*, 95-110.
- (30) Lucy, C. A.; Yeung, K. K. C.; Pang, X. J.; Chen, D. D. Y., *LC-GC* **1998**, *16*, 26.
- (31) Lauer, H. H.; McManigill, D., *TRAC-Trend. Anal. Chem.* **1986**, *5*, 11-15.
- (32) Kenndler, E., *Theory of Capillary Zone Electrophoresis*, John Wiley & Sons, Inc., Toronto, 1998.
- (33) Grushka, E.; McCormick, R. M., *J. Chromatogr.* **1989**, *471*, 421-428.
- (34) Freebairn, K. W.; Knox, J. H., *Chromatographia* **1984**, *19*, 37-47.
- (35) Grushka, E.; McCormick, R. M.; Kirkland, J. J., *Anal. Chem.* **1989**, *61*, 241-246.
- (36) Nelson, R. J.; Paulus, A.; Cohen, A. S.; Guttman, A.; Karger, B. L., *J. Chromatogr.* **1989**, *480*, 111-127.
- (37) Issaq, H. J.; Atamna, I. Z.; Muschik, G. M.; Janini, G. M., *Chromatographia* **1991**, *32*, 155-161.

- (38) Bushey, M. M.; Jorgenson, J. W., *J. Chromatogr.* **1989**, *480*, 301-310.
- (39) Mikkers, F. E. P.; Everaerts, F. M.; Verheggen, T., *J. Chromatogr.* **1979**, *169*, 1-10.
- (40) Yassine, M. M.; Lucy, C. A., *Electrophoresis* **2006**, *27*, 3066-3074.
- (41) Xu, X.; Kok, W. T.; Poppe, H., *J. Chromatogr. A* **1996**, *742*, 211-227.
- (42) Cifuentes, A.; Xu, X.; Kok, W. T.; Poppe, H., *J. Chromatogr. A* **1995**, *716*, 141-156.
- (43) Burgi, D. S.; Chien, R. L., *Anal. Chem.* **1991**, *63*, 2042-2047.
- (44) Chien, R. L.; Burgi, D. S., *Anal. Chem.* **1992**, *64*, 1046-1050.
- (45) Burgi, D. S.; Chien, R. L., *J. Microcol. Sep.* **1991**, *3*, 199-202.
- (46) Chien, R. L.; Burgi, D. S., *Anal. Chem.* **1992**, *64*, A489-A496.
- (47) Ermakov, S. V.; Zhukov, M. Y.; Capelli, L.; Righetti, P. G., *J. Chromatogr. A* **1995**, *699*, 297-313.
- (48) Kennedy, R. T., *Anal. Chim. Acta* **1999**, *400*, 163-180.
- (49) Schure, M. R.; Lenhoff, A. M., *Anal. Chem.* **1993**, *65*, 3024-3037.
- (50) Green, J. S.; Jorgenson, J. W., *J. Chromatogr.* **1989**, *478*, 63-70.
- (51) McCormick, R. M., *Anal. Chem.* **1988**, *60*, 2322-2328.
- (52) Lauer, H. H.; McManigill, D., *Anal. Chem.* **1986**, *58*, 166-170.
- (53) Hjerten, S., *J. Chromatogr.* **1985**, *347*, 191-198.
- (54) Bruin, G. J. M.; Chang, J. P.; Kuhlman, R. H.; Zegers, K.; Kraak, J. C.; Poppe, H., *J. Chromatogr.* **1989**, *471*, 429-436.
- (55) Melanson, J. E.; Baryla, N. E.; Lucy, C. A., *Anal. Chem.* **2000**, *72*, 4110-4114.
- (56) Bezkorovainy, A., *Basic Protein Chemistry*, Charles C. Thomas, Springfield, 1970.
- (57) Lucy, C. A.; MacDonald, A. M.; Gulcev, M. D., *J. Chromatogr. A* **2008**, *1184*, 81-105.

- (58) Towns, J. K.; Regnier, F. E., *Anal. Chem.* **1992**, *64*, 2473-2478.
- (59) Norde, W.; Haynes, C. A., in *Proteins at Interfaces II: Fundamentals and Applications*, American Chemical Society, Washington, D.C., 1995, vol. 602, pp. 26-40.
- (60) Norde, W., in *Physical Chemistry of Biological Interfaces*, eds. A. Baskin and W. Norde, Marcel Dekker, New York, 2000, pp. 115-135.
- (61) Malmsten, M., *J. Colloid Interf. Sci.* **1998**, *207*, 186-199.
- (62) Graf, M.; Garcia, R. G.; Watzig, H., *Electrophoresis* **2005**, *26*, 2409-2417.
- (63) Norde, W., in *Surfactant Science Series (Biopolymers at Interfaces)*, Marcel Dekker Inc., New York, 2003, vol. 110, pp. 21-43.
- (64) Yao, Y.; Lenhoff, A. M., *Anal. Chem.* **2004**, *76*, 6743-6752.
- (65) Yao, Y.; Lenhoff, A. M., *Anal. Chem.* **2005**, *77*, 2157-2165.
- (66) Kauzmann, W., *Adv. Protein Chem.* **1959**, *14*, 1-63.
- (67) Nakanishi, K.; Sakiyama, T.; Imamura, K., *J. Biosci. Bioeng.* **2001**, *91*, 233-244.
- (68) Leduc, C. A.; Vroman, L.; Leonard, E. F., *Ind. Eng. Chem. Res.* **1995**, *34*, 3488-3495.
- (69) Bhaduri, A. D., K.P., *J. Disper. Sci. Technol.* **1999**, *20*, 1097-1123.
- (70) Bidlingmeyer, B. A.; Warren, F. V., Jr., *Anal. Chem.* **1984**, *56*, 1583A-1596A.
- (71) Towns, J. K.; Regnier, F. E., *Anal. Chem.* **1991**, *63*, 1126-1132.
- (72) Yeung, K. K. C.; Lucy, C. A., *Anal. Chem.* **1997**, *69*, 3435-3441.
- (73) Baryla, N. E.; Melanson, J. E.; McDermott, M. T.; Lucy, C. A., *Anal. Chem.* **2001**, *73*, 4558-4565.
- (74) Baryla, N. E.; Lucy, C. A., *Anal. Chem.* **2000**, *72*, 2280-2284.
- (75) Verzola, B.; Gelfi, C.; Righetti, P. G., *J. Chromatogr. A* **2000**, *868*, 85-99.
- (76) Righetti, P. G.; Gelfi, C.; Sebastiano, R.; Citterio, A., *J. Chromatogr. A* **2004**, *1053*, 15-26.
- (77) Baryla, N. E., Ph.D., Department of Chemistry, University of Alberta, 2002.

- (78) Fang, N.; Li, J. W.; Yeung, E. S., *Anal. Chem.* **2007**, *79*, 5343-5350.
- (79) Fang, N.; Zhang, H.; Li, J. W.; Li, H. W.; Yeung, E. S., *Anal. Chem.* **2007**, *79*, 6047-6054.
- (80) Liu, Y. J.; Foote, R. S.; Culbertson, C. T.; Jacobson, S. C.; Ramsey, R. S.; Ramsey, J. M., *J. Microcol. Sep.* **2000**, *12*, 407-411.
- (81) Guzman, N. A.; Moschera, J.; Iqbal, K.; Malick, A. W., *J. Chromatogr.* **1992**, *608*, 197-204.
- (82) Hines, H. B.; Brueggemann, E. E., *J. Chromatogr. A* **1994**, *670*, 199-208.
- (83) Mandrup, G., *J. Chromatogr.* **1992**, *604*, 267-281.
- (84) Miura, T.; Funato, T.; Yabuki, S.; Sasaki, T.; Kaku, M., *Clin. Chim. Acta* **2000**, *299*, 87-99.
- (85) Gong, B. Y.; Ho, J. W., *Electrophoresis* **1997**, *18*, 732-735.
- (86) Stadalius, M. A.; Berus, J. S.; Snyder, L. R., *LC-GC* **1988**, *6*, 494.
- (87) Nahum, A.; Horvath, C., *J. Chromatogr.* **1981**, *203*, 53-63.
- (88) Govindaraju, K.; Ahmed, A.; Lloyd, D. K., *J. Chromatogr. A* **1997**, *768*, 3-8.
- (89) Oda, R. P.; Madden, B. J.; Spelsberg, T. C.; Landers, J. P., *J. Chromatogr. A* **1994**, *680*, 85-92.
- (90) Corradini, D.; Cannarsa, G., *Electrophoresis* **1995**, *16*, 630-635.
- (91) Corradini, D.; Bevilacqua, L.; Nicoletti, I., *Chromatographia* **2005**, *62*, S43-S50.
- (92) Rundlett, K. L.; Armstrong, D. W., *Anal. Chem.* **1996**, *68*, 3493-3497.
- (93) Varghese, J.; Cole, R. B., *J. Chromatogr. A* **1993**, *652*, 369-376.
- (94) Doherty, E. A. S.; Meagher, R. J.; Albarghouthi, M. N.; Barron, A. E., *Electrophoresis* **2003**, *24*, 34-54.
- (95) Liu, C. Y., *Electrophoresis* **2001**, *22*, 612-628.
- (96) Gao, L.; Liu, S. R., *Anal. Chem.* **2004**, *76*, 7179-7186.

- (97) Schmalzing, D.; Piggee, C. A.; Foret, F.; Carrilho, E.; Karger, B. L., *J. Chromatogr. A* **1993**, *652*, 149-159.
- (98) Nashabeh, W.; Elrassi, Z., *J. Chromatogr.* **1991**, *559*, 367-383.
- (99) Meagher, R. J.; Seong, J.; Laibinis, P. E.; Barron, A. E., *Electrophoresis* **2004**, *25*, 405-414.
- (100) Xu, R. J.; VidalMadjar, C.; Sebillé, B.; DiezMasa, J. C., *J. Chromatogr. A* **1996**, *730*, 289-295.
- (101) Sigma-Aldrich, www.sigma-aldrich.com, accessed April 2005.
- (102) Horvath, J.; Dolnik, V., *Electrophoresis* **2001**, *22*, 644-655.
- (103) Shao, X. W.; Shen, Y. F.; O'Neill, K.; Lee, M. L., *J. Chromatogr. A* **1999**, *830*, 415-422.
- (104) Liu, S. R.; Gao, L.; Pu, Q. S.; Lu, J. J.; Wang, X. J., *J. Proteome Res.* **2006**, *5*, 323-329.
- (105) Israelachvili, J. N.; Mitchell, D. J.; Ninham, B. W., *J. Chem. Soc. Farad. T2* **1976**, *72*, 1525-1568.
- (106) Israelachvili, J. N., *Intermolecular and Surface Forces*, 2nd edn., Academic Press, London, 1992.
- (107) Vinson, P. K.; Bellare, J. R.; Davis, H. T.; Miller, W. G.; Scriven, L. E., *J. Colloid Interf. Sci.* **1991**, *142*, 74-91.
- (108) Zhang, R.; Somasundaran, P., *Adv. Colloid Interfac. Sci.* **2006**, *123*, 213-229.
- (109) Liu, J. F.; Ducker, W. A., *J. Phys. Chem. B* **1999**, *103*, 8558-8567.
- (110) Patrick, H. N.; Warr, G. G.; Manne, S.; Aksay, I. A., *Langmuir* **1999**, *15*, 1685-1692.
- (111) Manne, S.; Cleveland, J. P.; Gaub, H. E.; Stucky, G. D.; Hansma, P. K., *Langmuir* **1994**, *10*, 4409-4413.
- (112) Lucy, C. A.; Underhill, R. S., *Anal. Chem.* **1996**, *68*, 300-305.
- (113) Mohabbati, S.; Westerlund, D., *J. Chromatogr. A* **2006**, *1121*, 32-39.
- (114) Yassine, M. M.; Lucy, C. A., *Anal. Chem.* **2004**, *76*, 2983-2990.

- (115) Bostrom, M.; Williams, D. R. M.; Ninham, B. W., *Langmuir* **2002**, *18*, 6010-6014.
- (116) Svitova, T. F.; Smirnova, Y. P.; Pisarev, S. A.; Berezina, N. A., *Colloid. Surf. A* **1995**, *98*, 107-115.
- (117) Yassine, M. M.; Lucy, C. A., *Anal. Chem.* **2005**, *77*, 620-625.
- (118) Cunliffe, J. M.; Baryla, N. E.; Lucy, C. A., *Anal. Chem.* **2002**, *74*, 776-783.
- (119) Zhang, H. X.; Zhang, C. J.; Lajoie, G. A.; Yeung, K. K. C., *Anal. Chem.* **2005**, *77*, 6078-6084.
- (120) Zhang, H. X.; Yeung, K. K. C., *Anal. Chem.* **2004**, *76*, 6814-6818.
- (121) Linden, M. V.; Wiedmer, S. K.; Hakala, R. M. S.; Riekkola, M. L., *J. Chromatogr. A* **2004**, *1051*, 61-68.
- (122) Baryla, N. E.; Lucy, C. A., *J. Chromatogr. A* **2002**, *956*, 271-277.
- (123) Jurcic, K.; Nesbitt, C. A.; Yeung, K. K. C., *J. Chromatogr. A* **2006**, *1134*, 317-325.
- (124) Kuldvee, R.; Linden, M. V.; Wiedmer, S. K.; Riekkola, M. L., *Anal. Bioanal. Chem.* **2004**, *380*, 293-302.
- (125) Wang, C. Z.; Lucy, C. A., *Electrophoresis* **2004**, *25*, 825-832.
- (126) Wang, C. Z.; Lucy, C. A., *Anal. Chem.* **2005**, *77*, 2015-2021.
- (127) Mansfield, E.; Ross, E. E.; Aspinwall, C. A., *Anal. Chem.* **2007**, *79*, 3135-3141.
- (128) Blom, A.; Drummond, C.; Wanless, E. J.; Richetti, P.; Warr, G. G., *Langmuir* **2005**, *21*, 2779-2788.
- (129) Iki, N.; Yeung, E. S., *J. Chromatogr. A* **1996**, *731*, 273-282.
- (130) Cifuentes, A.; Defrutos, M.; Diezmasa, J. C., *J. Dairy Sci.* **1993**, *76*, 1870-1875.
- (131) Tseng, W. L.; Lin, Y. W.; Chang, H. T., *Anal. Chem.* **2002**, *74*, 4828-4834.
- (132) Harris, J. M.; Zalipsky, S., *Poly(ethylene glycol) : Chemistry and Biological Applications*, American Chemical Society, Washington, 1997.
- (133) Leckband, D.; Sheth, S.; Halperin, A., *J. Biomat. Sci.-Polym. E* **1999**, *10*, 1125-1147.

- (134) Gilges, M.; Kleemiss, M. H.; Schomburg, G., *Anal. Chem.* **1994**, *66*, 2038-2046.
- (135) Gilges, M.; Husmann, H.; Kleemiss, M. H.; Motsch, S. R.; Schomburg, G., *HRC-J. High Res. Chrom.* **1992**, *15*, 452-457.
- (136) Belder, D.; Deege, A.; Husmann, H.; Kohler, F.; Ludwig, M., *Electrophoresis* **2001**, *22*, 3813-3818.
- (137) Verzola, B.; Gelfi, C.; Righetti, P. G., *J. Chromatogr. A* **2000**, *874*, 293-303.
- (138) Cifuentes, A.; Rodriguez, M. A.; GarciaMontelongo, F. J., *J. Chromatogr. A* **1996**, *742*, 257-266.
- (139) Ng, C. L.; Lee, H. K.; Li, S. F. Y., *J. Chromatogr. A* **1994**, *659*, 427-434.
- (140) Albarghouthi, M. N.; Stein, T. M.; Barron, A. E., *Electrophoresis* **2003**, *24*, 1166-1175.
- (141) Cretich, M.; Stastna, M.; Chrambach, A.; Chiari, M., *Electrophoresis* **2002**, *23*, 2274-2278.
- (142) Shou, C. Q.; Zhou, C. L.; Zhao, C. B.; Zhang, Z. L.; Li, G. B.; Chen, L. R., *Talanta* **2004**, *63*, 887-891.
- (143) Busch, M. H. A.; Kraak, J. C.; Poppe, H., *J. Chromatogr. A* **1995**, *695*, 287-296.
- (144) Yu, C. J.; Tseng, W. L., *Electrophoresis* **2006**, *27*, 3569-3577.
- (145) Lin, C. Y.; Yu, C. J.; Chen, Y. M.; Chang, H. C.; Tseng, W. L., *J. Chromatogr. A* **2007**, *1165*, 219-225.
- (146) Yao, Y. J.; Li, S. F. Y., *J. Chromatogr. A* **1994**, *663*, 97-104.
- (147) Erim, F. B.; Cifuentes, A.; Poppe, H.; Kraak, J. C., *J. Chromatogr. A* **1995**, *708*, 356-361.
- (148) Chiu, R. W.; Jimenez, J. C.; Monnig, C. A., *Anal. Chim. Acta* **1995**, *307*, 193-201.
- (149) Graul, T. W.; Schlenoff, J. B., *Anal. Chem.* **1999**, *71*, 4007-4013.
- (150) Ullsten, S.; Zuberovic, A.; Wetterhall, M.; Hardenborg, E.; Markides, K. E.; Bergquist, J., *Electrophoresis* **2004**, *25*, 2090-2099.
- (151) Puerta, A.; Axen, J.; Soderberg, L.; Bergquist, J., *J. Chromatogr. B-Anal. Technol. Biomed. Life Sci.* **2006**, *838*, 113-121.

- (152) Huang, X. J.; Wang, Q. Q.; Huang, B. L., *Talanta* **2006**, *69*, 463-468.
- (153) Ullsten, S.; Soderberg, L.; Folestad, S.; Markides, K. E., *Analyst* **2004**, *129*, 410-415.
- (154) Katayama, H.; Ishihama, Y.; Asakawa, N., *Anal. Chem.* **1998**, *70*, 2254-2260.
- (155) Katayama, H.; Ishihama, Y.; Asakawa, N., *Anal. Chem.* **1998**, *70*, 5272-5277.
- (156) Catai, J. R.; Tervahauta, H. A.; de Jong, G. J.; Somsen, G. W., *J. Chromatogr. A* **2005**, *1083*, 185-192.
- (157) Catai, J. R.; Torano, J. S.; de Jong, G. J.; Somsen, G. W., *Analyst* **2007**, *132*, 75-81.

Chapter Two: Enhancement of Electroosmotic Flow in Capillary

Electrophoresis using Zwitterionic Additives*

2.1 Introduction

Capillary electrophoresis (CE) is a very useful separation technique for many areas of analysis, as discussed in Chapter 1. In order to achieve the maximum benefits of CE it is important to understand the chemistry in the capillary. A fundamental phenomenon in CE is electroosmotic flow (EOF). As discussed in Section 1.2.2, EOF is a consequence of the surface charge on the capillary wall, and controls the amount of time that an analyte spends in the capillary.^{1,2} The EOF determines the reproducibility of sample migration and accuracy of mobility measurements.³ Thus, the ability to manipulate the EOF is important. In the analysis of small anions, the EOF is often reversed as it normally moves in the opposite direction to the natural migration of the anions.⁴ Otherwise the separation time would be greatly increased and in some cases, the anions may never reach the detector. In protein/peptide analysis, wall coatings are often used to suppress the EOF and prevent protein adsorption onto the capillary walls.⁵⁻⁸

Another method to adjust the EOF is to modify the pH of the buffer. A low pH has been used to protonate the silanol groups³ and a high pH has been used in protein separations to ensure all proteins are negatively charged.⁹ However, extreme pH may denature proteins.

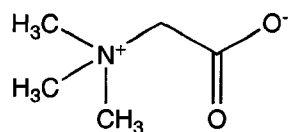
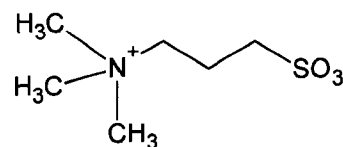
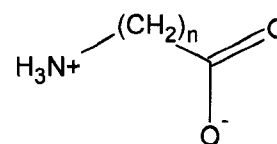
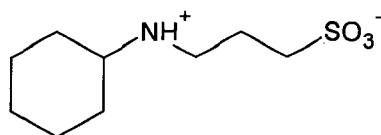
Ions can also be added to the background buffer as a means of minimizing silanol effects and manipulating the EOF. As discussed in Section 1.5.1, amines pair with

* A version of this chapter has been published. MacDonald, A.M., Sheppard, M.A.W., Lucy, C.A., *Electrophoresis*, **2005**, 26, 4421-4428.

negatively charged silanol groups, competing with the analyte for these positions.¹⁰ High salt concentrations increase the ionic strength of the buffer and compete for cation exchange sites. These additives increase conductivity and Joule heating.¹¹⁻¹³ This is where zwitterionic additives have an advantage: they do not increase the conductivity of the buffer. This allows for larger voltages and higher additive concentrations to be used.

The unique properties of zwitterions have led to their use in different applications. Bushey and Jorgenson¹² have investigated five zwitterions for their effectiveness in preventing protein adsorption. Trimethylglycine hydroxide (betaine, Figure 2.1) was the most successful, but the efficiencies were still low (< 30 000 plates/m). Betaine has been used as a buffer additive for protein separations on microchips to improve the separation.¹⁴ Sun and coworkers¹⁵ demonstrated trimethylammoniumalkyl sulfonate zwitterions increase protein efficiency and mobility. The propyl-form of this zwitterion has been marketed by Waters as the Accupure Z1-Methyl additive for the prevention of protein-wall interactions. A 20-fold increase in protein efficiency was observed upon addition of 2.0 M Z1-Methyl to the buffer. Guzman et al. obtained an improvement in peak area reproducibility in the separation of monoclonal antibodies with the use of 0.025 M Z1-Methyl.¹⁶ Z1-Methyl has also been used to prevent adsorption in the determination of ricin (a toxic glycoprotein),¹⁷ free fatty acids,¹⁸ deamidation products in insulin solutions¹⁹ and monoclonal proteins.²⁰

Thus, zwitterionic salts have been widely used as a buffer additive to improve separation efficiency.^{14,16-21} This chapter investigates the effect of Z1-Methyl as well as a series of other zwitterionic additives on EOF.

**Betaine****Z1-Methyl****3-amino-1-propane sulfonic acid****Aminocarboxylic Acids****n=1 glycine****n=3 4-aminobutyric acid****n=5 6-aminocaproic acid****n=7 8-aminocaprylic acid****CAPS****Figure 2.1:** Structures of Zwitterions

2.2 Experimental

2.2.1 Apparatus

All EOF measurements were performed with a Beckman P/ACE 2100 capillary electrophoresis system (Beckman Instruments, Fullerton, CA) equipped with a UV absorbance detector upgraded to 5000 series optics. Detection was performed at 254 nm. Instrument control and data acquisition was achieved using P/ACE station software for Windows 95 (Beckman Instruments, Fullerton, CA). The capillaries were untreated fused silica (Polymicro Technologies, Phoenix, AZ) with an I.D. of 50 μm , an O.D. of 360 μm , and a total length of 47 cm (40 cm to the detector).

2.2.2 Chemicals

All solutions were prepared in Nanopure 18 M Ω water (Barnstead, Chicago, IL). Buffers were prepared from stock solutions of reagent grade orthophosphoric acid (BDH, Toronto, ON), glacial acetic acid (Anachemia, Rouses Point, NY), or succinic acid (Anachemia). The pH of the buffers was adjusted with reagent grade sodium hydroxide (EM Science, Gibbstown, NJ), potassium hydroxide (BDH) or lithium hydroxide (Aldrich, Milwaukee, WI). The pH was measured using a Corning digital pH meter model 445 (Corning, Acton, MA). Glycine (reagent grade, Fisher Scientific, Fair Lawn, NJ), 4-aminobutyric acid (97%), 6-aminocaproic acid (98%), 8-aminocaprylic acid (99%), 3-amino-1-propane sulfonic acid (97%) (all from Aldrich), 3-[cyclohexylamino]-1-propanesulfonic acid (CAPS, Sigma, St. Louis, MO), and Z1-Methyl (reagent grade, Waters, Milford, MA) were used without further purification. The structures of these compounds are shown in Figure 2.1. These additives were added in varying concentrations directly to the running buffer. pH was checked after addition of the

additives to the buffers and was adjusted as required with reagent grade sodium hydroxide, lithium hydroxide, or potassium hydroxide. Mesityl oxide (Aldrich) was used as the neutral EOF marker.

2.2.3 EOF Measurement

New capillaries were used for each new buffer system to avoid hysteresis effects. The capillaries were conditioned with a high-pressure (20 psi) rinse of 0.1 M NaOH for 5 min and distilled water for 2 min. The capillary was rinsed between runs for 1 min with 0.1 M NaOH, 1 min with distilled water, and 2 min with the running buffer. In studies of the effect of buffer cation on EOF, the conditioning was as above, except the capillary was preconditioned with the corresponding metal hydroxide salt. Mesityl oxide (2 mM in water) was injected into a 47 cm capillary using hydrodynamic injection (0.5 psi) for 2 s. A constant voltage of +20 kV was applied at 25°C. Duplicate runs were carried out for each buffer system, with additive concentrations run in random order. Concentrations of additive ranged from 0 mM to 750 mM. As discussed in Section 2.1, an advantage of zwitterions over ionic additives is they do not increase the conductivity of the buffer. This characteristic allowed the use of these high concentrations, as well as the relatively high applied voltage of +20 kV, without the occurrence of Joule heating. A plot of the current versus additive concentration for all additives used is shown in Figure 2.2. The current is actually observed to decrease over the concentration range for all additives studied except for 3-amino-1-propane sulfonic acid. There is only a 7 μ A increase over a 750 mM concentration increase for this additive, which is still lower than expected for ionic additives. The increase may be a result of ionic impurities in the 3-amino-1-propane sulfonic acid additive. The electroosmotic mobility (μ_{eof}) was calculated from

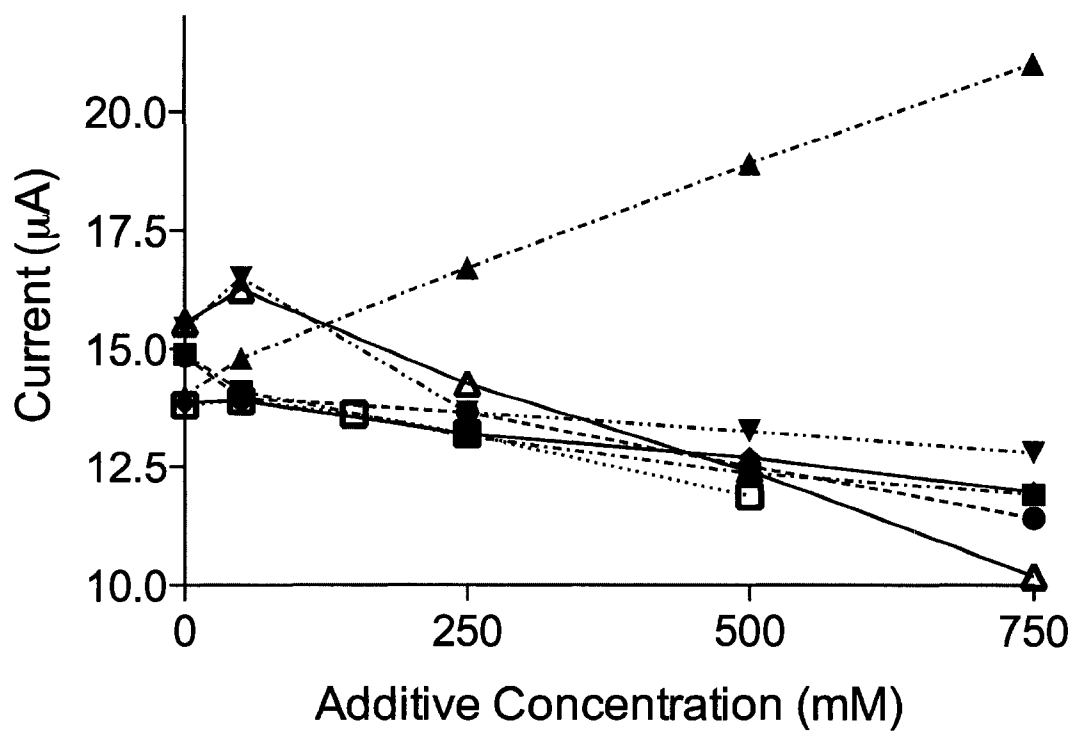


Figure 2.2: Current through the Capillary vs. Additive Concentration in 10 mM Phosphate Buffer (pH 7.2) for glycine (▼), 3-amino-1-propane sulfonic acid (▲), Z1-Methyl (■), 3-(cyclohexylamino)-1-propanesulfonic acid (CAPS) (△), 4-aminobutyric acid (◆), 6-aminocaproic acid (●), and 8-aminocaprylic acid (□)

Experimental conditions: applied voltage, +20 kV; capillary, 47 cm×50 µm I.D. (40 cm to detector); injection, 2 s hydrodynamic injection of 2 mM mesityl oxide; λ , 254 nm; and temperature, 25°C.

the migration time of the neutral marker (t_{eof}) using:

$$\mu_{eof} = \frac{L_t L_d}{V t_{eof}} \quad (2.1)$$

where L_t is the total length of the capillary, L_d is the length to the detector, and V is the voltage applied. To determine the effect of pH on EOF, the EOF was measured in 10 mM phosphate buffer at pH 7.2, and 11.4 and in 10 mM succinate buffer at pH 5.6 with 0 mM, 350 mM, and 750 mM Z1-Methyl added.

2.2.4 Relative Viscosity Measurements

Viscosities were measured relative to the 10 mM phosphate buffer without zwitterionic additive. Mesityl oxide was injected (2 s at 0.5 psi) and pushed to the detector using low pressure (0.5 psi).²² The relative viscosities (η_{rel}) were determined by ratioing mesityl oxide migration times in the buffer containing additives (t_{zwit}) vs. that in pure phosphate buffer (t_{buf}).

$$\eta_{rel} = \frac{t_{zwit}}{t_{buf}} \quad (2.2)$$

The average relative viscosities for each additive investigated are plotted in Figure 2.3 versus additive concentration. The effect is significant, especially at higher additive concentrations. Therefore, the relative viscosity (η_{rel}) of each buffer was measured as described above, and the observed EOF was corrected for viscosity:

$$\mu'_{eof} = \mu_{eof} \times \eta_{rel} \quad (2.3)$$

where μ_{eof} is the measured EOF mobility and μ'_{eof} is the EOF mobility corrected for viscosity. The observed viscosity increases are consistent with literature reports for glycine and 4-aminobutyric acid.²³

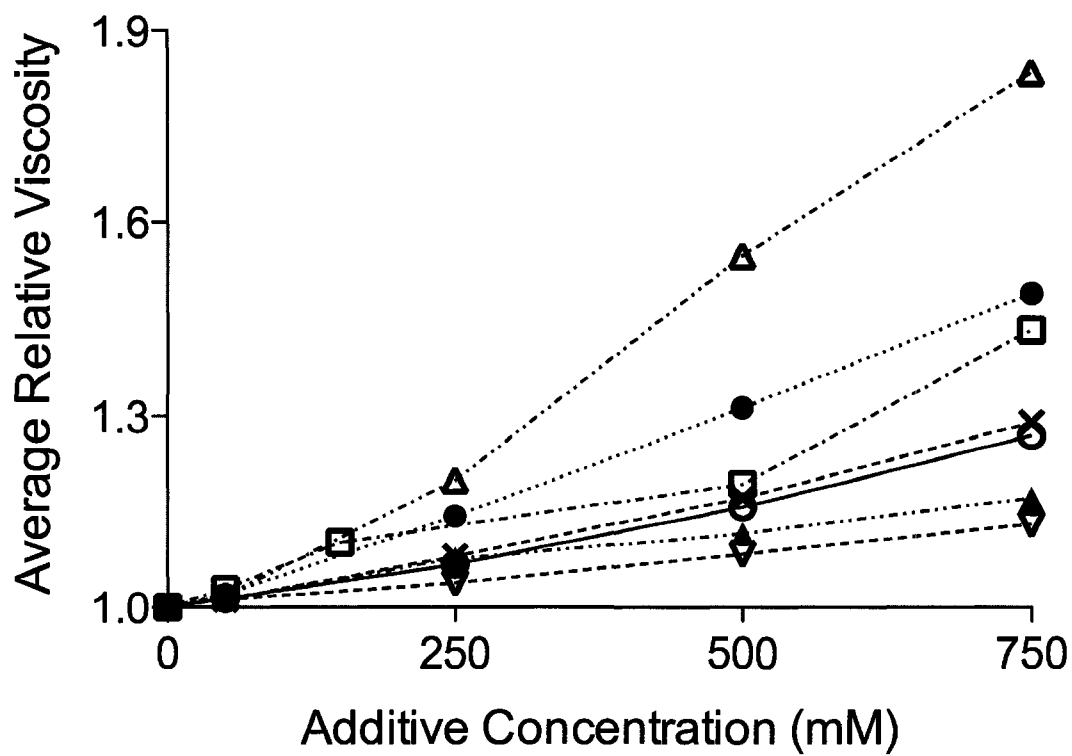


Figure 2.3: Average Relative Viscosity of 10 mM Phosphate Buffers (pH 7.2) Containing Zwitterionic Additive vs. Zwitterion Concentration for glycine (▽), 3-amino-1-propane sulfonic acid (▲), Z1-Methyl (○), (CAPS) (△), 4-aminobutyric acid (×), 6-aminocaproic acid (●), and 8-aminocaproic acid (□)

Experimental conditions: capillary, 47 cm×50 μm I.D. (40 cm to detector); injection, 2 s hydrodynamic injection of 2 mM mesityl oxide; λ, 254 nm; and temperature, 25°C.

2.3 Results

Preliminary studies performed by Mary Sheppard (nee Woodland) demonstrated separations of proteins were possible using zwitterionic additives (Figure 2.4). This is consistent with the work of Bushey and Jorgenson.¹² However the efficiency of the separation is much lower than the 1-2 million plates/m predicted by theory. This indicates zwitterionic additives are not effective for preventing protein adsorption (Section 1.4.2.1). Rather Woodland concluded that although zwitterions did not provide significant benefits with regard to protein adsorption, they did cause an increase in EOF and electrophoretic mobility.

As the primary focus of my research is prevention of protein adsorption, I did not study the use of zwitterionic additives for protein separations further. Rather I explored the use of hydrophilic self-assembled coatings, which is the subject of Chapters 3 and 4. However, as noted by Mary, the zwitterionic additives did have interesting effects on the EOF, which is the subject of this chapter.

2.3.1 Z1-Methyl

There have been reports of changes in EOF upon addition of Z1-Methyl to an electrolyte buffer. In the separation of metallochromic ligands, Macka et al. found the addition of 400 mM Z1-Methyl to the background electrolyte resulted in an increase in EOF from $+5.86 \times 10^{-4} \text{ cm}^2/\text{Vs}$ to $+6.91 \times 10^{-4} \text{ cm}^2/\text{Vs}$.²⁴ Buchberger and Winna observed an approximately 30% increase in EOF when 500 mM Z1-Methyl was added to the carrier electrolyte.¹⁸ Reichmuth et al. noted a 20% increase in flow for electrokinetic pumps when 1 M Z1-Methyl was added to the buffer.²⁵

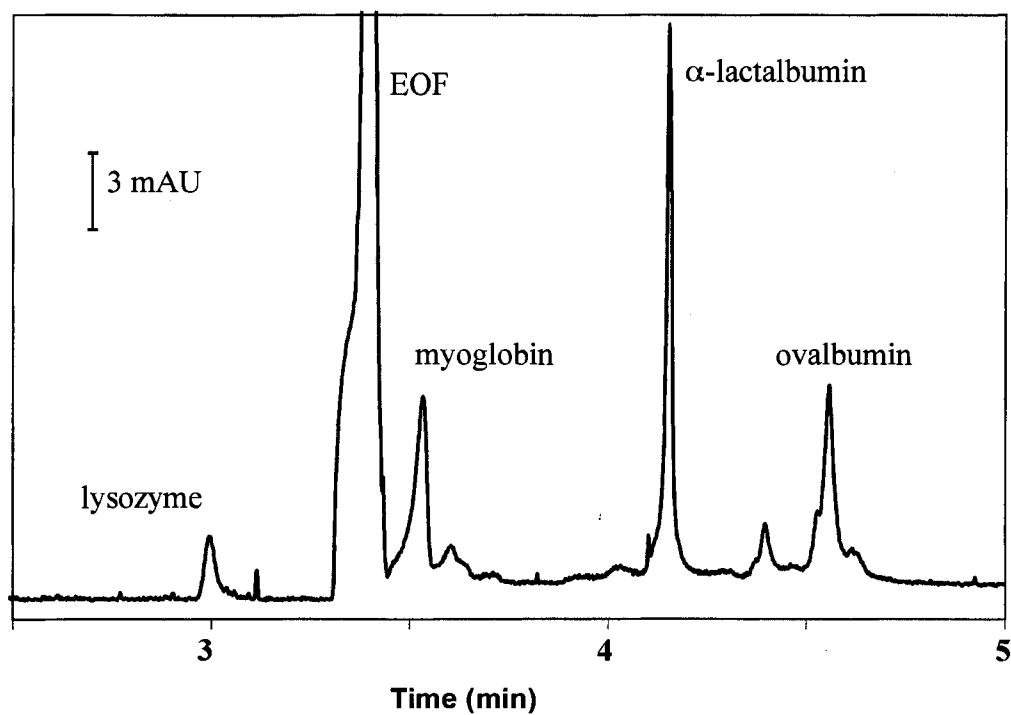


Figure 2.4 (Figure 3.8 from Mary Woodland's thesis): Protein Separation Using 100 mM Phosphate Buffer at pH 7.21 with 1.0 M Z1-Methyl

Experimental conditions: capillary, 27 cm \times 50 μ m I.D. (20 cm to detector); injection, 4 s hydrodynamic injection of 0.25 mg/mL lysozyme, and 0.15 mg/mL ovalbumin, myoglobin and α -lactalbumin; applied voltage, +7.5 kV; λ , 214 nm; and temperature, 25°C.

To investigate the effect of Z1-Methyl on EOF, the EOF was measured in 10 mM phosphate buffer at pH 7.2 as a function of Z1-Methyl concentration (0-750 mM). The EOF was then corrected for viscosity as described in Section 2.2.4. Figure 2.5 shows the viscosity corrected EOF (μ'_{eof}) vs. the concentration of Z1-Methyl (\blacktriangledown). The EOF increases linearly ($r^2=0.996$) with Z1-Methyl concentration (C), following the general behavior:

$$\mu'_{eof} = SC + \mu_{eof,buf} \quad (2.4)$$

where S is the EOF enhancement factor (i.e., the slope of the Z1-Methyl behaviour in Figure 2.5) and $\mu_{eof,buf}$ is the EOF mobility in the buffer containing no zwitterion. Similar EOF increases are noted in the literature, as discussed at the beginning of Section 2.3.1. Also, a similar linear dependence between streaming potential (i.e., the potential that develops across the capillary as a result of pressure induced flow) and concentration of zwitterions was observed by Reichmuth and Kirby.²⁶

The EOF enhancement caused by Z1-Methyl may be a function either of the interchange distance between the quaternary amine and sulfonate, or of the nature of the charged functionalities. Additional zwitterions were examined to determine which or if both of these factors cause the EOF enhancement.

2.3.2 Effect of Charge Separation

ω -Amino acids of the general structure $^+\text{NH}_3-(\text{CH}_2)_n-\text{COO}^-$ were investigated to determine the effect of charge separation, which is the distance between the positively and negatively charged functionalities in the zwitterion. As for Z1-Methyl, the EOF was monitored as a function of the concentration of zwitterion, and was corrected for

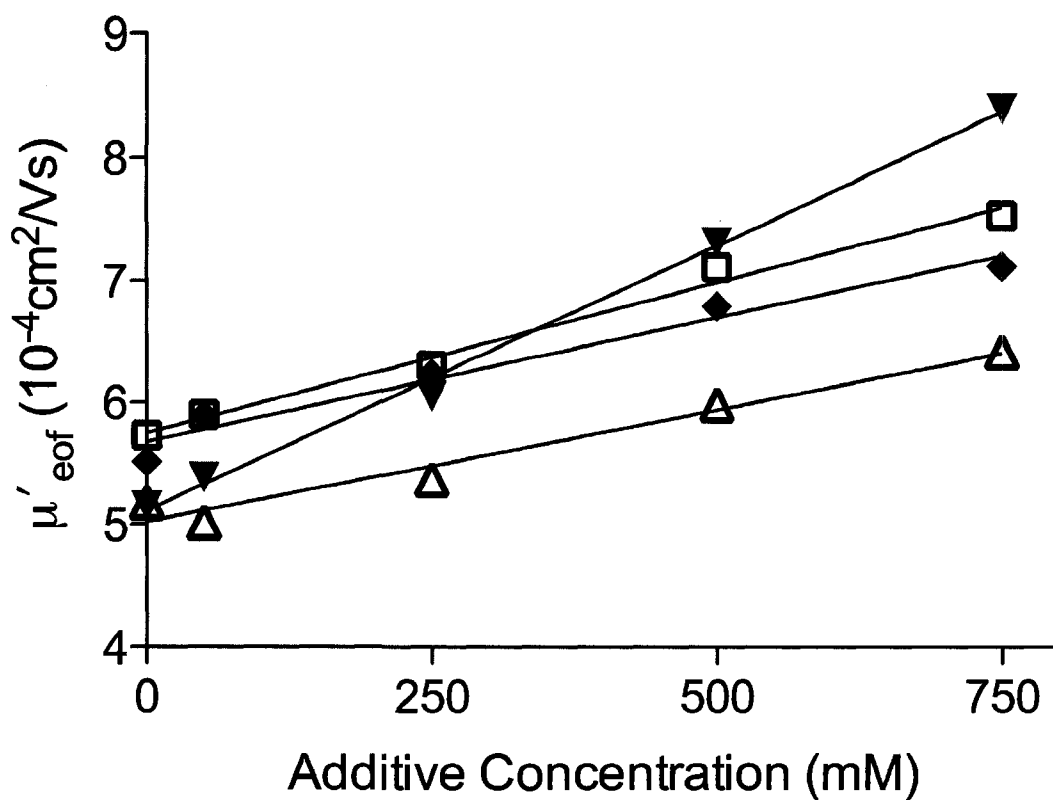


Figure 2.5: Viscosity Corrected EOF vs. Concentration of Z1-Methyl (▼), 3-amino-1-propane sulfonic acid (◆), 4-aminobutyric acid (△), and CAPS (□). The line is based on linear regression. Coefficients of the fit are given in Table 2.1.

Experimental conditions: applied voltage, +20 kV; capillary, 47 cm×50 μm I.D. (40 cm to detector); buffer, 10 mM phosphate (pH 7.2); injection, 2 s hydrodynamic injection of 2 mM mesityl oxide; λ , 254 nm; and temperature, 25°C.

for viscosity using equation 2.3. The solution pH (7.2) is near the isoelectric point of these aminocarboxylic acids, and at least 1.5 pH units from their pK_a . Thus, 10 mM phosphate buffer was sufficient to maintain the solution pH.

Figure 2.6 shows the viscosity corrected EOF (μ'_{eof}) vs. the zwitterion concentration for the aminocarboxylic acid additives (n=1-7). The EOF increases linearly with additive concentration (C) for all of the zwitterions, following the general behavior described by equation 2.4. The correlation coefficients (r^2) for all of the aminocarboxylic acids are greater than 0.96 (Table 2.1), with the residuals being randomly distributed. The intercepts given in Table 2.1 represent the EOF mobility without any zwitterions in solution (*i.e.*, $\mu_{eof,buf}$ in eq. 2.4). Some variation in the EOF in the absence of zwitterion was observed over the 2 weeks taken to collect this data.

As can be seen in Figure 2.6 and Table 2.1, the enhancement factor (S) increases with the number of methylenes (n) in the aminocarboxylic acid structure from glycine (n=1) to 8-aminocaprylic acid (n=7). Indeed the EOF increases 69% upon addition of 500 mM 8-aminocaprylic acid. Plotting the enhancement factors (S) vs. the number of methylenes in the interchange region results in a rectilinear ($R^2=0.968$) relationship (Figure 2.7). Reichmuth and Kirby measured the enhancement of streaming potential for solutions of a homologous series of cyclohexylamino alkyl sulfonates (*i.e.*, CHES, CAPS, CABS (4-(cyclohexylamino)-1-butanefulfonic acid)).²⁶ Plotting their data in a comparable fashion to Figure 2.7 reveals a similar rectilinear behavior, with possible positive deviation (Figure 2.8). Further, using dielectric measurements Galin et al.²⁷ noted a linear increase in charge separation with increasing chain length for a series of ammonioalkanesulfonates. Chevalier et al.²⁸ observed a linear increase in charge

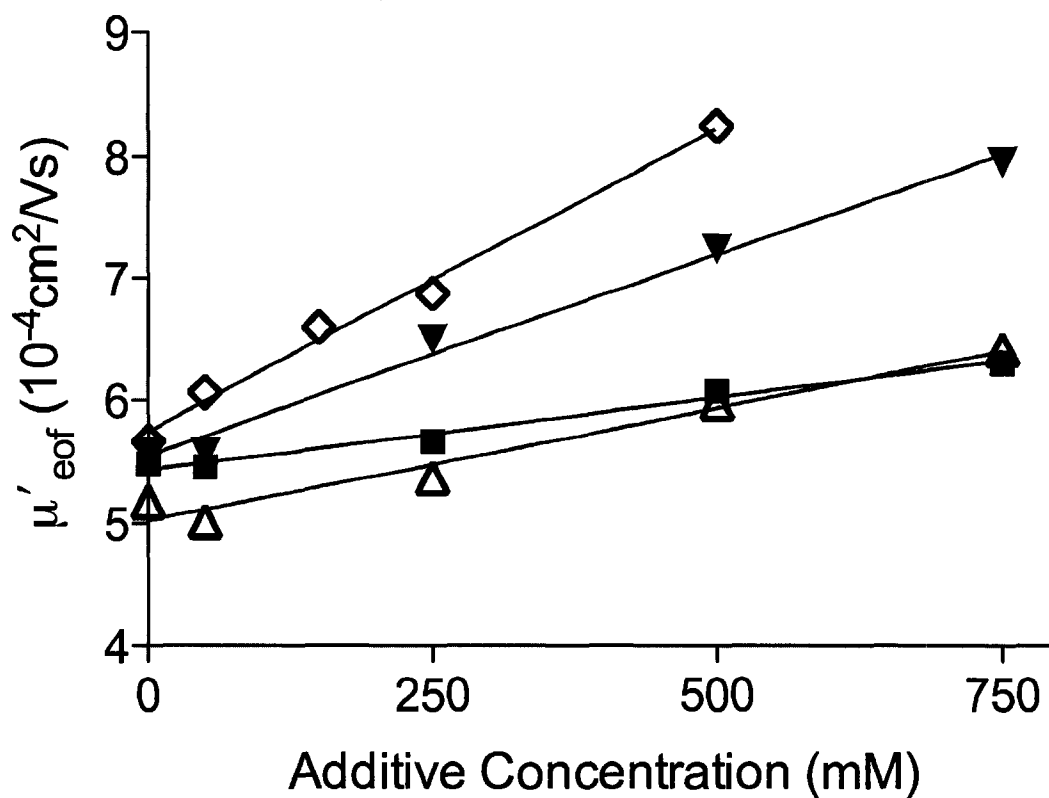


Figure 2.6: Viscosity Corrected EOF vs. Concentration of glycine(■), 4-aminobutyric acid (△), 6-aminocaproic acid (▼), and 8-aminocaprylic acid (◇)

Experimental conditions: applied voltage, +20 kV; capillary, 47 cm×50 μm I.D. (40 cm to detector); buffer, 10 mM phosphate (pH 7.2); injection, 2 s hydrodynamic injection of 2 mM mesityl oxide; λ , 254 nm, and temperature, 25°C.

Table 2.1: EOF Enhancement Factor, $\mu'_{eof, buf}$ in Pure Phosphate Buffer, Correlation Coefficient, and Dielectric Increment for Zwitterionic Additives from μ'_{eof} vs. Additive Concentration Plots^a

Zwitterion	n ^b	S (10 ⁻⁴ cm ² /(MV ^s)) ^c	$\mu'_{eof, buf}$ (10 ⁻⁴ cm ² /Vs) ^c	r ²	Literature δ ($\Delta\epsilon/\Delta C$)
Z1-Methyl (⁺ N(CH ₃) ₃ CH ₂ CH ₂ CH ₂ SO ₃ ⁻)	3	4.34 ± 0.15	5.11 ± 0.06	0.996	-
Glycine (⁺ NH ₃ (CH ₂) ₁ COO ⁻)	1	1.17 ± 0.09	5.44 ± 0.04	0.981	24 ²⁹
4-aminobutyric acid	3	1.83 ± 0.20	5.02 ± 0.08	0.965	53 ²⁹
6-aminocaproic acid	5	3.29 ± 0.18	5.55 ± 0.08	0.991	82 ²⁹
8-aminocaprylic acid	7	4.97 ± 0.27	5.75 ± 0.07	0.991	109 ²⁹
3-amino-1-propane sulfonic acid	3	2.03 ± 0.22	5.68 ± 0.09	0.966	56.8 ²⁹
CAPS	3	2.46 ± 0.15	5.75 ± 0.06	0.990	-
Triethylammonium propane sulfonic acid	3	-	-	-	58.6 ²⁷

^a Experimental conditions as in Figure 2.5.

^b Number of methylene groups between positively and negatively charged groups.

^c Uncertainties are the standard deviation of the slope and intercept.

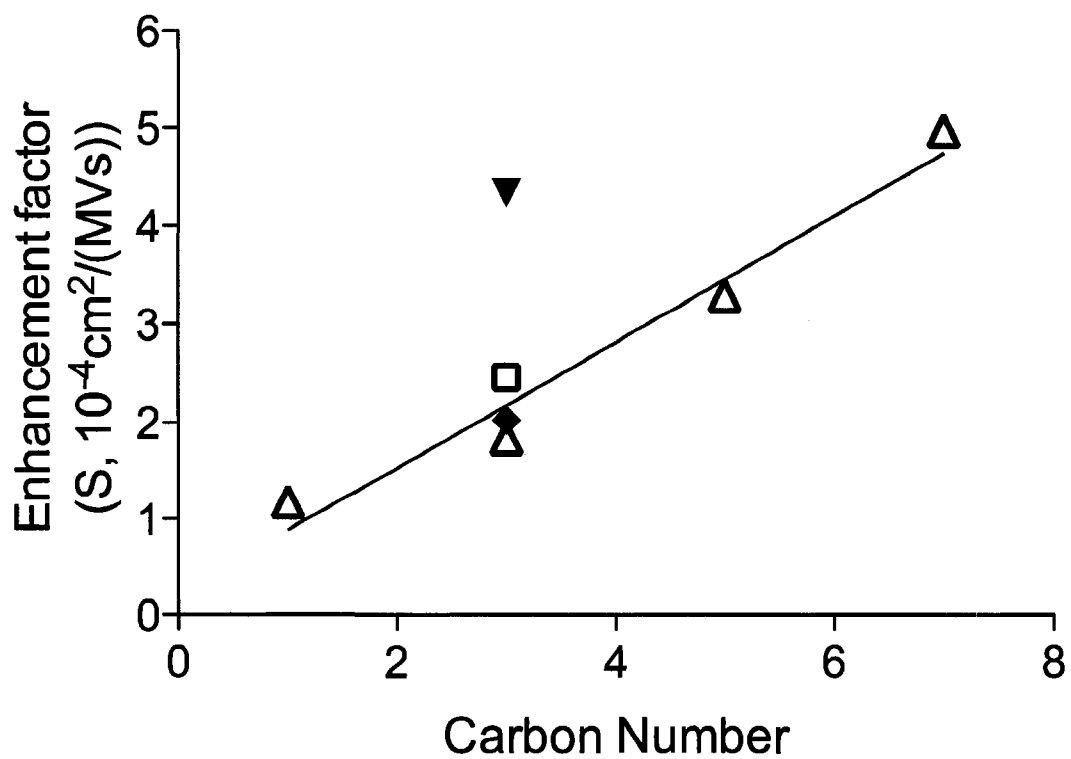


Figure 2.7: Slope of the Viscosity Corrected EOF Plots (Figure 2.5 and 2.6) vs. Carbon Number for the Aminocarboxylic Acid Additives (Δ), Z1-Methyl (▼), 3-amino-1-propane sulfonic acid (◆), and CAPS (□)

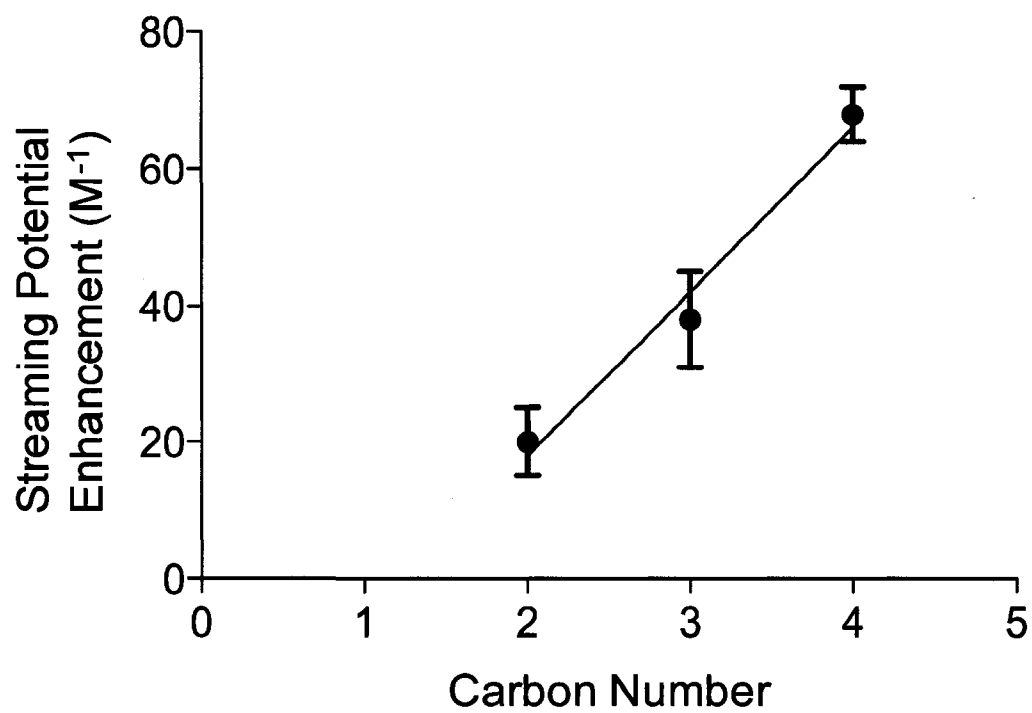


Figure 2.8: Plot of Streaming Potential Enhancement vs. Carbon Number for a Homologous Series of Cyclohexylamino alkyl sulfonates (CHES, CAPS, CABS) (plotted from data in Table 3 of ref²⁶)

separation with increasing chain length for low values of n (2-7), but at higher values a deviation from linearity was observed ($n=10$). For the interchange distance examined in this work, a linear relationship between charge separation and chain length was observed. This will be examined further in Section 2.4.

2.3.3 Effect of Functional Group

As can be seen in Figure 2.6 and Table 2.1, Z1-Methyl has an EOF enhancement effect (S) approximately double that of an aminocarboxylic additive of the equivalent chain length (i.e., 4-aminobutyric acid). This suggests EOF enhancement is not solely a function of charge separation. To further explore the effect of the functional group, 3-amino-1-propane sulfonic acid and 3-(cyclohexylamino)-1-propane sulfonic acid (CAPS) were studied. Like Z1-Methyl, these zwitterions have a propyl linkage ($n=3$) and contain sulfonate groups. However, Z1-Methyl has a quaternary amino group while 3-amino-1-propane sulfonic acid and 4-aminobutyric acid contain a primary amino group, and CAPS contains a secondary amino group. The observed EOF behaviour was studied as above, and is plotted in Figure 2.5. 3-Amino-1-propane sulfonic acid and CAPS show the same linear dependence between zwitterion concentration and EOF as did Z1-Methyl and the aminocarboxylic acids (Figures 2.5 and 2.6, respectively). The EOF enhancement due to 3-amino-1-propane sulfonic acid is statistically equivalent (95% confidence interval) to that of 4-aminobutyric acid. This suggests the structure of the anionic functionality does not influence the EOF enhancement.

The structure of the amine functionality, however, does have a strong influence on the EOF enhancement, as shown in Figure 2.9. CAPS, possessing a secondary amine, has an enhancement greater than those of 4-aminobutyric acid and 3-amino-1-propane

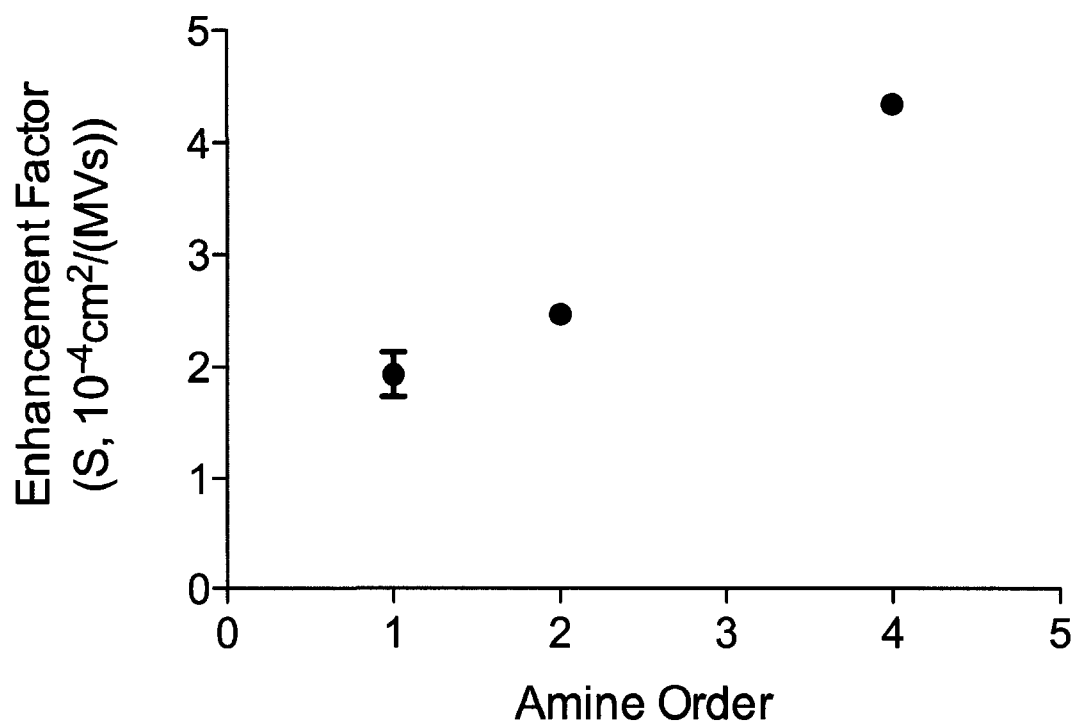


Figure 2.9: Plot of Enhancement Factor vs. Amine Order for Additives Containing Primary (average of 4-Aminobutyric acid and 3-Aminopropane sulfonic acid), Secondary (CAPS), and Quaternary (Z1-methyl) Amino Groups

sulfonic acid at the 95% confidence limit. While Z1-Methyl, with a quaternary amine functionality, shows about double the EOF enhancement of the primary amine zwitterions and substantially more enhancement than CAPS (Figure 2.9). Reichmuth and Kirby observed streaming potentials were enhanced more by Z1-Methyl than CAPS, consistent with the results in Table 2.1.²⁶

2.3.4 pH and Buffer Cation

The results above have focused on the influence of the nature of the zwitterions on EOF enhancement. Studies were also performed to determine whether buffer conditions affected the EOF enhancement caused by the zwitterionic additives. The effect of pH on the EOF was studied using Z1-Methyl, as the other additives studied above are zwitterionic only near pH 7. The enhancement factors (S) for each of the buffers studied are given in Table 2.2. The S values are statistically equivalent at the 95% confidence interval. Therefore, no systematic trend in μ'_{eof} increase with pH was observed over the range of pH and buffers studied.

Table 2.2: Effect of pH on EOF Enhancement^a

Buffer	μ'_{eof} (10^{-4} cm ² /Vs) with no zwitterion	S (10^{-4} cm ² /(MV s))
10 mM succinate and Z1-Methyl pH 5.6	5.44 ± 0.01	4.00 ± 0.22
10 mM sodium phosphate and Z1-Methyl pH 7.2	5.70 ± 0.03	4.13 ± 0.16
10 mM sodium phosphate and Z1-Methyl pH 11.4	6.78 ± 0.01	3.96 ± 0.30

^a Applied voltage, +20 kV; capillary, 47 cm×50 μm I.D. (40 cm to detector); injection, 2 s hydrodynamic injection of 25 mM mesityl oxide; λ , 254 nm; temperature, 25°C. Measurements made at 0, 350 and 750 mM Z1-Methyl.

The effect of buffer cation on the EOF enhancement was studied using 10 mM phosphate buffer (pH 7.2) prepared with lithium, sodium and potassium counter-ions (Table 2.3). In the absence of Z1-Methyl, the EOF for K^+ is statistically lower than that observed for Li^+ and Na^+ . This is consistent with the results of Salomen et al.³⁰ and Mammen et al.³¹ who found that electroosmotic velocity increases with the hydrated radius of the cation. The enhancement factors for all buffer cations are statistically equivalent at the 95% confidence interval, indicating that there is no systematic trend between buffer cation and μ'_{eof} . It can be concluded from these results that the buffer has no effect on the EOF enhancement.

Table 2.3: Effect of Cation on the EOF Increase with Z1-Methyl^a

Buffer	$\mu'_{eof, buf}$ ($10^{-4} \text{ cm}^2/\text{Vs}$) with no zwitterion	S ($10^{-4} \text{ cm}^2/(\text{MV s})$)
10 mM lithium phosphate pH 7.21	6.04 ± 0.02	4.24 ± 0.12
10 mM sodium phosphate pH 7.21	5.70 ± 0.03	4.13 ± 0.16
10 mM potassium phosphate pH 7.21	5.61 ± 0.01	4.19 ± 0.22

^a Applied voltage, +20 kV; capillary, 47 cm×50 μm I.D. (40 cm to detector); injection, 2 s hydrodynamic injection of 25 mM mesityl oxide; λ , 254 nm; temperature, 25°C. Measurements made at 0, 350 and 750 mM zwitterion.

2.4 Discussion

EOF is described by the von Smoluchowski equation:

$$\mu_{eof} = -\frac{\zeta \epsilon}{\eta} \quad (1.4)$$

Thus, the EOF mobility may be a function of the zeta potential (ζ), the dielectric constant (ϵ) and viscosity (η) of the solution.

The data presented in Sections 2.3.1-2.3.3 indicate that the EOF is enhanced by the addition of zwitterions to the running buffer. Equation 1.4 suggests that an enhanced EOF could be due to a decrease in viscosity. However, this explanation is not feasible since all of the zwitterions increase viscosity (Figure 2.3) and the EOF has been corrected for viscosity changes (eq. 2.3). Thus, the enhancement in EOF observed above must be due to either a change in the dielectric constant of the solution or the zeta potential, based on equation 1.4. Indeed, both of these have been cited in the literature as the cause of the EOF enhancement. Buchberger et al. suggested the increase in electroosmotic mobility might be due to a change in the zeta potential.¹⁸ Reichmuth and Kirby stated the large positive dielectric increments of the zwitterions studied are responsible for increased efficiency of electrokinetic pumping.²⁵ This possible mechanism is explored in the next section.

2.4.1 Dielectric Constant

The von Smoluchowski equation (eq. 1.4) indicates a direct relationship between the dielectric constant and the EOF. Changes in EOF upon addition of organic solvents such as methanol to CE buffers have been rationalized based on changes in the dielectric constant and viscosity.^{32,33} Organic solvents typically have significantly lower dielectric constants than water. Thus, these studies have observed only lowered EOF. Most non-zwitterions lower the dielectric constant of water.³⁴ However, zwitterion solutions have dielectric constants greater than that of pure water.^{26,27,29,35-37}

The addition of additives to an aqueous solution alters the dielectric constant of a solution through the relationship:

$$\varepsilon = \varepsilon_w + \delta C \quad (2.6)$$

where ϵ_w is the dielectric constant of pure water at 25°C (78.54),³⁵ δ is the dielectric increment of the additive and C is the additive concentration. Organic solvents such as acetonitrile³⁶ and dissociated electrolytes such as NaCl³⁷ have a negative dielectric increment. Thus aqueous solutions of acetonitrile and NaCl have a lower dielectric constant than that of pure water. In contrast, zwitterions display strong positive dielectric increments.³⁶ Table 2.1 shows literature dielectric increment values for the zwitterions studied.

Based on equation 2.6, the dielectric constant of the solution increases linearly with the concentration of the zwitterionic additive. Figures 2.5 and 2.6 show the EOF increases linearly with the concentration of each of the zwitterions. This EOF increase is consistent with predictions by the von Smoluchowski equation for solutions possessing higher dielectric constants.

Theory predicts the dielectric increment of zwitterions correlates with the square of the length of the dipole.²⁹ A number of studies have shown that intramolecular pairing does not occur with zwitterionic additives.^{27,38,39} In other words, the two charged end groups do not wrap around to form an ion pair with themselves. Rather the zwitterions adopt an extended conformation in aqueous solution, such that the intercharge distance increases proportionally to the number of methylene groups in the linkage.²⁹ This is true for the shorter chain zwitterions, whereas the longer chain zwitterions display some slight coiling. Galin et al. have shown the dipole moment of quaternary ammonioalkylsulfonates increases with the number of methylene groups in the linkage.²⁷ Thus, as can be seen in Figure 2.10, the dielectric increment increases linearly with the number of methylene groups in the linkage.^{29,36,40}

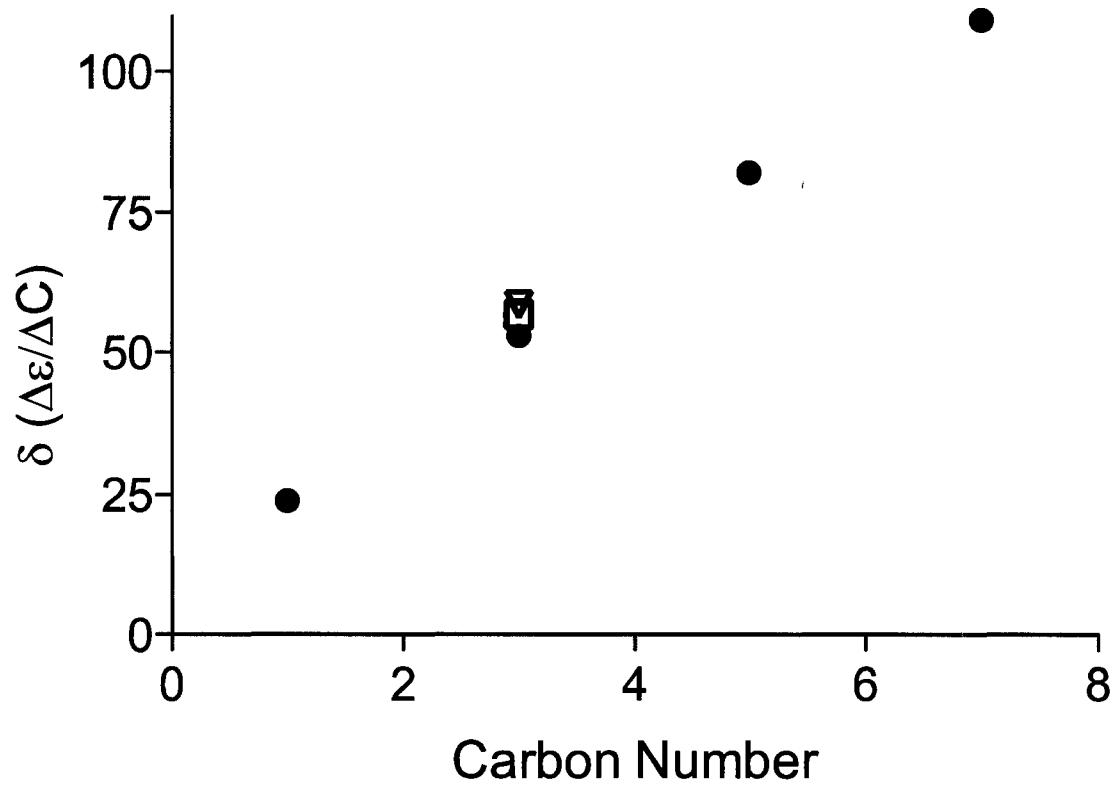


Figure 2.10: Dielectric Increment^{27,29} of the Zwitterionic Additives Aminocarboxylic Acids (●), 3-Aminopropane sulfonic acid (□), Triethylammoniumpropane sulfonate (▽), vs. Carbon Number in the Additive Chain

Figure 2.6 shows a linear increase in EOF enhancement with the number of methylenes in the interchange region of the aminocarboxylic acids. Further, the enhancement factors (S) for the aminocarboxylic acid series parallel the dielectric increments (Table 2.1). A plot of the EOF enhancement vs. the literature dielectric increments yields a rectilinear plot ($r^2=0.963$) with a slope of $0.0451 \pm (0.006)$ MVs/cm² and an intercept of $-0.207 \pm (0.47)$ (Figure 2.11). Therefore, the increase in EOF enhancement along the ω -amino acid series (Figure 2.6) is due to an increase in the dielectric constant of the solution. Thus the enhancement observed in the EOF upon addition of zwitterions is at least in part due to the change in the dielectric constant of the solution.

A plot of the observed viscosity corrected EOF mobility ($\mu'_{eof, obs}$) vs. the viscosity corrected EOF mobility predicted from dielectric increment measurements ($\mu'_{eof, pred}$) is shown in Figure 2.12. The predicted values were calculated from the following equation:

$$\mu'_{eof, pred} = \mu'_{eof, buf} * \left(\frac{\epsilon_w + \delta C}{\epsilon_w} \right) \quad (2.7)$$

The slope of the plot in Figure 2.12 is 0.895 ± 0.064 with a correlation coefficient of $r^2=0.990$. This data also suggests the change in dielectric constant of the solutions containing zwitterionic additives is contributing to the observed changes in EOF mobility.

However, Nandi et al. argue the dipole moments of zwitterions such as glycine are too low to account for the substantial increase in the dielectric constant of amino acid, peptide and protein solutions.⁴⁰ Further, Fersht and Sternberg conclude that no simple

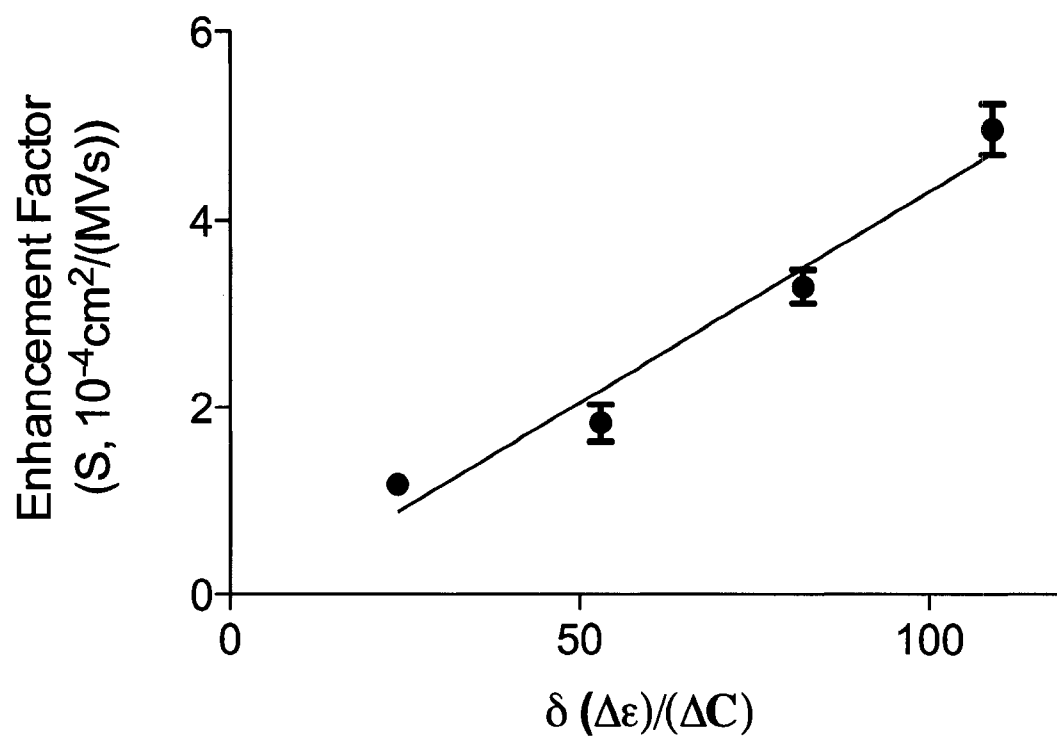


Figure 2.11: Enhancement Factors of the Aminocarboxylic Acid Additive Series vs. Literature Dielectric Increments²⁹

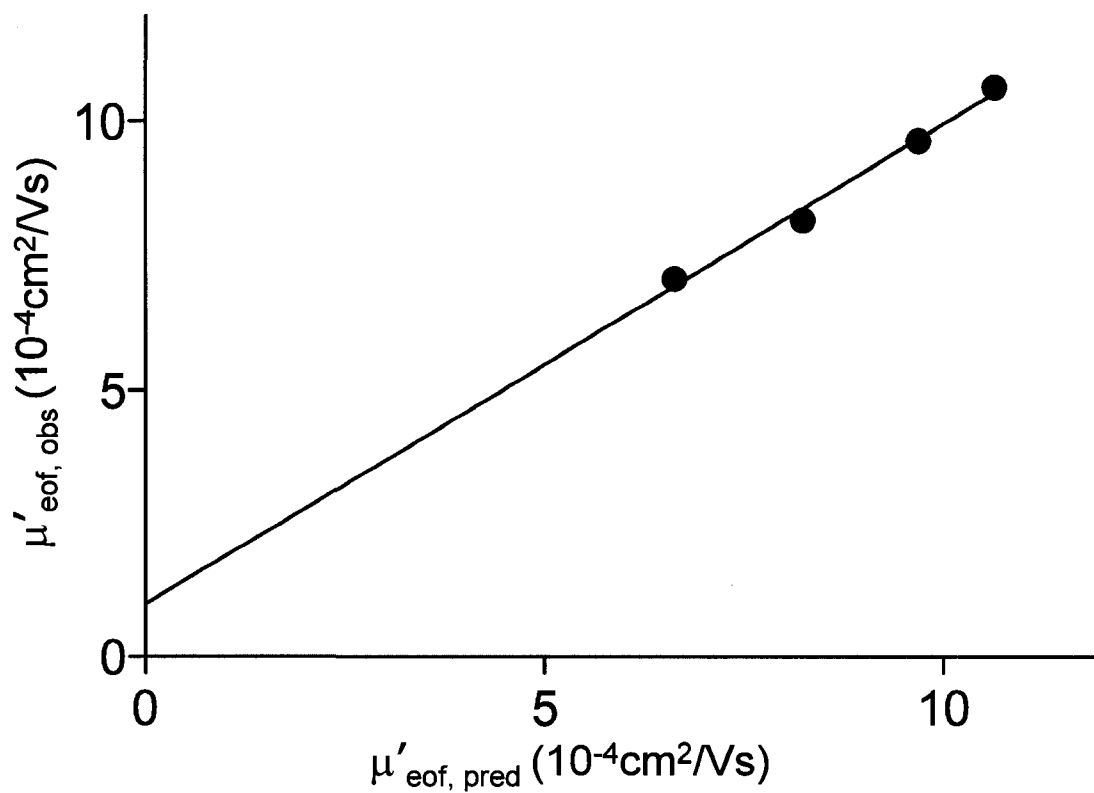


Figure 2.12: Observed Viscosity Corrected EOF Mobility vs. Viscosity Corrected EOF Mobility Predicted from Literature Dielectric Increment Measurements²⁹ for Aminocarboxylic Acid Additives, each at a Concentration of 400 mM

relationship exists between the effective dielectric constant and the intercharge distance.⁴¹

To explore whether factors other than intercharge distance are operative, the enhancements observed for propyl linkage additives with differing endgroups (i.e., Z1-Methyl, 3-amino-1-propane sulfonic acid, 4-aminobutyric acid, CAPS) were studied. Surprisingly, Table 2.1 shows that these additives do cause differing amounts of EOF enhancement, whereas the dielectric increments are about constant. This suggests that the structure of the charged functionalities influence the EOF, in addition to the direct effect of the additive on the dielectric constant. As mentioned in Section 2.3.3, the EOF enhancements due to 3-amino-1-propane sulfonic acid and 4-aminobutyric acid (Table 2.1) are statistically equivalent, indicating that the anionic group has little effect on the EOF. However, the nature of the amino group appears to have a strong effect on the EOF enhancement. Indeed, Z1-Methyl has an enhancement factor similar to an additive with double its chain length. Although no literature value for the dielectric increment of Z1-Methyl could be found, the dielectric increment of a propyl linkage additive containing a triethylamino group is given in Table 2.1. The dielectric increment of Z1-Methyl is estimated to be intermediate between this value and those given for 3-amino-1-propane sulfonate and 4-aminobutyric acid. All of these values are considerably lower than that of 6-aminocaproic acid (Table 2.1). Thus the dielectric constant of the solution is not the only factor contributing to the increased EOF with addition of these zwitterions to the running buffer. There appears to be an additional effect related to either the order or the hydrophobicity of the amine functionality. However, at this point any explanation for this additional effect would be speculative.

2.4.2 Zeta Potential

Some researchers have suggested the EOF enhancement observed above could be due to the zwitterion competing with buffer cations for association with the silanols on the capillary wall.¹⁶⁻¹⁸ If this were true, it is likely that Z1-Methyl would replace the cations in the double layer that are responsible for the EOF. As discussed in Section 1.2.2, the zeta potential is defined as the potential at the plane of shear located between the Stern layer (closest to the capillary wall) and the diffuse layer (furthest from the capillary wall). If the zwitterions, which have no mobility, did displace a cation in the double layer, it would result in a decrease in the zeta potential. Recalling equation 1.4, a decrease in the zeta potential should result in a decrease in EOF. Therefore, one would expect the displacement of a cation in the double layer by a zwitterion possessing zero mobility would result in a decrease in EOF. However, as shown in Figure 2.5, the EOF increases upon addition of Z1-Methyl.

A change in the pH of the running buffer would also affect the negative charge density on the silica surface. If the zwitterions ion exchanged with the negative sites on silica, a change in this ion exchange behavior would be expected upon changing pH. However, the results in Table 2.2 show no difference in enhancement as the pH is varied.

Further, if there were competition for the silanols on the capillary wall, the ion exchange capability of the cation would have an effect on the resultant change in EOF. One would have expected a larger increase in EOF when the buffer cation is lithium (a weak exchanging cation) compared to potassium (a stronger ion exchanging cation)⁴² if a competition type mechanism was at work. Instead the increase in EOF remains constant as the cation is varied (Table 2.3).

Even further, given the negligible conductivity of a zwitterion solution, use of such an eluent would be ideal for ion chromatography. Nonetheless, extensive searches of the ion chromatography literature reveal no reports of zwitterions such as used herein being used as an eluent. Thus it must be concluded that zwitterions such as Z1-Methyl do not compete with cations such as Li^+ or Na^+ for cation exchange sites. Therefore zwitterions do not affect the zeta potential.

2.5 Concluding Remarks

Addition of zwitterionic additives to the running buffers causes increases in the EOF. The increases in EOF are a function of both length of the linkage and the end group functionalities. Increases in the dielectric constant of the zwitterion solutions are a factor behind the EOF enhancements. The amino functionality also influences the EOF enhancement, but more study is needed before any real conclusions can be drawn. However as zwitterionic additives do not effectively prevent protein adsorption, such studies were beyond the scope of this thesis.

2.6 References

- (1) Muzikar, J.; van de Goor, T.; Gas, B.; Kenndler, E., *J. Chromatogr. A* **2002**, *960*, 199-208.
- (2) Corradini, D.; Spreccacenero, L., *Chromatographia* **2003**, *58*, 587-596.
- (3) McCormick, R. M., *Anal. Chem.* **1988**, *60*, 2322-2328.
- (4) Baryla, N. E.; Lucy, C. A., *J. Chromatogr. A* **2002**, *956*, 271-277.
- (5) Albarghouthi, M. N.; Stein, T. M.; Barron, A. E., *Electrophoresis* **2003**, *24*, 1166-1175.
- (6) Chiari, M.; Cretich, M.; Stastna, M.; Radko, S. P.; Chrambach, A., *Electrophoresis* **2001**, *22*, 656-659.
- (7) Gonzalez, N.; Elvira, C.; San Roman, J.; Cifuentes, A., *J. Chromatogr. A* **2003**, *1012*, 95-101.
- (8) Jiang, T. F.; Gu, Y. L.; Liang, B.; Li, J. B.; Shi, Y. P.; Ou, Q. Y., *Anal. Chim. Acta* **2003**, *479*, 249-254.
- (9) Lauer, H. H.; McManigill, D., *Anal. Chem.* **1986**, *58*, 166-170.
- (10) Corradini, D., *J. Chromatogr. B* **1997**, *699*, 221-256.
- (11) Green, J. S.; Jorgenson, J. W., *J. Chromatogr.* **1989**, *478*, 63-70.
- (12) Bushey, M. M.; Jorgenson, J. W., *J. Chromatogr.* **1989**, *480*, 301-310.
- (13) Chen, F. A.; Kelly, L.; Palmieri, R.; Biehler, R.; Schwartz, H., *J. Liq. Chromatogr.* **1992**, *15*, 1143-1161.
- (14) Liu, Y. J.; Foote, R. S.; Culbertson, C. T.; Jacobson, S. C.; Ramsey, R. S.; Ramsey, J. M., *J. Microcolumn Sep.* **2000**, *12*, 407-411.
- (15) Fang, X. H.; Zhu, T.; Sun, V. H., *J. High Res. Chromatog.* **1994**, *17*, 749-752.
- (16) Guzman, N. A.; Moschera, J.; Iqbal, K.; Malick, A. W., *J. Chromatogr.* **1992**, *608*, 197-204.
- (17) Hines, H. B.; Brueggemann, E. E., *J. Chromatogr. A* **1994**, *670*, 199-208.
- (18) Buchberger, W.; Winna, K., *Mikrochim. Acta* **1996**, *122*, 45-52.

- (19) Mandrup, G., *J. Chromatogr.* **1992**, *604*, 267-281.
- (20) Miura, T.; Funato, T.; Yabuki, S.; Sasaki, T.; Kaku, M., *Clin. Chim. Acta* **2000**, *299*, 87-99.
- (21) Gong, B. Y.; Ho, J. W., *Electrophoresis* **1997**, *18*, 732-735.
- (22) Peng, X. J.; Bowser, M. T.; BritzMcKibbin, P.; Bebault, G. M.; Morris, J. R.; Chen, D. D. Y., *Electrophoresis* **1997**, *18*, 706-716.
- (23) Islam, M. N.; Wadi, R. K., *Phys. Chem. Liq.* **2003**, *41*, 533-544.
- (24) Macka, M.; Haddad, P. R.; Buchberger, W., *J. Chromatogr. A* **1995**, *706*, 493-501.
- (25) Reichmuth, D. S.; Chirica, G. S.; Kirby, B. J., *Sensor. Actuat. B - Chem.* **2003**, *92*, 37-43.
- (26) Reichmuth, D. S.; Kirby, B. J., *J. Chromatogr. A* **2003**, *1013*, 93-101.
- (27) Galin, M.; Chapoton, A.; Galin, J. C., *J. Chem. Soc. Perk. T.2* **1993**, 545-553.
- (28) Chevalier, Y.; Storet, Y.; Pourchet, S.; Leperchec, P., *Langmuir* **1991**, *7*, 848-853.
- (29) Kirchnerova, J.; Farrell, P. G.; Edward, J. T., *J. Phys. Chem.* **1976**, *80*, 1974-1980.
- (30) Salomon, K.; Burgi, D. S.; Helmer, J. C., *J. Chromatogr.* **1991**, *559*, 69-80.
- (31) Mammen, M.; Carbeck, J. D.; Simanek, E. E.; Whitesides, G. M., *J. Am. Chem. Soc.* **1997**, *119*, 3469-3476.
- (32) Schwer, C.; Kenndler, E., *Anal. Chem.* **1991**, *63*, 1801-1807.
- (33) Wright, P. B.; Lister, A. S.; Dorsey, J. G., *Anal. Chem.* **1997**, *69*, 3251-3259.
- (34) Wyman, J.; McMeekin, T. L., *J. Am. Chem. Soc.* **1933**, *55*, 910-916.
- (35) Wyman, J. J., *J. Am. Chem. Soc.* **1934**, *56*, 536-544.
- (36) Wyman, J. J., *Chem. Rev.* **1936**, *19*, 213-239.
- (37) Lessard, J. G.; Fragata, M., *J. Phys. Chem.* **1986**, *90*, 811-817.
- (38) Weers, J. G.; Rathman, J. F.; Axe, F. U.; Crichlow, C. A.; Foland, L. D.; Scheuing, D. R.; Wiersema, R. J.; Zielske, A. G., *Langmuir* **1991**, *7*, 854-867.

- (39) Edward, J. T.; Farrell, P. G.; Job, J. L., *J. Am. Chem. Soc.* **1974**, *96*, 902-906.
- (40) Nandi, N.; Bhattacharyya, K.; Bagchi, B., *Chem. Rev.* **2000**, *100*, 2013-2045.
- (41) Fersht, A. R.; Sternberg, M. J. E., *Protein Eng.* **1989**, *2*, 527-530.
- (42) Haddad, P. R.; Jackson, P. E., *Ion Chromatography: Principles and Applications*, Elsevier, Amsterdam, 1990.

Chapter Three: Highly Efficient Protein Separations in Capillary Electrophoresis Using a Supported Bilayer/Diblock Copolymer Coating*

3.1 Introduction

Capillary electrophoresis (CE) is a powerful tool for separating a range of analytes from small ions^{1,2} to large biomolecules.^{3,4} However, the separation of proteins by CE experiences some obstacles, including lack of EOF control, coating stability, and protein adsorption onto the capillary walls. Irreproducible EOF can adversely affect resolution and reproducibility.^{5,6} Alternately, if the coating generates a high EOF, the proteins may migrate off the capillary before resolution is achieved. Suppression of the EOF enables greater protein resolution to be attained.⁷

Adsorption of proteins onto the capillary wall can lead to poor reproducibility,⁸ band-broadening,⁹ and low sample recovery.¹⁰ As discussed in Chapter 1, coating the capillary wall is the most frequently used method for minimizing protein adsorption. Coatings reduce the interactions between proteins and the capillary wall. They can be covalently bonded polymers,¹¹⁻¹³ physically adsorbed polymers,¹⁴⁻¹⁶ or adsorbed surfactants (dynamic coatings),¹⁷⁻¹⁹ the latter two being the focus of the review in Chapter 1.²⁰ Dynamic coatings are very attractive due to their versatility, ease of use, and cost effectiveness. It is known that double-chain cationic surfactants form a bilayer structure on the capillary wall,²¹ which results in excellent coating stability.²² A capillary coated with a double-chain cationic surfactant also enables very efficient separations of basic proteins.²² However, the strong reversed EOF ($-5.8 \pm (0.2) \times 10^{-4} \text{ cm}^2/\text{Vs}$)²² overwhelms

* A version of this chapter has been published. MacDonald, A.M. and Lucy, C.A., *J Chromatogr. A*, **2006**, 1130, 265-271.

the mobility of most proteins, limiting resolution. A reduced EOF enables the mobility of the proteins to come to the forefront so better resolution can be attained. Further, acidic proteins will adsorb to cationic coatings such as a didodecyldimethylammonium bromide (DDAB) bilayer. A bare capillary is another option for separating acidic proteins and peptides, however, this results in long analysis times.²³ To overcome these problems, zwitterionic surfactants,^{19,24-26} phospholipids,^{7,27} catanionic (i.e., mixture of cationic and anionic surfactants) mixtures,^{28,29} and successive multiple ionic-polymer layer (SMIL) coatings^{30,31} have been used for acidic and basic protein separations as they have been shown to resist adsorption.³² One shortcoming of the zwitterionic coatings is they are fully dynamic, meaning the surfactant monomer must be present in the running buffer to establish a stable coating.³³ This characteristic makes these coatings incompatible with electrospray – mass spectrometric detection since ionization of the analyte would be suppressed by the surfactant (Section 1.5.1). A problem with the phospholipid coatings is that they can be difficult to prepare.^{7,27} Moderate to high efficiencies are typically obtained for basic and acidic proteins with the SMIL coatings, however, the coating procedure requires more than an hour.^{30,31}

Polyoxyethylene (POE) has been used extensively as a covalently bonded wall coating in CE³³⁻³⁶ as it forms a neutral hydrophilic surface that is well known to be resistant to protein adsorption.³⁷⁻⁴⁰ However, the preparation of covalently bonded coatings is very time consuming. POE has also been used as a non-bonded coating whereby the POE molecules are held to the capillary wall by weak interactions.^{38,41} This procedure requires 45 minutes of capillary pretreatment between protein separations.

Warr and co-workers⁴² have modified a DDAB bilayer with POE 100 stearate, where 100 is the number of oxyethylene units in the diblock copolymer structure, and examined its surface properties. A schematic structure of the DDAB/POE 100 stearate aggregate is shown in Figure 3.1. The DDAB surfactant forms a bilayer on the silica surface and the stearate portion of the polymer interacts hydrophobically with the bilayer. The POE extends from the surface of the bilayer. At low polymer concentration, such as used herein, there is little interaction between the adsorbed polymer molecules. The tethered polymer adopts a mushroom configuration thus creating a neutral, hydrophilic surface (Section 4.3.1.1).

I prepared a novel coating using dioctadecyldimethylammonium bromide (DODAB) and POE 40 stearate. DODAB, the C₁₈ analogue of DDAB, has been shown to form similar wall coatings to DDAB, but with greater stability.²² It is expected that DODAB/POE 40 stearate will form a similar aggregate structure to the DDAB/POE 100 stearate system studied by Warr and co-workers⁴² (Figure 3.1). In this work POE 40 stearate was used rather than POE 100 stearate or POE 8 stearate as preliminary studies showed POE 40 stearate resulted in a more stable coating. The DODAB/POE 40 stearate coatings are semi-permanent and can be used for the efficient separation of both basic and acidic proteins over a wide pH range.

3.2 Experimental

3.2.1 Apparatus

All CE experiments were performed using a Beckman P/ACE 2100 system (Beckman Instruments, Fullerton, CA, USA) equipped with an UV absorbance detector

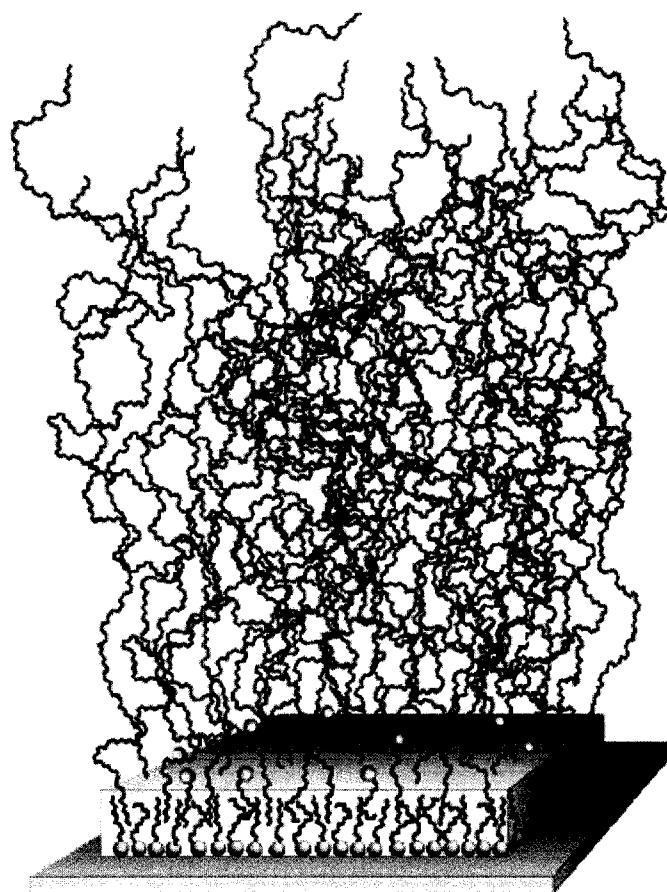


Figure 3.1: Schematic of the DDAB/POE 100 Stearate Coating, adapted from Figure 10 of reference⁴². Reprinted with permission.

upgraded to 5000 series optics. Detection at 254 nm was used for EOF stability studies and 214 nm for protein separations. The data acquisition rate was 5 Hz and the detector time constant was 0.5 s. Instrument control and data acquisition were managed using P/ACE station software for Windows 95 (Beckman Instruments). Untreated fused silica capillaries (Polymicro Technologies, Phoenix, AZ, USA) with an I.D. of 50 μm , O.D. of 360 μm , and total length of 47 cm (40 cm to the detector) were used unless otherwise stated. The capillary was thermostated at 25°C.

3.2.2 Chemicals

All solutions were prepared in Nanopure 18 M Ω water (Barnstead, Chicago, IL, USA). Buffers were prepared from stock solutions of sodium dihydrogen phosphate salt (BDH, Toronto, ON, Canada), ammonium formate (Fisher Scientific, Fair Lawn, NJ, USA), Ultrapure tris(hydroxymethyl)aminomethane (Tris; Schwarz/Mann Biotech, Cleveland, OH, USA), and (2-[N-cyclohexylamino]ethane-sulfonic acid) (CHES, 99%; Sigma, St. Louis, MO, USA). Phosphate buffers were adjusted to pH 3.0 using orthophosphoric acid (BDH). Ammonium formate buffers were adjusted to pH 3.5 using formic acid (EM Science, Gibbstown, NJ, USA). Tris buffers were adjusted to pH 7.4 using reagent grade hydrochloric acid (Anachemia, Rouses Point, NY, USA) or glacial acetic acid (Anachemia). CHES buffers were adjusted to pH 10.0 using reagent grade sodium hydroxide (EM Science). The pH was measured using a Corning digital pH meter model 445 (Corning, Acton, MA, USA). The cationic surfactant DODAB was used as received from Aldrich (Milwaukee, WI, USA). The polymers POE 8 stearate, POE 40 stearate, and POE 100 stearate were used as received from Sigma. The structures of the surfactant and polymers used are shown in Figure 3.2. A solution of

2 mM mesityl oxide (Aldrich) was used as the neutral EOF marker. The proteins lysozyme (chicken egg white), cytochrome *c* (bovine and equine heart), ribonuclease A (bovine pancreas), α -chymotrypsinogen A (bovine pancreas), insulin chain A oxidized ammonium salt (bovine insulin), trypsin inhibitor (soybean), and α -lactalbumin (bovine milk) were used as received from Sigma. The physical properties of the proteins used are given in Table 3.1. Benzylamine (Aldrich) and benzoic acid (reagent grade, BDH) were used as internal standards for the basic and acidic protein recovery studies, respectively.

3.2.3 Preparation of the DODAB/POE 40 Stearate Coating

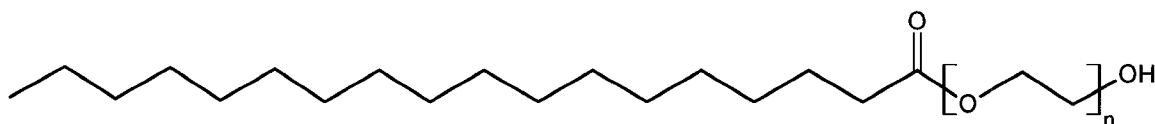
DODAB/POE 40 stearate solutions were prepared using a variation of the method used by Yassine and Lucy.²² The surfactant salt and the polymer were added together to nanopure water and sonicated (Aquasonic 75 HT, VWR Scientific Products, West Chester, PA, USA) for 30 min at 75°C. The solution was then stirred at room temperature for 20 min. This process produced a clear solution. The coating procedure consisted of flowing the DODAB/POE 40 stearate solution through the capillary at a high pressure (20 psi), as described in Section 3.2.4.

3.2.4 EOF Measurements

To avoid hysteresis effects, fresh capillaries were used with each new buffer system. New capillaries were rinsed with 0.1 M NaOH for 10 min using high pressure (20 psi) and then with distilled water for 5 min. 0.1 mM DODAB/0.1% POE 40 stearate solution was flowed through the capillary for 20 min to coat the capillary. As the EOF is suppressed by the POE, the three injection method described by Williams and Vigh⁴⁵ was used to determine its magnitude. Mesityl oxide (2 mM) was hydrodynamically injected onto the capillary for 3 s using low-pressure (0.5 psi). This was followed by a



Dimethyldioctadecylammonium bromide (DODAB)



Polyoxyethylene (POE) stearate

Figure 3.2: Surfactant and Polymer Structures

Table 3.1: Physical Properties of Proteins⁴³

Protein	Sigma Product Number	Molecular Weight (Daltons)	pI
cytochrome <i>c</i>	C2037	12 300	10-10.5
lysozyme	L6876	14 300	11.35
ribonuclease A	R4875	13 700	9.6
α -chymotrypsinogen A	C4879	25 600	8.97
insulin chain A	I1633	2 531.64	5.3 ^a
trypsin inhibitor	T9003	20 100	4.0 – 4.3
α -lactalbumin	L6010	14 200	4.5

^a pI for native insulin chain A⁴⁴

low-pressure (0.5 psi) buffer rinse for 1 min to push this band onto the capillary. A second band of mesityl oxide was introduced onto the capillary in the same way as the first, and both bands were pushed further onto the capillary by another 1 min low-pressure buffer rinse. A constant voltage of -5 kV was applied across the capillary for 1 min. During this time both mesityl oxide bands move towards the detector as a result of the suppressed reversed EOF. A third mesityl oxide injection was made in the same manner and all three bands are pushed towards the detector using low pressure (0.5 psi). Detection was at 254 nm. The magnitude of the EOF was then determined by comparing the spacing between the second and third band to that between the first and second band, as described in reference.⁴⁵

3.2.5 Coating Stability

The stability of the DODAB/POE 40 stearate coating was evaluated by monitoring the EOF as a function of hydrodynamic rinse time.⁴⁶ The capillary was regenerated by rinsing with 0.1 M NaOH for 2.5 min followed by a 5 min 0.1 mM DODAB/0.1% POE 40 stearate coat time at 20 psi. The capillary was then rinsed with buffer for an initial period of 0.5 min followed by increasingly longer rinse times and the EOF was determined using the three-injection method described previously. This procedure was repeated for rinse times up to 60 min.

3.2.6 Protein Separations

A new capillary ($L_d=40$ cm, $L_t=47$ cm) was initially rinsed with 0.1 M NaOH for 10 min followed by distilled water for 5 min at 20 psi. The capillary was then coated for 20 min with 0.1 mM DODAB/0.1% POE 40 stearate in water, followed by a 0.5 min buffer rinse (20 psi) to remove any excess surfactant/polymer mixture. All protein

mixtures (0.2 mg/mL) were injected for 3 s at 0.5 psi. Separation of the proteins was performed using: 50 mM sodium phosphate pH 3.0, 50 mM or 75 mM Tris-acetate pH 7.4, or 50 mM CHES pH 10.0 buffer devoid of surfactant/polymer mixture. The applied voltage was +20 kV (for basic protein mixtures) or -20 kV (for acidic protein mixtures). The maximum working voltage was determined by preparing an Ohm's plot for the buffer system in question. An Ohm's plot for the 0.1 mM DODAB/0.1% POE 40 stearate coating with a 50 mM ammonium formate pH 3.5 buffer is shown in Figure 3.3.

As $r^2 = 0.999$ for the Ohm's plot (Figure 3.3) with the 20 kV data point included, it was determined that no Joule heating was occurring at this voltage. Detection of proteins was performed at a wavelength of 214 nm. Between runs the capillary was rinsed for 2.5 min (20 psi) with 0.1 M NaOH followed by 5 min (20 psi) with 0.1 mM DODAB/0.1% POE 40 stearate and a 0.5 min (20 psi) buffer rinse. Rinse times of 1 min with 0.1 M NaOH and a recoat time of 3 min with 0.1 mM DODAB/0.1% POE 40 stearate resulted in comparable RSD values and efficiencies except for insulin chain A, which had an efficiency that was lower by approximately 65%. Efficiencies were calculated using the Foley-Dorsey method⁴⁷ unless otherwise stated. This is a more rigorous method than the width-at-half-height method, which is the algorithm used by the Beckman software. The efficiencies determined using the Foley-Dorsey method are calculated using the following equation:

$$N = \frac{41.7(t_m / W_{0.1})^2}{B/A + 1.25} \quad (3.1)$$

where t_m is the migration time of the analyte peak, $W_{0.1}$ is the width at 10% of the peak height, and B/A is the asymmetry factor (Figure 3.4).

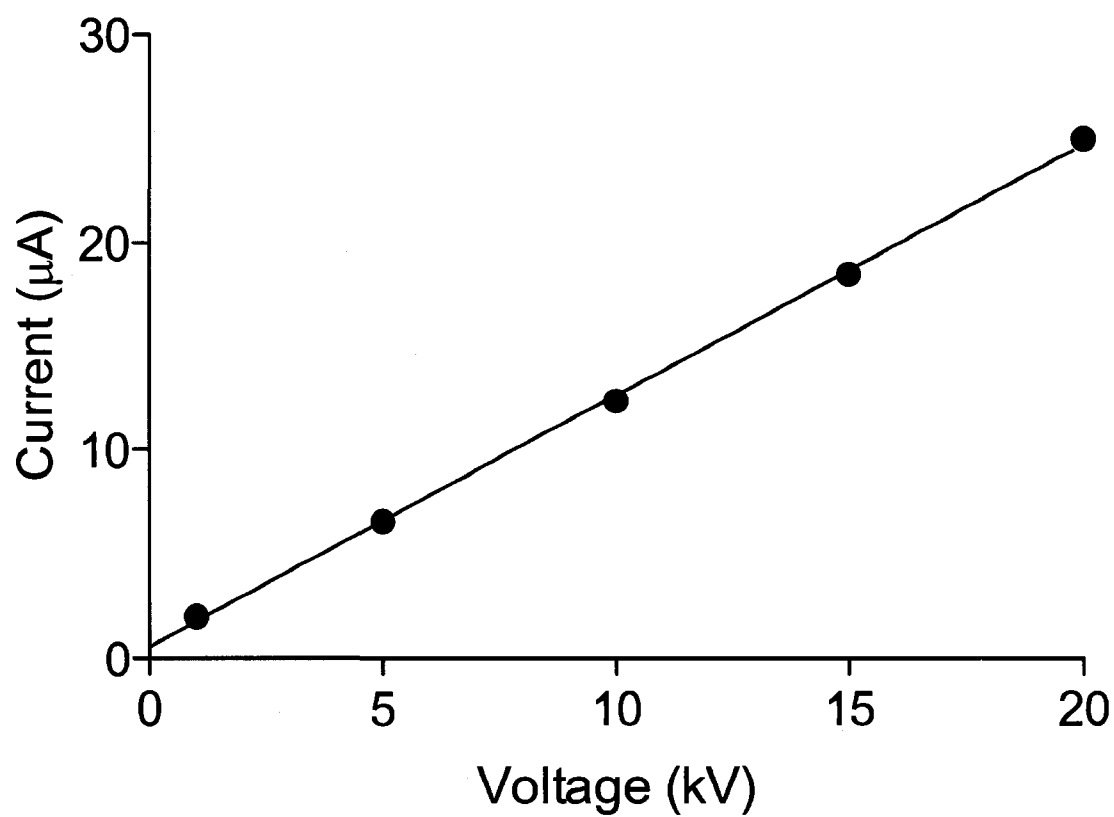


Figure 3.3: Ohm's Plot for the 50 mM Ammonium Formate pH 3.5 Buffer System with a 0.1 mM DODAB/0.1% POE 40 Stearate Coated Capillary. Points are experimental data fit to a linear regression equation with intercept.

Experimental Conditions: capillary, 27 cm x 50 µm I.D. (20 cm to the detector); neutral marker, 2 mM mesityl oxide; temperature, 25°C.

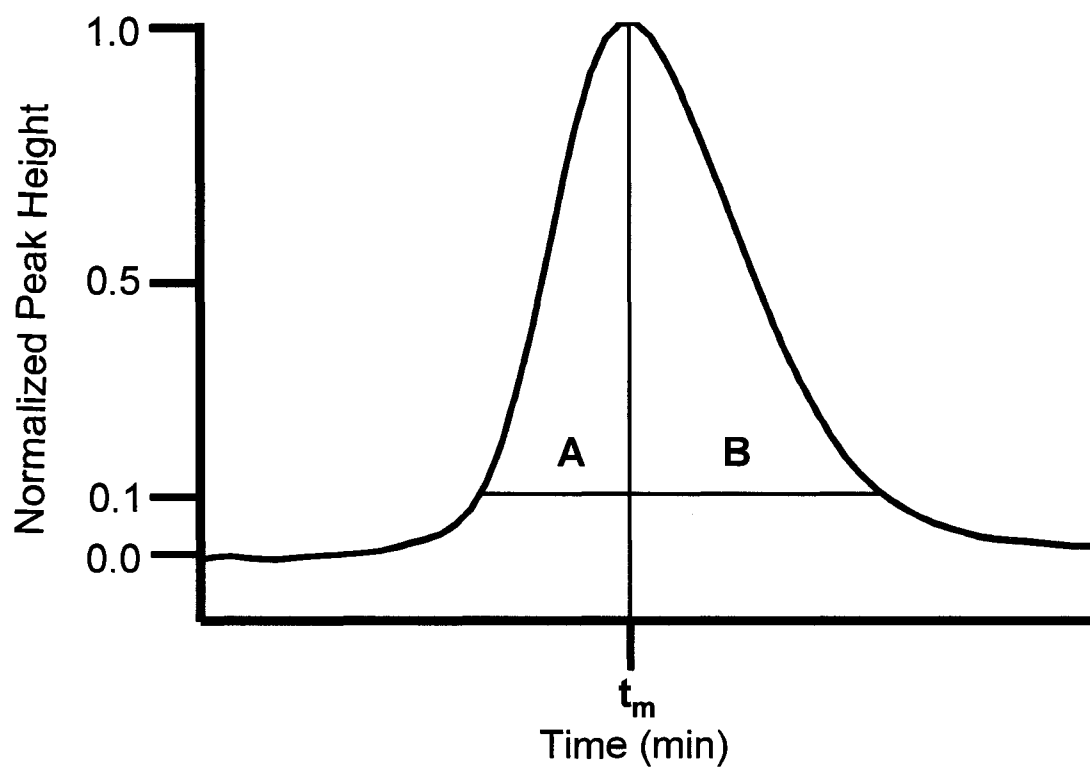


Figure 3.4: Peak Asymmetry Measure (B/A) at 10% of the Peak Height⁴⁷ (eq. 3.1)

Migration time reproducibilities were determined by performing 10 replicate injections on two different days. The method of Towns and Regnier⁴⁸ (Section 1.4.2.2.1) modified for a one detector CE¹⁹ was used for the protein recovery studies. A new 47 cm (40 cm to the detector) was used for the study. Six replicate injections of a protein mixture were performed as described previously. The capillary was then cut to 27 cm (20 cm to detector) and six replicate injections were performed on this shorter length capillary. Injection time and pressure were adjusted to correct for the shortened capillary length. Further, an internal standard (benzylamine or benzoic acid) was used to correct for any remaining injection volume variations (i.e., peak areas of the proteins were divided by the peak area of the benzylamine). Recoveries of the proteins were determined by comparing the peak area between the long and short portions of the capillary.

For the cytochrome *c* separations, a new capillary ($L_d=47$ cm, $L_t=40$ cm) was pretreated and coated as described above. A 0.2 mg/mL sample of a mixture of bovine and equine cytochrome *c* was injected for 3 s at 0.5 psi. Separation was performed in 50 mM Tris-acetate pH 7.4 buffer devoid of DODAB/POE 40 stearate. The applied voltage was +20 kV with detection at 214 nm.

3.3 Results and Discussion

Proteins can interact with surfaces in two different ways: biospecifically and nonspecifically.⁴⁹ In this case, nonspecific interactions are the dominant forces. They include electrostatic interactions, hydrophobic interactions and Van der Waals forces. When a protein comes into contact with a surface, either reversible adsorption or denaturation/irreversible adsorption of the protein on the surface can occur.⁴⁹ Reversible

adsorption leads to a distortion of the analyte peak,⁵⁰ resulting in peak broadening or tailing (Section 1.4.2.1). Therefore, determining the extent of peak broadening is important in establishing a coating's performance. Irreversible adsorption of protein on the capillary wall results in the deposition of more and more protein until the wall can become saturated with adsorbed protein.⁵¹ However, the irreversible adsorption that may accompany denaturation at the surface may not be reflected in peak efficiencies. Thus, some type of protein recovery measurement must be carried out to determine the extent of irreversible adsorption that occurs on the coating (Section 1.4.2.2). Extensive studies have been carried out by Righetti and co-workers to determine and assess methods to quantify and quench protein adsorption.⁵¹⁻⁵⁴

In this chapter, the performance of the surfactant/polymer coating is assessed by examining three measures: protein peak efficiency to monitor reversible adsorption; protein recovery⁴⁸ to gauge irreversible adsorption; and stability. Ideally, broadening in CE is related only to longitudinal diffusion, which depends on analyte mobility, the applied voltage and the diffusion coefficient, and not on capillary length⁵⁵ (Section 1.3.1). However, any interaction between the analyte and the capillary wall introduces a C-term (i.e., a resistance to mass transfer term) into the broadening behavior.⁹ Under such conditions it would be most appropriate to refer to a plate height⁴⁸ or moment analysis⁹ to characterize the peaks. However, it has been the convention in the protein CE literature to quote plates/m (e.g., refs^{13,15,49,56-58}) to describe the band broadening in the presence of wall adsorption. Therefore plates/m will be quoted herein to allow comparison to the literature. Finally, stability is monitored because the DODAB/POE 40 stearate coating is

semi-permanent. Thus it is essential to determine the stability of the resultant coating before performing protein separations.

3.3.1 Coating Stability

EOF measurements under a number of conditions can be used to indirectly determine the stability of a semi-permanent coating. In this case, the capillary was coated with the DODAB/POE 40 stearate solution using high pressure (see Section 3.2.5 for details). The unadsorbed surfactant/polymer mixture was rinsed from the capillary with buffer. These rinse times varied from 0.5 min up to 60 min, and the effect on EOF with rinse time was monitored. The DODAB and POE 40 stearate concentrations were optimized using this method. As can be seen in Figure 3.5, 0.1 mM DODAB/0.1% POE 40 stearate and 0.2 mM DODAB/0.5% POE 40 stearate were the most stable. The 0.1 mM DODAB/0.1% POE 40 stearate was chosen as the coating because fewer sonication/stir cycles were required than for the 0.2 mM DODAB/0.5% POE 40 stearate coating. It is apparent that the 0.1 mM DODAB/0.1% POE 40 stearate coating remains stable even after an hour long high-pressure rinse (Figure 3.5). The pH was increased to 3.5 for this coating as previous work in the lab had determined that the cationic surfactant coatings were more stable as the pH was increased.⁴⁶ However, at pH 3.0 the 0.1 mM DODAB/0.1% POE 40 stearate coating was also stable, as shown in Figure 3.6. Since the DODAB surfactant is forming the bilayer on the capillary wall, a stable coating is to be expected.²² The 0.1 mM DODAB/0.1% POE 40 stearate coating was observed to be stable over the pH range used in this study (Figure 3.6). However, the EOF is over a factor of ten lower than that observed with DODAB alone.²² The average value of the EOF with the DODAB/POE 40 stearate coating in Tris-acetate pH 7.4 buffer is

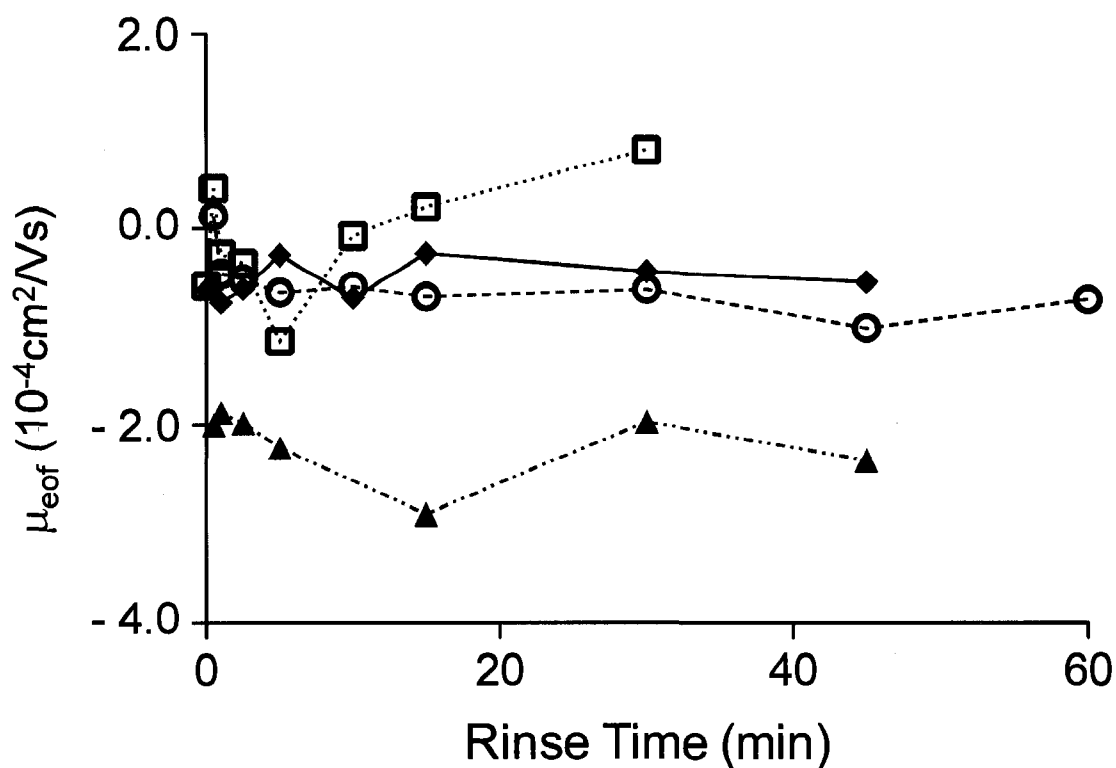


Figure 3.5: Coating Stability of Various DODAB/POE Stearate Concentrations reflected as EOF Mobility vs. High Pressure Rinse Time with the following Concentrations: 0.2 mM DODAB/1% POE 40 stearate, pH 2.5 (▲), 0.2 mM DODAB/0.5% POE 40 stearate, pH 2.5 (◆), 0.2 mM DODAB/0.1% POE 40 stearate, pH 2.5 (□), and 0.1 mM DODAB/0.1% POE 40 stearate, pH 3.5 (○).

Experimental conditions: applied voltage, -1 or -5 kV; capillary, 27 cm x 50 μ m I.D. (20 cm to the detector); buffers, 50 mM sodium phosphate pH 2.5, 50 mM ammonium formate pH 3.5; neutral marker, 2 mM mesityl oxide; λ , 254 nm; temperature, 25°C. The three-injection method was used to determine the EOF mobility following each buffer rinse.

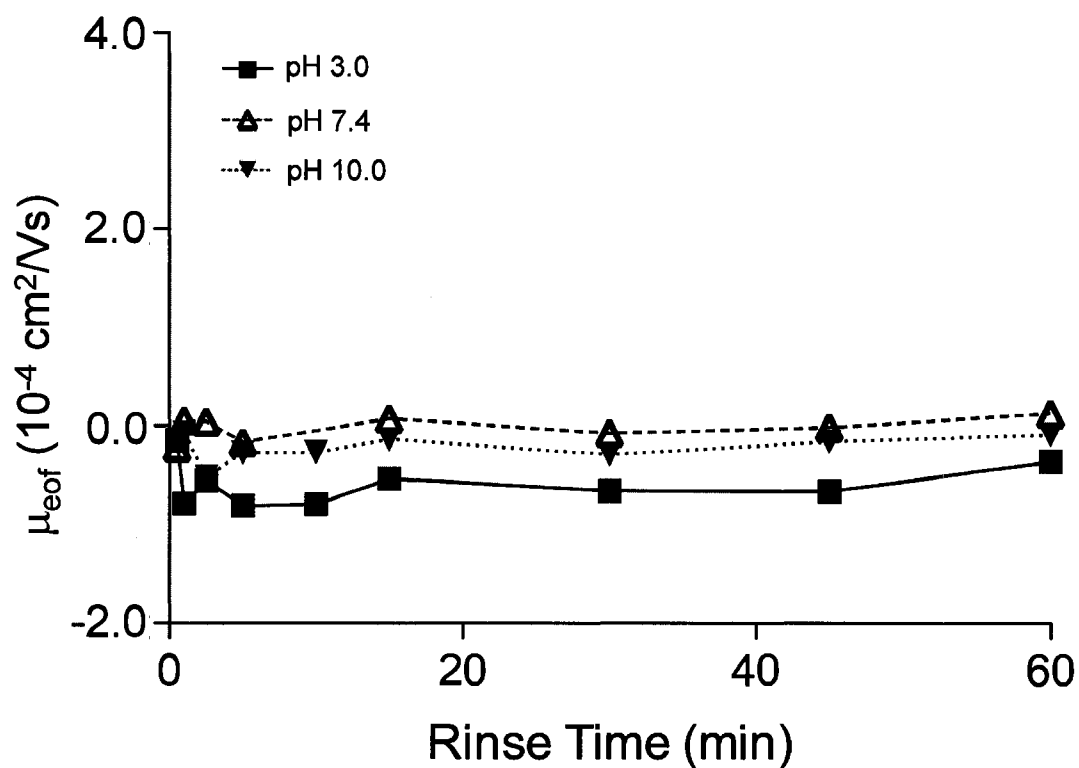


Figure 3.6: pH Stability of the DODAB/0.1% POE 40 Stearate Coating

Experimental conditions: DODAB concentration, 0.1 mM for pH 3.0 and 7.4, 0.2 mM for pH 10.0; applied voltage, -5 kV; capillary, 47 cm x 50 μm I.D. (40 cm to the detector); buffers, 75 mM sodium phosphate pH 3.0, 75 mM Tris acetate pH 7.4; 20 mM CHES pH 10.0; neutral marker, 2 mM mesityl oxide; λ , 254 nm; temperature, 25°C. The three-injection method was used to determine the EOF mobility following each buffer rinse.

$-0.45 \pm (0.23) \times 10^{-4} \text{ cm}^2/\text{Vs}$. This is more suppressed than the EOF observed with the zwitterionic phospholipid coating: $+1.4 \times 10^{-4} \text{ cm}^2/\text{Vs}$ at pH 7.4.⁷ The EOF generated on the DODAB/POE 40 stearate coating is similar to that observed with non-bonded POE coatings, allowing for the reversed EOF caused by the DODAB. Preisler and Yeung⁴¹ and Tran et al.⁵⁶ observed the EOF on non-bonded POE coatings to be approximately $+0.25 \times 10^{-4} \text{ cm}^2/\text{Vs}$ and $+0.5 \times 10^{-4} \text{ cm}^2/\text{Vs}$, respectively. The pH did not have a significant effect on the EOF of the DODAB/POE 40 stearate coating as the value in CHES pH 10.0 buffer is $-0.21 \pm (0.15) \times 10^{-4} \text{ cm}^2/\text{Vs}$, while in sodium phosphate pH 3.0 buffer the EOF is $-0.56 \pm (0.24) \times 10^{-4} \text{ cm}^2/\text{Vs}$.

3.3.2 Protein Separations using the DODAB/POE 40 Stearate Coating

The suppressed EOF allows for separations of both basic and acidic proteins. The separation of four basic proteins (lysozyme, cytochrome *c*, ribonuclease A, and α -chymotrypsinogen A) at pH 3.0 on the DODAB/POE 40 stearate coating is shown in Figure 3.7. These proteins were chosen as they are recommended as test proteins by Mazzeo and Krull,⁵⁹ and are also commonly used in the literature as standard proteins to test the effectiveness of coatings. All of these proteins will be highly positively charged, as pH 3.0 is well below their pI. The separation occurs in less than 15 minutes with efficiencies ranging from 0.85 million – 1.3 million plates/m (Table 3.2). These efficiencies are comparable to and, in the case of ribonuclease A and α -chymotrypsinogen A, higher than efficiencies obtained for these proteins on other semi-permanent, surfactant-based coatings.^{7,26,28} The efficiencies are also superior to those observed with permanent coatings.^{34,35,57} For example, Mohabbati et al. were able to achieve between 0.46 million to 1.6 million plates/m for these proteins on a

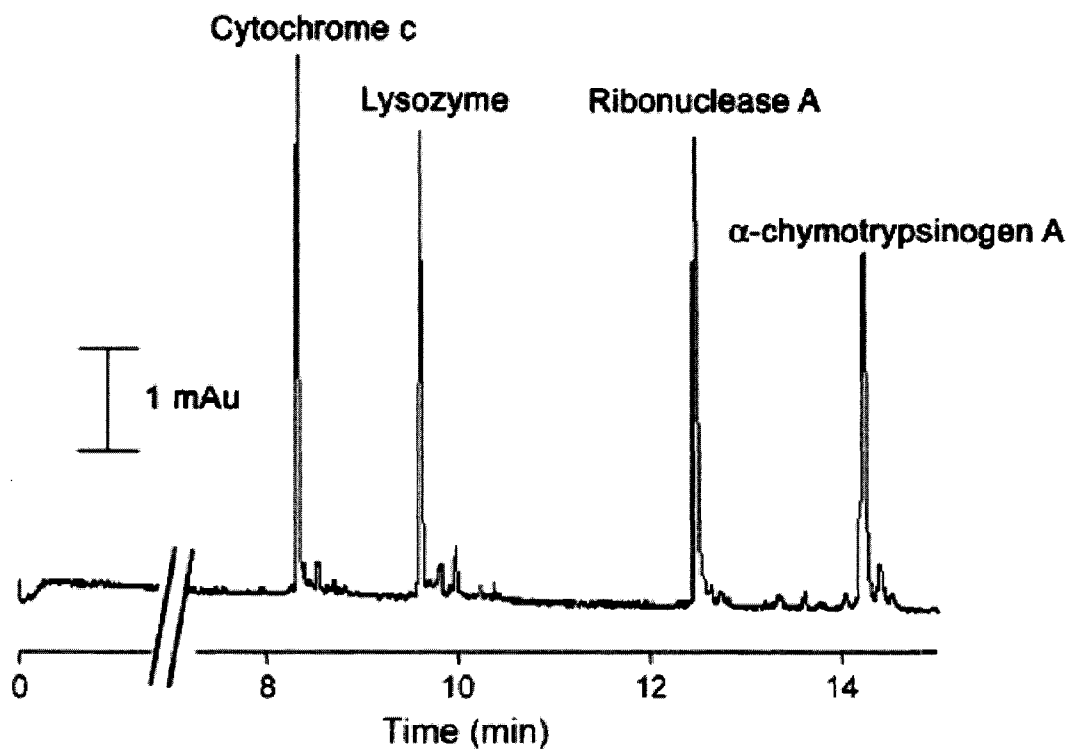


Figure 3.7: Separation of Basic Proteins on a 0.1 mM DODAB/0.1% POE 40 Stearate Coating

Experimental conditions: applied voltage, +20 kV; capillary, 47 cm x 50 μ m I.D. (40 cm to the detector); buffer, 50 mM sodium phosphate, pH 3.0; λ , 214 nm; 0.2 mg/mL protein sample dissolved in water and injected hydrodynamically at 0.5 psi for 3 s.

Table 3.2: Separation Characteristics of Basic Proteins Using a 0.1 mM DODAB/0.1% POE 40 Stearate Coated Capillary with 50 mM Sodium Phosphate Buffer pH 3.0

Protein	N ^a (x10 ³ plates/m)	% RSD (migration time)		% Recovery
		run to run ^a	day to day ^b	
cytochrome <i>c</i>	1 260	0.9	1.4	97 \pm 1
lysozyme	1 340	1.1	1.7	94 \pm 3
ribonuclease A	850	1.5	2.1	92 \pm 6
α -chymotrypsinogen	1 040	1.7	2.3	96 \pm 4

^a Values obtained from an average of 10 runs; calculated using the Foley-Dorsey method

^b % RSD over two days

poly(acrylamide) coated capillary.⁵⁷ Their values for ribonuclease A and α -chymotrypsinogen A are higher than the values obtained in this work. However, their coating is much more time consuming to prepare. In theory the peak efficiencies should be between 1-2 million plates/m.⁵⁹ Not all of our values are within this range, which suggests there is a phenomenon occurring, such as electrodispersion, which is reducing efficiency. This effect will be discussed in detail in Chapter 5. The small peaks observed next to the main analyte peaks are also noted in separations of these proteins on other coatings having a suppressed EOF.^{60,61} The smaller peak succeeding cytochrome *c* may be the result of a difference between the oxidized and reduced form of cytochrome *c*, while the small peak migrating after α -chymotrypsinogen A may be chymotrypsin (activated form of α -chymotrypsinogen A).⁶²

Figure 3.8 shows the separation of three proteins (insulin chain A, trypsin inhibitor, and α -lactalbumin) on the DODAB/POE 40 stearate coating at pH 7.4. The protein separations were run with and without recoating between runs. No recoating allows faster throughput. Efficiencies for the acidic proteins are higher if the capillary is rinsed with the coating solution between runs (Table 3.3). The pI of these acidic proteins is well below this pH, resulting in all of these proteins being negatively charged. Efficiencies (Table 3.3) for these proteins are superior to those obtained in previous separations using a zwitterionic semi-permanent coating,⁷ except for the α -lactalbumin (with no recoating). Similarly, many physically adsorbed coatings result in lower protein efficiencies than achieved in Table 3.3.^{15,63,64} A separation of three acidic proteins was achieved by Chiari et al. using a hydrophilic, adsorbed, acrylic polymer.⁶³ Our

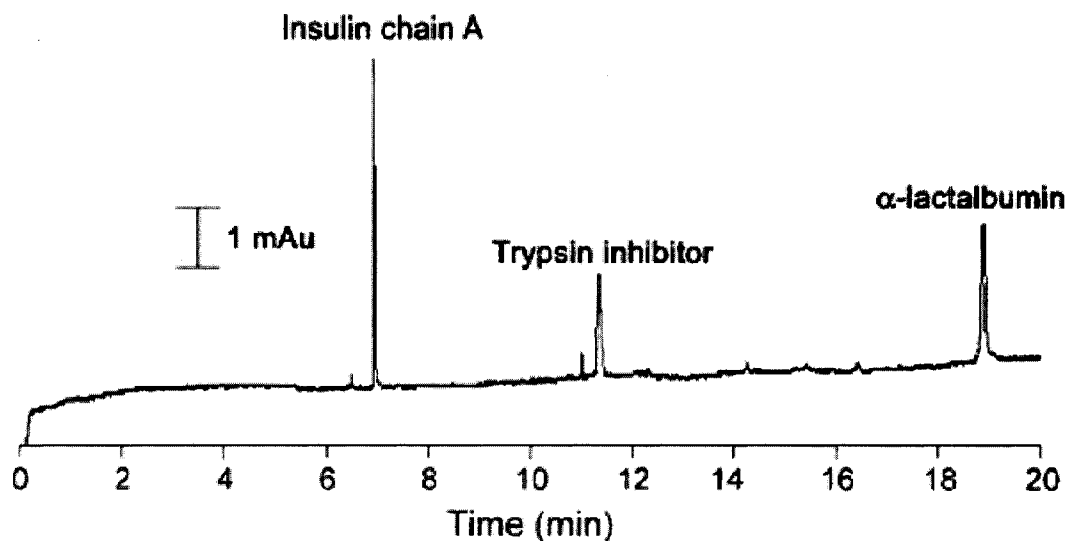


Figure 3.8: Separation of Acidic Proteins on a 0.1 mM DODAB/0.1% POE 40 Stearate Coating

Experimental conditions: applied voltage, -20 kV; capillary, 47 cm x 50 μ m I.D. (40 cm to the detector); buffer, 75 mM Tris-acetate, pH 7.4; λ , 214 nm; 0.2 mg/mL protein sample dissolved in water and injected hydrodynamically at 0.5 psi for 3 s.

Table 3.3: Efficiency and Migration Time Reproducibility of Acidic Proteins Using a 0.1 mM DODAB/0.1% POE 40 Stearate Coated Capillary with 75 mM Tris-acetate pH 7.4 Buffer with and without Re-coating between Runs

Protein	N ($\times 10^3$ plates/m) ^a		% RSD (migration time) with re-coating		% RSD (migration time) no re-coating	
	Re-coating	No re-coating	run to run ^a	day to day ^b	run to run ^a	day to day ^b
insulin chain A	640	280	0.9	0.8	0.5	0.6
trypsin inhibitor	320	220	1.3	1.1	1.0	1.0
α -lactalbumin	360	120	2.1	1.7	1.8	1.8

^aValues obtained from an average of 10 runs; calculated using the Foley-Dorsey method

^b% RSD over two days

measurements estimate the efficiencies to be only 100 000-190 000 plates/m for their coating. Further, the β -lactoglobulin A is not present in their electropherogram after the second coating regeneration. Comparable values to those found in Table 3.3 were reported using a SMIL coating.^{30,31} Also, our values were calculated using the Foley-Dorsey method, which is more rigorous than the width-at-half-height method (Section 5.3.1).

Figure 3.9 shows the separation of the basic proteins at pH 7.4. As the recovery of this protein was quantitative at pH 3.0, we assume the proteins do not adsorb to a great extent at pH 7.4. Efficiencies at pH 7.4 are lower than obtained at pH 3.0 (Table 3.4). As the coating has a slightly reversed EOF, this indicates a positive charge is present on the coating. Therefore, the proteins could interact electrostatically with the coating as a result of less electrostatic repulsion than is present at pH 3.0. This interaction could lead to the increased peak widths in Figure 3.9, and thus, lower efficiencies.

A separation of insulin chain A, trypsin inhibitor, and α -lactalbumin was also performed at pH 10.0, where all proteins would be highly negatively charged (Figure 3.10). The efficiencies are greater than those obtained at pH 7.4, except for the value for α -lactalbumin with recoating, which is greater at pH 7.4 (Table 3.5).

If there is no adsorption of the proteins onto the capillary wall, the migration times should be reproducible from run-to-run and from day-to-day. For the proteins studied, the migration time RSDs were as low as 0.8% from run-to-run and 0.9% from day-to-day. The values for each pH are given in Tables 3.2-3.5. Unless otherwise noted, the coating was regenerated between runs. This coating also yields very good reproducibility even without any regeneration between runs, as can be seen in Table 3.3.

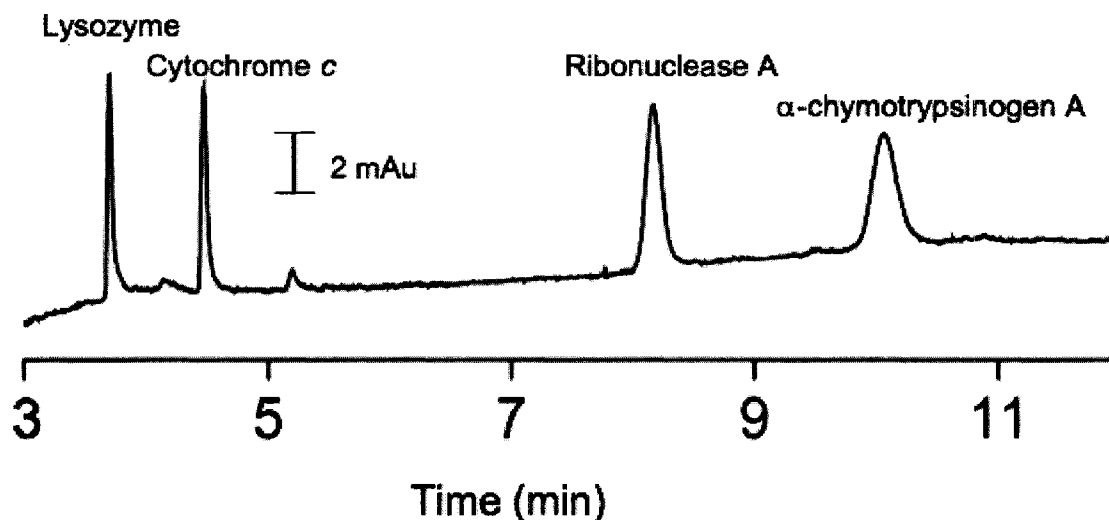


Figure 3.9: Separation of Basic Proteins on a 0.1 mM DODAB/0.1% POE 40 Stearate Coating

Experimental conditions: applied voltage, +15 kV; capillary, 27 cm x 50 μ m I.D. (20 cm to the detector); buffer, 75 mM Tris-acetate, pH 7.4; λ , 214 nm; 0.2 mg/mL protein sample dissolved in water and injected hydrodynamically at 0.5 psi for 3 s.

Table 3.4: Efficiency and Migration Time Reproducibility of Basic Proteins Using a 0.1 mM DODAB/0.1 % POE 40 Stearate Coated Capillary with 75 mM Tris-acetate pH 7.4 Buffer

Protein	N ($\times 10^3$ plates/m) ^a	% RSD (migration time) run to run ^a
lysozyme	110	2.7
cytochrome <i>c</i>	100	3.2
ribonuclease A	90	5.0
α -chymotrypsinogen A	50	6.1

^aValues obtained from an average of 5 runs; calculated using the Foley-Dorsey method

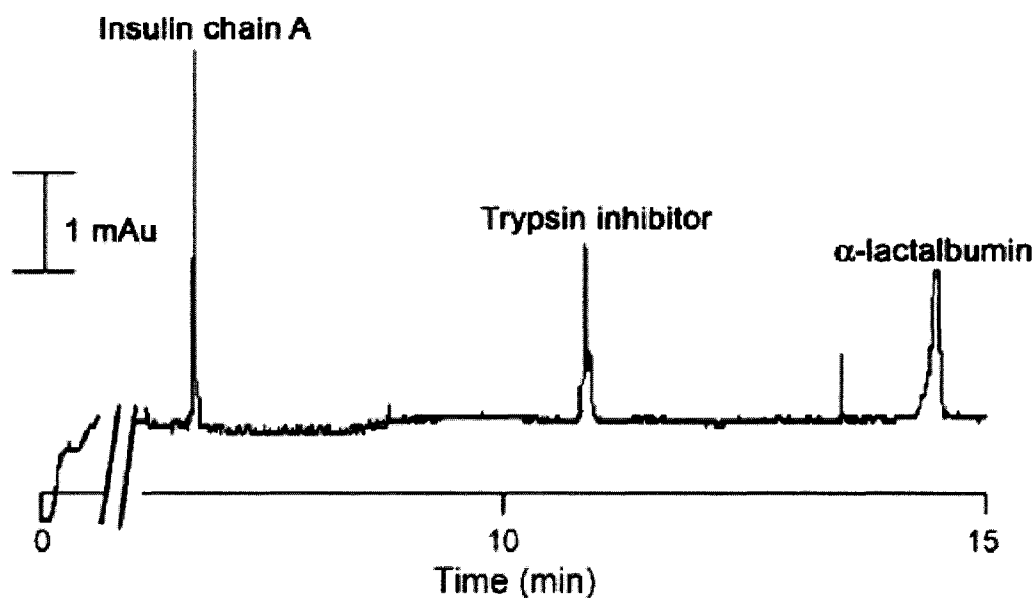


Figure 3.10: Separation of Acidic proteins on a 0.1 mM DODAB/0.1% POE 40 Stearate Coating at pH 10.0

Experimental conditions: applied voltage, -20 kV; capillary, 47 cm x 50 μ m I.D. (40 cm to the detector); buffer, 50 mM CHES, pH 10; λ , 214 nm; 0.2 mg/mL protein sample dissolved in water and injected hydrodynamically at 0.5 psi for 3 s.

Table 3.5: Efficiency, Migration Time Reproducibility, and Percent Recoveries of Acidic Proteins Using a 0.1 mM DODAB/0.1% POE 40 Stearate Coated Capillary with 50 mM CHES pH 10.0 Buffer

Protein	N ($\times 10^3$ plates/m) ^a	% RSD (migration time)		% Recovery
		run to run ^a	day to day ^b	
insulin chain A	1 310	1.3	2.0	92 \pm 4
trypsin inhibitor	900 *	2.2	3.2	95 \pm 6
α -lactalbumin	280	2.9	4.2	84 \pm 6

^a Values obtained from an average of 10 runs; calculated using the Foley-Dorsey method

^b % RSD over two days

* calculated using the width-at-half-height method

However, the efficiencies observed without regeneration are lower than those obtained with regeneration. Therefore, all other experiments were done with a recoating step between runs.

Protein recovery studies were carried out for the pH 3.0 and pH 10.0 separations (Table 3.2, Table 3.5). Recovery studies were not performed at pH 7.4 as the EOF was too suppressed to elute the internal standard in a reasonable amount of time. Recoveries are 92% or greater, except for α -lactalbumin for which a value of 84% was obtained. Therefore, little to no protein adsorption occurs at the capillary wall. Previous work in our group found that using a DDAB coated capillary resulted in recoveries for the basic proteins that were quantitative or nearly quantitative.^{21,65} The values obtained in the DODAB/POE 40 stearate work were comparable to and, for some proteins, better than those using zwitterionic coatings.^{7,26,66} Towns and Regnier achieved very good recoveries for both basic and acidic proteins using a nonionic surfactant coating.⁴⁸ However, the capillary first had to be derivatized with alkylsilane. Tran et al. used a non-covalent POE coating to study a highly basic protein, kin17, and its recovery was 79%.⁵⁶

To test the capillary coating, a separation of bovine and equine cytochrome *c*, which differ by only 3 amino acid residues,⁶⁷ was performed (Figure 3.11). If the electrophoretic mobility and EOF are equal in magnitude but opposite in direction, ultra-high resolution separations can be achieved,⁶⁸ including the separation of isotopomers.⁶⁸⁻⁷² The DDAB coating has a high reversed EOF, which allows proteins to be separated in a very short time. However, resolution will be reduced. For example, the four basic proteins studied in this work were separated on a DDAB coating⁴⁶ and our calculations determined the average resolution to be about 3, whereas the average resolution obtained

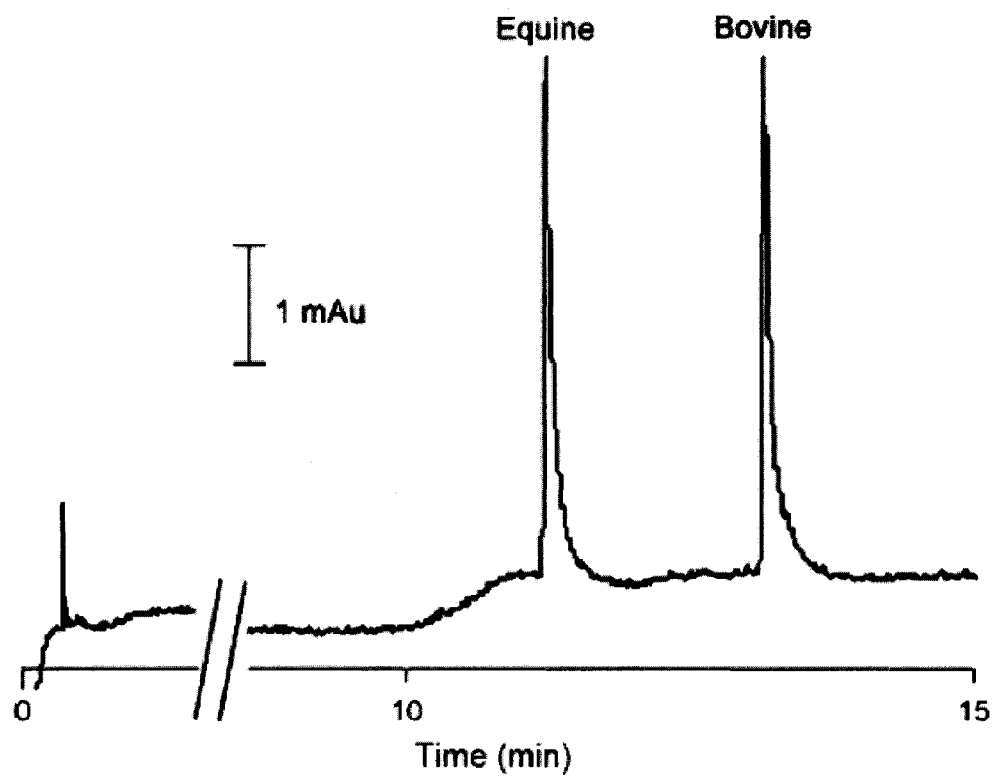


Figure 3.11: Separation of Equine and Bovine Cytochrome *c* on a 0.1 mM DODAB/0.1% POE 40 Stearate Coating

Experimental conditions: applied voltage, +20 kV; capillary, 47 cm x 50 μ m I.D. (40 cm to the detector); buffer, 50 mM Tris-acetate, pH 7.4; λ , 214 nm; 0.2 mg/mL protein sample dissolved in water and injected hydrodynamically at 0.5 psi for 3 s.

in Figure 3.7 is 15. Figure 3.11 shows the separation of equine and bovine cytochrome *c* at pH 7.4 using the DODAB/POE 40 stearate coating. Peak efficiencies are lower for the equine form (60 000 plates/m) than the bovine form (130 000 plates/m) when separated using this coating. These values for the efficiencies are lower than that obtained on a 2C₁₄DAB coating (700 000 plates/m).⁷³ However, the resolution achieved is 6.4 on the DODAB/POE 40 stearate coating versus only 4.7 on the 2C₁₄DAB coated capillary.

3.4 Concluding Remarks

The DODAB/POE 40 stearate coating was demonstrated to be stable, simple to prepare, and useful over a broad pH range. It effectively suppresses the EOF and prevents adsorption of basic and acidic proteins. High efficiencies are obtained for both types of protein separations at pH 3.0 and 10.0 and are comparable to or better than those obtained in the literature for similar coatings. Proteins differing in a small number of amino acid residues can be separated using this coating with better resolution than observed on a cationic surfactant coating. Improvements in the stability of the coating by way of a different coating method are investigated in Chapter 4, while sources of band broadening other than adsorption are minimized in Chapter 5.

3.5 References

- (1) Fritz, J. S., *J. Chromatogr. A* **2000**, 884, 261-275.
- (2) Timerbaev, A. R., *Electrophoresis* **2002**, 23, 3884-3906.
- (3) Hutterer, K.; Dolnik, V., *Electrophoresis* **2003**, 24, 3998-4012.
- (4) Wang, H. L.; Lu, M. L.; Mei, N.; Lee, J.; Weinfeld, M.; Le, X. C., *Anal. Chim. Acta* **2003**, 500, 13-20.
- (5) Melanson, J. E.; Baryla, N. E.; Lucy, C. A., *Trac-Trend. Anal. Chem.* **2001**, 20, 365-374.
- (6) Zhu, M. D.; Rodriguez, R.; Hansen, D.; Wehr, T., *J. Chromatogr.* **1990**, 516, 123-131.
- (7) Cunliffe, J. M.; Baryla, N. E.; Lucy, C. A., *Anal. Chem.* **2002**, 74, 776-783.
- (8) Lauer, H. H.; McManigill, D., *Anal. Chem.* **1986**, 58, 166-170.
- (9) Schure, M. R.; Lenhoff, A. M., *Anal. Chem.* **1993**, 65, 3024-3037.
- (10) Towns, J. K.; Regnier, F. E., *Anal. Chem.* **1992**, 64, 2473-2478.
- (11) Towns, J. K.; Regnier, F. E., *J. Chromatogr.* **1990**, 516, 69-78.
- (12) Huang, X. Y.; Doneski, L. J.; Wirth, M. J., *Anal. Chem.* **1998**, 70, 4023-4029.
- (13) Schmalzing, D.; Piggee, C. A.; Foret, F.; Carrilho, E.; Karger, B. L., *J. Chromatogr. A* **1993**, 652, 149-159.
- (14) Hardenborg, E.; Zuberovic, A.; Ullsten, S.; Soderberg, L.; Heldin, E.; Markides, K. E., *J. Chromatogr. A* **2003**, 1003, 217-221.
- (15) Gonzalez, N.; Elvira, C.; San Roman, J.; Cifuentes, A., *J. Chromatogr. A* **2003**, 1012, 95-101.
- (16) Cordova, E.; Gao, J. M.; Whitesides, G. M., *Anal. Chem.* **1997**, 69, 1370-1379.
- (17) Baryla, N. E.; Lucy, C. A., *J. Chromatogr. A* **2002**, 956, 271-277.
- (18) Giordano, B. C.; Muza, M.; Trout, A.; Landers, J. P., *J. Chromatogr. B Biomed* **2000**, 742, 79-89.
- (19) Yeung, K. K. C.; Lucy, C. A., *Anal. Chem.* **1997**, 69, 3435-3441.

- (20) Lucy, C. A.; MacDonald, A. M.; Gulcev, M. D., *J. Chromatogr. A* **2008**, *1184*, 81-105.
- (21) Baryla, N. E.; Melanson, J. E.; McDermott, M. T.; Lucy, C. A., *Anal. Chem.* **2001**, *73*, 4558-4565.
- (22) Yassine, M. M.; Lucy, C. A., *Anal. Chem.* **2005**, *77*, 620-625.
- (23) Gamble, T. N.; Ramachandran, C.; Bateman, K. P., *Anal. Chem.* **1999**, *71*, 3469-3476.
- (24) Emmer, A.; Jansson, M.; Roeraade, J., *J. Chromatogr. A* **1994**, *672*, 231-236.
- (25) Gong, B. Y.; Ho, J. W., *Electrophoresis* **1997**, *18*, 732-735.
- (26) Baryla, N. E.; Lucy, C. A., *Anal. Chem.* **2000**, *72*, 2280-2284.
- (27) Gulcev, M. D.; Lucy, C. A., *Anal. Chem.* **2008**, *80*, 1806-1812.
- (28) Wang, C. Z.; Lucy, C. A., *Electrophoresis* **2004**, *25*, 825-832.
- (29) Hult, E. L.; Emmer, A.; Roeraade, J., *J. Chromatogr. A* **1997**, *757*, 255-262.
- (30) Katayama, H.; Ishihama, Y.; Asakawa, N., *Anal. Chem.* **1998**, *70*, 5272-5277.
- (31) Catai, J. R.; Tervahauta, H. A.; de Jong, G. J.; Somsen, G. W., *J. Chromatogr. A* **2005**, *1083*, 185-192.
- (32) Holmlin, R. E.; Chen, X. X.; Chapman, R. G.; Takayama, S.; Whitesides, G. M., *Langmuir* **2001**, *17*, 2841-2850.
- (33) Herren, B. J.; Shafer, S. G.; Vanalstine, J.; Harris, J. M.; Snyder, R. S., *J. Colloid Interf. Sci.* **1987**, *115*, 46-55.
- (34) Bruin, G. J. M.; Chang, J. P.; Kuhlman, R. H.; Zegers, K.; Kraak, J. C.; Poppe, H., *J. Chromatogr.* **1989**, *471*, 429-436.
- (35) Nashabeh, W.; El Rassi, Z., *J. Chromatogr.* **1991**, *559*, 367-383.
- (36) Zhao, Z. X.; Malik, A.; Lee, M. L., *Anal. Chem.* **1993**, *65*, 2747-2752.
- (37) Zalipsky, S.; Harris, J. M., *Poly(ethylene glycol) : chemistry and biological applications*, American Chemical Society, Washington, D.C., 1997.
- (38) Iki, N.; Yeung, E. S., *J. Chromatogr. A* **1996**, *731*, 273-282.

- (39) Leckband, D.; Sheth, S.; Halperin, A., *J. Biomat. Sci. Polym. E* **1999**, *10*, 1125-1147.
- (40) Ostuni, E.; Chapman, R. G.; Holmlin, R. E.; Takayama, S.; Whitesides, G. M., *Langmuir* **2001**, *17*, 5605-5620.
- (41) Preisler, J.; Yeung, E. S., *Anal. Chem.* **1996**, *68*, 2885-2889.
- (42) Blom, A.; Drummond, C.; Wanless, E. J.; Richetti, P.; Warr, G. G., *Langmuir* **2005**, *21*, 2779-2788.
- (43) Sigma Aldrich Datasheets, www.sigma-aldrich.com, (accessed April 2005).
- (44) Conway, J. A.; Lewin, L. M., *Anal. Biochem.* **1971**, *43*, 394.
- (45) Williams, B. A.; Vigh, C., *Anal. Chem.* **1996**, *68*, 1174-1180.
- (46) Yassine, M. M.; Lucy, C. A., *Anal. Chem.* **2004**, *76*, 2983-2990.
- (47) Foley, J. P.; Dorsey, J. G., *Anal. Chem.* **1983**, *55*, 730-737.
- (48) Towns, J. K.; Regnier, F. E., *Anal. Chem.* **1991**, *63*, 1126-1132.
- (49) Doherty, E. A. S.; Meagher, R. J.; Albarghouthi, M. N.; Barron, A. E., *Electrophoresis* **2003**, *24*, 34-54.
- (50) Stedry, M.; Gas, B.; Kenndler, E., *Electrophoresis* **1995**, *16*, 2027-2033.
- (51) Castelletti, L.; Verzola, B.; Gelfi, C.; Stoyanov, A.; Righetti, P. G., *J. Chromatogr. A* **2000**, *894*, 281-289.
- (52) Olivieri, E.; Sebastiano, R.; Citterio, A.; Gelfi, C.; Righetti, P. G., *J. Chromatogr. A* **2000**, *894*, 273-280.
- (53) Verzola, B.; Gelfi, C.; Righetti, P. G., *J. Chromatogr. A* **2000**, *868*, 85-99.
- (54) Verzola, B.; Gelfi, C.; Righetti, P. G., *J. Chromatogr. A* **2000**, *874*, 293-303.
- (55) Gas, B.; Stedry, M.; Kenndler, E., *Electrophoresis* **1997**, *18*, 2123-2133.
- (56) Tran, N. T.; Taverna, M.; Miccoli, L.; Angulo, J. F., *Electrophoresis* **2005**, *26*, 3105-3112.
- (57) Mohabbati, S.; Hjerten, S.; Westerlund, D., *J. Chromatogr. A* **2004**, *1053*, 201-216.

- (58) Yeung, K. K. C.; Kiceniuk, A. G.; Li, L., *J. Chromatogr. A* **2001**, *931*, 153-162.
- (59) Mazzeo, J. R.; Krull, I. S., *Handbook of Capillary Electrophoresis*, CRC Press, Boca Raton, 1994.
- (60) Liu, S. R.; Gao, L.; Pu, Q. S.; Lu, J. J.; Wang, X. J., *J. Proteome Res.* **2006**, *5*, 323-329.
- (61) Gilges, M.; Kleemiss, M. H.; Schomburg, G., *Anal. Chem.* **1994**, *66*, 2038-2046.
- (62) Hempen, P. to MacDonald, A., Sigma Aldrich, August 22, 2008, E-mail correspondence.
- (63) Chiari, M.; Cretich, M.; Damin, F.; Ceriotti, L.; Consonni, R., *Electrophoresis* **2000**, *21*, 909-916.
- (64) Albarghouthi, M. N.; Stein, T. M.; Barron, A. E., *Electrophoresis* **2003**, *24*, 1166-1175.
- (65) Melanson, J. E.; Baryla, N. E.; Lucy, C. A., *Anal. Chem.* **2000**, *72*, 4110-4114.
- (66) Yeung, K. K. C.; Atwal, K. K.; Zhang, H. X., *Analyst* **2003**, *128*, 566-570.
- (67) Moza, B.; Qureshi, S. H.; Ahmad, F., *Biochim. Biophys. Acta Protein. Proteom.* **2003**, *1646*, 49-56.
- (68) Terabe, S.; Yashima, T.; Tanaka, N.; Araki, M., *Anal. Chem.* **1988**, *60*, 1673-1677.
- (69) Yeung, K. K. C.; Lucy, C. A., *Anal. Chem.* **1998**, *70*, 3286-3290.
- (70) Yeung, K. K. C.; Lucy, C. A., *Electrophoresis* **1999**, *20*, 2554-2559.
- (71) Lucy, C. A.; McDonald, T. L., *Anal. Chem.* **1995**, *67*, 1074-1078.
- (72) Henley, T. H.; Wilburn, R. T.; Crouch, A. M.; Jorgenson, J. W., *Anal. Chem.* **2005**, *77*, 7024-7031.
- (73) Yassine, M. M.; Lucy, C. A., *Electrophoresis* **2006**, *27*, 3066-3074.

Chapter Four: A Modified Supported Bilayer/Diblock Copolymer - Working Towards a Tunable Coating for Capillary Electrophoresis

4.1 Introduction

A common challenge in the capillary electrophoresis (CE) of proteins and biomolecules is the adsorption of these molecules onto the surface of the capillary.^{1,2} Adsorption can lead to undesirable effects such as band broadening,³ poor migration time reproducibility,⁴ and low sample recovery.⁵ The most common method to eliminate these problems is to coat the capillary. Such coatings can be broadly classified as covalent,⁶⁻⁸ physically adsorbed polymers,⁹⁻¹¹ or small molecule additives.¹²⁻¹⁵ Physically adsorbed polymers and surfactant coatings possess the attractive qualities of being easy to prepare, regenerable, and cost effective. A recent review on physically adsorbed polymer and surfactant coatings details the advantages and disadvantages of a number of the most widely-used varieties.¹⁶

As detailed in Chapter 3 we recently developed a neutral, hydrophilic coating enabling high efficiency separations of proteins.¹⁷ This coating was based on work by Warr and coworkers,¹⁸ who examined the surface properties of a didodecyldimethylammonium bromide (DDAB) bilayer modified with polyoxyethylene (POE) 100 stearate (Figure 3.1). The DDAB forms a bilayer on the surface and the C₁₈ chain of the stearate is anchored by the hydrophobic portion of the bilayer while the hydrophilic POE moieties protrude into the surrounding solution.

The coating discussed in Chapter 3 consisted of a dioctadecyldimethylammonium bromide (DODAB) (Figure 3.2) bilayer modified with POE 40 stearate polymer. Previous work in our lab has shown DODAB bilayers to be more stable than DDAB

bilayers.¹³ Therefore, DODAB was used to form the bilayer for the coating studied in Chapter 3, as well as all coatings discussed here.

One of the benefits of the DODAB/POE 40 stearate coating is its suppressed electroosmotic flow (EOF) – approximately -0.45×10^{-4} cm²/Vs at pH 7.4. A suppressed EOF allows for high resolution of protein peaks, which can be advantageous when working with complex samples. However, a highly suppressed EOF results in long migration times. For this reason, a coating with similar properties to the one developed in Chapter 3, but with an EOF that could be easily tuned is desirable.

With many tunable coatings the adjustable EOF is in response to changing the buffer pH. Smith and El Rassi developed a coating for separation of biomolecules that consisted of unreacted silanol groups, quaternary ammonium groups, and a hydrophilic layer of polyether chains to prevent adsorption.¹⁹ The net charge on the surface of the coating was a balance between the positive charge of the quaternary amine groups and the ionization of the silanol groups. Varying the pH of the buffer altered the magnitude and direction of the EOF from -1.8×10^{-4} to $+0.8 \times 10^{-4}$ cm²/Vs. Efficiencies of 180 000 plates/m were observed for model basic proteins, but baseline shifts indicating irreversible adsorption (Sec. 1.4.2.1) were evident. A sol gel version of the pH adjustable coating based on the relative concentration of SiO^- and $-\text{N}(\text{CH}_3)_3^+$ but lacking the protective polyether chains²⁰ yielded poor efficiencies ($< 50\,000$ plates/m) in the separation of basic proteins at pH 3.0.²¹ Colon and co-workers developed a sol gel coating using an aminopropyltriethoxysilane precursor, which enabled broad control over the EOF (-4×10^{-4} to $+5 \times 10^{-4}$ cm²/Vs) and moderate efficiencies (350 000 plates/m) for basic proteins at pH 3.9.²² However, pH is an important variable in the optimization of a

protein separation. Having both the EOF and separation selectivity governed by the same variable restricts method development.

The EOF in the presence of a coating can also be tuned using additives. As discussed in Section 1.5.1, amines are the most common small molecule additive. Corradini et al. noted a change in EOF from $+0.18 \times 10^{-4} \text{ cm}^2/\text{Vs}$ at pH 3.0 to $+0.89 \times 10^{-4} \text{ cm}^2/\text{Vs}$ at pH 8.0 when 40 mM diethylaminetriamine was added to the running buffer.¹² Separations of basic proteins with efficiencies ranging from 240 000 – 780 000 plates/m were obtained over this pH range. Quaternary amines have also demonstrated effectiveness at tuning the EOF. An advantage of the quaternary amines over the polyamines is they remain protonated at high pH, which makes them more effective at higher pH. Buchberger et al. varied the EOF from $+7.5 \times 10^{-4} \text{ cm}^2/\text{Vs}$ to $+5 \times 10^{-4} \text{ cm}^2/\text{Vs}$ at pH 11 by adding 0.8 mM hexamethonium bromide.²³ Baryla and Lucy manipulated the EOF by adding polarizable anions to a buffer containing zwitterionic surfactant.²⁴ This increased the cathodic EOF to approximately $+3 \times 10^{-4} \text{ cm}^2/\text{Vs}$ and enabled simultaneous separations of acidic and basic proteins with efficiencies of over 1.5 million plates/m. Often a mixture of two surfactant types is used and the EOF is tuned by varying the ratio. Hult et al. used a mixture of cationic and anionic fluorosurfactants to obtain a coating with an EOF that could be tuned by adjusting the amounts of cationic and anionic surfactant.²⁵ The EOF could be tuned over the range of $+8 \times 10^{-4} \text{ cm}^2/\text{Vs}$ to $-8 \times 10^{-4} \text{ cm}^2/\text{Vs}$. A greater concentration of anionic surfactant resulted in a more cathodic EOF, while more cationic surfactant produced a more anodic EOF. A mixture of acidic and basic proteins could be separated in less than two minutes. Wang and Lucy used a mixture of a cationic surfactant (CTAB) and anionic surfactant (SDS) to vary the EOF

from $+5 \times 10^{-4} \text{ cm}^2/\text{Vs}$ to approximately $-3 \times 10^{-4} \text{ cm}^2/\text{Vs}$, depending on the surfactant ratio.²⁶ Basic proteins were separated with efficiencies ranging from 360 000 – 560 000 plates/m. Recently Liu et al. studied a similar system whereby DDAB or a long chain gemini surfactant (i.e., two conventional surfactant molecules whose headgroups are chemically bonded together by a spacer) was used with SDS to impart more stability to the coating,²⁷ however, the EOF was only tuned from $4 \times 10^{-4} \text{ cm}^2/\text{Vs}$ to $8 \times 10^{-4} \text{ cm}^2/\text{Vs}$ by varying SDS concentration. Efficiencies on the DDAB/SDS and the gemini/SDS coatings ranged from 440 000 – 520 000 plates/m at pH 5.²⁷ In addition to mixing cationic and anionic surfactants, cationic and zwitterionic surfactants have been mixed to produce a tunable coating. Emmer and Roeraade mixed cationic and zwitterionic fluorosurfactants to tune the EOF so that it was anodic below pH 8 and cathodic above pH 8.²⁸ A mixture of proteins were separated at pH 4, 5, and 6 with efficiencies of approximately 200 000 plates/m. Yeung and Lucy could vary the EOF from approximately $+0.5 \times 10^{-4} \text{ cm}^2/\text{Vs}$ to $-4.5 \times 10^{-4} \text{ cm}^2/\text{Vs}$ by changing the ratio of a cationic (tetradecyltrimethylammonium bromide (TTAB)) and zwitterionic (coco amidopropylhydroxydimethylsulfobetaine (CAS U)) surfactant.²⁹

The coatings developed in this chapter vary the EOF of the DODAB/POE stearate coating by modifying the concentration or the chain length of the polymer while keeping the DODAB concentration constant. In Chapter 3 only POE 40 stearate was used. Chapter 4 examines POE 8 and POE 100 stearate as well. The extension of the POE portion of the POE 100 stearate into solution has been calculated as 5.5 nm, assuming a good solvent.¹⁸ If a total thickness for the DODAB and POE 100 stearate is approximated to be 10 nm (as the thickness of the adsorbed DODAB bilayer depends on

the buffer and pH conditions³⁰), this layer would not interfere with the EOF flow profile for the 50 μm capillary used in this work.³¹ The performance of the modified coatings was evaluated by examining stability, efficiency of protein separations, and ease of preparation. The ability to control the EOF enabled the separation of acidic and basic proteins, including a histone protein. The development of a tunable coating also led to the establishment of a simpler method of coating preparation.

4.2 Experimental

4.2.1 Apparatus

All CE experiments were performed using a Beckman P/ACE 2100 system (Beckman Instruments, Fullerton, CA, USA) equipped with an UV absorbance detector upgraded to 5000 series optics, or a Beckman P/ACE 5500 system with an on-column diode array UV absorbance detector (Beckman). Detection at 214 nm was used for EOF stability studies and for protein separations. The data acquisition rate was 5 Hz and the detector time constant was 0.5 s for the P/ACE 2100 system. The data acquisition rate was 4 Hz for the P/ACE 5500 system. Instrument control and data acquisition were controlled using P/ACE station software for Windows 95 (Beckman). Untreated fused silica capillaries (Polymicro Technologies, Phoenix, AZ, USA) with an I.D. of 50 μm , O.D. of 360 μm , and total length of 47 cm or 27 cm (40 cm or 20 cm to the detector, respectively) were used unless otherwise stated. The capillary was thermostated at 25°C.

4.2.2 Chemicals

All solutions were prepared in Nanopure 18 M Ω water (Barnstead, Chicago, IL, USA). Buffers were prepared from stock solutions of sodium dihydrogen phosphate salt (BDH, Toronto, ON, Canada), Ultrapure tris(hydroxymethyl)aminomethane (Tris;

Schwarz/Mann Biotech, Cleveland, OH, USA), boric acid (BDH), (2-[N-cyclohexylamino]ethane-sulfonic acid) (CHES, 99%; Sigma, St. Louis, MO, USA), and formic acid (EM Science, Gibbstown, NJ, USA). Phosphate buffers were adjusted to pH 3.0 using reagent grade orthophosphoric acid (BDH). Tris acetate buffers were adjusted to pH 7.4 using reagent grade glacial acetic acid (Anachemia, Rouses Point, NY, USA). Borate and CHES buffers were adjusted to pH 10.0 using reagent grade sodium hydroxide (EM Science). Tris formate buffers were adjusted to pH 4.0 using formic acid (EM Science). The pH was measured using a Corning digital pH meter model 445 (Corning, Acton, MA, USA). The cationic surfactant DODAB was used as received from Aldrich (Milwaukee, WI, USA). The polymers POE 8 stearate, POE 40 stearate, and POE 100 stearate were also purchased from Aldrich. A solution of 2 mM benzyl alcohol (Aldrich) was used as the neutral EOF marker. The proteins lysozyme (chicken egg white), cytochrome *c* (bovine heart), ribonuclease A (bovine pancreas), α -chymotrypsinogen A (bovine pancreas), insulin chain A oxidized (bovine insulin), trypsin inhibitor (soybean), α -lactalbumin (bovine milk), and histone type III-S (calf thymus) were used as received from Sigma.

4.2.3 Preparation and Coating of the Surfactant/Polymer Solutions

Two different methods were used to prepare the DODAB/POE 40 stearate solutions (Figure 4.1). In the first “mixed” method, which was used in Chapter 3, the surfactant salt and the polymer were both added to nanopure water and sonicated (Aquasonic 75 HT, VWR Scientific Products, West Chester, PA, USA) for 30 min at 75°C. The solution was then stirred at room temperature for 20 min. This process was repeated until a clear solution was obtained. A new 47 cm capillary was rinsed with

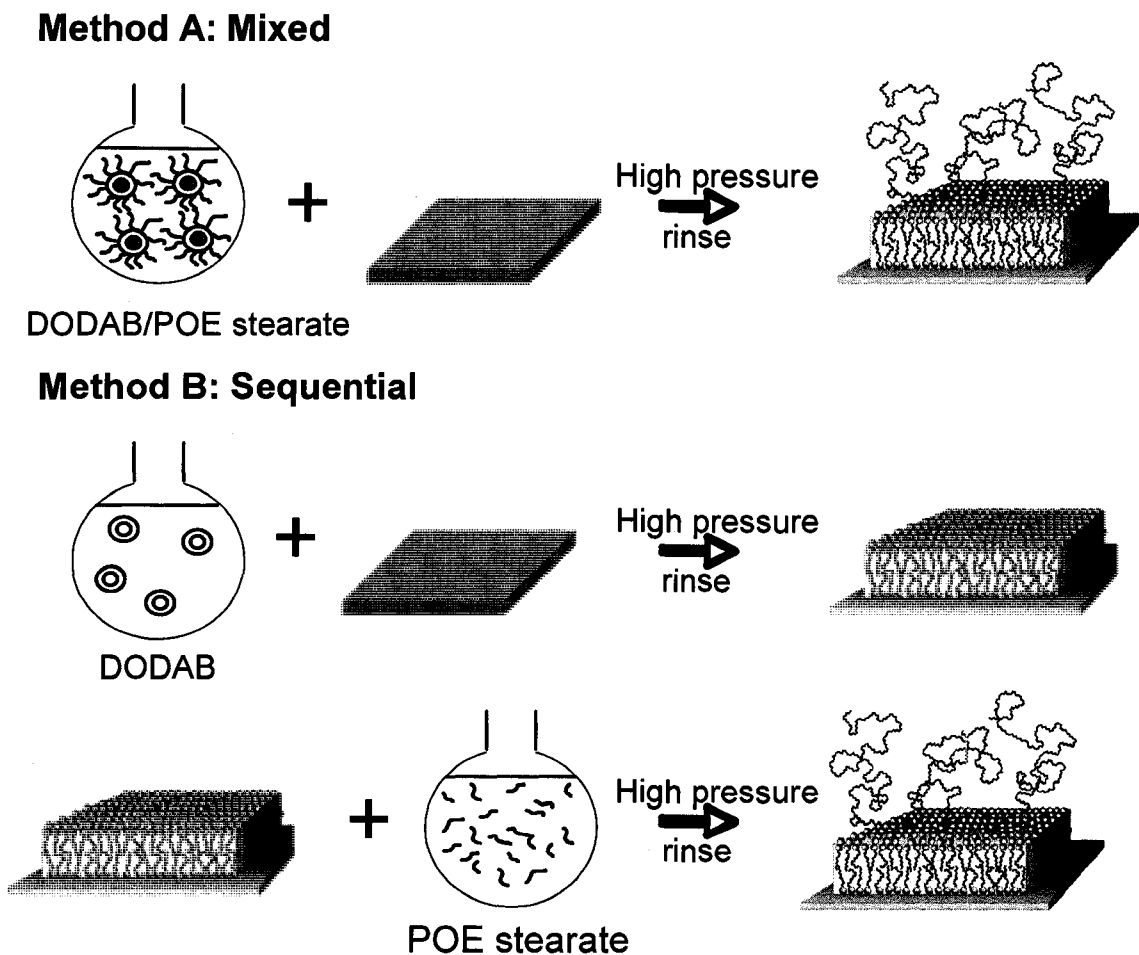


Figure 4.1: Schematic of the Mixed and Sequential Coating Methods. For the mixed method, (A), DODAB and POE stearate are added to a flask, sonicated and stirred, and then rinsed through the capillary. For the sequential method, (B), a DODAB solution is first rinsed through the capillary to form a bilayer on the wall. A POE stearate solution is then rinsed through the capillary and the stearate chains intercalate into the bilayer. Bilayer structures reprinted with permission from reference¹⁸.

0.1 M NaOH for 10 min using high pressure (20 psi). Fresh capillaries were used with each new buffer system to avoid hysteresis effects. This was followed by a 20 min flow (20 psi) of the DODAB/POE 8, 40, or 100 stearate solution to coat the capillary. A 0.5 min buffer rinse (20 psi) was then performed to remove any excess coating (corresponds to 1.6 capillary volumes). Rinse and coat times were adjusted for 27 cm capillaries.

In the second “sequential” method (Figure 4.1B), a 0.1 mM solution of DODAB was prepared using a variation of the sonication/stir method,¹³ as described in Section 3.2.3. POE 8, 40, and 100 stearate solutions of a range of concentrations (POE 8: 0.001 - 0.01%; POE 40: 0.0004 - 1%; POE 100: 0.0005 - 0.01%) were prepared separately with no DODAB present using the sonication/stir method. The capillary was rinsed for 10 min with 0.1 M NaOH (20 psi) followed by a 10 min flow (20 psi) of 0.1 mM DODAB. The DODAB coated capillary was then immediately rinsed for 10 min (20 psi) with a POE 40 stearate solution of the concentration of interest. A 0.5 min buffer rinse was performed to remove excess coating solution from the capillary.

4.2.4 EOF Measurements

The EOF was measured in two ways. Suppressed EOF ($< 1 \times 10^{-4} \text{ cm}^2/\text{Vs}$) were measured using the 3 injection method described by Williams and Vigh,³² as described in detail in Section 3.2.4. For coatings prepared using POE 100 stearate or non-suppressed EOF, the direct voltage method was used to measure EOF. A 3 s hydrodynamic injection of benzyl alcohol was followed by the application of voltage across the capillary. The EOF was then calculated using:

$$\mu_{eof} = \frac{L_d L_t}{V t_m} \quad (4.1)$$

where L_t and L_d are the total length of the capillary and the capillary length to the detector, respectively, V is the voltage applied, and t_m is the migration time of the neutral marker. Detection was at 214 nm.

4.2.5 Protein Separations

A new capillary ($L_d=40$ cm, $L_t=47$ cm) was initially rinsed with 0.1 M NaOH for 5 min at 20 psi. For the mixed coating method (Figure 4.1A), the DODAB/POE stearate coating solution was flowed through the capillary for 20 min (20 psi). The capillary was then rinsed for 0.5 min with buffer (20 psi) to remove excess surfactant/polymer. All protein mixtures were injected for 3 s at 0.5 psi. Protein separation was performed using: 50 mM sodium phosphate pH 3.0, 75 mM Tris-acetate pH 7.4, 50 mM CHES pH 10.0, or 50 mM borate pH 10.0 buffer devoid of surfactant/polymer mixture. The applied voltage was +17.5 kV, unless otherwise noted. Detection of proteins was performed at 214 nm. Between runs the capillary was rinsed for 2 min (20 psi) with 0.1 M NaOH followed by a 5 min (20 psi) flow of the surfactant/polymer mixture of interest and a 1 min (20 psi) buffer rinse. For each coating the identity of the peaks was determined by injecting each protein separately and monitoring the migration time. Efficiencies were calculated using the Foley Dorsey method,³³ unless otherwise noted.

For the sequential coating method (Figure 4.1B), the new capillaries were coated for 10 min with 0.1 mM DODAB followed by a 10 min flow of the POE stearate solution. In subsequent runs, a 5 min flow of each coating solution was performed. For the histone sample, a new capillary ($L_d=60$ cm, $L_t=67$ cm) was rinsed for 10 min (20 psi) with methanol, 5 min (20 psi) with 0.1 M NaOH, coated for 10 min with 0.1 mM DODAB (20 psi), coated for 10 min with 0.075% POE 40 stearate (20 psi), and rinsed for

2 min (20 psi) with 75 mM Tris formate pH 4.0. A 0.25 mg/mL solution of the histone type III-S was injected hydrodynamically (0.5 psi) for 4 s and a voltage of +15 kV was applied. The width-at-half-height method was used for the histone separations as the baseline was not conducive to measurements using the Foley-Dorsey method.

4.3 Results and Discussion

4.3.1 Mixed DODAB/POE stearate

4.3.1.1 Tunability of EOF

The DODAB/POE stearate coating consists of a DODAB surfactant bilayer adsorbed to the capillary wall, which is modified with a POE stearate diblock copolymer. The stearate chain interacts hydrophobically with the carbon chains of the DODAB while the hydrophilic POE portion protrudes into solution,¹⁸ as discussed in Chapter 3. POE alone can suppress the EOF as a semi-permanent coating.³⁴⁻³⁶ Preisler and Yeung observed that the EOF decreased by more than an order of magnitude for a non-bonded POE coated capillary compared to a bare capillary at pH 7.³⁵ Tran et al. determined the EOF to be $0.5 \times 10^{-4} \text{ cm}^2/\text{Vs}$ at pH 7.5, a fivefold decrease from the EOF on a bare capillary at this pH.³⁶

In this chapter, the magnitude of the reversed EOF caused by the DODAB bilayer will be modulated by altering the POE stearate concentration. The hypothesis is at lower POE stearate concentrations, there will be fewer polyoxyethylene chains extending into solution. Therefore, the positive charge on the DODAB quaternary ammonium headgroup will be less shielded by the neutral POE, resulting in a stronger reversed EOF. A similar phenomenon has been noted with polyethylene glycol (PEG)-grafted polymethacryl oxyethyl trimethylammonium chloride (PMOTAC) coatings.³⁷ PEG has

the same monomeric structure as POE (Section 1.5.2). Grafting PMOTAC with PEG results in a weaker anodic EOF than PMOTAC alone. This was attributed to the shielding of some of the positive charge on the PMOTAC by the PEG.³⁷ A more fundamental study of negatively charged liposomes grafted with PEG showed a decrease in both the absolute value of the zeta potential and surface charge of the liposomes with increasing mole fraction of PEG.³⁸ This is a result of the shielding of the negative charge on the liposome by the PEG.

The EOF tunability of the mixed DODAB/POE 40 stearate coating was studied over the pH range 3-10. The DODAB concentration was constant at 0.1 mM, while the POE 40 stearate concentration was varied from 0 to 1%. The EOF was measured for each POE 40 stearate concentration at pH 3.0, 7.4, and 10.0 (Figure 4.2). In the absence of POE stearate, the EOF is strongly reversed ($-4.5 \times 10^{-4} \text{ cm}^2/\text{Vs}$) due to DODAB's cationic headgroup. This EOF is consistent with that demonstrated by Yassine et al.¹³ for DODAB under various conditions and for comparable DDAB coatings.³⁹⁻⁴¹ When as little as 0.01% (w/v in water) POE 40 stearate is added to the DODAB, the EOF becomes much less reversed ($-0.4 \times 10^{-4} \text{ cm}^2/\text{Vs}$ at pH 7.4). This 12-fold suppression of EOF is similar to the 5-fold³⁶ and > 10-fold³⁵ EOF suppression observed for semi-permanent POE coatings on bare capillaries.

The EOF remains suppressed and reversed from 0.01% to 0.5% POE 40 stearate for pH 3.0 and 7.4. At pH 10.0 with 0.5% POE stearate, however, the EOF is strong and normal ($+5 \times 10^{-4} \text{ cm}^2/\text{Vs}$). This is statistically equivalent to the EOF of a bare capillary (right-hand points in Figure 4.2). Similarly, at all pH studied POE 40 stearate

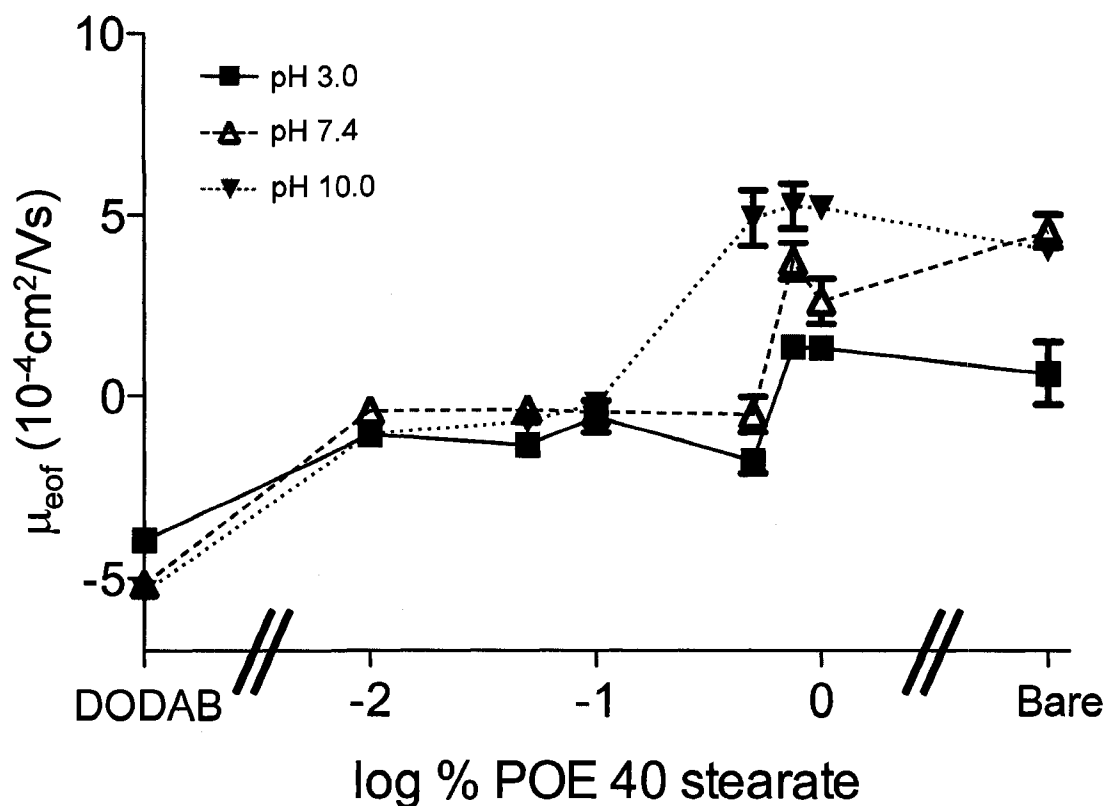


Figure 4.2: EOF at Various Percentages of POE 40 Stearate. Shown as log % POE 40 concentration, and a constant concentration of 0.1 mM DODAB, reflected as EOF mobility. pH 3.0 data displayed in Table 4.1

Experimental conditions: applied voltage, ± 1 kV for runs using the three injection method, ± 15 kV for runs using the voltage method; capillary, 27 or 47 cm x 50 μm I.D. (20 cm or 40 cm to the detector); buffers, 50 mM sodium phosphate pH 3.0, 75 mM Tris-acetate pH 7.4, 50 mM CHES pH 10.0, 50 mM borate, pH 10; neutral marker, 2 mM benzyl alcohol ($\lambda=214$ nm) or 2 mM mesityl oxide ($\lambda=254$ nm); temperature, 25°C.

concentrations of $\geq 0.75\%$ result in a normal EOF equivalent to that of a bare capillary (right-hand side of Figure 4.2).

For the DODAB/POE stearate coating, hydrophilicity increases with both the POE stearate concentration and POE chain length (to be discussed in Section 4.3.1.3). Hydrophilic polymeric coatings such as polyethylene glycol (PEG) are favored for protein and biomolecule separations as a result of their ability to reduce nonspecific adsorption and EOF.⁴² Reduction of EOF is desirable for protein separations as it enables the mobility of the proteins to come to the forefront so that better resolution can be attained. However, there is generally an optimum hydrophilicity that can be attained for semi-permanent coatings.^{34,43,44} Semi-permanent coatings tend to be unstable if they are very hydrophilic. In a study of a variety of non-covalent coatings for DNA separations, Madabhushi noted weaker adsorption of PEG onto the capillary wall than other more hydrophobic coatings.⁴⁵ This is attributed to water being a good solvent for PEG. Therefore, PEG would be more weakly adsorbed to the wall than a more hydrophobic polymer such as polydimethylacrylamide (PDMA) for which water is a poor solvent. Another possible explanation for the high normal EOF values at high POE 40 stearate concentrations could be steric hindrance. Grafted polymer chains adopt different conformations depending on factors including: the radius of gyration of the polymer (i.e., the average distance from the centre of gravity of the polymer to the chain segment), the distance between points of attachment on the surface, and the quality of the solvent.⁴⁶ These conformations, or regimes, are known as the pancake regime (low grafting densities), the mushroom regime (intermediate grafting densities), and the brush regime (high grafting densities).^{46,47} Warr and coworkers calculated the length of POE 100

stearate chains physigrafted on a DDAB bilayer using both adsorption and force measurements.¹⁸ The extension of the chains increased with increasing concentration of POE 100 stearate, as can be seen in Figures 4.3a and b. The strength of the layer of POE chains also increases at $\sim 0.4\%$ POE 100 stearate, suggesting a mushroom (left-hand side of Figure 4.3b) to brush (right-hand side of Figure 4.3b) conformational change.

Thus at low concentrations of POE 100 stearate ($<0.4\%$), the POE extending from the DODAB vesicles is flexible (mushroom structure) such that it does not interfere with vesicle adsorbing and fusing onto the capillary wall. Hence suppressed EOF are observed under these conditions (Figure 4.2, for POE 40 stearate). At higher concentrations of POE 100 stearate ($> 0.4\%$), Warr and co-workers observed an inflexible brush structure.¹⁸ The large number of inflexible hydrophilic chains on the outer surface of the vesicle could prevent the DODAB from interacting with the capillary wall. This could be compounded by the fact that the POE is in a good solvent (water) and a full coating would not be formed on the capillary wall. Hence an EOF typical of a bare capillary is observed at high POE 40 stearate concentrations (Figure 4.2). The hypothesis is supported by the success of the sequential method of forming DODAB/POE stearate coatings (Section 4.3.2) even in the presence of high concentrations of POE stearate.

4.3.1.2 Coat Time Study

The time required for a stable EOF to be achieved using a mixed DODAB/POE 40 stearate coating was studied. This experiment was carried out in a similar fashion to that used in previous studies of the adsorption of phospholipids.⁴⁸ The POE 40 stearate concentration was held constant at 0.01%. A new 47 cm capillary was first rinsed for 10

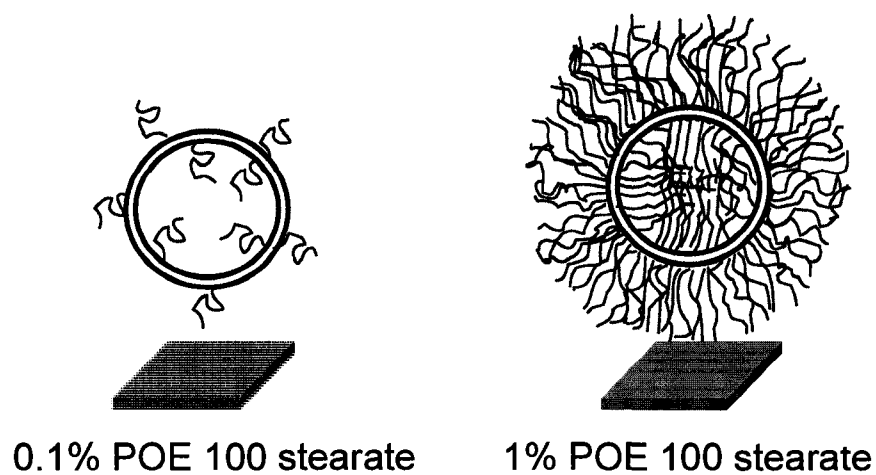


Figure 4.3a: Schematic of Vesicle Formation at Low and High Concentrations of POE 100 Stearate

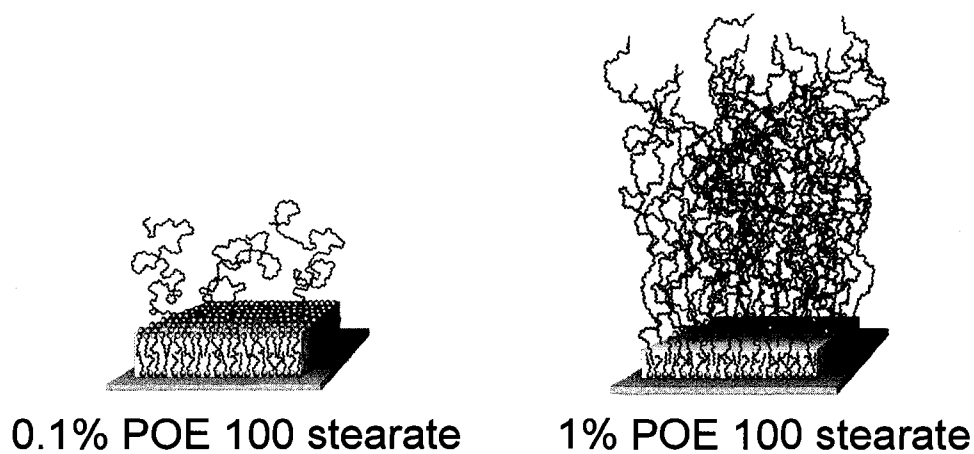


Figure 4.3b: Representation of the Surfactant Bilayer/Polymer Structure at Low and High Concentrations of POE 100 Stearate. Reprinted with permission from ¹⁸.

min with methanol. This was followed by a 5 min rinse with NaOH and a 5 min rinse with water. A 0.5 min flow of the DODAB/0.01% POE 40 stearate solution was then followed by a 0.5 min rinse with buffer to remove any excess coating material. Benzyl alcohol was injected and the EOF was determined. This was followed by a flow of the coating solution for another 0.5 min followed by a 0.5 min buffer rinse, and the EOF was measured again. The coating/EOF measurement was repeated with successively longer coating times. The results are shown in Figure 4.4. This experiment was run for 90 min of coating time, but is only shown up to 30 min as the EOF remained stable after this time. The EOF does not change significantly after the first 5 min of coating indicating that a complete coating has been formed. A 20 min coating time (20 psi) was used to initially coat all new capillaries with DODAB/POE stearate using the mixed procedure, with a 5 min recoat between consecutive runs.

4.3.1.3 Protein Separations with mixed DODAB/POE 40 stearate

In Chapter 3 the separation of model proteins was extensively investigated for coatings prepared using 0.1 mM DODAB/0.1% POE 40 stearate.¹⁷ This coating enabled separation of both basic and acidic proteins over a pH range of 3-10 due to its neutral, hydrophilic nature (Figures 3.7 - 3.10). Efficiencies as high as 1.3 million plates/m were achieved.¹⁷ In this section protein separations were performed on capillaries coated with DODAB/POE 40 stearate prepared using various concentrations of the POE 40 stearate. The efficiencies for model basic proteins (cytochrome *c*, lysozyme, ribonuclease A, and α -chymotrypsinogen A) separated at pH 3.0 are summarized in Table 4.1. Figure 4.5 shows the separation of the four proteins on a DODAB coated capillary, while Figure 4.6 shows the separation on a DODAB/0.5% POE 40 stearate coated capillary.

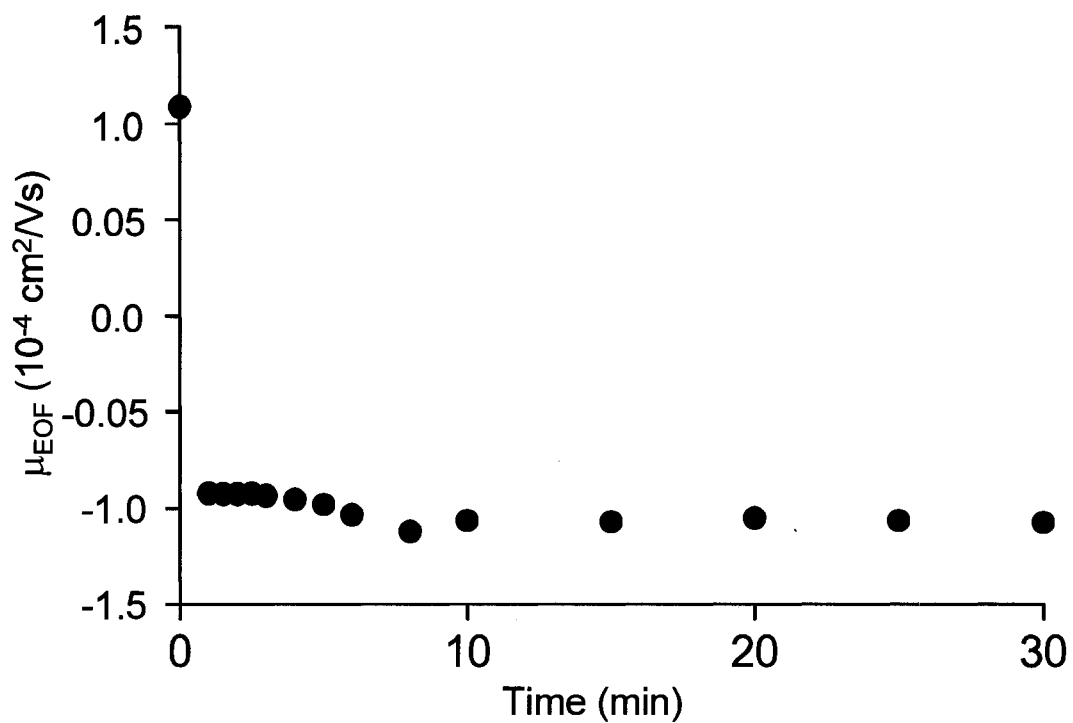


Figure 4.4: Coat Time Study for 0.1 mM DODAB/0.01% POE 40 Stearate

Experimental conditions: applied voltage, +15 kV; 27 cm \times 50 μm I.D. capillary (20 cm to detector); 50 mM sodium phosphate buffer, pH 3.0; λ , 214 nm; 2 mM benzyl alcohol injected for 3 s at 0.5 psi; temperature, 25°C.

Table 4.1: EOF Values and Efficiencies for Mixed 0.1 mM DODAB/POE 40 Stearate Coatings with 0.1 mg/mL Basic Proteins, unless otherwise Noted

Coating ^a	μ_{eof} ($\times 10^{-4}$ cm ² /Vs)	N, plates/m ($\times 10^3$) (Foley-Dorsey)			
		cyt c	lys	RNase A	α -chym A
DODAB ^b	-3.96 ± 0.01	115	130	150	120
DODAB/0.01% POE 40 stearate	-1.07 ± 0.15	280	850	470	510
DODAB/0.05% POE 40 stearate	-1.35 ± 0.02	220	780	500	390
DODAB/0.1% POE 40 stearate	-0.57 ± 0.44	410	1 030	600	620
DODAB/0.5% POE 40 stearate	-1.79 ± 0.34	280 ^c	550	640	930
DODAB/0.75% POE 40 stearate	1.35 ± 0.19				
DODAB/1% POE 40 stearate ^b	1.32 ± 0.30	490	710	590	670

^a 0.1 mM DODAB, 50 mM Na₃PO₄ buffer, pH 3.0

^b Sample concentration is 0.2 mg/mL, capillary length is 27 cm (total), width-at-half-height efficiencies ($N_{1/2}$)

^c Calculated using width-at-half-height method

In the absence of POE 40 stearate, the efficiencies observed for the model basic proteins are low (< 200 000 plates/m). Baseline resolution is not achieved between α -chymotrypsinogen A and ribonuclease A on DODAB alone (Figure 4.5). Upon addition of POE 40 stearate, the efficiencies were moderate (200 000 – 500 000 plates/m) to high (> 500 000 plates/m) (Table 4.1). The higher efficiency enables baseline resolution to be achieved between α -chymotrypsinogen A and ribonuclease A, as can be observed in Figure 4.6 for a 0.1 mM DODAB/0.5% POE 40 stearate coating. The migration order is reversed as compared to the separation on DODAB alone (Figure 4.5), as a result of the DODAB causing a reversal of the EOF.

From Table 4.1 it is apparent that when POE 40 stearate is introduced into the coating solution, efficiencies increase. The efficiency values obtained using the 0.1 mM DODAB/1% POE 40 stearate coating are at least a factor of four greater than those

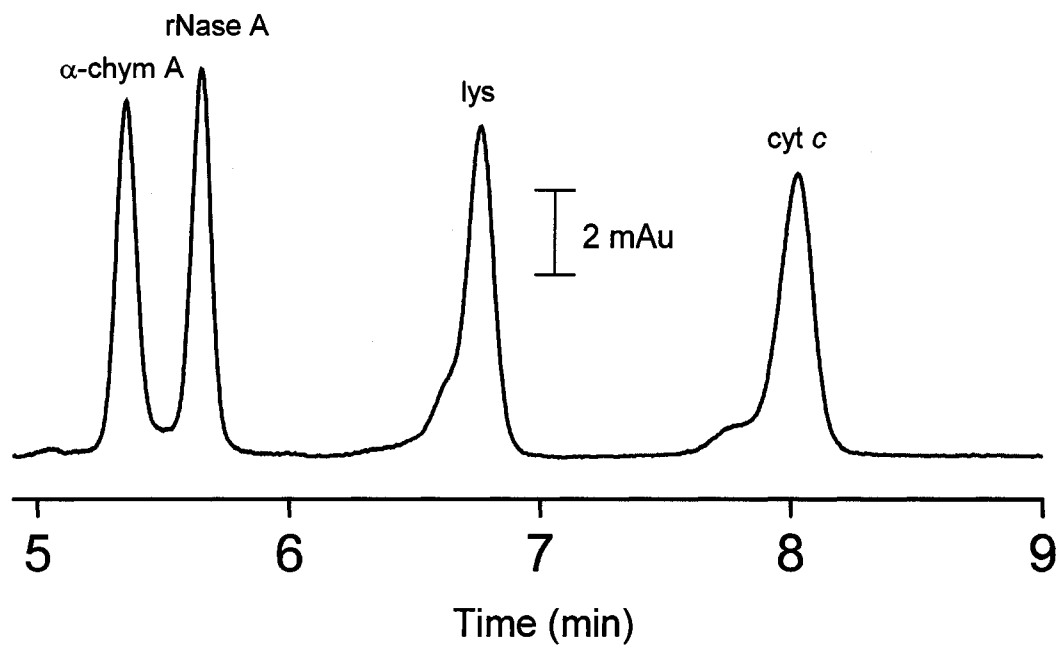


Figure 4.5: Separation of Basic Proteins on a 0.1 mM DODAB Coated Capillary
Experimental conditions: applied voltage, -10 kV; 27 cm \times 50 μ m I.D. capillary (20 cm to detector); 50 mM sodium phosphate buffer, pH 3.0; λ , 214 nm; 0.2 mg/mL of each protein; temperature, 25°C.

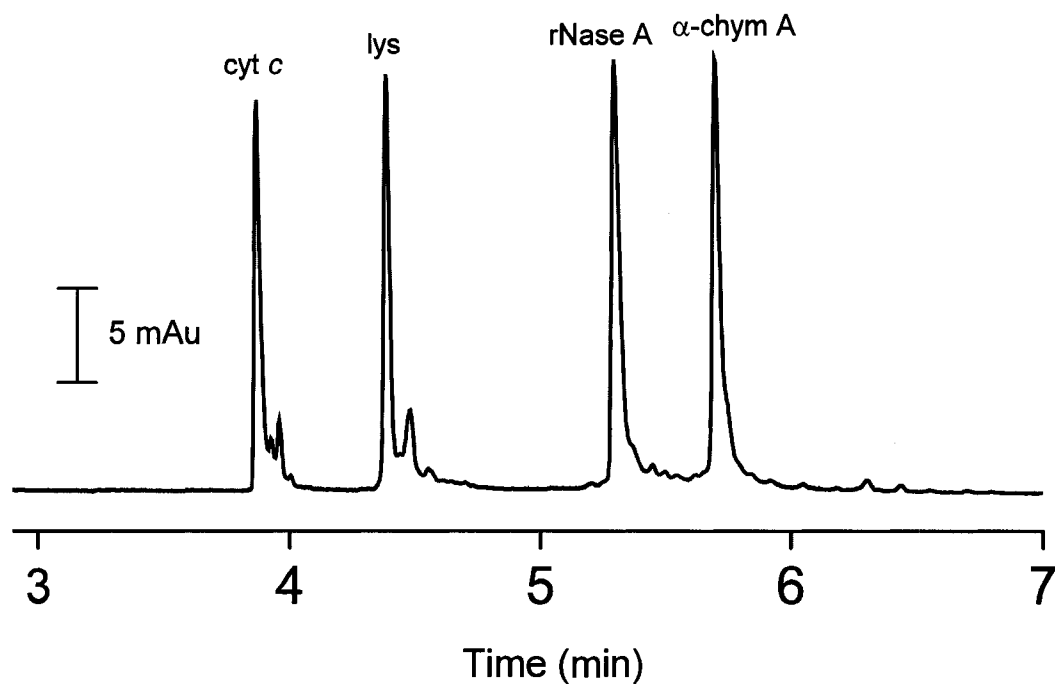


Figure 4.6: Separation of Basic Proteins on a 0.1 mM DODAB/0.5% POE 40 Stearate Coated Capillary

Experimental conditions: applied voltage, +10 kV; 27 cm \times 50 μ m I.D. capillary (20 cm to detector); 50 mM sodium phosphate buffer, pH 3.0; λ , 214 nm; 0.2 mg/mL of each protein; temperature, 25°C.

obtained on DODAB alone under the same conditions (both were calculated using the width-at-half-height method). As discussed in Section 4.3.1.1, the 0.1 mM DODAB/1% POE 40 stearate coating has an EOF not significantly different from that obtained on a bare capillary. However, the efficiencies obtained with this coating are approximately an order of magnitude larger than those obtained on a bare capillary under the same conditions (40 000 – 70 000 plates/m). An absence of protein adsorbing onto the wall results in higher efficiencies than if adsorption occurs (Section 1.4.2.1). As discussed in Section 3.1, POE is effective at reducing protein adsorption as a result of its neutral, hydrophilic nature. McPherson et al. studied the prevention of adsorption by using grafted PEO-PPO-PEO polymers containing a similar number of oxyethylene units as the POE 100 stearate.⁴⁹ Increasing the concentration of various chain lengths of the POE resulted in an initial decrease in protein adsorption. This was followed by a plateau in the amount of protein adsorbed as the polymer concentration increased. This trend reflects the observation made in Table 4.1 for the efficiencies as the concentration of POE 40 stearate in the coating solution increases. Upon introduction of the POE 40 stearate into the coating, the efficiencies increase and remain moderate to very high overall as the POE 40 stearate concentration increases.

4.3.1.4 Adjustment of Polymer Chain Length with Mixed DODAB/POE stearate

4.3.1.4.1 EOF Modification

Another method of tuning the EOF is to vary the POE chain length protruding from the DODAB bilayer. The three POE stearate polymers used in this work (8, 40 and 100) were each added (at a concentration of 0.01%) to the DODAB surfactant to form the coatings (Figure 4.1, Method A). The EOF for each coating measured at pH 3.0 is given

in Table 4.2. The EOF is anodic for all three polymer chain lengths, however, it is the most highly reversed for the smaller chain POE 8 stearate with a value of -2.97×10^{-4} cm^2/Vs . The EOF for the POE 40 stearate is -1.07×10^{-4} cm^2/Vs , which is suppressed by approximately a factor of three relative to the POE 8 stearate coating. Increasing the POE chain length to 100 units suppresses the EOF further to a value of -0.16×10^{-4} cm^2/Vs . In the separation of DNA using physically adsorbed polymeric coatings, Doherty et al. noted that as the contour length (i.e., maximum end-to-end distance of a linear polymer chain) of a polymer increases, the EOF within the capillary decreases significantly.⁵⁰ If the polymers contained approximately 2000 to 5000 monomer units, the EOF decreased by an order of magnitude compared to that obtained on a bare capillary. An even greater suppression of the EOF was noted if the polymer contained 15 000 or more monomer units. Cretich et al. observed an EOF suppressed by more than a factor of ten for a coating prepared from polydimethylacrylamide (PDMA) with a molecular mass of 73 kDa (longer chain) versus a coating prepared from PDMA with a molecular mass of 26 kDa (shorter chain).⁵¹

Table 4.2: EOF Values for the 0.01% POE 8, 40, and 100 Stearate Coatings

Coating ^a	$\mu_{\text{eof}} (10^{-4} \text{ cm}^2/\text{Vs})$
DODAB/0.01% POE 8 stearate	-2.97 (± 0.03)
DODAB/0.01% POE 40 stearate	-1.07 (± 0.16)
DODAB/0.01% POE 100 stearate	-0.16 (± 0.02)

^a All DODAB concentrations are 0.1 mM, polymer concentrations are %w/v, 50 mM Na_3PO_4 pH 3.0, SD in brackets

4.3.1.4.2 Protein Separation with mixed DODAB/POE 8 stearate

As discussed above, POE is well-known to reduce protein adsorption.⁵² Chapter 3 showed combining this polymer with a DODAB bilayer produced a very effective coating for separating proteins.¹⁷ However the coating's highly suppressed EOF prohibited separation of acidic and basic proteins simultaneously. Rather separate runs had to be performed (Figure 3.7 - 3.10). Simultaneous separation of acidic and basic proteins is a challenging task because an EOF is needed to push the proteins towards the detector as the positively and negatively charged proteins have mobilities in the opposite direction to each other. In addition, a coating must be present to prevent adsorption. To prevent adsorption of both types of protein, a neutral coating would be the obvious choice, but this normally results in an EOF of near zero. As shown in Figure 4.2, adjusting the POE 40 stearate concentration did not provide the controllable change in the EOF needed for simultaneous separations. However, reducing the POE chain length from 40 to 8 monomer units results in a stronger reversed EOF (Table 4.2), which could be used for simultaneous separations.

Figure 4.7 shows the simultaneous separation of three acidic proteins and two basic proteins using a coating consisting of 0.1 mM DODAB/0.01% POE 8 stearate ($\mu_{\text{eof}} = -1.4 (\pm 0.05) \times 10^{-4} \text{ cm}^2/\text{Vs}$). The dip in the baseline following the α -lactalbumin peak represents the EOF. It is not present in the other electropherograms as the EOF is too suppressed for it to migrate off the capillary in a reasonable time. Calcium chloride was added to the run buffer. It was expected that the calcium would reduce the electrostatic interaction of the acidic proteins (negatively charged) with any DODAB (positively charged) that is exposed. Calcium was added to the run buffer in a separation of

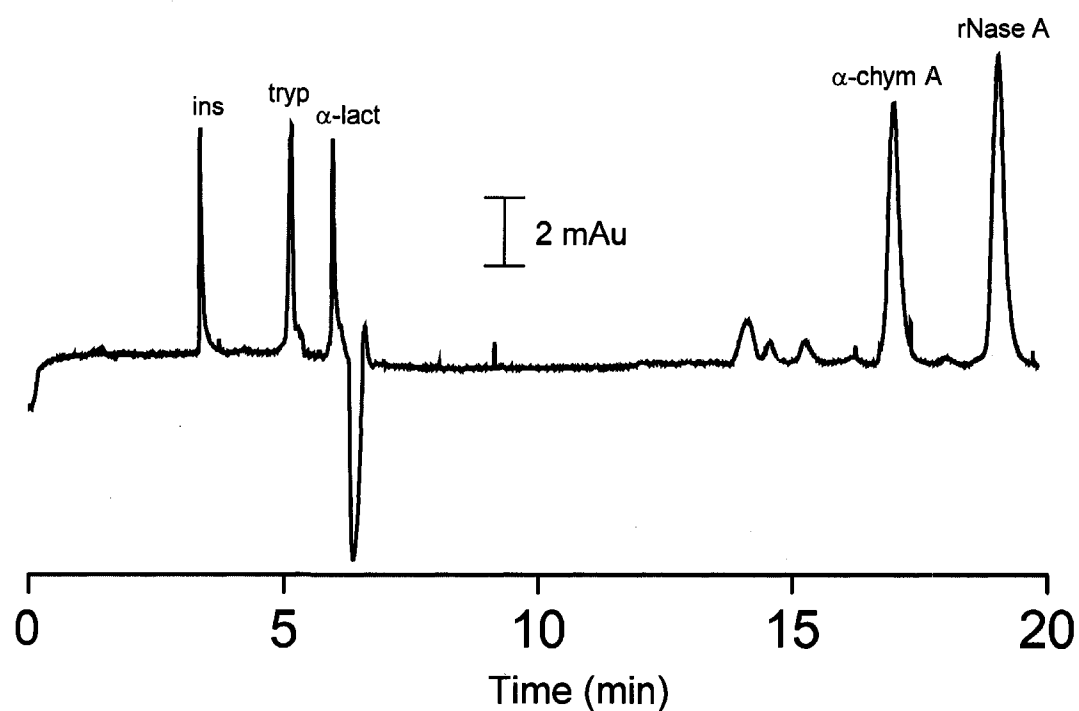


Figure 4.7: Separation of Three Acidic and Two Basic Proteins on a 0.1 mM DODAB/0.01% POE 8 Stearate Coated Capillary
Experimental conditions: applied voltage, -10 kV; 27 cm × 50 μm I.D. capillary (20 cm to detector); 75 mM Tris-acetate with 20 mM CaCl₂ buffer, pH 6.4; λ, 214 nm; 0.2 mg/mL of each protein; temperature, 25°C.

recombinant human deoxyribonuclease (rhDNA) and was found to dramatically improve resolution as a result of the calcium binding to the rhDNA.⁵³ In the absence of calcium, the resolution of the acidic proteins degraded after the first run on a 0.1 mM DODAB/0.02% POE 8 stearate coating at pH 7.4. Therefore, calcium was kept in the running buffer for the simultaneous separation on the 0.1 mM DODAB/0.01%POE stearate. The efficiencies range from 20 000 – 90 000 plates/m for the acidic proteins and 110 000 – 140 000 plates/m for the basic proteins. The values for the acidic proteins are lower than those obtained for the same proteins at pH 7.4 on the 0.1 mM DODAB/0.1% POE 40 stearate coating (Section 3.3.2), whereas the value for the ribonuclease A on the 0.1 mM DODAB/0.01% POE 8 stearate coating is higher than that obtained at pH 7.4 on the 0.1 mM DODAB/0.1% POE 40 stearate coating. These efficiencies are lower than those calculated for a simultaneous acidic and basic protein separation using a zwitterionic additive (560 000 – 840 000 plates/m),²⁴ and for those achieved on a 1,2-dilauroyl-*sn*-phosphatidylcholine (DLPC)/DDAB coating (> 400 000 plates/m).⁵⁴ The efficiencies are comparable to those obtained using low concentrations (< 0.8%) of polydiallyldimethylammonium chloride (PDADMAC) as a buffer additive.⁵⁵ Six consecutive runs were performed with a full strip (Sec. 4.3.1.5) and recoat between each run (RSDs: 1.5 – 4.8%). Injection of cytochrome *c* or lysozyme yielded no peaks within 60 min, due to these proteins having a higher mobility than the EOF.

4.3.1.5 Capillary Age

The effect of capillary age on the coating was also studied. A freshly cut capillary was coated with the 0.1 mM DODAB/0.5% POE 40 stearate. A separation of four basic proteins on this capillary at pH 3.0 is shown in Figure 4.8 (top trace). The same

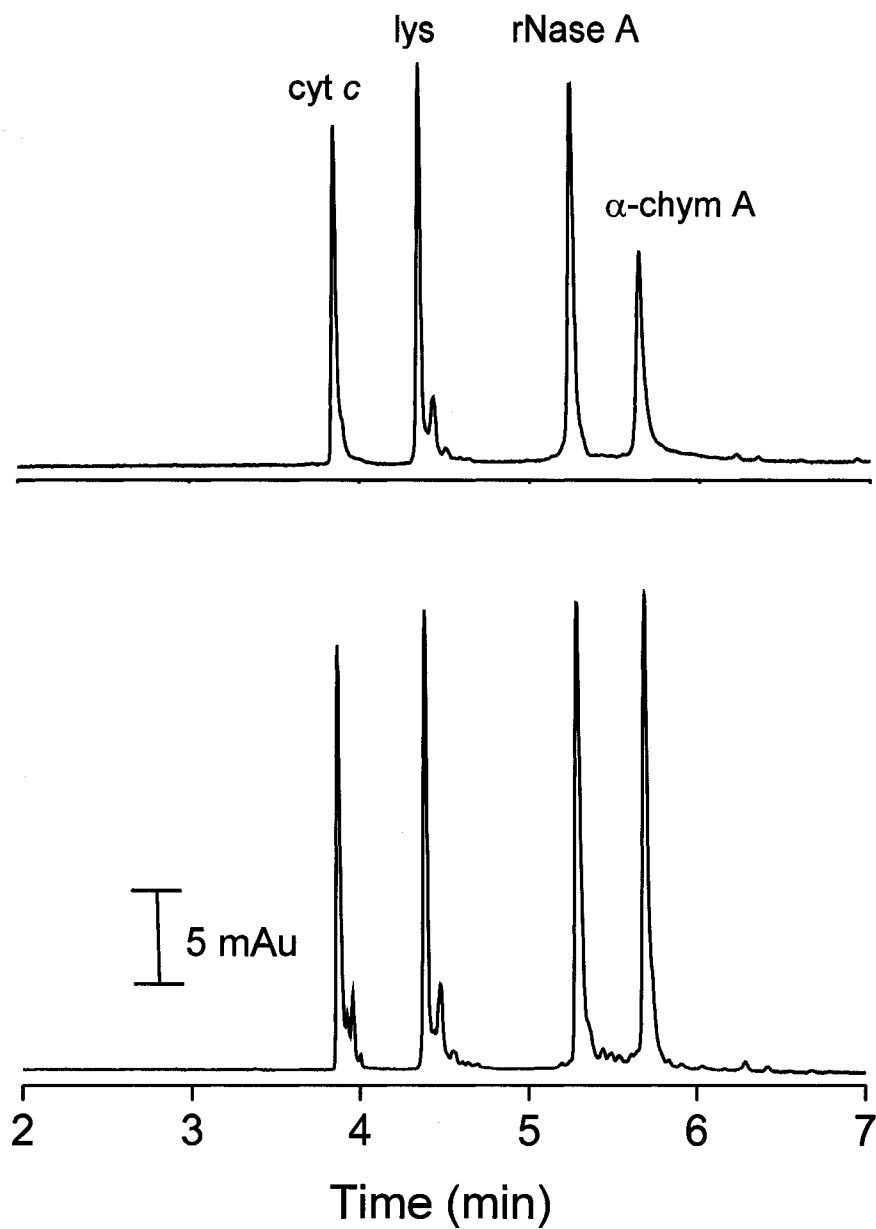


Figure 4.8: Separation of Basic Proteins on a New (top trace) and a Previously Coated Stripped (bottom trace) Capillary Freshly Coated with 0.1 mM DODAB/0.5% POE 40 Stearate

Experimental conditions: applied voltage, +10 kV; 27 cm \times 50 μ m I.D. capillary (20 cm to detector); 50 mM sodium phosphate buffer, pH 3.0; λ , 214 nm; 0.2 mg/mL of each protein; temperature, 25°C.

separation (bottom trace in Figure 4.8) was carried out on a capillary that had previously been coated over a period of five weeks with other DODAB/POE stearate coatings at pH 3.0 and stripped (i.e., rinsed with methanol) before each new coating was applied.

Efficiencies for all proteins do not change significantly after a period of five weeks of continuous use of the capillary. This result suggests that there is limited if any irreversible adsorption occurring over this period of time.

4.3.1.6 Coating Stability

Double chain surfactants can be used as semi-permanent coatings due to the stability imparted by the surfactant's ability to form bilayers on the capillary wall.⁵⁶ A number of factors influence the stability of such semi-permanent coatings.⁴⁰ Factors that minimize the critical micelle concentration (cmc) of the surfactant (e.g., increased ionic strength and a buffer counter-ion that interacts more strongly with quaternary amines) increase the stability of the bilayer.⁴⁰ Increasing the hydrophobicity of the surfactant by increasing the carbon chain length also decreases the cmc and thus increases the stability of the bilayer.¹³ For this reason, DODAB was chosen for the surfactant portion of the coating used in Chapters 3 and 4.

A DODAB/0.075% POE 40 stearate coating was prepared by flowing 0.1 mM DODAB/0.075% POE 40 stearate through a capillary for 10 min. The coating stability was monitored by injecting a sample of four basic proteins fourteen times with no recoating between runs. Table 4.3 summarizes the results. The migration times for the basic proteins gradually increased with successive injections, resulting in an upward drift in migration times and a higher %RSD.

The mixed method of preparing the coating results in POE stearate both inside and outside of the vesicle (Figure 4.1, Method A). The POE chains on the outside of the vesicle may interfere with the ability of the DODAB to adhere to the walls as discussed in Section 4.3.1.1. One way of overcoming this is to use another coating method whereby the DODAB is first rinsed through the capillary followed by the POE stearate, as will be discussed in Section 4.3.2.

4.3.2 Sequential Coating Method

Coatings prepared from double-chain surfactants have been shown to produce stable semi-permanent coatings.^{13,39,57,58} To increase the stability and flexibility of the surfactant/diblock copolymer coating used in this work, a different coating method was investigated (Figure 4.1, Method B). With this method, the DODAB solution is first flowed through the capillary to form the bilayer on the capillary wall. This is followed by a flow of POE stearate solution. The stearate chains of the polymer are hypothesized to intercalate into the hydrophobic portion of the DODAB bilayer. Drummond et al. examined the interaction of POE 100 stearate with a trimeric surfactant on a surface and

Table 4.3: Efficiency Range and %RSD of Basic Protein Migration Times for Mixed and Sequential Coating Methods Using 0.1 mM DODAB and 0.075% POE 40 Stearate^a

Coating Method	Efficiency Range (x10 ³ plates/m) ^b	Number of Consecutive Runs	% RSD Range
Mixed	500 - 790	14	2.4 – 4.6
Sequential	740 - 960	28	0.4 – 0.5

^a 3 s injection of cytochrome *c*, lysozyme, ribonuclease A, and α -chymotrypsinogen A, no recoating between runs, 50 mM Na₃PO₄, pH 3.0, +17.5 kV

^b Efficiencies calculated using width-at-half-height method.

noted that the polymers became co-adsorbed into the surfactant bilayer and were not just adsorbed onto the surface.⁵⁹

4.3.2.1 Temporal Coating Studies

As mentioned above, Drummond et al. studied the interaction of a trimeric surfactant and POE 100 stearate with mica surfaces.⁵⁹ The surfactant was left to form a bilayer on the surface overnight and the polymer was added the following day. The exchange of the polymer molecules with the cationic surfactant molecules was observed to be a slow process. Changes in the thickness of the film and adhesion energy were noted up to 30 hours after the polymer was added to the solution. Therefore, the kinetics of formation of a sequential DODAB then POE stearate coating was monitored in a similar fashion to that used in previous studies of the desorption of DDAB,⁴⁰ adsorption of phospholipids⁴⁸ and the coating time studies for the mixed method in Section 4.3.1.2. A new capillary was coated with DODAB for 10 min and temporal coating studies were carried out for POE 8, POE 40, and POE 100 stearate. That is, POE 40 stearate solution was flowed through the DODAB coated capillary for 0.5 min, followed by a 0.5 min buffer rinse to remove any excess coating material. Benzyl alcohol was injected and the EOF was determined. Subsequent runs were carried out in which the capillary was rinsed for increasingly longer periods of time with polymer followed by 0.5 min with buffer and the EOF was measured again.

Figures 4.9 to 4.11 shows the results of the coat time studies for various concentrations and lengths of POE stearate. Prior to flowing POE stearate through the capillary (time = 0), the capillary possesses a DODAB bilayer coating, which results in a strongly anodic (reversed) EOF ($\mu_{eof,DODAB}$). Upon rinsing the DODAB coated capillary

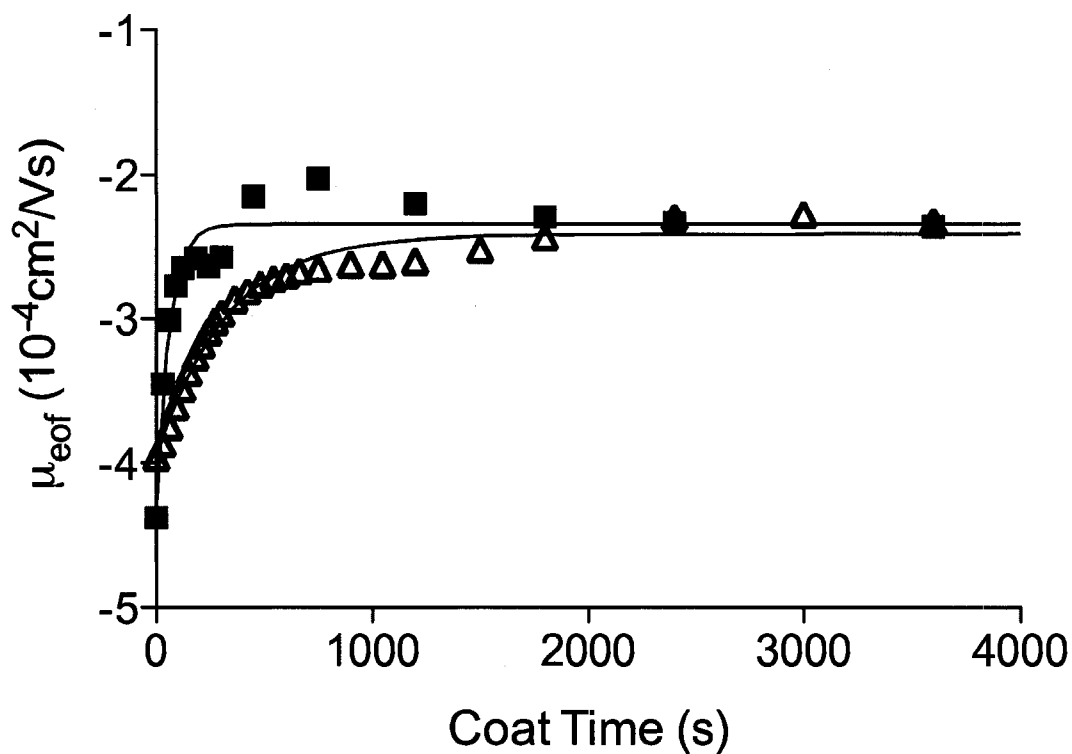


Figure 4.9: Effect of POE 8 Stearate Concentration on Intercalation Rate into the DODAB Bilayer. Concentrations used: 0.01% (1.6×10^{-4} M) (■) and 0.003% (0.5×10^{-4} M) (△) POE 8 stearate.

Experimental conditions: DODAB concentration, 0.1 mM; applied voltage, -15 kV; 47 cm \times 50 μm I.D. capillary (40 cm to detector); 50 mM sodium phosphate buffer, pH 3.0; λ , 214 nm; 2 mM benzyl alcohol injected for 3 s at 0.5 psi; temperature, 25°C; data is fit to equation 4.2.

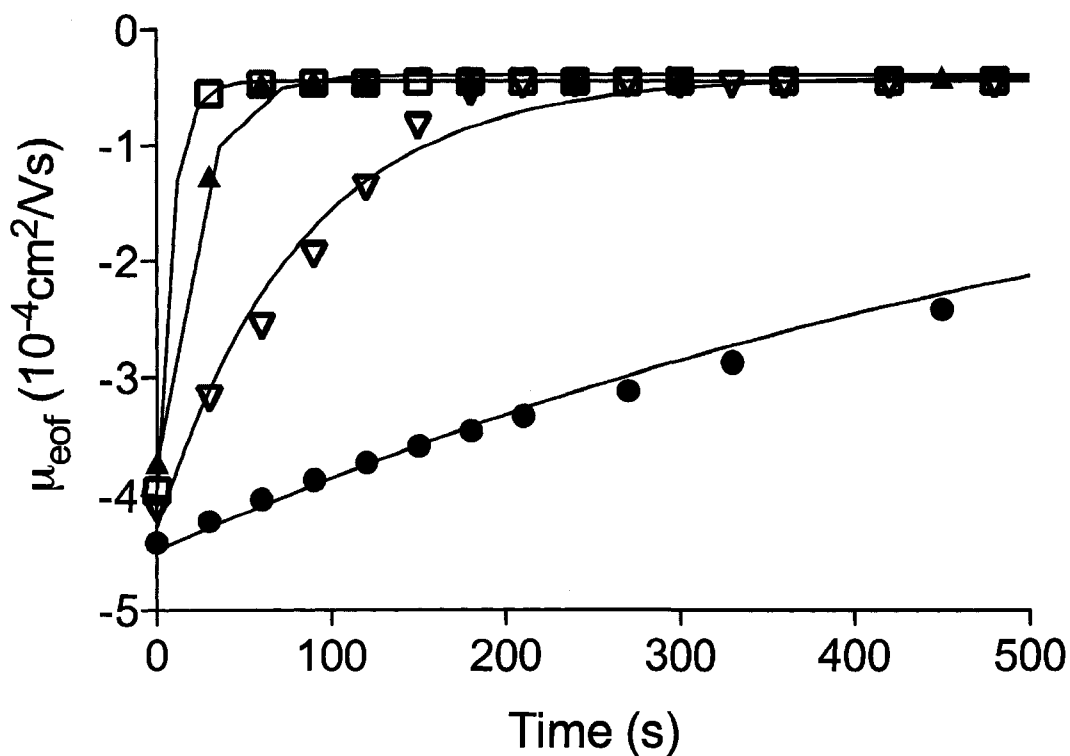


Figure 4.10: Effect of POE 40 Stearate Concentration on the Intercalation Rate into the DODAB Bilayer. Concentrations used: 0.01% (0.5×10^{-4} M) (\square), 0.006% (0.3×10^{-4} M) (\blacktriangle), 0.002% (0.1×10^{-4} M) (∇), and 0.0004% (0.02×10^{-4} M) (\bullet) POE 40 stearate.

Experimental conditions: DODAB concentration, 0.1 mM; applied voltage, -15 or -17.5 kV; 47 cm \times 50 μ m I.D. capillary (40 cm to detector); 50 mM sodium phosphate buffer, pH 3.0; λ , 214 nm; 2 mM benzyl alcohol injected for 3 s at 0.5 psi; temperature, 25°C; data is fit to equation 4.2.

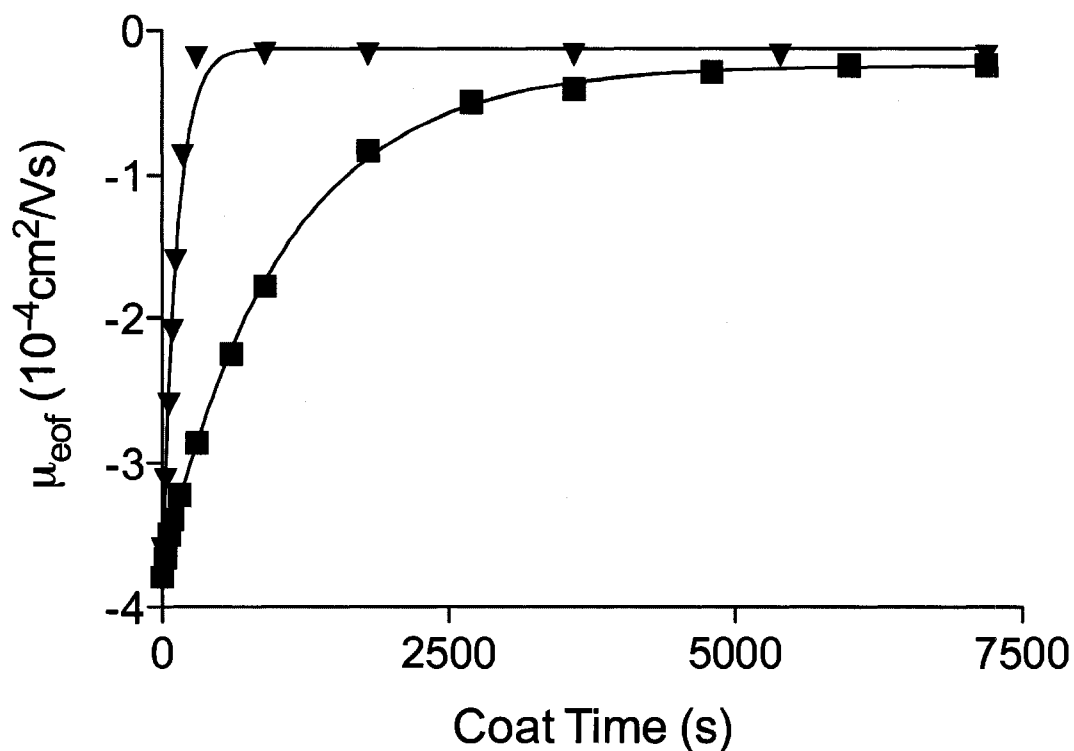


Figure 4.11: Effect of POE 100 Stearate Concentration on Intercalation Rate into the DODAB Bilayer. Concentrations used: 0.0009% (0.02×10^{-4} M) (\blacktriangledown) and 0.0005% (0.01×10^{-4} M) (\blacksquare) POE 100 stearate.

Experimental conditions: DODAB concentration, 0.1 mM; applied voltage, -15 or -17.5 kV; 47 cm \times 50 μm I.D. capillary (40 cm to detector); 50 mM sodium phosphate buffer, pH 3.0; λ , 214 nm; 2 mM benzyl alcohol injected for 3 s at 0.5 psi; temperature, 25°C; data is fit to equation 4.2.

with POE stearate, the EOF gradually becomes more attenuated until it reaches the more suppressed EOF characteristic of a fully formed DODAB/POE stearate coating ($\mu_{eof, DODAB+POE\ stearate}$). The curves in Figures 4.9-4.11 were fit to the first order kinetic expression:

$$\mu_{eof} = \mu_{eof, DODAB} + ((\mu_{eof, DODAB+POE\ stearate} - \mu_{eof, DODAB}) * (1 - e^{-kt})) \quad (4.2)$$

using Prism (version 4.00, GraphPad Software Inc., San Diego, CA) where μ_{eof} is the observed EOF and k is the formation constant for the coating. With the exception of the most concentrated POE 8 stearate, which exhibits an increase in EOF before plateauing, equation 4.2 fit the data with correlation coefficients (r^2) greater than 0.98 (Table 4.4). As was observed with the mixed coating procedure (Table 4.2), the EOF of the DODAB/POE stearate coating ($\mu_{eof, DODAB+POE\ stearate}$) becomes more suppressed as the length of the POE block increases. The EOF in the presence of the coating is weakly dependent on the concentration of the POE stearate at the low concentrations studied above.

For all POE stearate lengths, the rate of DODAB/POE stearate coating formation (k) increased with increasing concentration of POE stearate. Figure 4.12 shows a plot of the formation constants for the DODAB/POE 40 stearate coating versus the % POE 40 stearate (limited data precludes preparing similar plots for POE 8 and 100 stearate). Figure 4.12 suggests the rate of the POE stearate intercalating into the bilayer increases linearly with the POE 40 stearate concentration.

It was noted in Figures 4.9 to 4.11 that the EOF stabilizes more quickly with increasing polymer concentration. This is reflected in the rate constants for each concentration examined. The trend is similar to that observed with phospholipid bilayer

Table 4.4: EOF Mobility, Rate Constant and Correlation Coefficient for Sequential DODAB then POE Stearate Coatings^{a,b}

Stearate Polymer	Polymer Concentration %, ($\times 10^{-4} \text{M}$)	$\mu_{\text{eof,DODAB}}$ ($10^{-4} \text{ cm}^2/\text{Vs}$)	$\mu_{\text{eof,DODAB + POE}}$ ($10^{-4} \text{ cm}^2/\text{Vs}$) ^c	k (10^{-3} s^{-1}) ^d	r^2
POE 8	0.003 (0.5)	-4.0	-2.40 (± 0.01)	3.1 (± 0.2)	0.980
POE 8	0.01 (1.6)	-4.4	-2.37 (± 0.01)	16.5 (± 2.4)	0.938
POE 40	0.0004 (0.02)	-4.4	-0.50 (± 0.01)	1.6 (± 0.1)	0.992
POE 40	0.002 (0.1)	-4.1	-0.47 (± 0.004)	12.0 (± 0.8)	0.981
POE 40	0.006 (0.3)	-3.7	-0.37 (± 0.002)	46.9 (± 1.7)	0.998
POE 40	0.01 (0.5)	-4.0	-0.44 (± 0.01)	116.2 (± 3.8)	0.999
POE 100	0.0005 (0.01)	-3.8	-0.24 (± 0.03)	0.9 (± 0.0)	0.999
POE 100	0.0009 (0.02)	-3.6	-0.17 (± 0.005)	7.7 (± 0.6)	0.988

^a Data shown in Figures 4.9, 4.10 and 4.11

^b Capillary coated with 0.1 mM DODAB followed by successive polymer rinses, 50 mM Na_3PO_4 , pH 3.0

^c Standard deviation in brackets

^d Standard error (i.e., standard deviation divided by square root of the number of replicates) in brackets

coatings.⁴⁸ In this work the hydrophobic portion of the polymer is intercalating into the DODAB bilayer, whereas the phospholipid is coating the bare capillary. Still, the trend in rate constants is similar between the two types of coatings suggesting a comparable dependence on polymer/phospholipid concentration.

Table 4.4 also shows that for a given concentration, longer POE polymers form a stable coating more quickly than their shorter chain counterparts. For example at $0.5 \times 10^{-4} \text{ M}$ POE stearate, the rate constant is almost two orders of magnitude greater for the POE 40 stearate than the POE 8 stearate. This is reflected in Figure 4.10 by the early stabilization of the EOF (\blacklozenge). When comparing $0.02 \times 10^{-4} \text{ M}$ POE 40 and POE 100 stearate, the coating formation is a factor of three faster for the POE 100 stearate. All

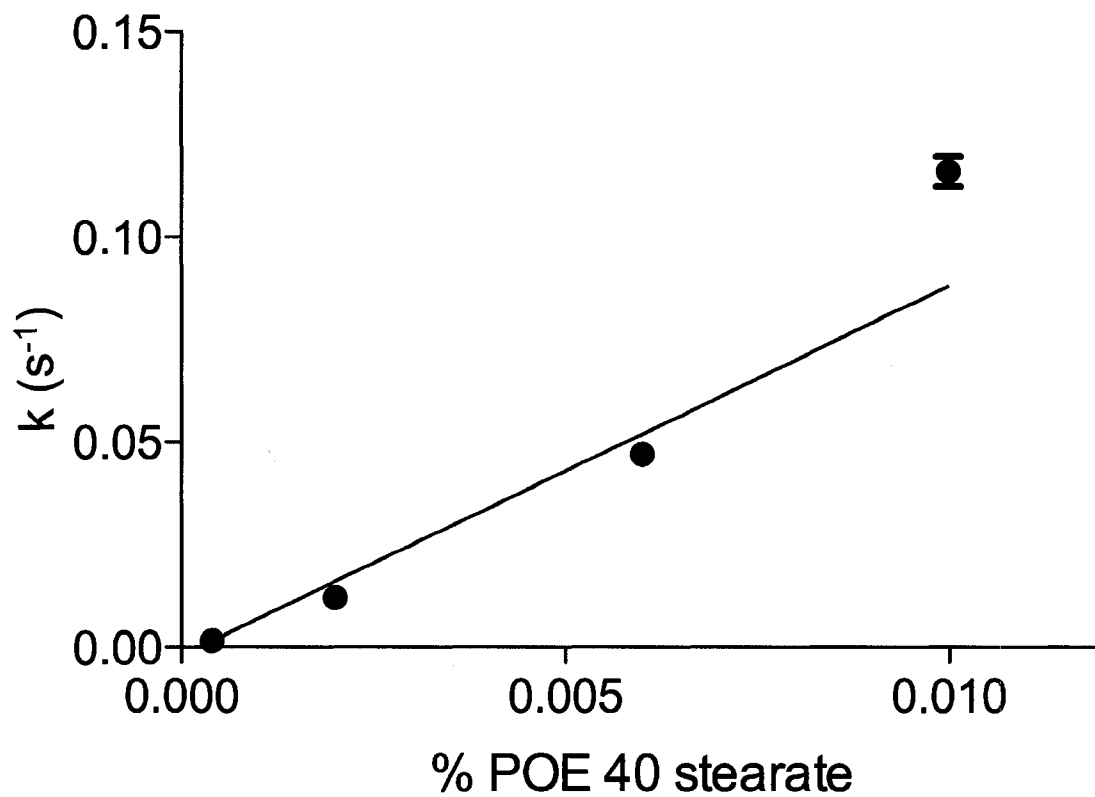


Figure 4.12: Rate Constant vs. POE 40 Stearate Concentration Rinsed through the DODAB Coated Capillary

Experimental conditions: See Figure 4.10. Points represent the rate constants determined from the fits of the plots in Figure 4.10. Data were fit to a weighted linear regression (weighted by $1/y^2$), as the error scales with the k values. Error bars represent the standard error for each of the fits.

further studies were conducted using POE stearate concentrations and rinse times that would yield a saturated surface.

4.3.2.2 EOF Studies

4.3.2.2.1 EOF with DODAB/POE stearate coatings

The EOF was measured for a number of coatings with various POE 40 stearate concentrations prepared using the sequential method (Figure 4.1, Method B) at pH 3.0. Figure 4.13 compares the EOF in the presence of the sequential DODAB/POE 40 stearate coatings with the EOF observed in the presence of coatings formed using the mixed method (Figure 4.1, Method B). With the sequential coating method, a constant EOF of $-0.3 \times 10^{-4} \text{ cm}^2/\text{Vs}$ was observed for $> 0.01\%$ POE 40 stearate (i.e., suppressed). In contrast, with the mixed coating method the EOF is partially suppressed below 0.5% POE stearate, and essentially that of a bare capillary above 0.5% indicating that a full coating may not be formed under such conditions (Section 4.3.1.1).

Table 4.5 shows that the magnitude of the EOF for a DODAB/POE stearate coating depends on the length of the POE block, with longer POE blocks yielding greater suppression. Further, as evident in Figure 4.13, changes in the concentration of the POE stearate do not alter the EOF significantly. Thus a particular POE stearate will generate a stable and reproducible EOF.

4.3.2.2.2 Adjustable EOF with DODAB/POE stearate coatings

The ability to control the magnitude of the EOF is important in optimizing separations.^{12,19,21,22,24-27,29} However, as shown in Table 4.5, a discrete EOF is observed for each length of POE stearate. In theory very fine control of the EOF could be achieved

Table 4.5: EOF Values for the 0.01% POE 8, 40, and 100 Stearate Sequential Coatings

Coating ^a	μ_{eof} (10^{-4} cm ² /Vs)
DODAB then POE 8 stearate	-2.44 ^b
DODAB then POE 40 stearate	-0.44 ^b
DODAB then POE 100 stearate	-0.20

^a All DODAB concentrations are 0.1 mM, 50 mM Na₃PO₄, pH 3.0

^b Values taken from plateau regions of Figures 4.9 and 4.10 for POE 8 and 40 stearate

using a series of POE stearate in which the POE blocks differ by one monomer unit.

However, the POE stearate polymers are somewhat polydisperse. Robelin et al. note that the POE 50 stearate polymer can range in POE block size from 39 to 57 if purchased from Sigma.⁶⁰ Therefore, it is not feasible to vary the POE block size by one POE moiety.

Previous studies^{25-27,29} have achieved fine control of the EOF by mixing two discrete additives each of which has an intrinsic and different EOF. For example, anionic/cationic surfactant mixtures²⁵⁻²⁷ and zwitterionic/cationic surfactant mixtures²⁹ have been used. In a similar manner the EOF can be fine-tuned using mixtures of two POE stearate polymers (Figure 4.14). The capillary was first coated with DODAB and then rinsed with a mixture of POE 8 and POE 40 stearate. The POE 8 stearate concentration was kept constant at 0.01%, and the POE 40 stearate concentration was varied. Figure 4.14 shows that the EOF can be controlled from a moderately reversed EOF to a strongly suppressed EOF using these mixtures.

A similar study was carried out using POE 40 and POE 100 stearate. However since both additives individually yield a strongly suppressed EOF, the EOF could only be

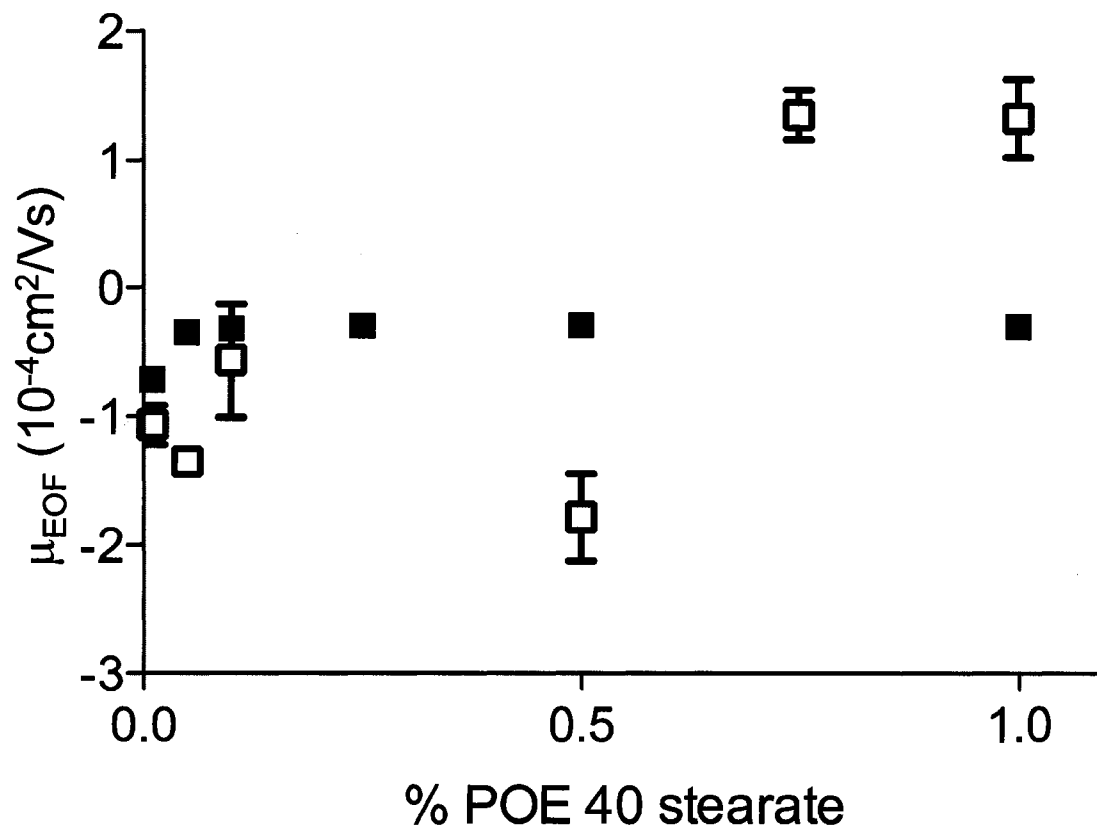


Figure 4.13: EOF stability for Mixed and Sequential Coating Methods using POE 40 Stearate

Experimental conditions: Sequential coating (\blacksquare): applied voltage, -15 kV; 47 cm \times 50 μm I.D. capillary (40 cm to detector); 50 mM sodium phosphate buffer, pH 3.0; λ , 214 nm; 2 mM benzyl alcohol injected for 3 s at 0.5 psi; temperature, 25°C; Mixed coating (\square): conditions as in Figure 4.2. The points are experimental data and error bars represent the standard deviation.

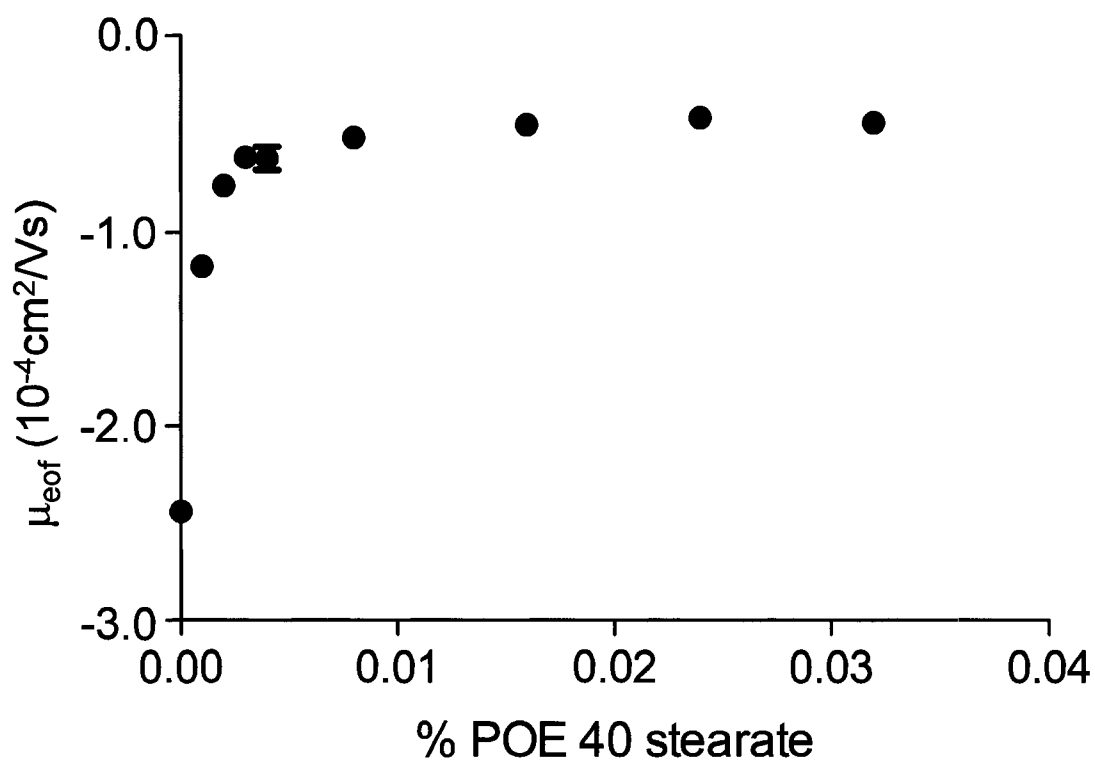


Figure 4.14: EOF vs. POE 40 Stearate Concentration on a Capillary first Coated with 0.1 mM DODAB followed by Coating with a Mixture of 0.01% POE 8 Stearate and POE 40 Stearate

Experimental conditions: applied voltage, -15 kV; 47 cm \times 50 μm I.D. capillary (40 cm to detector); 50 mM sodium phosphate buffer, pH 3.0; λ , 214 nm; 2 mM benzyl alcohol injected for 3 seconds at 0.5 psi; temperature, 25°C. Points are experimental data and error bars represent the standard deviation.

varied from $-0.36 \times 10^{-4} \text{ cm}^2/\text{Vs}$ to $-0.25 \times 10^{-4} \text{ cm}^2/\text{Vs}$ over the POE 100 stearate range of 0.00002% to 0.1% (with the POE 40 stearate concentration being held constant at 0.001%). The narrowness of this range precluded further study.

4.3.3 Protein Separations

Table 4.3 compares the performance of coatings prepared using the sequential method with comparable coatings formed using the mixed method (Figure 4.1). The same procedure was used to determine stability as was used for the mixed coating method (Section 4.3.1.6). As with the mixed method, there was no recoating performed between successive runs. Twice as many runs were performed with the sequential coating of DODAB then 0.075% POE 40 stearate than with the mixed method. A detectable drift was observed in migration times leading to high RSDs (2.4 - 4.6%) for migration times when the mixed method was used. No drift in migration times was observed for the sequential coating over 28 runs (double the number of runs on the mixed coating) and the RSDs were 0.4 - 0.5% (Figure 4.15). These values are lower than those obtained using DDAB alone (0.8 - 1%, $n=10$, with recoating between runs)³⁹ or when DDAB is mixed with the zwitterionic phospholipid, DLPC ($< 1.6\%$, $n=16$, with recoating between runs).⁵⁴ The RSDs for the protein migration times are also better than those obtained for a protein separation on an adsorbed PEO coating (0.8%, $n=5$)³⁶ and slightly higher than those on an adsorbed PEO-PPO-PEO coated capillary ($< 0.26\%$, $n=7$, no recoating).⁶¹ The peak efficiencies improve following the first run, as the peaks sharpen (Figure 4.15). The efficiencies over the next 28 runs remain high ($< 500\,000$ plates/m).

The efficiencies are also up to 30% greater with the sequential method (740,000 – 960,000 plates/m, Table 4.3). Both studies were completed with no recoating between

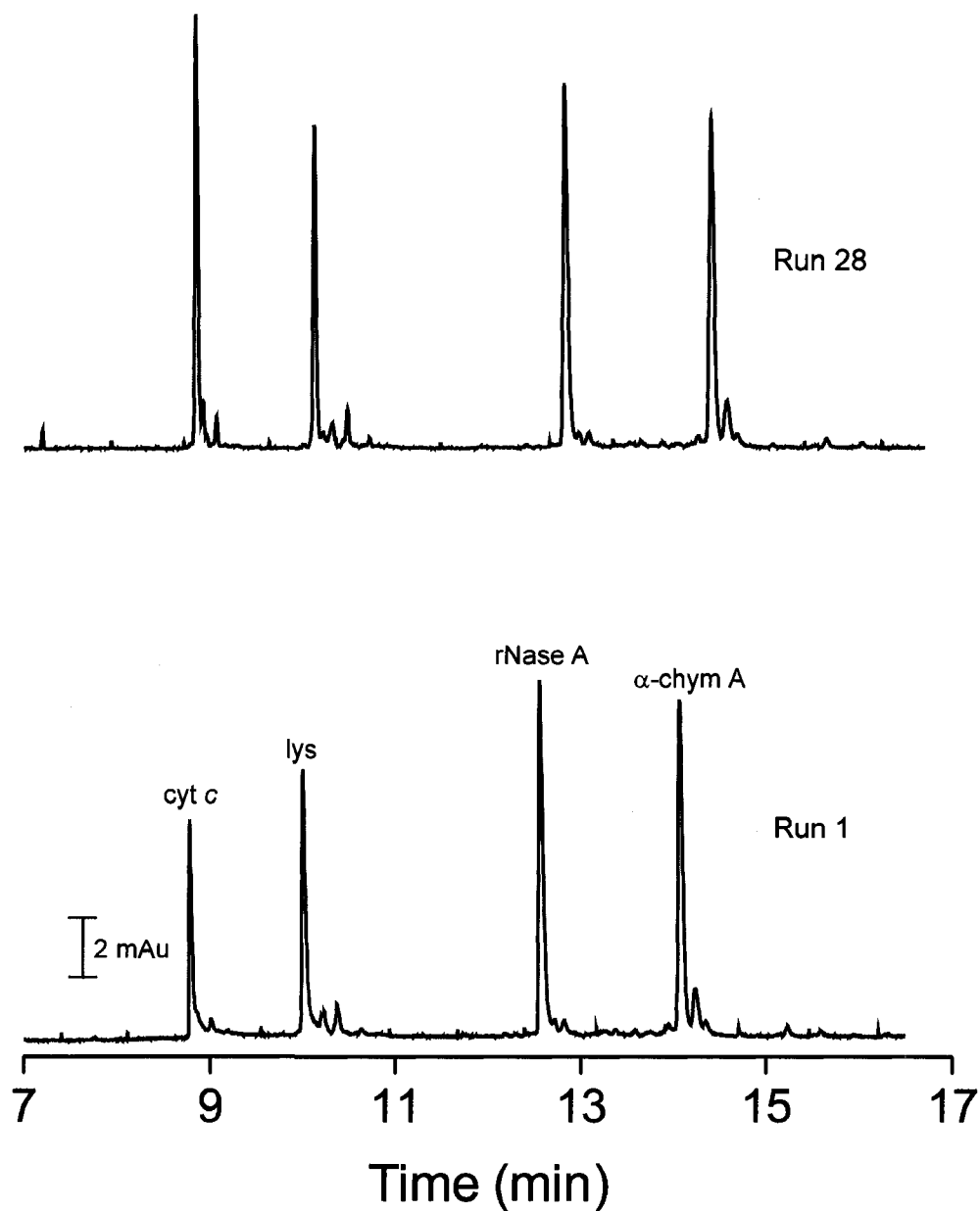


Figure 4.15: First and Twenty-eighth Separation of Basic Proteins on a Sequential 0.1 mM DODAB then 0.075% POE 40 Stearate Coating with no Recoating between Runs
Experimental conditions: applied voltage, -17.5 kV; 47 cm × 50 μm I.D. capillary (40 cm to detector); 50 mM sodium phosphate buffer, pH 3.0; λ, 214 nm; 0.1 mg/mL protein sample injected for 3 seconds at 0.5 psi; temperature, 25°C.

runs, demonstrating that the sequential method results in a very robust coating. This sequential method is superior to the mixed coating method in terms of coating stability.

As was done with the mixed DODAB/POE 40 stearate coatings, the separation of four standard basic proteins was carried out on coatings using a range of POE 40 stearate concentrations (0.01 - 1%) prepared using the sequential coating method (Table 4.6). The efficiencies are consistently higher than those obtained from separations on a coating formed using the mixed method (Table 4.1). These results indicate that in addition to the sequential method forming more stable coatings, it also results in coatings better able to perform separations of basic proteins.

4.3.4 Histone Separations

Histones are the major structural proteins of chromatin, which packs DNA into higher order structures to accommodate the full genome.^{62,63} There are different classes of histones, which are classified based on their lysine and arginine content. Within these

Table 4.6: Efficiency Ranges and EOF Values for Basic Proteins Separated on Sequential 0.1 mM DODAB then POE 40 Stearate Coatings

Coating ^a	μ_{eof} ($\times 10^{-4} \text{ cm}^2/\text{Vs}$)	N, plates/m ($\times 10^3$) (Foley-Dorsey)			
		cyt c	lys	RNase A	α -chym A
0.01% POE 40 stearate	-0.72 ± 0.009	310	1 200	580	680
0.05% POE 40 stearate	-0.36 ± 0.006	360	1 180	680	870
0.075% POE 40 stearate		220	1 230	780	940
0.1% POE 40 stearate	-0.33 ± 0.009	530 ^b	1 100	690	1 040
0.25% POE 40 stearate	-0.31 ± 0.004	430 ^b	1 020	720	910
0.5% POE 40 stearate	-0.30 ± 0.003	420 ^b	900	750	870
1% POE 40 stearate	-0.31 ± 0.005	320 ^b	1 040	680	850

^a All capillaries are first coated with 0.1 mM DODAB; 50 mM Na_3PO_4 buffer, pH 3.0, 40/47 cm capillary, 0.1 mg/mL proteins

^b Calculated using width-at-half-height method

classes there are several variants or subtypes, comprised of different amino acid sequences.⁶⁴ Type III-S histone from calf thymus is separated in this work. This histone is lysine rich and mainly H1 in character.⁶⁵ CE can be an useful method to separate individual histones if an effective coating is used to prevent their adsorption onto the capillary wall.^{62,66,67} Recently, histone type III-S from calf thymus was separated into three H1 subtypes at pH 4.0 using a zwitterionic phospholipid coating.⁴⁸ Aguilar et al. separated histone type III-S from calf thymus on a hydroxypropylmethylcellulose (HPMC) coated capillary and observed one broad peak.⁶² Figure 4.16 shows resolution of nine possible histone subtypes using a sequential 0.1 mM DODAB then 0.075% POE 40 stearate coating. As noted in Chapter 3, when the EOF is suppressed the protein mobilities are able to come to the forefront, enabling greater resolution. As the EOF on this coating was both suppressed and reversed, six more peaks were visible than on the phospholipid coating, which had a suppressed normal EOF.

The first run for all sets of histone separations had very low peak areas. Similarly with phospholipids coating poor resolution and low peak areas for the histones were observed on the first run.⁴⁸ Subsequent runs on the sequential 0.1mM DODAB then 0.075% POE 40 stearate coating resulted in efficiencies of as high as 1.2 million plates/m. The third, fifth and ninth runs are shown in Figure 4.16 as they are representative of all of the separations. The migration time RSDs were $\leq 0.5\%$, which are comparable to those obtained on the phospholipid coating.

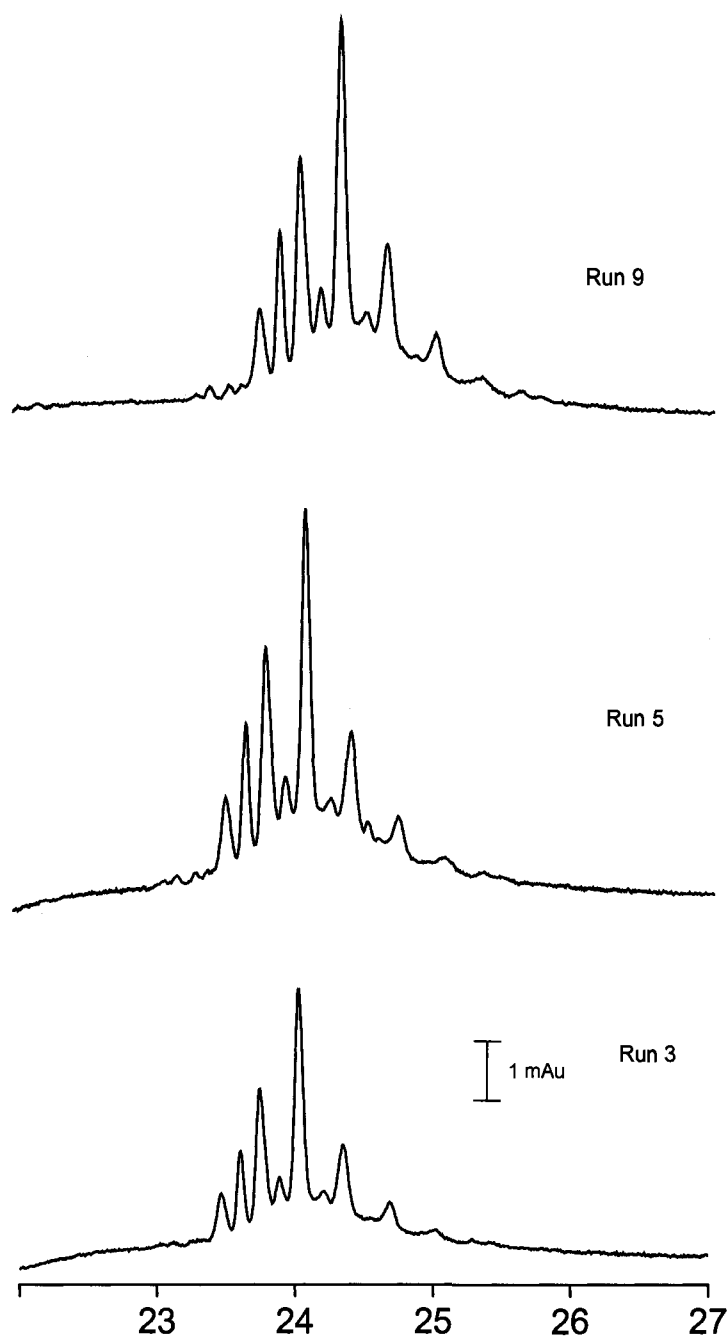


Figure 4.16: Histone Type III-S Separation on a 0.1 mM DODAB then 0.075% POE 40 Stearate Sequentially Coated Capillary

Experimental conditions: applied voltage, +15 kV; 67 cm \times 50 μ m I.D. capillary (60 cm to detector); 75 mM Tris formate buffer, pH 4.0; λ , 200 nm; 0.25 mg/mL histone type III-S injected for 4 s at 0.5 psi; temperature, 25°C.

4.4 Concluding Remarks

A coating prepared from DODAB and POE stearate polymer was demonstrated to be tunable by adjusting the polymer chain length. By modifying the POE length, a coating with a moderately reversed EOF that still possessed neutral, hydrophilic characteristics was obtained. A shorter POE length resulted in an EOF appropriate for the simultaneous separation of basic and acidic proteins. A sequential rather than mixed method for coating preparation produces a more stable coating that can separate basic proteins with higher efficiency. The EOF in the presence of this coating was tunable by varying polymer chain length, and by mixing polymer chains of different lengths. Histone proteins can be separated with high efficiency into a large number of subtypes on coatings formed using the sequential method.

4.5 References

- (1) Karger, B. L.; Chu, Y. H.; Foret, F., *Annu. Rev. Biophys. Biomed.* **1995**, *24*, 579-610.
- (2) Quigley, W. W. C.; Dovichi, N. J., *Anal. Chem.* **2004**, *76*, 4645-4658.
- (3) Schure, M. R.; Lenhoff, A. M., *Anal. Chem.* **1993**, *65*, 3024-3037.
- (4) Lauer, H. H.; McManigill, D., *Anal. Chem.* **1986**, *58*, 166-170.
- (5) Towns, J. K.; Regnier, F. E., *Anal. Chem.* **1991**, *63*, 1126-1132.
- (6) Jiang, W.; Awasum, J. N.; Irgum, K., *Anal. Chem.* **2003**, *75*, 2768-2774.
- (7) Towns, J. K.; Regnier, F. E., *J. Chromatogr.* **1990**, *516*, 69-78.
- (8) Cifuentes, A.; Diez-Masa, J. C.; Fritz, J.; Anselmetti, D.; Bruno, A. E., *Anal. Chem.* **1998**, *70*, 3458-3462.
- (9) Gilges, M.; Kleemiss, M. H.; Schomburg, G., *Anal. Chem.* **1994**, *66*, 2038-2046.
- (10) Chiu, R. W.; Jimenez, J. C.; Monnig, C. A., *Anal. Chim. Acta* **1995**, *307*, 193-201.
- (11) Graul, T. W.; Schlenoff, J. B., *Anal. Chem.* **1999**, *71*, 4007-4013.
- (12) Corradini, D.; Bevilacqua, L.; Nicoletti, I., *Chromatographia* **2005**, *62*, S43-S50.
- (13) Yassine, M. M.; Lucy, C. A., *Anal. Chem.* **2005**, *77*, 620-625.
- (14) Cunliffe, J. M.; Baryla, N. E.; Lucy, C. A., *Anal. Chem.* **2002**, *74*, 776-783.
- (15) Wang, C. Z.; Lucy, C. A., *Anal. Chem.* **2005**, *77*, 2015-2021.
- (16) Lucy, C. A.; MacDonald, A. M.; Gulcev, M. D., *J. Chromatogr. A* **2008**, *1184*, 81-105.
- (17) MacDonald, A. M.; Lucy, C. A., *J. Chromatogr. A* **2006**, *1130*, 265-271.
- (18) Blom, A.; Drummond, C.; Wanless, E. J.; Richetti, P.; Warr, G. G., *Langmuir* **2005**, *21*, 2779-2788.
- (19) Smith, J. T.; El Rassi, Z., *HRC-J. High Res. Chromatogr.* **1992**, *15*, 573-578.
- (20) Tien, P.; Chau, L. K.; Shieh, Y. Y.; Lin, W. C.; Wei, G. T., *Chem. Mater.* **2001**, *13*, 1124-1130.

- (21) Hsieh, Y. Y.; Lin, Y. H.; Yang, J. S.; Wei, G. T.; Tien, P.; Chau, L. K., *J. Chromatogr. A* **2002**, *952*, 255-266.
- (22) Guo, Y.; Imahori, G. A.; Colon, L. A., *J. Chromatogr. A* **1996**, *744*, 17-29.
- (23) Buchberger, W.; Haddad, P. R., *J. Chromatogr. A* **1994**, *687*, 343-349.
- (24) Baryla, N. E.; Lucy, C. A., *Anal. Chem.* **2000**, *72*, 2280-2284.
- (25) Hult, E. L.; Emmer; Roeraade, J., *J. Chromatogr. A* **1997**, *757*, 255-262.
- (26) Wang, C. Z.; Lucy, C. A., *Electrophoresis* **2004**, *25*, 825-832.
- (27) Liu, Q.; Yang, Y. M.; Yao, S. Z., *J. Chromatogr. A* **2008**, *1187*, 260-266.
- (28) Emmer, A.; Roeraade, J., *J. Liq. Chromatogr.* **1994**, *17*, 3831-3846.
- (29) Yeung, K. K. C.; Lucy, C. A., *J. Chromatogr. A* **1998**, *804*, 319-325.
- (30) Pereira, E. M. A.; Petri, D. F. S.; Carmona-Ribeiro, A. M., *J. Phys. Chem. B* **2006**, *110*, 10070-10074.
- (31) Ghosal, S., *Electrophoresis* **2004**, *25*, 214-228.
- (32) Williams, B. A.; Vigh, C., *Anal. Chem.* **1996**, *68*, 1174-1180.
- (33) Foley, J. P.; Dorsey, J. G., *Anal. Chem.* **1983**, *55*, 730-737.
- (34) Iki, N.; Yeung, E. S., *J. Chromatogr. A* **1996**, *731*, 273-282.
- (35) Preisler, J.; Yeung, E. S., *Anal. Chem.* **1996**, *68*, 2885-2889.
- (36) Tran, N. T.; Taverna, M.; Miccoli, L.; Angulo, J. F., *Electrophoresis* **2005**, *26*, 3105-3112.
- (37) Wiedmer, S. K.; Andersson, T.; Sundermann, M.; Riekkola, M. L.; Tenhu, H., *J. Polym. Sci. Pol. Phys.* **2007**, *45*, 2655-2663.
- (38) Yoshida, A.; Hashizaki, K.; Yamauchi, H.; Sakai, H.; Yokoyama, S.; Abe, M., *Langmuir* **1999**, *15*, 2333-2337.
- (39) Melanson, J. E.; Baryla, N. E.; Lucy, C. A., *Anal. Chem.* **2000**, *72*, 4110-4114.
- (40) Yassine, M. M.; Lucy, C. A., *Anal. Chem.* **2004**, *76*, 2983-2990.

- (41) Mohabbati, S.; Hjerten, S.; Westerlund, D., *Anal. Bioanal. Chem.* **2008**, *390*, 667-678.
- (42) Horvath, J.; Dolnik, V., *Electrophoresis* **2001**, *22*, 644-655.
- (43) Cretich, M.; Stastna, M.; Chrambach, A.; Chiari, M., *Electrophoresis* **2002**, *23*, 2274-2278.
- (44) Zhao, Z. X.; Malik, A.; Lee, M. L., *Anal. Chem.* **1993**, *65*, 2747-2752.
- (45) Madabhushi, R. S., *Electrophoresis* **1998**, *19*, 224-230.
- (46) Vermette, P.; Meagher, L., *Colloid. Surface. B* **2003**, *28*, 153-198.
- (47) Tsukanova, V.; Salesse, C., *J. Phys. Chem. B* **2004**, *108*, 10754-10764.
- (48) Gulcev, M. D.; Lucy, C. A., *Anal. Chem.* **2008**, *80*, 1806-1812.
- (49) McPherson, T.; Kidane, A.; Szleifer, I.; Park, K., *Langmuir* **1998**, *14*, 176-186.
- (50) Doherty, E. A. S.; Berglund, K. D.; Buchholz, B. A.; Kourkine, I. V.; Przybycien, T. M.; Tilton, R. D.; Barron, A. E., *Electrophoresis* **2002**, *23*, 2766-2776.
- (51) Cretich, M.; Chiari, M.; Pirri, G.; Crippa, A., *Electrophoresis* **2005**, *26*, 1913-1919.
- (52) Zalipsky, S.; Harris, J. M., *Poly(ethylene glycol): Chemistry and Biological Applications*, American Chemical Society, Washington, D.C., 1997.
- (53) Felten, C.; Quan, C. P.; Chen, A. B.; Canova-Davis, E.; McNerney, T.; Goetzinger, W. K.; Karger, B. L., *J. Chromatogr. A* **1999**, *853*, 295-308.
- (54) Baryla, N. E., Ph.D., Department of Chemistry, University of Alberta, 2002.
- (55) Lin, C. Y.; Yu, C. J.; Chen, Y. M.; Chang, H. C.; Tseng, W. L., *J. Chromatogr. A* **2007**, *1165*, 219-225.
- (56) Baryla, N. E.; Melanson, J. E.; McDermott, M. T.; Lucy, C. A., *Anal. Chem.* **2001**, *73*, 4558-4565.
- (57) Mohabbati, S.; Westerlund, D., *J. Chromatogr. A* **2006**, *1121*, 32-39.
- (58) Linden, M. V.; Wiedmer, S. K.; Hakala, R. M. S.; Riekkola, M. L., *J. Chromatogr. A* **2004**, *1051*, 61-68.
- (59) Drummond, C.; In, M.; Richetti, P., *Eur. Phys. J. E* **2004**, *15*, 159-165.

- (60) Robelin, C.; Duval, F. P.; Richetti, P.; Warr, G. G., *Langmuir* **2002**, *18*, 1634-1640.
- (61) Ng, C. L.; Lee, H. K.; Li, S. F. Y., *J. Chromatogr. A* **1994**, *659*, 427-434.
- (62) Aguilar, C.; Hofte, A. J. P.; Tjaden, U. R.; van der Greef, J., *J. Chromatogr. A* **2001**, *926*, 57-67.
- (63) von Holt, C., *BioEssays* **1985**, *3*, 120-124.
- (64) Bossi, A.; Gelfi, C.; Orsi, A.; Righetti, P. G., *J. Chromatogr. A* **1994**, *686*, 121-128.
- (65) Product Number H 5505, Product Information Sheet, Sigma Aldrich, Saint Louis, Missouri.
- (66) Gurley, L. R.; London, J. E.; Valdez, J. G., *J. Chromatogr.* **1991**, *559*, 431-443.
- (67) Lindner, H.; Helliger, W.; Dirschlmaier, A.; Talasz, H.; Wurm, M.; Sarg, B.; Jaquemar, M.; Puschendorf, B., *J. Chromatogr.* **1992**, *608*, 211-216.

Chapter Five: Factors Other Than Adsorption Affecting Peak Efficiencies in Capillary Electrophoretic Separations of Proteins*

5.1 Introduction

In theory, capillary electrophoresis (CE) should yield high efficiency separations of proteins. The charge on the proteins results in a high mobility, while the large voltages used and the low diffusion coefficient of proteins result in low longitudinal diffusion broadening (Section 1.3.1). In practice, protein adsorption onto the capillary seriously compromises separation performance. Substantial effort has gone into the creation of coatings to prevent adsorption. As detailed in Section 1.5, coatings can be grouped into three main classes: covalently bonded coatings, physically adsorbed polymeric coatings, and dynamic (e.g., surfactant) coatings.^{1,2}

Protein adsorption may be reversible and/or irreversible (Section 1.4.1). Thus, performance measures are required to monitor both types of adsorption. Peak efficiency and migration time reproducibility can be used as measures of reversible adsorption, while protein recovery, EOF reproducibility, and step changes in the baseline are indicators of irreversible adsorption (Section 1.4.2).² Of these factors, peak efficiencies are the most commonly quoted. However, the method used to calculate peak efficiency is often not mentioned. The calculation method can significantly affect the values obtained, especially if the peaks are asymmetrical.³

As discussed in Section 1.3.1, the only cause of band broadening in CE is ideally longitudinal diffusion.⁴ Often, conditions are not ideal, resulting in broadening from

* Experiments using the Agilent CE system were performed by a Chem 299 ROP student, Rachael DaCuhna, under my direction.

other sources⁵ such as Joule heating,^{4,6,7} interaction of the analyte with the capillary wall⁸⁻¹⁰ and analyte and buffer concentration issues.¹¹⁻¹³ All sources contributing to band broadening in CE can be illustrated by:

$$\sigma^2_{tot} = \sigma^2_{dif} + \sigma^2_{inj} + \sigma^2_{temp} + \sigma^2_{det} + \sigma^2_{emd} + \sigma^2_{ads} \quad (1.17)$$

where σ^2_{tot} is the total (observed) variance of an electrophoretic peak and σ^2_n are the individual contributions to the overall variance due to: longitudinal diffusion (σ^2_{dif}), injection band broadening (σ^2_{inj}), Joule heating (σ^2_{temp}), detector band broadening (σ^2_{det}), electromigration dispersion (σ^2_{emd}) and adsorption (σ^2_{ads}). These are discussed in detail in Section 1.3.¹⁴⁻¹⁶

Thus, factors other than protein adsorption can affect the efficiency measured for a protein separation. This was illustrated in the recent preparative CE studies by Yassine and Lucy, where the protein concentration, buffer concentration and buffer co-ion were all observed to affect the peak efficiencies of cytochrome *c*.¹⁷ Catai et al. studied the effect of buffer concentration on peptide separations on a PB-PVS SMIL coated capillary (Section 1.5.4).¹⁸ In the absence of stacking effects (Section 1.3.5), increasing the Tris-phosphate buffer concentration from 25 mM to 200 mM increased efficiencies from 300 000 – 500 000 plates/m for one positively charged peptide and from 200 000 – 900 000 plates/m for a second positively charged peptide. The enhanced performance in the presence of higher buffer concentrations was attributed to decreased interactions between the peptides and coating as well as a minimization of peak distortion by electromigration dispersion (EMD).¹⁸ Similar effects with higher buffer concentrations were noted by this group for protein separations at neutral pH on a PB-PVS coating.¹⁹

In this chapter, coating the capillary with DODAB/POE 40 stearate has effectively eliminated interactions between the proteins and the capillary wall. Recovery studies performed on this coating in Chapter 3 ranged from 92-97% for basic proteins and 84-95% recovery for acidic proteins. First, the effect of the method used to calculate peak efficiencies on peaks of various asymmetries is examined. The impact of instrumental and buffer conditions on band broadening under analytical conditions is investigated with capillaries coated with the DODAB/POE 40 stearate coating (Chapter 3) and on a commercially available polyvinyl alcohol coating (PVA). Specifically applied voltage, buffer concentration, buffer co-ion, and protein concentration are investigated with respect to the efficiency and asymmetry of basic proteins peaks. The effect of protein concentration is examined on DODAB/POE 40 stearate coatings prepared using both the mixed and sequential method (Chapter 4) under numerous solution conditions. Finally, the impact of buffer type and concentration on acidic protein separations performed on the DODAB/POE 40 stearate coating is investigated.

5.2 Experimental

5.2.1 Apparatus

All CE experiments were performed on either an Agilent HP^{3D} CE (Agilent Technologies, Palo Alto, CA, USA) instrument equipped with an on-column diode array UV absorbance detector or a Beckman P/ACE 2100 system (Beckman Instruments, Fullerton, CA, USA) equipped with an UV absorbance detector upgraded to 5000 series optics. Data acquisition (20 Hz) and control were performed on the Agilent instrument using ChemStation software (Agilent Technologies). For the P/ACE instrument the data acquisition rate was 5 Hz and the detector time constant was 0.5 s. Instrument control

and data acquisition were managed using P/ACE station software for Windows 95 (Beckman Instruments). EOF studies and protein separations were monitored at 214 nm. Benzyl alcohol (Aldrich, Milwaukee, WI, USA) was used as the neutral marker for the EOF studies. Untreated fused silica capillaries (Polymicro Technologies, Phoenix, AZ, USA) with an I.D. of 50 μm , O.D. of 360 μm , and total length of either 32 cm (23 cm to the detector) (Agilent) or 47 cm (40 cm to the detector) (Beckman) were used for the semi-permanent coating studies. A capillary coated with polyvinylalcohol (PVA) (Agilent) with an I.D. of 50 μm , O.D. of 360 μm , and total length of 32 cm (23 cm to the detector) was used as a commercially available comparison to the semi-permanent coating.

5.2.2 Chemicals

All solutions were prepared in Nanopure 18 M Ω water (Barnstead, Chicago, IL, USA). Buffers for the basic protein separations were prepared from orthophosphoric acid (BDH, Toronto, ON, Canada), and titrated to pH 3.0 with either sodium hydroxide (BDH), lithium hydroxide (BDH), or bis(2-hydroxyethyl)imino-tris(hydroxymethyl) methane (Bis-tris; Sigma, St. Louis, MO, USA). For the acidic protein separations, ultrapure tris(hydroxymethyl)aminomethane (Tris; Schwarz/Mann Biotech, Cleveland, OH, USA) was titrated to pH 7.4 with either reagent grade glacial acetic acid (Anachemia, Rouses Point, NY, USA) or reagent grade hydrochloric acid (Anachemia). The pH was measured using a Corning digital pH meter model 445 (Corning, Acton, MA, USA). The cationic surfactant dioctadecyldimethylammonium bromide (DODAB) was used as received from Aldrich. Polyoxyethylene (POE) (40) stearate was also purchased from Aldrich. The proteins lysozyme (chicken egg white), cytochrome *c*

(bovine heart), ribonuclease A (bovine pancreas), α -chymotrypsinogen A (bovine pancreas), insulin chain A oxidized (bovine insulin), trypsin inhibitor (soybean), and α -lactalbumin (bovine milk) were used as received from Sigma.

5.2.3 Preparation and Coating of the Surfactant/Polymer Solutions

Two methods were used to prepare the DODAB/POE 40 stearate solutions, the “mixed” method and the “sequential” method (Figure 4.1). These methods are described in detail in Section 4.2.3. For experiments performed on the Agilent instrument, only coatings prepared using the “mixed” method were used. A new bare fused silica capillary ($L_d=23$ cm, $L_t=32$ cm) was first rinsed for 10 min with 0.1 M NaOH. A 0.1 mM DODAB/0.1% POE 40 stearate solution was flowed through the capillary for 10 min to form the coating. Finally, a 1 min rinse with the buffer of interest was performed to remove excess surfactant/polymer solution. In subsequent runs, the coating procedure consisted of a 2.5 min 0.1 M NaOH rinse, a 7.5 min 0.1 mM DODAB/0.1% POE 40 stearate coat time, and a 1 min buffer rinse. For experiments using the PVA coated capillary ($L_d=23$ cm, $L_t=32$ cm), the only conditioning step performed was a 2 min buffer rinse before each injection, as per the manufacturer’s suggestion.²⁰

5.2.3 Protein Separations

All protein mixtures were injected for 3 s at 0.5 psi for experiments on the Beckman instrument. Protein separation was performed using sodium phosphate pH 3.0 buffer for the basic proteins and Tris-acetate or Tris-HCl pH 7.4 buffer for the anionic proteins. The buffers were devoid of the surfactant/polymer mixture. The applied voltage was +17.5 kV for basic protein separations and -20 kV for acidic protein separations, unless otherwise noted. Detection of proteins was performed at 214 nm.

All protein mixtures were 0.2 mg/mL and injected for 3 s at 0.5 psi for experiments performed using the Agilent instrument. Run buffers were sodium, lithium, and Bis-tris phosphate buffered at pH 3.0. The applied voltage was +10 kV, unless otherwise noted. Proteins were detected at 214 nm. Efficiencies were calculated using the Foley-Dorsey method²¹ or the width-at-half-height method, as noted. The effect of the method used on the measured efficiency is discussed in Section 5.3.1.

5.3 Results and Discussion

As demonstrated in Chapter 3, the 0.1 mM DODAB/0.1% POE 40 stearate coating is a stable, easily regenerated, semi-permanent coating that enables efficient protein separations. In Section 5.3.1, separation and buffer conditions are examined to assess how they affect protein peak efficiencies. In Section 5.3.2 comparison of this semi-permanent coating versus a commercially available, permanently coated PVA capillary is also carried out.

5.3.1 Measurement of N

There are numerous methods for calculating efficiencies in chromatographic and electrophoretic separations.³ For instance, in CE separations of proteins, papers have reported efficiencies based on width-at-half height²²⁻²⁵ and the Foley-Dorsey method.^{26,27} Even more commonly the method used to calculate efficiencies is not specified.²⁸⁻³¹ In many of the unspecified cases the width-at-half height method will have been used, as it is the implicit method with the Beckman and Agilent software.

The method used to calculate efficiencies can profoundly affect the measured values if the peaks are asymmetrical.³ Methods that assume a Gaussian peak shape (width-at-half-height, tangent method) bias efficiencies high. The magnitude of the bias

depends upon the degree of asymmetry and where along the peak the width is measured. Methods such as the width-at-half-height and tangent method, which make measurements high up on the peak, are considered the least accurate.³ As an alternate, the Foley-Dorsey method (Section 3.2.6) assumes an exponentially modified Gaussian (EMG) peak shape, and has been demonstrated with computer generated peaks to be accurate even for severely asymmetrical peaks.²¹

Thus, it is clear that methods such as the width-at-half-height should bias efficiency measurements high. However it was not clear how severe this effect would be for protein separations in CE. Therefore a comparison of efficiencies calculated using the width-at-half-height and the Foley-Dorsey method was made for lysozyme and ribonuclease A separated on a 0.1 mM DODAB/0.1% POE 40 stearate coated capillary under a variety of buffer conditions. In Figure 5.1a, the solid line indicates the expected behaviour if both calculation methods yielded the same efficiencies. Clearly, the efficiencies are biased high when the width-at-half-height method ($N_{1/2}$) is used. It is obvious there is a positive deviation from this line, particularly at low efficiencies. This is consistent with the simulations of Bidlingmeyer and Warren.³ Figure 5.1b depicts how this bias varies with peak shape. Fronting peaks ($B/A < 1$) and tailing peaks ($B/A > 1$) are more affected by the method used to calculate efficiencies than symmetrical peaks ($B/A = 1$) (i.e., higher % bias). The bias ranges from 1% for high efficiency symmetrical peaks to 82% for low efficiency asymmetrical peaks. This is also consistent with the simulations of Bidlingmeyer and Warren.³

A number of conclusions can be drawn from Figures 5.1a and b. Firstly, it is critical that the method used to calculate efficiencies be specified. Secondly, whenever

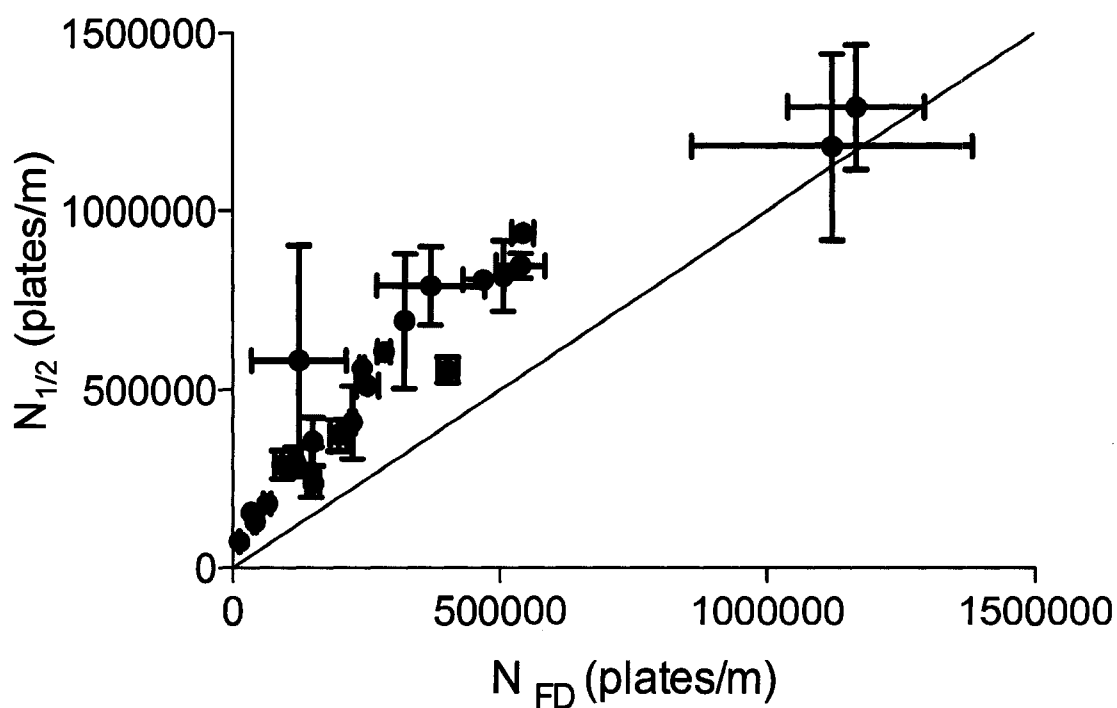


Figure 5.1a: Width-at-Half-Height Efficiencies ($N_{1/2}$) vs. Foley-Dorsey Efficiencies (N_{FD}) for Lysozyme and Ribonuclease A, on a 0.1 mM DODAB/0.1% POE 40 Stearate Coated Capillary. Error bars represent standard deviation.

Experimental conditions: capillary, 32 cm \times 50 μ m I.D. (23 cm to detector); 10, 20, 50 and 75 mM sodium, lithium, and Bis-tris phosphate buffers; injection, 3 s (0.5 psi) hydrodynamic injection of 0.2 mg/mL lysozyme and ribonuclease A; λ , 214 nm; temperature, 25°C; instrument, Agilent HP^{3D} CE.

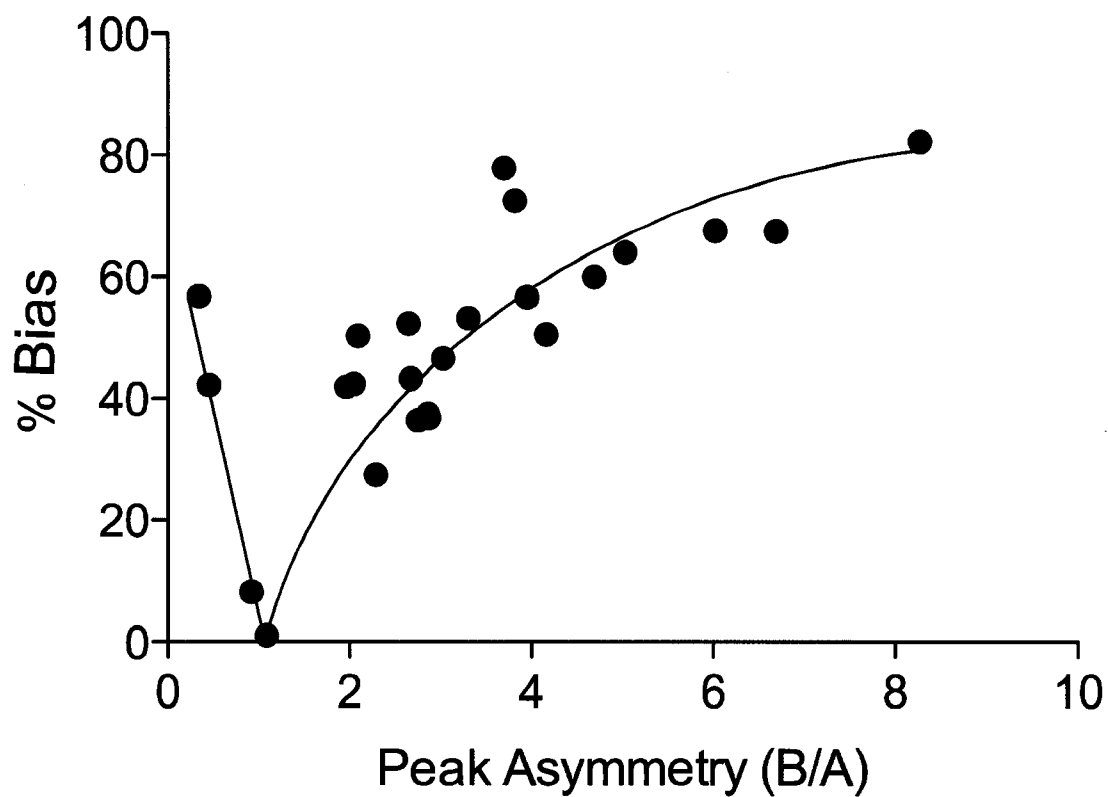


Figure 5.1b: % Bias of Peak Efficiencies as a result of Calculation Method vs. Peak Asymmetry (B/A) for Lysozyme and Ribonuclease A on a 0.1 mM DODAB/0.1% POE 40 Stearate Coated Capillary. Points are experimental data, line is a guide to the eye.
Experimental conditions: see Figure 5.1a

possible the Foley-Dorsey method should be used, as it is a fundamentally more accurate method to measure the efficiency of asymmetrical peaks. However, in some cases the use of the Foley-Dorsey method is not possible. For instance, cytochrome *c* and α -chymotrypsinogen A are excluded from the study in Figure 5.1 because a shoulder on these peaks made measurement of the asymmetry factor (and therefore the Foley-Dorsey efficiency) impossible. Thirdly, trends in efficiency are evident regardless of which method is used to measure *N*. Thus, the width-at-half-height method would be effective to monitor the effect of a particular variable on efficiency (as will be done below). This is consistent with Bidlingmeyer and Warren's conclusion that "*In some situations, the relative accuracy of the method may matter very little, as in the monitoring of a column throughout its useful lifetime. Here, it is the changes in efficiency...that are of interest.*"³

However, caution must be taken in comparing efficiencies if different measurement methods are used. Finally, Bidlingmeyer and Warren's recommendation of greater consideration of the peak asymmetry will be reflected in the following discussion.

5.3.2 Band broadening with DODAB/POE 40 Stearate Coated Capillaries

5.3.2.1 Effect of Voltage on Protein Separations

As discussed in Section 1.3.3, an Ohm's plot should always be performed to determine the maximum voltage that can be applied across the capillary without causing significant Joule heating.⁶ Under ideal conditions, the plot of current versus applied voltage is linear. When high electrolyte concentrations are used, resistance in the capillary is low. This leads to a high current, according to Ohm's law, as a result of the generation of Joule heat.³² In an Ohm's plot, the presence of significant Joule heat is indicated by deviations from linearity in the applied voltage vs. current plot. Ohm's plots

were constructed for each of the buffer co-ions and concentrations studied. Figure 5.2 shows an Ohm's plot constructed for the most concentrated buffer (100 mM sodium phosphate), for which Joule heating would be most significant. Above +10 kV curvature was evident, indicating Joule heating. Joule heating would be less significant for lower concentration sodium phosphate buffers. Also lithium and Bis-tris have a lower mobility than sodium (Table 5.1) and so conduct less current. Therefore, a voltage resulting in insignificant Joule heating for buffers containing sodium will also be within the useable voltage range for lithium and Bis-tris.

As discussed in Sections 1.3 and 5.3.1, peak efficiency is one of the most common measures for determining the effectiveness of a coating.² The efficiencies of protein separations on various DODAB/POE stearate coatings were measured in Chapters 3 and 4 using the optimum voltage determined by an Ohm's plot such as Figure 5.2. To examine the effect of voltage on peak efficiency, plots of efficiency versus voltage were constructed. Shown in Figure 5.3a and 5.3b are the plots of efficiency (width-at-half-height) vs. voltage for sodium phosphate and lithium phosphate buffers, respectively, for each of the four basic proteins investigated. Below +10 kV, efficiencies for all proteins in both buffers increase with voltage. This is in agreement with the improvement expected under ideal separation conditions (Section 1.3.1).³⁴ As the voltage increases, the time each analyte spends on the capillary decreases, allowing less time for longitudinal diffusion to occur and thus greater efficiency. However, at voltages higher than +10 kV, there is a general decrease in efficiencies. This is consistent with expectations from the Ohm's plot (Figure 5.2). It is also consistent with results in the literature. Hjerten observed van Deemter – like behaviour in a plot of plate height vs.

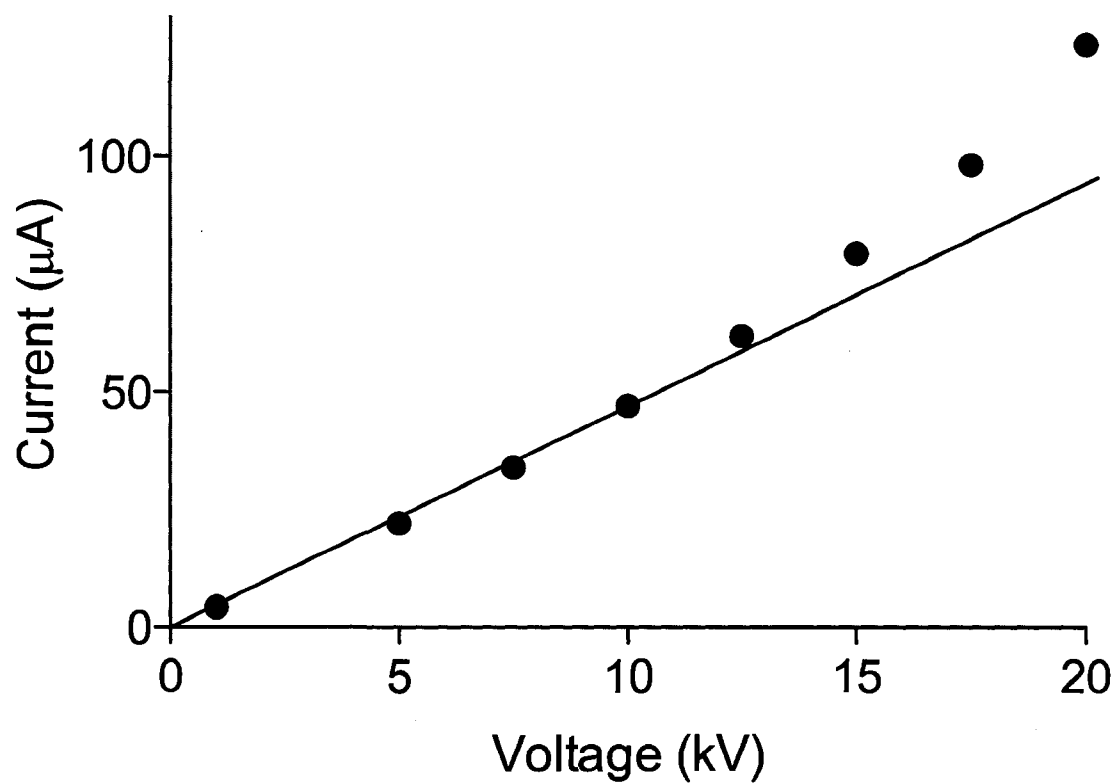


Figure 5.2: Ohm's Plot for 100 mM Sodium Phosphate, pH 3.0 on a 0.1 mM DODAB/0.1% POE 40 Stearate Coated Capillary.

Experimental conditions: capillary, 32 cm×50 µm I.D. (23 cm to detector); temperature, 25°C; instrument, Agilent HP^{3D} CE.

Table 5.1: Mobilities of Buffer Co-ions and Proteins in 75 mM Phosphate, pH 3.0

Buffer Co-ion	$\mu_{\text{co-ion}}^a$ ($10^{-4}\text{cm}^2/\text{Vs}$)	$\mu_{\text{cyt c}}$ ($10^{-4}\text{cm}^2/\text{Vs}$)	μ_{lys} ($10^{-4}\text{cm}^2/\text{Vs}$)	$\mu_{\text{rNase A}}$ ($10^{-4}\text{cm}^2/\text{Vs}$)	$\mu_{\alpha\text{-chym A}}$ ($10^{-4}\text{cm}^2/\text{Vs}$)
Na ⁺	4.4	2.4 ± 0.03	2.2 ± 0.03	1.8 ± 0.03	1.7 ± 0.03
Li ⁺	3.3	2.0 ± 0.1	1.8 ± 0.1	1.5 ± 0.001	1.3 ± 0.1
Bis-tris ⁺	1.9				

^a Calculated using Peakmaster version 5.1³³

electric field strength (i.e., applied voltage/cm) in capillary zone electrophoresis, indicating an optimum applied voltage.³⁵ Sepaniak and Cole observed similar behaviour in a study of factors affecting column efficiency in micellar electrokinetic chromatography (MEKC).³⁶ Ho Row et al. also noted that separation efficiency was highly dependent on separation voltage in an MEKC separation of nucleic acid constituents, and that an optimum existed.³⁷ All attributed this behaviour to Joule heating effects. In my work, above +10 kV the band broadening due to Joule heating overwhelms the increase in efficiency expected from the decreased longitudinal diffusion. Lysozyme in the lithium buffer is an exception in that no decrease in efficiencies is evident until +20 kV. In light of this data as well as the Ohm's plot (Figure 5.2), +10 kV was chosen as the applied voltage for all separations using the Agilent instrument.

5.3.2.2 Effect of Buffer Concentration

All buffer concentrations were more dilute than 100 mM to ensure Joule heating was not an issue during these separations. Buffer concentration has been shown to affect protein separations using bare capillaries, where adsorption would be significant. As early as 1989, Green and Jorgenson examined the effect of various concentrations of

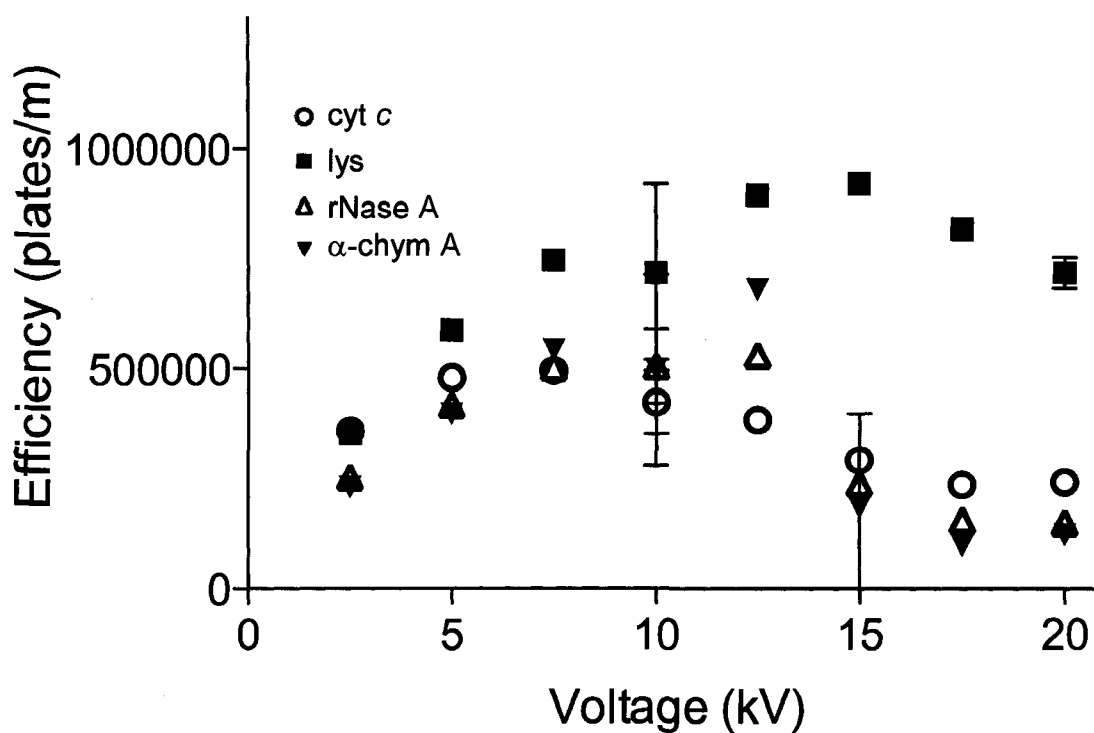


Figure 5.3a: Efficiency vs. Applied Voltage on a 0.1 mM DODAB/0.1% POE 40 Stearate Coated Capillary with 100 mM Sodium Phosphate Buffer, pH 3.0

Experimental conditions: capillary, 32 cm \times 50 μ m I.D. (23 cm to detector); injection, 3 s (0.5 psi) hydrodynamic injection of a mixture of 0.2 mg/mL basic proteins; λ , 214 nm; temperature, 25°C; instrument, Agilent HP^{3D} CE; efficiencies calculated using the width-at-half-height method.

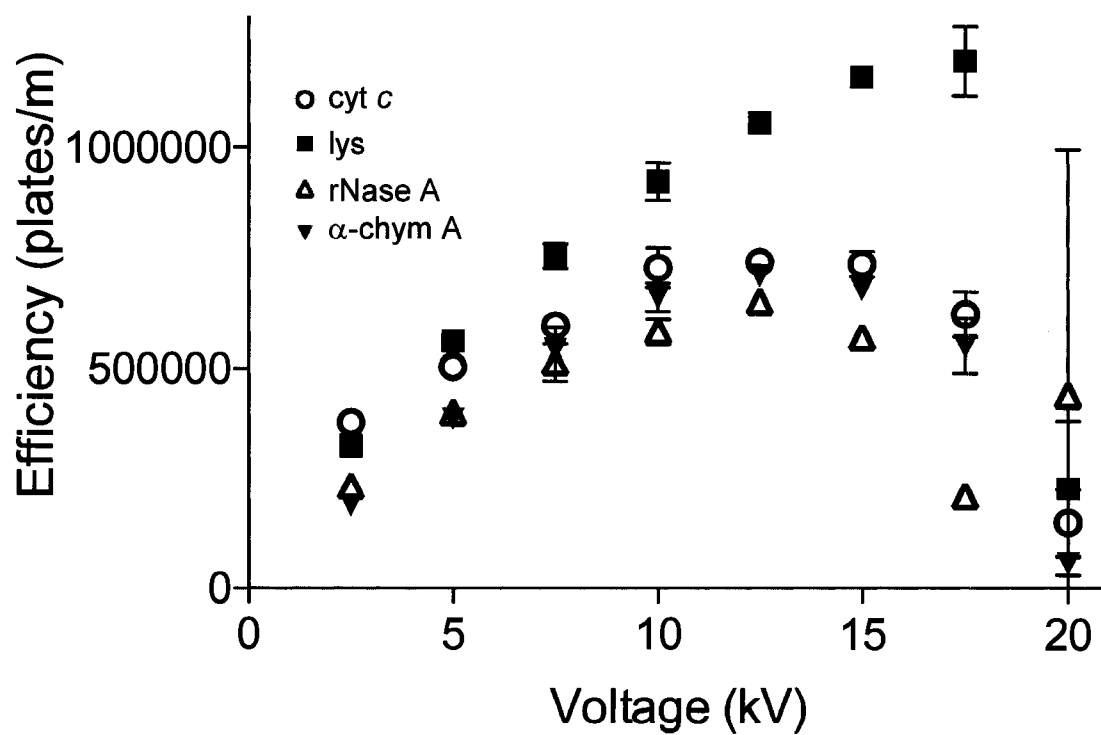


Figure 5.3b: Efficiency vs. Applied Voltage on a 0.1 mM DODAB/0.1% POE 40 Stearate Coated Capillary with 100 mM Lithium Phosphate Buffer, pH 3.0
Experimental conditions: See Figure 5.3a

alkali metal salts in the buffer on protein retention behaviour on a bare fused silica capillary.³⁸ Lysozyme and trypsinogen bound irreversibly to the capillary wall in the absence of added salt. No adsorption was observed when 250 mM potassium sulfate was added to the separation buffer due to the electrostatic screening provided by the buffer. This work was followed up by examining zwitterionic additives in buffers to prevent adsorption²⁸ as they do not increase conductivity at high concentrations. However, protein separations performed in the presence of these additives resulted in low efficiencies (< 30 000 plates/m). Efficiencies were low to moderate (170 000 - 250 000 plates/m) when both the zwitterionic betaine and potassium sulfate were added to a sodium phosphate buffer.²⁸ Although zwitterionic additives are not advantageous for preventing protein adsorption, they do show interesting effects on EOF enhancement, as discussed in Chapter 2.

As mentioned in Section 5.1, Catai et al. demonstrated that buffer concentration has a significant effect on peak efficiency in the presence of a coating.^{18,19} Protein peak efficiency increased from < 125 000 plates/m to 125 000 – 700 000 plates/m by increasing the Tris phosphate buffer concentration from 25 mM to 400 mM.¹⁹ This effect was attributed in part to fewer interactions between the proteins and coating at higher buffer concentrations.

Alternately if a buffer additive adsorbs onto the bare capillary, an increase in the additive concentration may improve efficiency by reducing protein adsorption (Section 1.5.1). For instance, increasing the concentration of diethylaminetriamine in the buffer from 20 to \geq 40 mM at pH 6.5 increased efficiencies for cytochrome *c* from 12 000 to 516 000 plates/m.²⁹

Recent studies have also observed efficiency improvements with higher buffer concentrations under conditions where adsorption broadening was not expected to be significant. Previous studies in our group have demonstrated that cationic bilayer coatings based on DDAB yield high efficiencies (560 000 – 750 000 plates/m) and quantitative recoveries for basic proteins.²² Nevertheless, a 3-fold increase in peak efficiency was observed upon increasing the concentration of sodium acetate buffer (pH 5.0) from 5 to 50 mM.³⁹

Similarly Chapter 3 demonstrated that the DODAB/POE 40 stearate coating also yields high efficiencies (850 000 - 1 340 000 plates/m) and quantitative recoveries for model basic proteins. Yet, plots of efficiency vs. buffer concentration for each basic protein studied (Figures 5.4a-d) show increased efficiencies with higher buffer concentration.

Plots of peak asymmetry vs. buffer concentration for lysozyme and ribonuclease A separated on a capillary coated with 0.1 mM DODAB/0.1% POE 40 stearate are shown in Figures 5.5a-b. Similar plots are not shown for cytochrome *c* and α -chymotrypsinogen A because shoulder peaks overlap with protein peaks making measurement of the width at 10% of the peak height impossible. A peak asymmetry factor of 1 corresponds to a symmetrical peak, and is indicated on Figures 5.5a-b by the dotted line. Asymmetry factors less than 1 are fronting peaks, and greater than 1 are tailing peaks (Figure 3.4).

In sodium phosphate (inverted triangles in Figures 5.5a-b) the asymmetry decreases significantly (from tailing to near symmetrical) as the buffer concentration increases. This is consistent with the increase in efficiencies observed for these proteins in sodium phosphate (Figures 5.4b-c). In lithium phosphate buffer (open squares, Figures

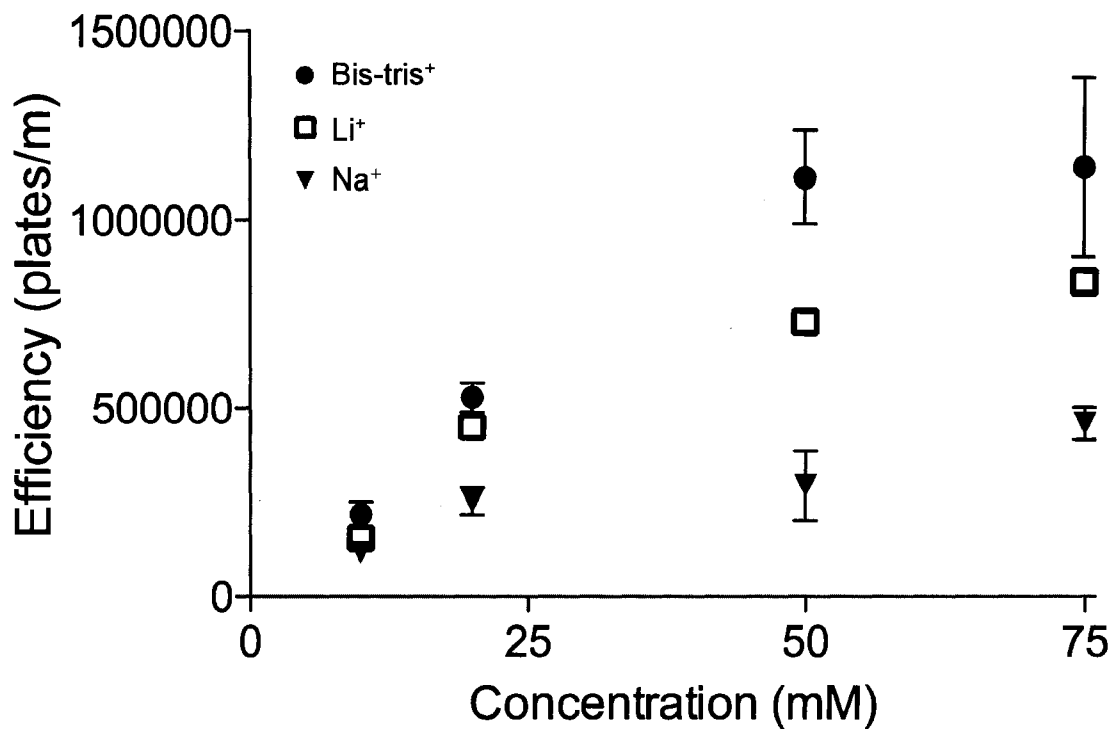


Figure 5.4a: Efficiency of Cytochrome *c* vs. Buffer Concentration on a 0.1 mM DODAB/0.1% POE 40 Stearate Coated Capillary

Experimental conditions: capillary, 32 cm×50 μm I.D. (23 cm to detector); injection, 3 s (0.5 psi) hydrodynamic injection of a mixture of 0.2 mg/mL cytochrome *c*, lysozyme, ribonuclease A, and α-chymotrypsinogen A; pH, 3.0; λ, 214 nm; temperature, 25°C; instrument, Agilent HP^{3D} CE; efficiencies calculated using width-at-half-height method.

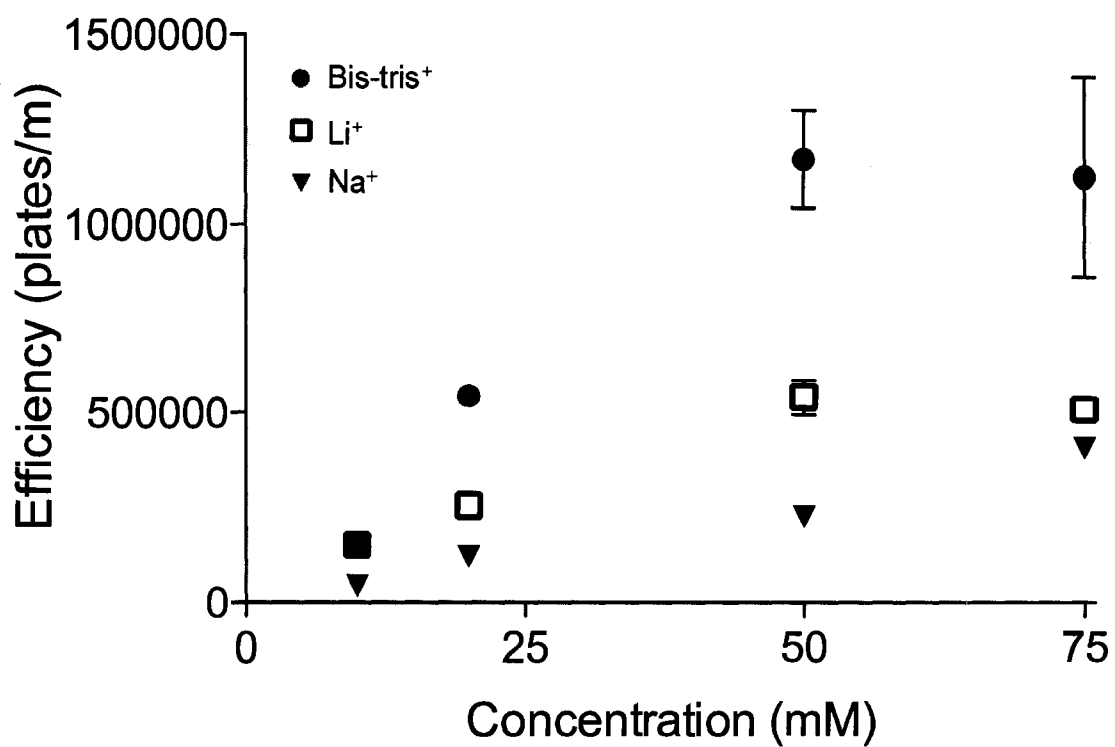


Figure 5.4b: Efficiency of Lysozyme vs. Buffer Concentration on a 0.1 mM DODAB/0.1% POE 40 Stearate Coated Capillary
Experimental conditions: see Figure 5.4a; efficiencies calculated using the Foley-Dorsey method.

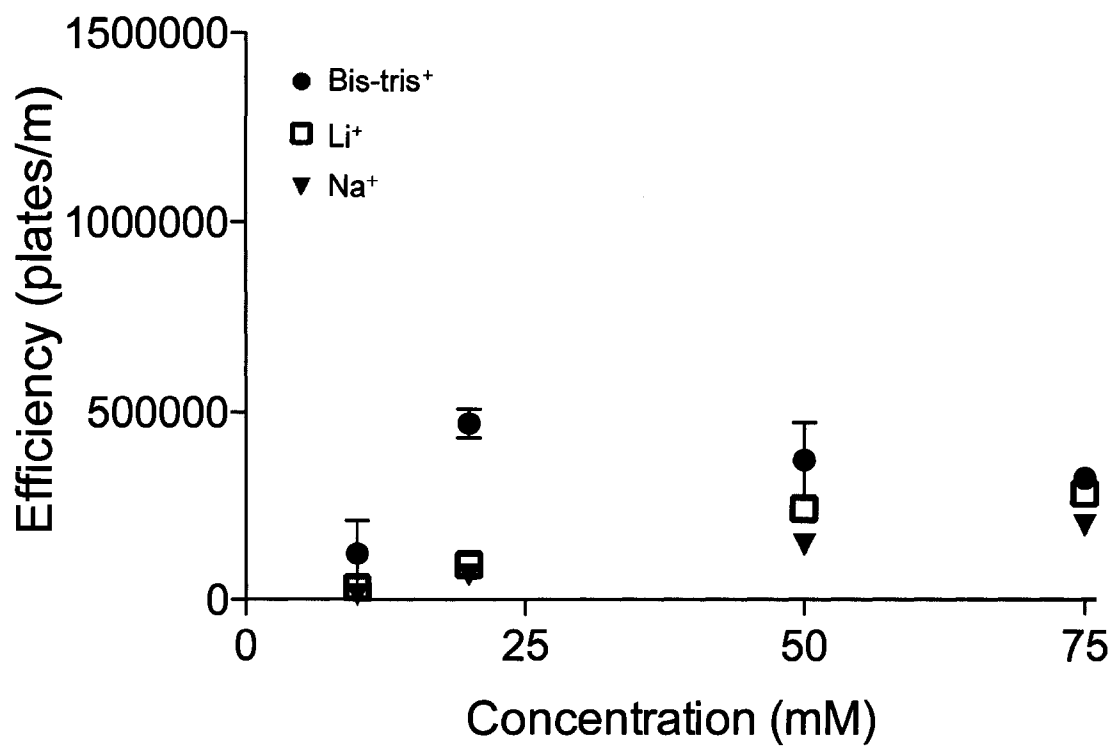


Figure 5.4c: Efficiency of Ribonuclease A vs. Buffer Concentration on a 0.1 mM DODAB/0.1% POE 40 Stearate Coated Capillary
Experimental conditions: see Figure 5.4a; efficiencies calculated using the Foley-Dorsey method.

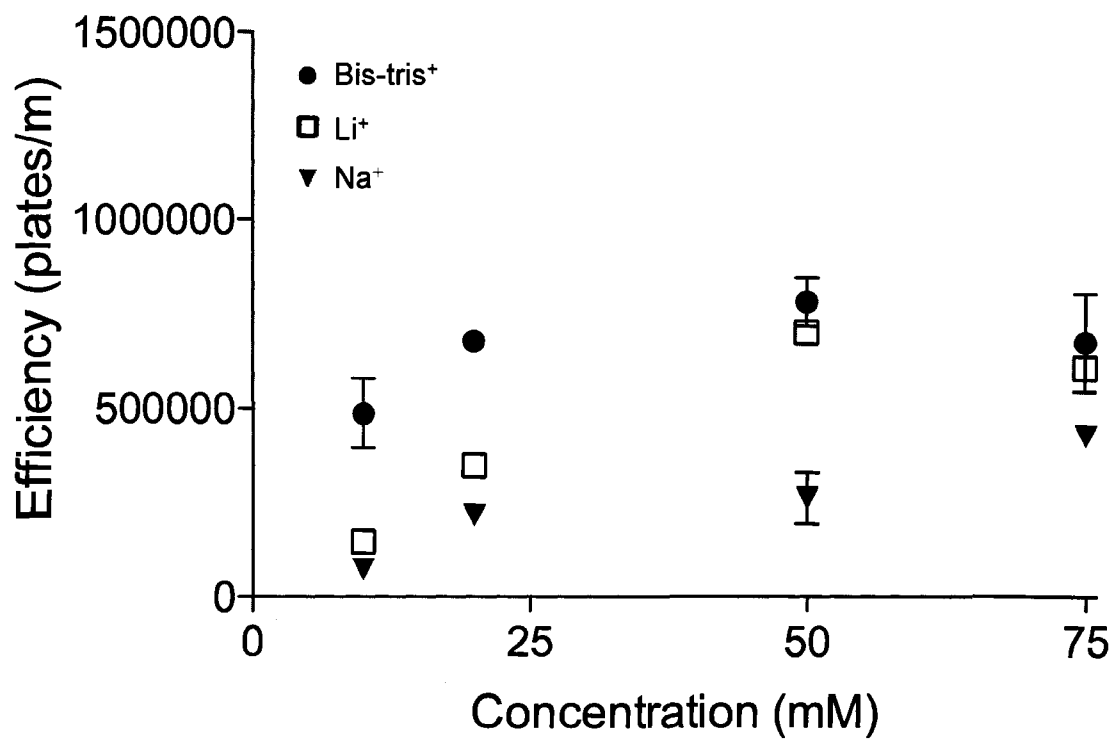


Figure 5.4d: Efficiency of α -chymotrypsinogen A vs. Buffer Concentration on a 0.1 mM DODAB/0.1% POE 40 Stearate Coated Capillary
Experimental conditions: See Figure 5.4a; efficiencies calculated using the width at half height method.

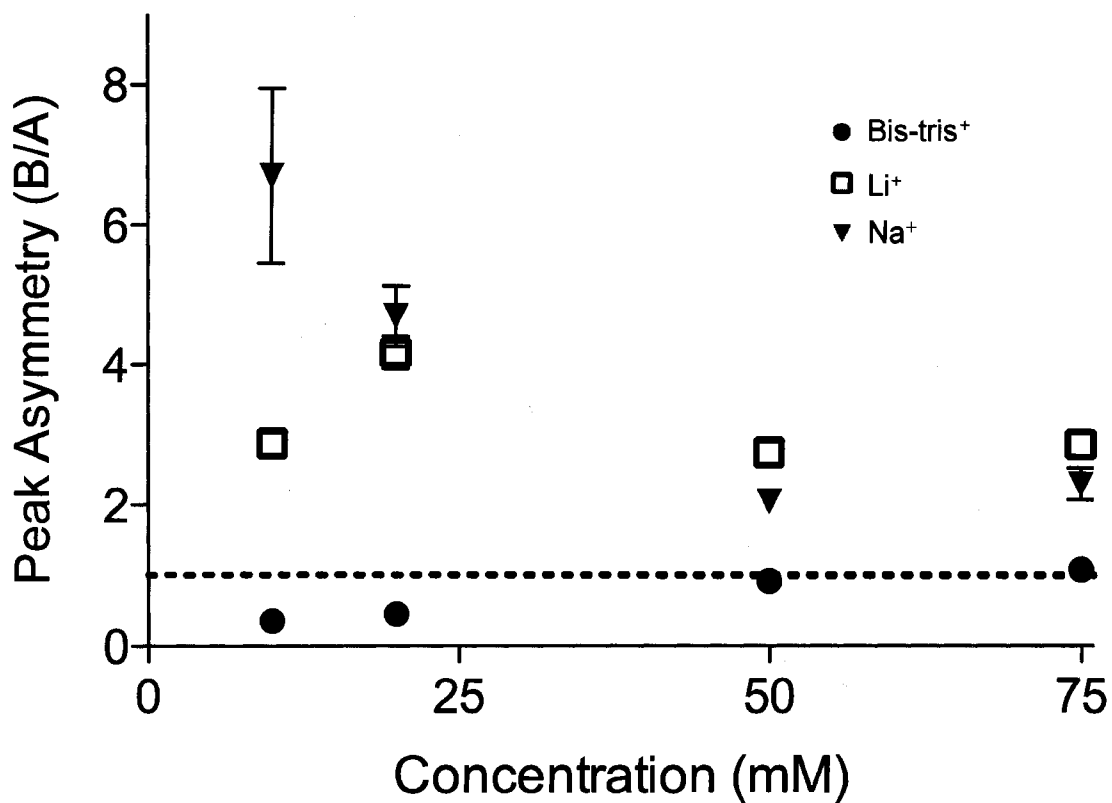


Figure 5.5a: Peak Asymmetry vs. Buffer Concentration for Lysozyme at pH 3.0.

Experimental conditions: capillary, 32 cm×50 μ m I.D. (23 cm to detector) coated with 0.1 mM DODAB/0.1% POE 40 stearate; injection, 3 s (0.5 psi) hydrodynamic injection of a mixture of 0.2 mg/mL cytochrome *c*, lysozyme, ribonuclease A, and α -chymotrypsinogen A; buffer concentration, 50 mM; λ , 214 nm; temperature, 25°C.; instrument, Agilent HP^{3D} CE.

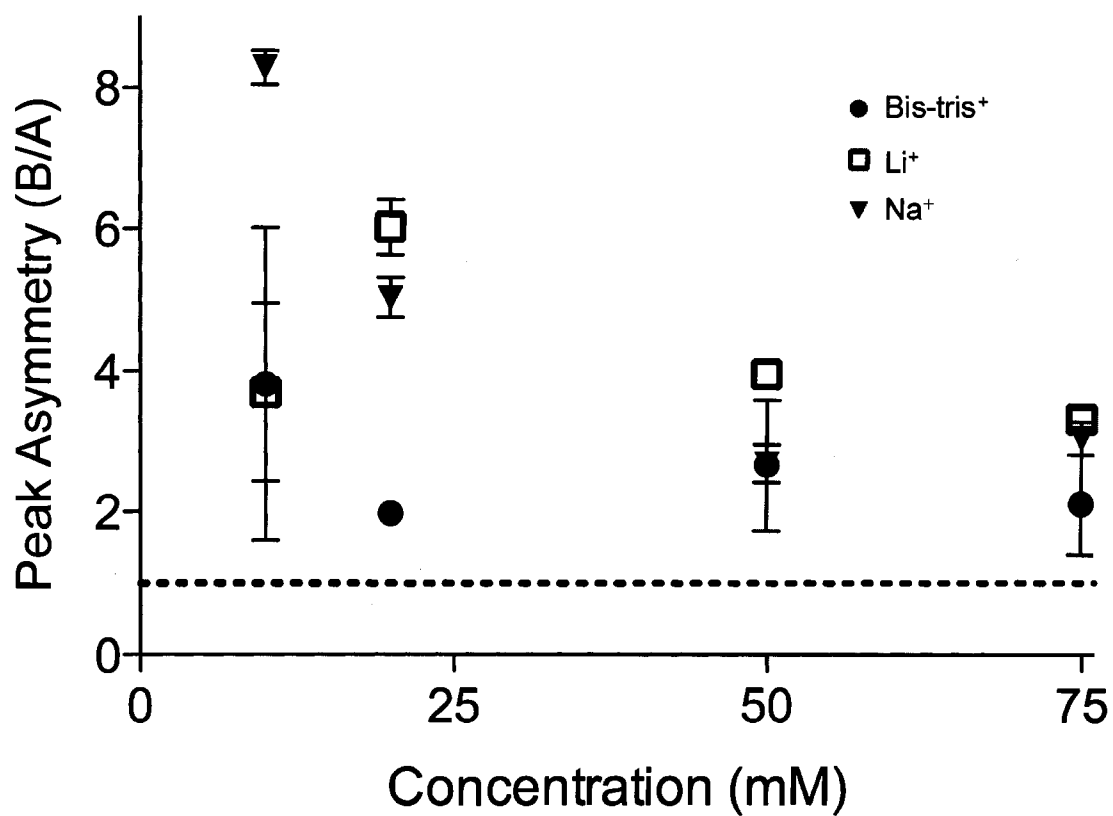


Figure 5.5b: Peak Asymmetry vs. Buffer Concentration for Ribonuclease A at pH 3.0.
Experimental conditions: See Figure 5.5a.

5.5a-b) asymmetry is lower and no consistent trend is evident for either protein. In Bis-tris phosphate buffer (circles, Figure 5.5a-b) no trend in asymmetries is evident for ribonuclease A. However, the lysozyme peak is fronting ($B/A < 1$) in low concentrations of Bis-tris and becomes more symmetrical ($B/A \approx 1$) as the buffer concentration increases. Similar trends in peak fronting were noted in a study of preparative separations of cytochrome *c* by CE.¹⁷ Yassine and Lucy observed more strongly fronting peaks at lower buffer concentrations. Peak asymmetries for bovine cytochrome *c* increased from < 0.1 in 10 mM lithium phosphate to 0.60 in 150 mM lithium phosphate.¹⁷

To examine whether the improvement in efficiency with increasing buffer concentration is unique to the basic proteins studied, the effect of the buffer concentration on acidic protein separations was also examined. Table 5.2 displays efficiencies observed for acidic proteins with Tris-HCl or Tris-acetate buffer using a 0.1 mM DODAB/0.1% POE 40 stearate coated capillary. No universal trend in efficiency is evident, with peak efficiencies increasing, staying constant, and decreasing with increasing buffer concentration. The peak asymmetries in Table 5.2 shows more consistent behavior, in that generally the acidic protein peaks become more symmetrical (B/A closer to 1) as the buffer concentration is increased.

5.3.2.3 Effect of Buffer Co-ion

Section 5.3.1.2 determined that higher buffer concentrations generally result in higher efficiencies and greater peak symmetry. However a second factor at play within Figures 5.4 and 5.5 and Table 5.2 is the effect of buffer co-ion (i.e., the buffer component with the same sign of charge as the protein).

Table 5.2: Peak Efficiencies^a and Asymmetry Factors for Acidic Proteins at pH 7.4

Buffer	N, plates/m (x10 ³)			Asymmetry Factor (B/A)		
	ins	tryp	α -lact	ins	tryp	α -lact
20 mM Tris-HCl	20±10	50±40	160±10	8.0±1.4	2.8±0.5	2.1±0.3
50 mM Tris-HCl	30±10	160±20	140±90	6.1±0.4	2.1±0.3	0.7±0.2
20 mM Tris-acetate	1 ^b	210±20	520±20	12.2 ^b	2.2±0.2	2.1±0.4
50 mM Tris-acetate	2±1	200±50	250±180	9.2±3.3	1.9±0.1	0.8±0.5
75 mM Tris-acetate	640±20	240±10	280±20	2.2±0.2	1.7±0.1	0.7±0.1
100 mM Tris-acetate	550±340	230±50	80±30	2.6±1.0	1.7±0.2	1.4±0.9

^a Calculated using Foley-Dorsey method

^b Calculated from one electropherogram

Previous work in our group has shown the buffer co-ion plays an important role in determining the effectiveness of preparative separations.¹⁷ Yassine and Lucy attributed peak broadening under preparative CE conditions to a mismatch in the mobilities of the sample and buffer co-ions, resulting in electromigration dispersion (EMD). As discussed in Section 1.3.5, EMD occurs when the mobility or conductance of the sample zone in the capillary is either higher or lower than that of the surrounding buffer zone (Figure 1.9).

The peak variance due to EMD is governed by:

$$\sigma_{emd}^2 = \frac{2El_{inj}C_{s,0}|k_{EMD}|}{9C_B v} \quad (1.30)$$

where E is the applied electric field, l_{inj} is the injection length, $C_{s,0}$ is the initial sample concentration, k_{EMD} is the EMD factor, C_B is the buffer concentration, and v is the apparent velocity of the analyte.^{11,17} The EMD factor (k_{EMD}) is:

$$k_{EMD} = \frac{(\mu_a - \mu_s)(\mu_b - \mu_s)}{(-\mu_a + \mu_b)\mu_s} \quad (1.31)$$

where μ_a , μ_b , and μ_s are the mobilities of the buffer co-ion, buffer counter-ion, and

analyte ion, respectively.^{17,40,41} The EMD factor (eq. 1.31) can be minimized by decreasing the mobility difference between sample and buffer co-ions, which in turn will result in a decrease in the peak variance (eq. 1.30).

To investigate the effect of the buffer co-ion on the efficiency of basic proteins, three buffer co-ions were chosen: sodium, lithium, and Bis-tris. The buffer co-ion migrates in the same direction as the sample ions and will be the main current carrier. As the buffer counter-ion moves in the opposite direction to sample migration, the counter-ion mobility will have less of an effect on the observed EMD. Therefore, only the effect of buffer co-ion on the separations was studied. The mobility of each of the buffer co-ions is given in Table 5.1, along with the protein mobilities. The mobilities are not reported for the proteins in Bis-tris buffer as the mobility of the suppressed EOF (μ_{eof}) could not be measured. Limitations in the pressure control on the Agilent system prohibited using the three injection method⁴² (Section 3.2.4). However, the protein mobilities differ only slightly between the sodium and lithium buffers (Table 5.1). Also Yassine and Lucy observed the protein mobilities in the Bis-tris buffer were very similar to those in lithium and sodium phosphate buffers.¹⁷ Thus it is assumed in this work that the protein mobilities in the Bis-tris buffer are similar to those in the other buffers.

In Figures 5.4a-d the efficiencies are generally highest for Bis-tris, moderate for lithium and lowest for sodium buffers. This is consistent with the trend observed in preparative separations on 2C₁₄DAB coated capillaries.¹⁷ The protein mobilities most closely match the mobility of the Bis-Tris ion (Table 5.1), followed by lithium and then sodium. As expected, the mobilities of the co-ions decrease and become more similar to the protein mobilities as the size of the co-ion increases. Thus the trend in efficiencies

noted in Figures 5.4a-d follows what would be expected from the EMD broadening: the buffer co-ions with the most closely matched mobilities to those of the samples result in a smaller k_{EMD} (eq. 1.31), and thus a smaller peak variance (eq. 1.30). As there is an inverse relationship between peak variance and plate number (eq. 1.14), higher plate numbers are achieved. Only the previous studies by Catai et al. and Yassine and Lucy had alluded to EMD within peptide or protein separations.^{17,18} Most commonly, EMD broadening has been discussed only in inorganic anion separations using indirect UV detection.^{43,44} The use of indirect detection necessitated the use of very dilute (2-5 mM) buffers.

From Figure 1.9, if the mobility of the sample zone is lower than that of the buffer zone, the peak should be fronting as it travels on the capillary, and would appear tailed on the electropherogram. This is the case for the proteins ($B/A > 1$) when separated in sodium or lithium phosphate buffer. The peak asymmetries for Bis-tris phosphate indicate tailing to a lesser extent than in sodium or lithium phosphate. At low Bis-tris phosphate concentrations lysozyme is fronting. As the mobility of the proteins could not be directly calculated in the Bis-tris buffer, it is possible that the mobility of lysozyme in Bis-tris may be higher than the Bis-tris ion (Table 5.1). This would result in a fronting peak and the effect would be magnified at lower buffer concentrations (eq. 1.31). Regardless, matching the buffer co-ion and analyte mobility results in more symmetrical peaks overall.

The effect of the buffer co-ion on peak efficiency was also examined for the acidic proteins (Table 5.2). In general, the trends are less distinct with the acidic proteins than the basic proteins described above (possibly due to the poorer match in mobilities

than for the basic proteins), but are consistent with EMD. Efficiencies for trypsin inhibitor and α -lactalbumin A increase in going from 20 mM Tris-HCl to 20 mM Tris-acetate. The mobility of acetate is more similar to the mobilities of the acidic proteins than that of chloride (Table 5.3), and so less EMD would be expected for separations in acetate. However, this effect is muted at higher concentrations, in part due to the greater uncertainty in the efficiency measurements. The peak asymmetry values in these two concentrations of buffer are not statistically different between buffers for these proteins.

Table 5.3: Mobility of Buffer Co-ions in 50mM Tris Buffer, pH 7.4

Buffer Co-ion	$\mu_{\text{co-ion}}^a$ ($10^{-4}\text{cm}^2/\text{Vs}$)	μ_{ins} ($10^{-4}\text{cm}^2/\text{Vs}$)	μ_{tryp} ($10^{-4}\text{cm}^2/\text{Vs}$)	$\mu_{\alpha\text{-lact}}$ ($10^{-4}\text{cm}^2/\text{Vs}$)
Cl^-	-7.1	-1.9	-1.0	-0.4
CH_3COO^-	-3.6	-2.0	-1.2	-0.6

^a Calculated using Peakmaster Version 5.1³³

5.3.2.4 Effect of Protein Concentration

As indicated in equation 1.30, increasing the analyte concentration ($C_{s,0}$) will increase EMD. The presence of the sample in the buffer can change the conductance of the buffer. The conductance can be increased if the sample behaves as an additional conducting electrolyte. The sample can also decrease the conductance if it adsorbs small ions.⁴ These effects are magnified if the concentration of the sample is high.^{11,17,41} From equation 1.30, if the sample concentration increases, so will the variance, which decreases the plate number. Yassine and Lucy¹⁷ studied the effect of analyte concentration for cytochrome *c* separations on a 2C₁₄DAB coated capillary. Both

analytical and preparative scale concentrations were examined. Strongly fronting peaks were observed in the preparative concentration range (1 to 10 mg/mL). However, even at analytical scale concentrations, a decrease in efficiency of 23% was noted as the concentration increased over the range 0.05 – 1 mg/mL.¹⁷

The effect of the concentration of the protein sample on the peak efficiencies was examined on DODAB/POE 40 stearate coatings prepared using the mixed method and the sequential method (Figure 4.1). A plot of efficiencies vs. ribonuclease A concentration is shown in Figure 5.6a for separations performed on 0.1 mM DODAB/0.075% POE 40 stearate (mixed method) in 50 mM sodium phosphate buffer at pH 3.0. The efficiencies decrease by 87% as the protein concentration increases from 0.05 – 0.5 mg/mL. Figure 5.6b shows a similar decrease in efficiency with increased protein concentration for sodium, lithium and Bis-tris buffers on a coating prepared using the sequential method (capillary coated first with 0.1 mM DODAB followed by 0.075% POE 40 stearate). The efficiencies are highest overall in the Bis-tris buffer, consistent with the results from Sections 5.3.2.2 and 5.3.2.3. The efficiencies in lithium buffer are not significantly different from the efficiencies obtained in the sodium buffer, consistent with Sections 5.3.2.2 and 5.3.2.3. Higher efficiencies on the sequentially prepared coatings are also observed, consistent with results in Section 4.3.3.

Electropherograms for separations performed with three concentrations of ribonuclease A on the sequential 0.1 mM DODAB then 0.075% POE 40 stearate coating are shown in Figure 5.7. The peaks become more asymmetrical (Figure 5.8), (i.e., a statistically significant deviation away from 1) as the protein concentration increases. This is in agreement with EMD theory (eqn. 1.30), which states that the EMD will

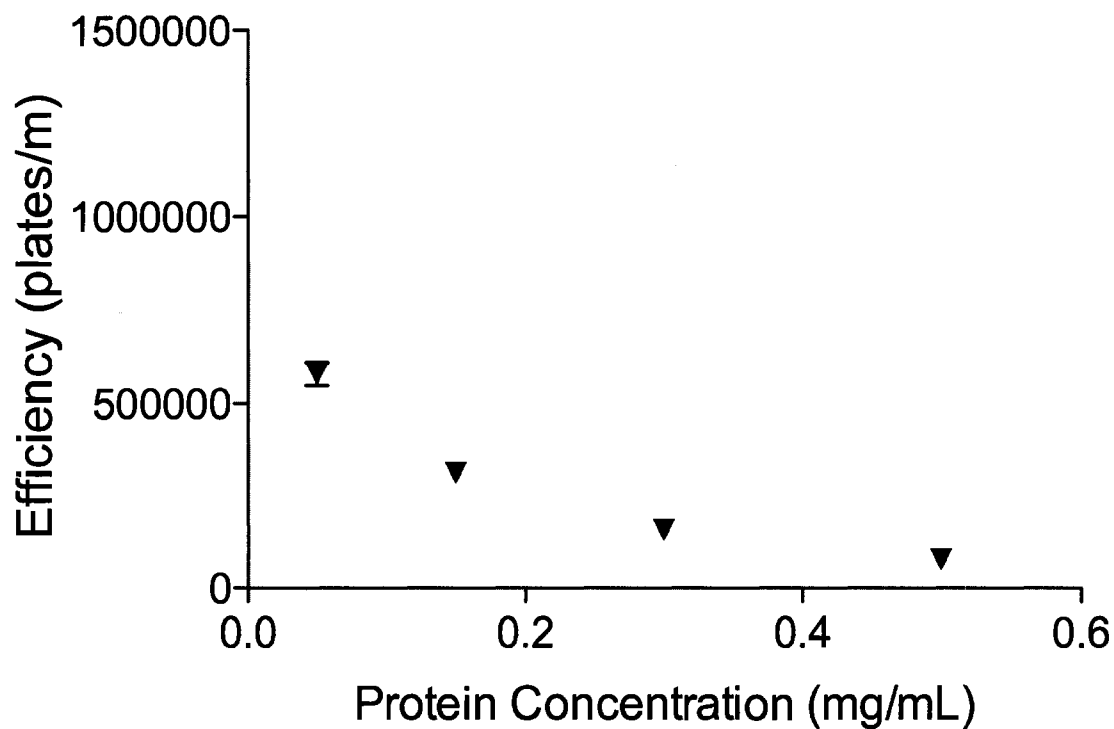


Figure 5.6a: Efficiencies vs. Ribonuclease A Concentration for Separations in 50 mM Sodium Phosphate Buffer on a 0.1 mM DODAB/0.075% POE 40 Stearate Coated Capillary

Experimental conditions: capillary, 47 cm \times 50 μ m I.D. (40 cm to detector); injection, 3 s (0.5 psi) hydrodynamic injection of a mixture of various concentrations of cytochrome *c*, lysozyme, ribonuclease A, and α -chymotrypsinogen A; pH, 3.0; applied voltage, +17.5 kV; λ , 214 nm; temperature, 25°C; instrument, Beckman 2100. Efficiencies calculated using the Foley-Dorsey method.

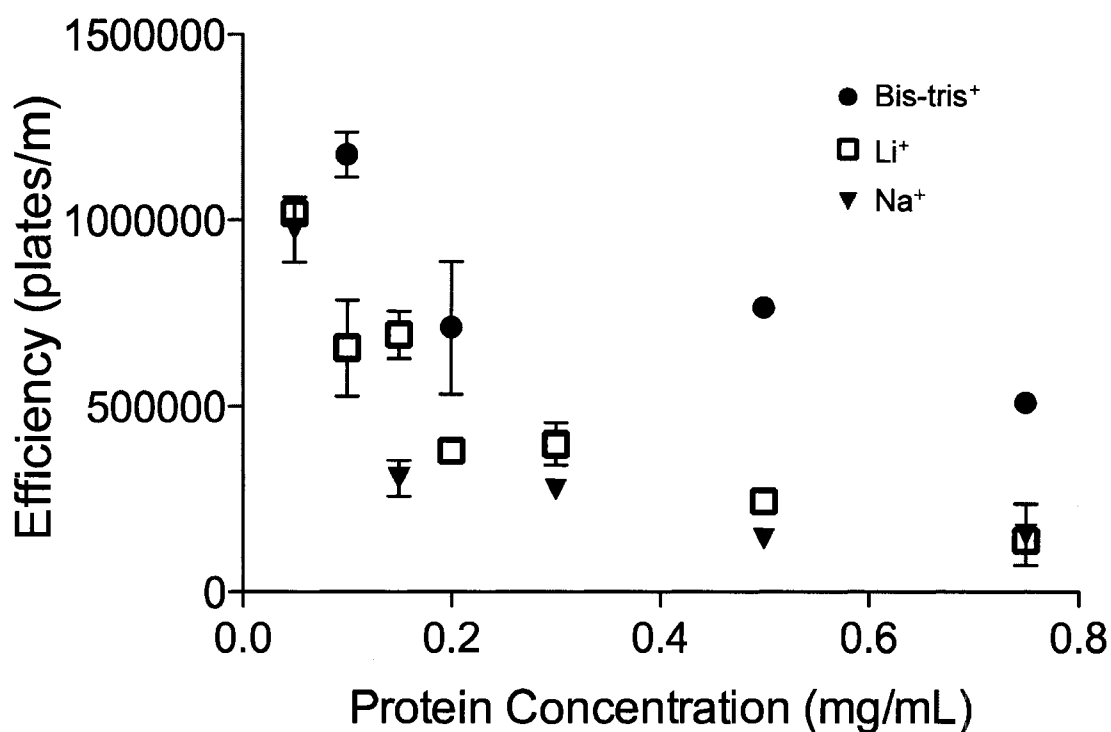


Figure 5.6b: Efficiencies vs. Ribonuclease A Concentration for Separations in Sodium Phosphate, Lithium Phosphate, and Bis-tris Phosphate Buffers on a Sequential 0.1 mM DODAB the 0.075% POE 40 Stearate Coating

Experimental conditions: capillary, 47 cm×50 μ m I.D. (40 cm to detector); injection, 3 s (0.5 psi) hydrodynamic injection of a mixture of cytochrome *c*, lysozyme, ribonuclease A, and α -chymotrypsinogen A (for the Bis-tris phosphate experiments, only lysozyme and ribonuclease A were injected); buffer concentration, 50 mM; pH, 3.0; applied voltage, +17.5 kV; λ , 214 nm; temperature, 25°C; instrument, Beckman 2100. Efficiencies calculated using the Foley-Dorsey method.

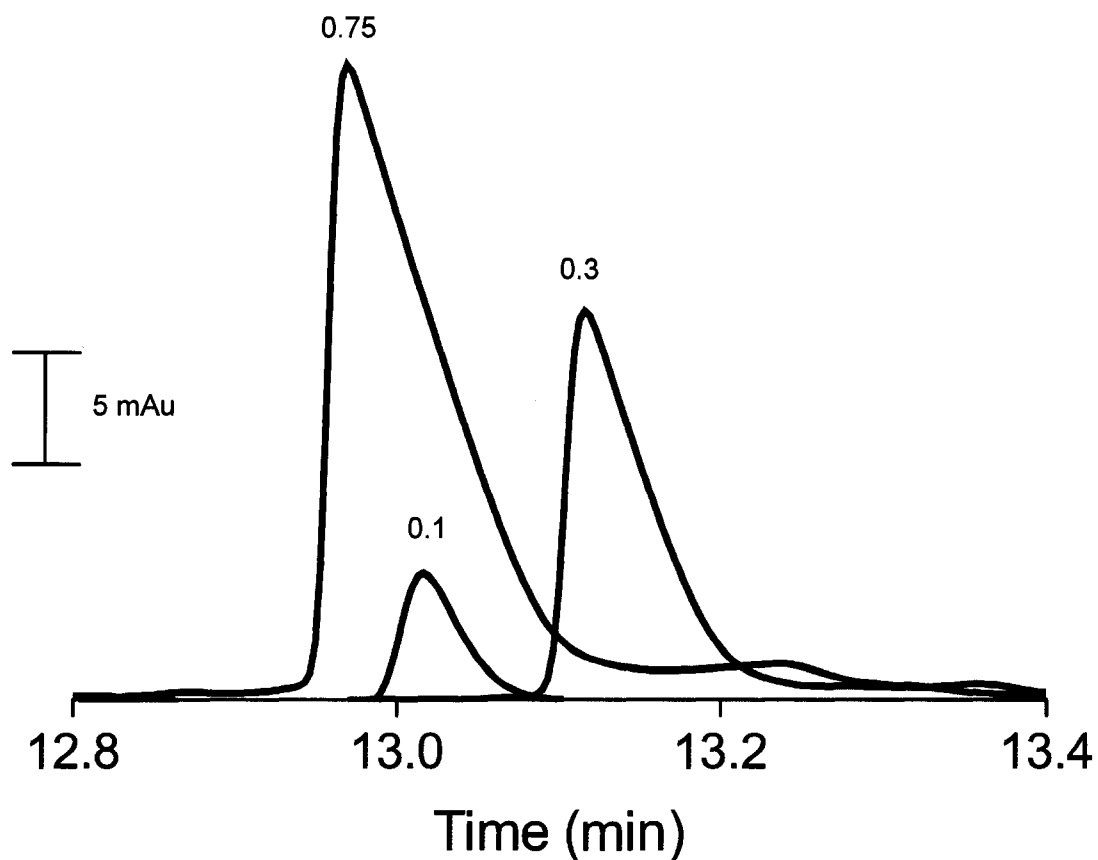


Figure 5.7: Ribonuclease A at Various Concentrations (shown in mg/mL above each peak) on a Sequential Coating of 0.1 mM DODAB then 0.075% POE 40 in 50 mM Lithium Phosphate, pH 3.0.

Experimental conditions: capillary, 47 cm×50 μ m I.D. (40 cm to detector); injection, 3 s (0.5 psi) hydrodynamic injection of a mixture of cytochrome *c*, lysozyme, ribonuclease A, and α -chymotrypsinogen A; applied voltage, +17.5 kV; λ , 214 nm; temperature, 25°C; instrument, Beckman 2100.

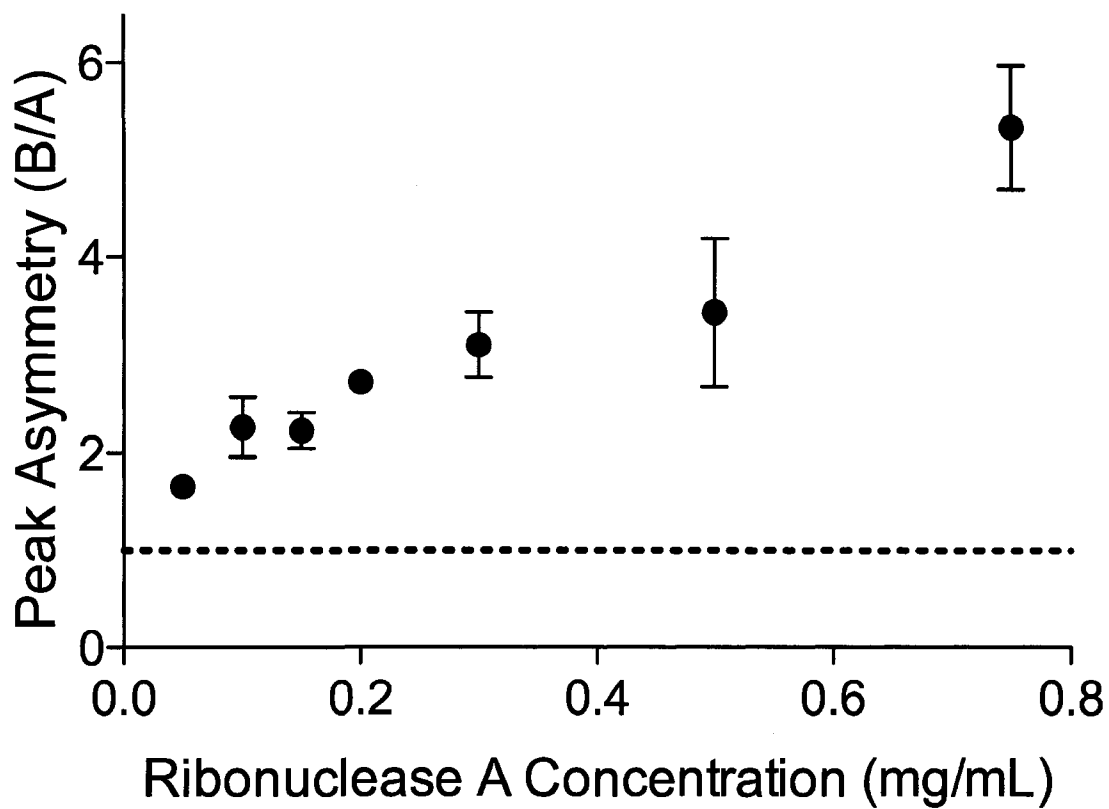


Figure 5.8: Peak Asymmetry vs. Ribonuclease A Concentration for Separations on a Sequential Coating of 0.1 mM DODAB followed by 0.075% POE 40 Stearate with 50 mM Lithium Phosphate, pH 3.0. Dotted line depicts a peak asymmetry of 1.
Experimental conditions: See Figure 5.7

become more pronounced at higher sample concentrations.^{11,41} A similar trend was noted by Yassine and Lucy.¹⁷

5.3.3 Protein Separations with Commercial Coatings

Commercially available coated capillaries can be appealing as they do not require any preparation of a coating before use. Polyacrylamide and polyvinyl alcohol (PVA) are two polymer coatings that are commercially available^{45,46} as a linear bonded polyacrylamide (LPA) and a permanently coated PVA, respectively. Their structures are shown in Figure 5.9. Both types of coating have achieved efficient protein separations in the literature⁴⁷⁻⁵¹ and so were chosen as comparison standards for the DODAB/POE 40 stearate coating. Their performance is investigated below and compared with that of the DODAB/POE 40 stearate coating used in this and previous chapters.

Figure 5.10 depicts a separation of the model basic proteins on LPA, PVA and 0.1 mM DODAB/0.1% POE 40 stearate in 75 mM lithium phosphate buffer. In our work the separations on the LPA coated capillaries yielded poor separations performed poorly all buffers (sodium, lithium, and Bis-tris phosphate) as evident in Figure 5.10. A known problem with LPA coatings is the acrylamide molecules do not completely cover the surface, leading to adsorption of proteins and changes in the EOF.⁵² Improved performance has been noted in the literature with crosslinked polyacrylamide coatings over the linear version.⁵²⁻⁵⁴ However, such capillaries are not commercially available. Therefore, polyacrylamide coatings were not studied further.

PVA demonstrated better performance than LPA in Figure 5.10, and so it was chosen for further study. The Agilent website states that the PVA is permanently adsorbed to the capillary wall.⁴⁶ Blanco et al. examined protein separation on a variety of

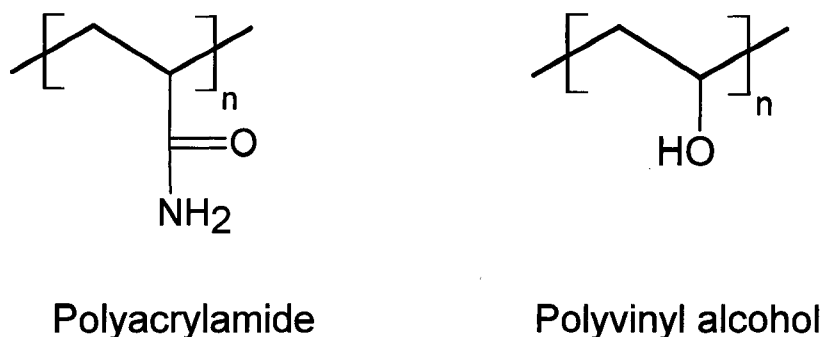


Figure 5.9: Commercial Polymer Coating Structures

coatings, including a permanent PVA coating purchased from Hewlett-Packard (now Agilent).⁵¹

Efficiencies of approximately 700 000 plates/m were achieved for lysozyme with a 50 mM sodium phosphate buffer. This is similar to 600 000 plates/m we observed in the 75 mM lithium phosphate buffer (Figure 5.10).

Figures 5.11a-d show the efficiencies observed for the model basic proteins on a PVA coated capillary under a variety of buffer conditions. The efficiencies for cytochrome *c*, lysozyme, and α -chymotrypsinogen A had to be calculated using the width-at-half-height method due to shoulders on these peaks. The efficiencies in Figures 5.11a-d are substantially lower than those observed with the DODAB/POE 40 stearate coating (Figures 5.4a-d), suggesting that reversible adsorption is occurring. Also the increase in the baseline after each peak in Figure 5.10 suggests that some protein is being irreversibly adsorbed on the PVA coated capillary.

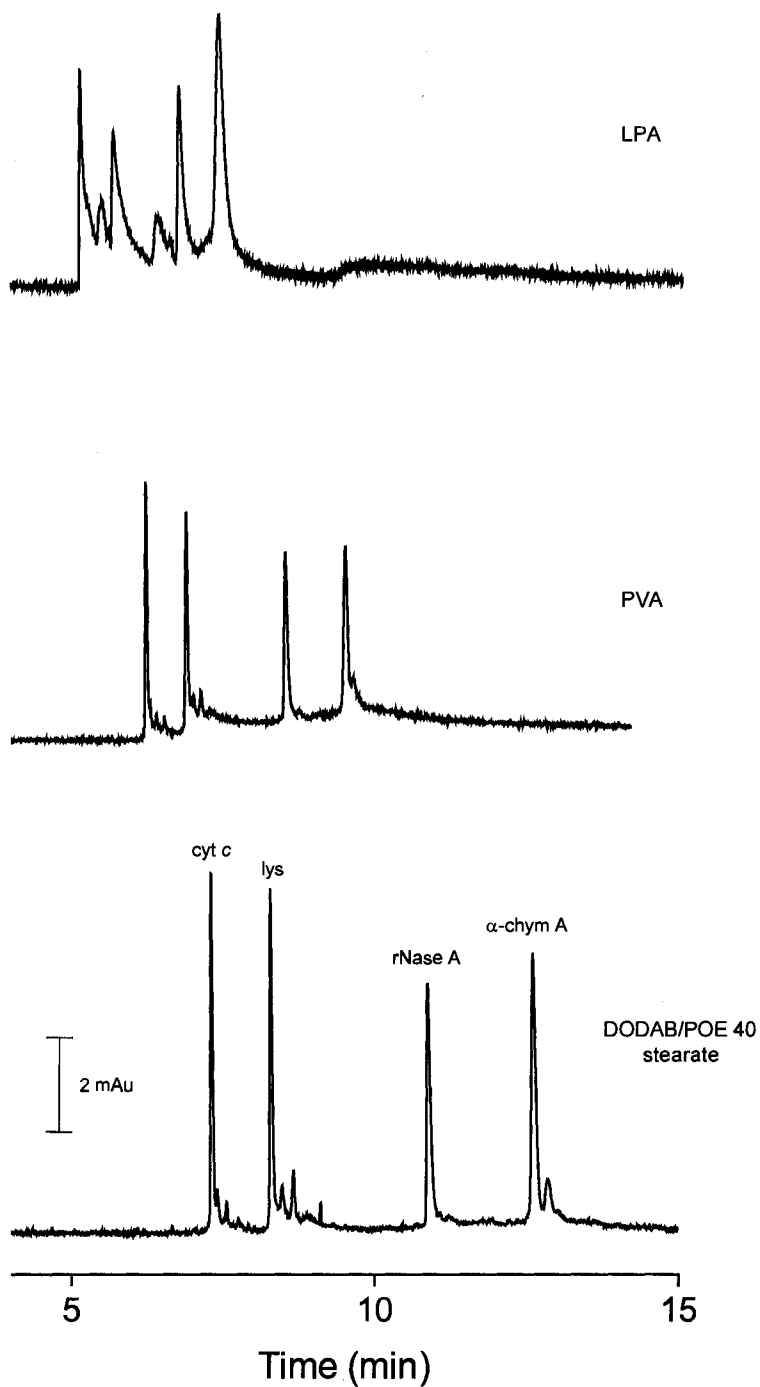


Figure 5.10: Basic Protein Separation on LPA, PVA, and 0.1 mM DODAB/0.1% POE 40 Stearate with 75 mM Lithium Phosphate, pH 3.0.

Experimental conditions: capillary, 32 cm \times 50 μ m I.D. (23 cm to detector); injection, 3 s (0.5 psi) hydrodynamic injection of a mixture of 0.2 mg/mL cytochrome *c*, lysozyme, ribonuclease A, and α -chymotrypsinogen A; λ , 214 nm; temperature, 25°C; instrument, Agilent HP^{3D} CE.

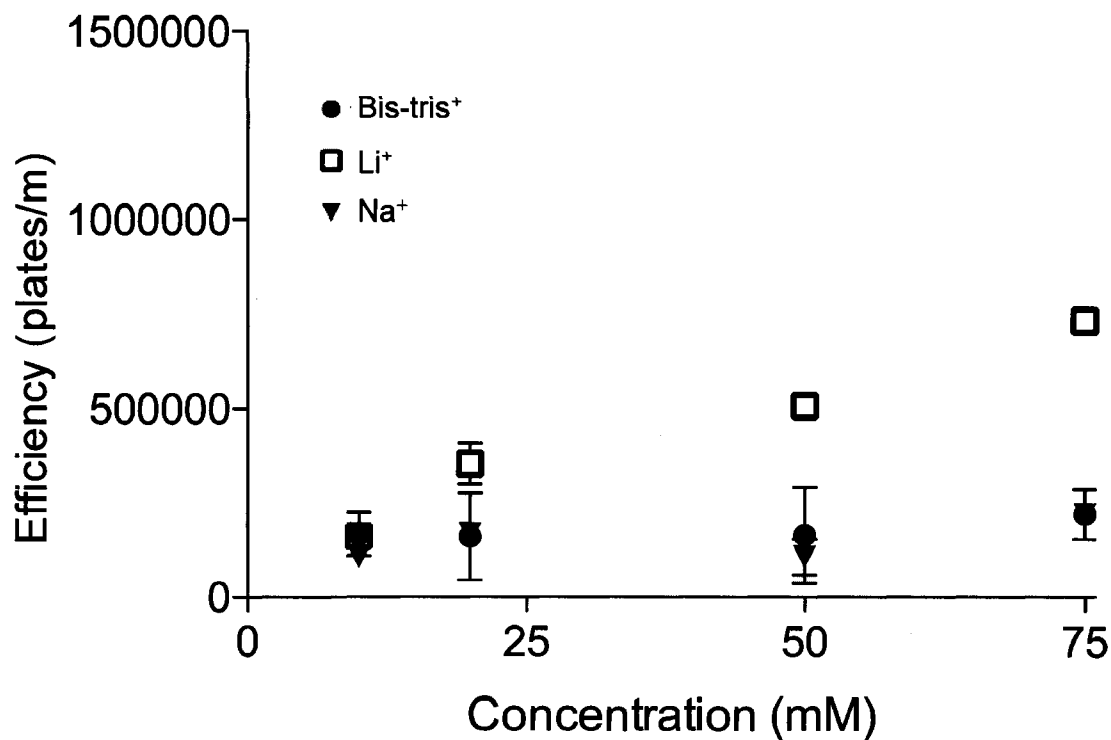


Figure 5.11a: Efficiency of Cytochrome *c* vs. Buffer Concentration in Various Buffers at pH 3.0 on a PVA Coated Capillary.

Experimental conditions: capillary, 32 cm×50 μ m I.D. (23 cm to detector); injection, 3 s (0.5 psi) hydrodynamic injection of a mixture of 0.2 mg/mL cytochrome *c*, lysozyme, ribonuclease A, and α -chymotrypsinogen A; λ , 214 nm; and temperature, 25°C; efficiencies calculated using width-at-half-height method.

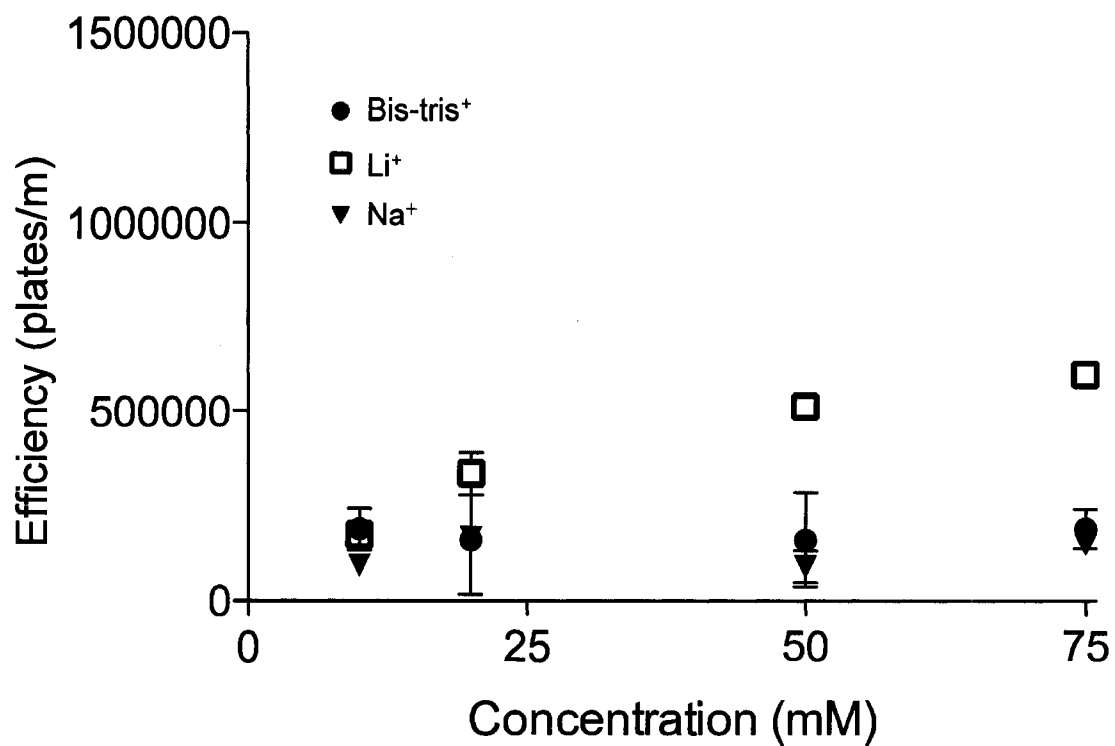


Figure 5.11b: Efficiency of Lysozyme vs. Buffer Concentration in Various Buffers on a PVA Coated Capillary at pH 3.0.

Experimental Conditions: See Figure 5.11a.

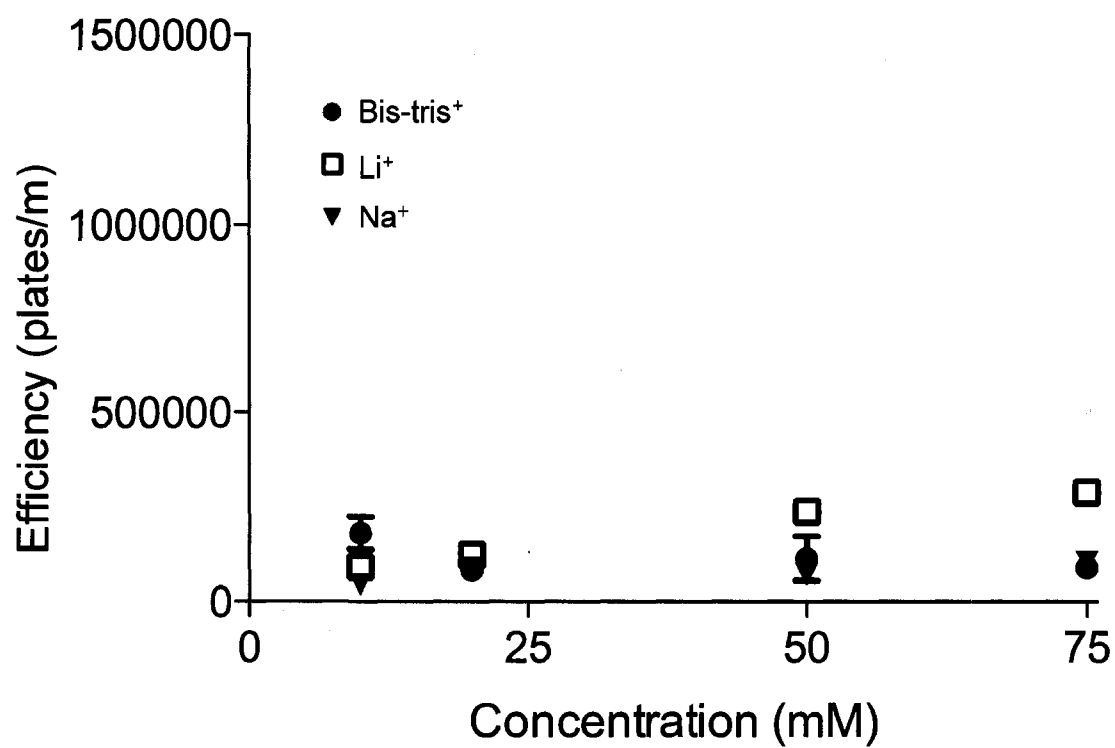


Figure 5.11c: Efficiency of Ribonuclease A vs. Buffer Concentration in Various Buffers at pH 3.0 on a PVA Coated Capillary

Experimental conditions: See Figure 5.11a, except efficiencies were calculated using the Foley-Dorsey method

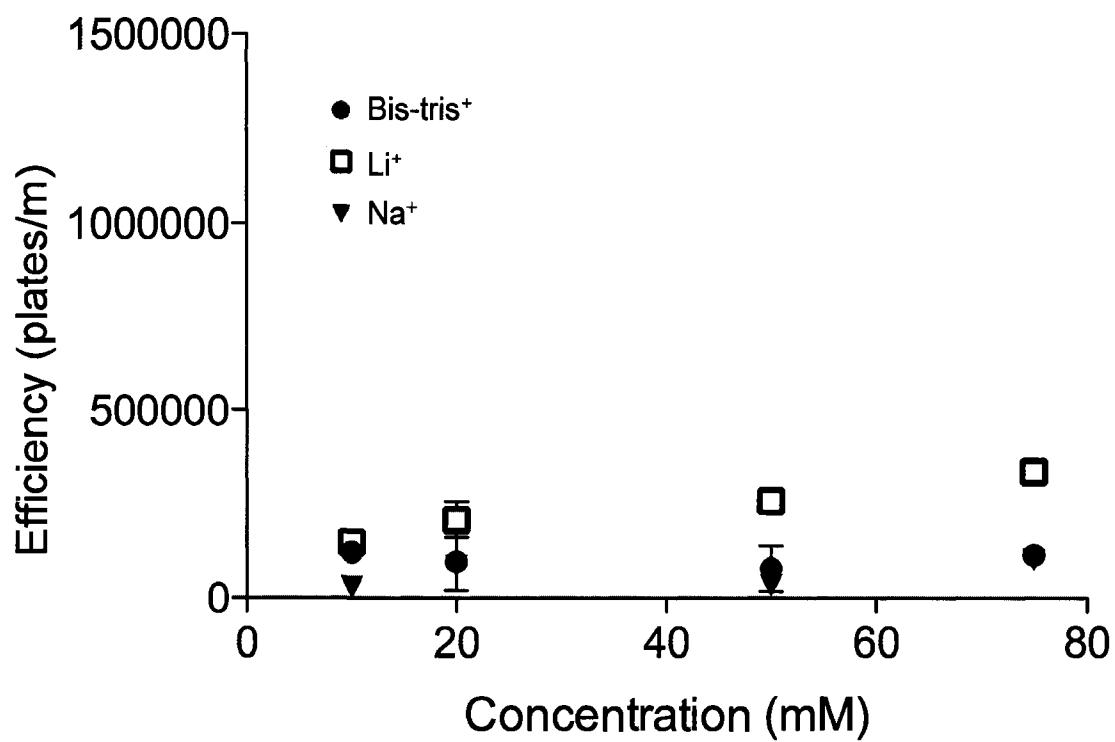


Figure 5.11d: Efficiency of α -chymotrypsinogen A vs. Buffer Concentration in Various Buffers at pH 3.0 on a PVA Coated Capillary
Experimental conditions: See Figure 5.11a.

Despite the poorer performance of the PVA capillary, some trends are evident in Figures 5.11 a-d. Using lithium phosphate buffer, the efficiencies for cytochrome *c* on PVA (160 000 – 730 000 plates/m) are comparable to those observed on the 0.1 mM DODAB/0.1% POE 40 stearate coated capillary (150 000 – 840 000 plates/m). As with the DODAB/POE 40 stearate coating (Figures 5.4a-d), efficiencies on PVA improved with increasing lithium phosphate buffer concentration. The efficiencies in sodium or Bis-tris phosphate were much lower (< 250 000 plates/m) on the PVA coating - as much as a factor of 10 lower when high concentrations of sodium or Bis-tris phosphate buffers were used. No statistically significant increase in efficiency was observed for increased concentrations of the sodium or Bis-Tris phosphate buffers.

Figure 5.12 shows the peak asymmetry vs. buffer concentration for ribonuclease A in the three buffers studied. Statistically lower B/A values are noted in sodium and lithium buffers at higher buffer concentrations than at lower buffer concentrations, with the exception of 10 mM lithium. However, Bis-tris shows anomalous behaviour on the PVA coating in that an increase in asymmetry factors is observed at higher concentrations. No change in the EOF was observed with Bis-tris concentration, discounting the possibility that the buffer ion was adsorbing to the PVA surface. Regardless, Bis-tris is not an effective buffer for use with a PVA coating.

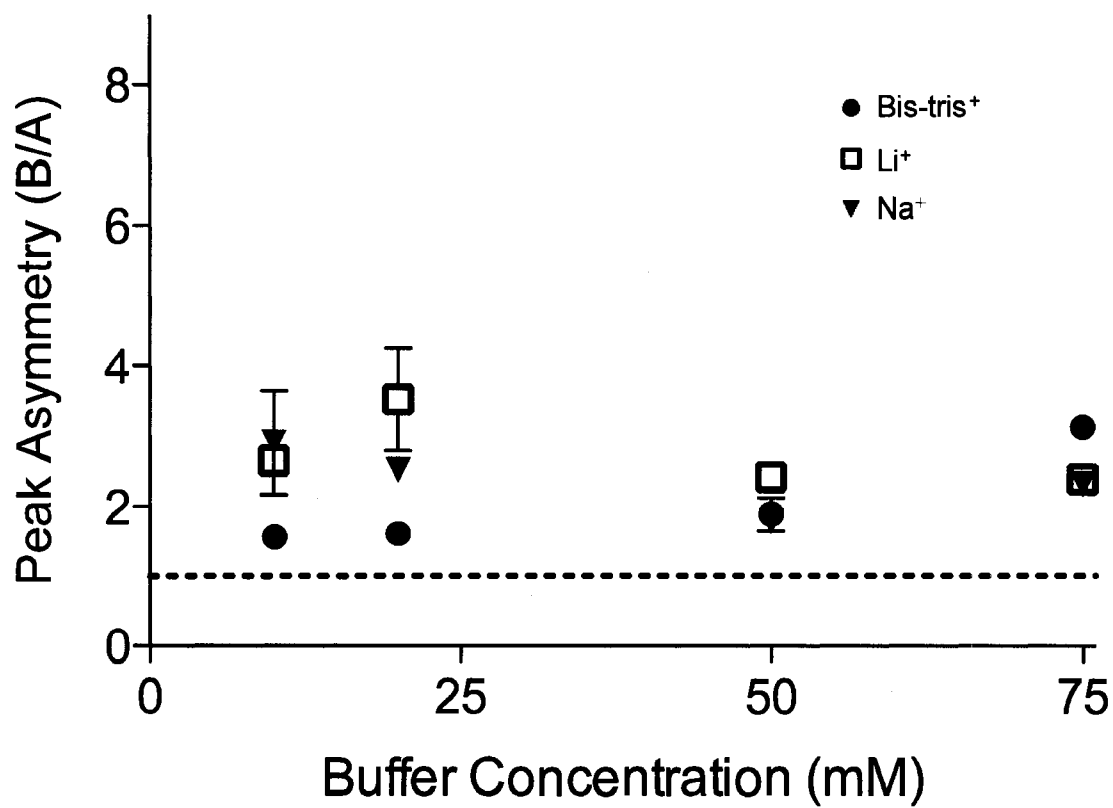


Figure 5.12: Peak Asymmetry vs. Buffer Concentration for Ribonuclease A at pH 3.0 on a PVA Coated Capillary.

Experimental conditions: See Figure 5.11a.

5.4 Concluding Remarks

As discussed in our recent review,² peak efficiency is a metric often used to determine the effectiveness of a coating. However as shown herein on both a DODAB/POE 40 stearate coated capillary and a commercial PVA capillary, experimental factors in addition to the coating can significantly affect the efficiency measurements. Firstly, the method used to calculate the efficiencies (Foley-Dorsey vs. width-at-half-height) can cause a > 80% bias in the efficiencies measured. Second, buffer concentration strongly affects efficiencies. Higher buffer concentrations yield better efficiencies by reducing both adsorption (based on literature studies of bare capillaries) and electromigration dispersion. Thirdly, buffer co-ion influences band broadening due to electromigration dispersion, even at analytical protein concentrations. In general use of a buffer co-ion that closely matches the protein mobility improves efficiencies.

5.5 References

- (1) Doherty, E. A. S.; Meagher, R. J.; Albarghouthi, M. N.; Barron, A. E., *Electrophoresis* **2003**, *24*, 34-54.
- (2) Lucy, C. A.; MacDonald, A. M.; Gulcev, M. D., *J. Chromatogr. A* **2008**, *1184*, 81-105.
- (3) Bidlingmeyer, B. A.; Warren, F. V., Jr., *Anal. Chem.* **1984**, *56*, 1583A-1596A.
- (4) Jorgenson, J. W.; Lukacs, K. D., *Science* **1983**, *222*, 266-272.
- (5) Foret, F.; Deml, M.; Bocek, P., *J. Chromatogr.* **1988**, *452*, 601-613.
- (6) Nelson, R. J.; Paulus, A.; Cohen, A. S.; Guttman, A.; Karger, B. L., *J. Chromatogr.* **1989**, *480*, 111-127.
- (7) Terabe, S.; Otsuka, K.; Ando, T., *Anal. Chem.* **1985**, *57*, 834-841.
- (8) Gas, B.; Stedry, M.; Rizzi, A.; Kenndler, E., *Electrophoresis* **1995**, *16*, 958-967.
- (9) Towns, J. K.; Regnier, F. E., *Anal. Chem.* **1992**, *64*, 2473-2478.
- (10) Schure, M. R.; Lenhoff, A. M., *Anal. Chem.* **1993**, *65*, 3024-3037.
- (11) Xu, X.; Kok, W. T.; Poppe, H., *J. Chromatogr. A* **1996**, *742*, 211-227.
- (12) Mikkers, F. E. P.; Everaerts, F. M.; Verheggen, T., *J. Chromatogr.* **1979**, *169*, 11-20.
- (13) Beckers, J. L., *J. Chromatogr. A* **1995**, *693*, 347-357.
- (14) Huang, X. H.; Coleman, W. F.; Zare, R. N., *J. Chromatogr.* **1989**, *480*, 95-110.
- (15) Grossman, P. D.; Colburn, J. C., *Capillary Electrophoresis Theory and Practice*, Academic Press, Inc., Toronto, 1992.
- (16) Lauer, H. H.; McManigill, D., *TRAC-Trend. Anal. Chem.* **1986**, *5*, 11-15.
- (17) Yassine, M. M.; Lucy, C. A., *Electrophoresis* **2006**, *27*, 3066-3074.
- (18) Catai, J. R.; Somsen, G. W.; de Jong, G. J., *Electrophoresis* **2004**, *25*, 817-824.
- (19) Catai, J. R.; Tervahauta, H. A.; de Jong, G. J.; Somsen, G. W., *J. Chromatogr. A* **2005**, *1083*, 185-192.

- (20) Wenner, A., Information Sheet, *Agilent Technologies* **2006**.
- (21) Foley, J. P.; Dorsey, J. G., *Anal. Chem.* **1983**, *55*, 730-737.
- (22) Melanson, J. E.; Baryla, N. E.; Lucy, C. A., *Anal. Chem.* **2000**, *72*, 4110-4114.
- (23) Yassine, M. M.; Lucy, C. A., *Anal. Chem.* **2005**, *77*, 620-625.
- (24) Cunliffe, J. M.; Baryla, N. E.; Lucy, C. A., *Anal. Chem.* **2002**, *74*, 776-783.
- (25) Wang, C. Z.; Lucy, C. A., *Electrophoresis* **2004**, *25*, 825-832.
- (26) Gulcev, M. D.; Lucy, C. A., *Anal. Chem.* **2008**, *80*, 1806-1812.
- (27) MacDonald, A. M.; Lucy, C. A., *J. Chromatogr. A* **2006**, *1130*, 265-271.
- (28) Bushey, M. M.; Jorgenson, J. W., *J. Chromatogr.* **1989**, *480*, 301-310.
- (29) Corradini, D.; Bevilacqua, L.; Nicoletti, I., *Chromatographia* **2005**, *62*, S43-S50.
- (30) Albarghouthi, M. N.; Stein, T. M.; Barron, A. E., *Electrophoresis* **2003**, *24*, 1166-1175.
- (31) Meagher, R. J.; Seong, J.; Laibinis, P. E.; Barron, A. E., *Electrophoresis* **2004**, *25*, 405-414.
- (32) Rabanal, B.; de Paz, E.; Merino, G.; Negro, A., *J. Chromatogr. B* **2000**, *738*, 293-303.
- (33) Gas, B.; Jaros, M.; Hruska, V.; Zuskova, I.; Stedry, M., *LC GC Europe* **2005**, *18*, 282-288.
- (34) Jorgenson, J. W.; Lukacs, K. D., *Anal. Chem.* **1981**, *53*, 1298-1302.
- (35) Hjerten, S., *Electrophoresis* **1990**, *11*, 665-690.
- (36) Sepaniak, M. J.; Cole, R. O., *Anal. Chem.* **1987**, *59*, 472-476.
- (37) Ho Row, K.; Griest, W. H.; Maskarinec, M. P., *J. Chromatogr. A* **1987**, *409*, 193-203.
- (38) Green, J. S.; Jorgenson, J. W., *J. Chromatogr.* **1989**, *478*, 63-70.
- (39) Yassine, M. M.; Lucy, C. A., *Anal. Chem.* **2004**, *76*, 2983-2990.

- (40) Cifuentes, A.; Xu, X.; Kok, W. T.; Poppe, H., *J. Chromatogr. A* **1995**, *716*, 141-156.
- (41) Mikkers, F. E. P.; Everaerts, F. M.; Verheggen, T., *J. Chromatogr.* **1979**, *169*, 1-10.
- (42) Williams, B. A.; Vigh, C., *Anal. Chem.* **1996**, *68*, 1174-1180.
- (43) Doble, P.; Macka, M.; Haddad, P. R., *TRAC-Trend. Anal. Chem.* **2000**, *19*, 10-17.
- (44) Landers, J. P., *Handbook of Capillary Electrophoresis*, CRC Press, Boca Raton, 1994.
- (45) Microsolv Technology Corp., http://www.mtc-usa.com/wcode_eof-cat.asp, accessed August 9, 2007.
- (46) Agilent Technologies, <http://www.chem.agilent.com/Scripts/PDS.asp?lPage=2248>, accessed July 23, 2007.
- (47) Huang, X. Y.; Doneski, L. J.; Wirth, M. J., *Anal. Chem.* **1998**, *70*, 4023-4029.
- (48) Cifuentes, A.; Diez-Masa, J. C.; Fritz, J.; Anselmetti, D.; Bruno, A. E., *Anal. Chem.* **1998**, *70*, 3458-3462.
- (49) Gilges, M.; Kleemiss, M. H.; Schomburg, G., *Anal. Chem.* **1994**, *66*, 2038-2046.
- (50) Belder, D.; Deege, A.; Husmann, H.; Kohler, F.; Ludwig, M., *Electrophoresis* **2001**, *22*, 3813-3818.
- (51) Blanco, D.; Herrero, I.; Laviana, L.; Gutierrez, M. D., *J. Liq. Chrom. Rel. Tech.* **2002**, *25*, 1171-1185.
- (52) Gao, L.; Liu, S. R., *Anal. Chem.* **2004**, *76*, 7179-7186.
- (53) Schmalzing, D.; Piggee, C. A.; Foret, F.; Carrilho, E.; Karger, B. L., *J. Chromatogr. A* **1993**, *652*, 149-159.
- (54) Huang, M. X.; Vorkink, W. P.; Lee, M. L., *J. Microcol. Sep.* **1992**, *4*, 233-238.

Chapter 6: Summary and Future Work

6.1 Summary

The main goal of this thesis was to develop a method of preventing protein adsorption in capillary electrophoresis that is simple and cost-effective. Factors affecting separations beside adsorption were also investigated. The role of the EOF is highlighted throughout. In Chapter 2 the EOF enhancement resulting from zwitterionic additives was examined, as well as the underlying causes for this enhancement. These additives demonstrated interesting effects on the EOF, but were not effective at preventing protein adsorption. Therefore, coating methods to prevent protein adsorption were studied. A review of coating procedures is provided in Chapter 1. Building on these procedures a novel semi-permanent coating was developed in Chapter 3 to prevent protein adsorption. My coating consists of a surfactant bilayer and a diblock copolymer, and results in a suppressed EOF. The efficacy of this coating for separations of both anionic and cationic proteins was demonstrated. The possibility of modifying certain aspects of the coating in order to tune the EOF and provide the most efficient protein separations was investigated in Chapter 4. Chapter 5 examined factors causing band broadening other than adsorption. Such studies were made possible by the effective elimination of protein adsorption by the bilayer/diblock copolymer coating.

6.1.1 Chapter 2

In Chapter 2 the effect of zwitterionic additives on the EOF was examined. It had been previously demonstrated in our lab that zwitterionic additives were less effective than many coatings at preventing adsorption. Therefore, the main focus of Chapter 2 was an examination of the effect of zwitterions on EOF. Z1-methyl

(trimethylammoniumpropyl sulfonate) was the first zwitterion investigated. The EOF was monitored in the presence of 0 - 750 mM Z1-Methyl. The EOF increased in magnitude 63% over that of a buffer containing no zwitterion.

The cause of this enhancement was investigated by first studying a homologous series of aminocarboxylic acids. The EOF enhancement increased with carbon chain length and thus the intercharge separation. The end group also had a demonstrable effect on the EOF enhancement. Z1-methyl, with a quaternary amine functionality, had approximately double the enhancement of an aminocarboxylic acid (i.e., primary amine) of the same length. The anionic functionality did not significantly affect the enhancement. Buffer conditions such as pH and buffer cation had no effect. The EOF enhancement observed with the aminocarboxylic acids studied is in agreement with the increase in dielectric constant within this series (Section 2.4.1). However, the literature dielectric increments for the same chain length additives having different endgroups are not significantly different. Therefore, the dielectric constant does have an effect on EOF, but cannot fully explain the observed enhancement. Both an increase in the order of the amine and the dielectric increment of the zwitterionic additives increase the EOF.

6.1.2 Chapter 3

As the ultimate goal of this thesis was to develop a cost effective and reliable method of preventing protein adsorption, a semi-permanent coating was developed for this purpose in Chapter 3. This coating consists of a long chain surfactant (DODAB, i.e., 2C₁₈DAB) and a neutral hydrophilic diblock copolymer (POE stearate). The DODAB surfactant forms a bilayer on the capillary wall. The hydrocarbon chains of the POE stearate intercalate with those of DODAB, while the hydrophilic POE portion protrudes

into solution. This creates a neutral hydrophilic surface, which suppresses the EOF and allows for better resolution of peaks. The stability of the coating was measured by first coating the capillary and rinsing with buffer for increasingly longer times. Even after a rinse time of 60 min, the EOF remained stable and ten times more suppressed than DODAB alone. pH did not have a significant effect on the stability or the value of the EOF.

Basic proteins could be separated with efficiencies ranging from 0.85 million – 1.3 million plates/m at pH 3.0. These values are comparable or better than those obtained on other types of coatings. Recoveries of these proteins ranged from 92 – 97%, and so are nearly or fully quantitative.

Acidic standard proteins were separated at pH 7.4 with efficiencies ranging from 0.3 million – 0.6 million plates/m. Optimal efficiencies were achieved when the capillary was recoated between runs. These proteins were also separated at pH 10.0 with efficiencies of 0.3 – 1.3 million plates/m. Recoveries were 84 – 95% for these proteins at pH 10.0.

Day to day migration time reproducibilities were 0.6 – 4.2% for all proteins and pH examined. As a further test, bovine and equine cytochrome *c*, which differ by only three amino acids, were separated at pH 7.4 with excellent resolution. Overall, little to no adsorption occurs on this coating and it is very stable under harsh conditions.

6.1.3 Chapter 4

6.1.3.1 Mixed DODAB/POE Stearate Coating

As the DODAB/POE stearate coating was simple to prepare and enabled efficient protein separations, modifying it to gain EOF tunability as well as better stability and

separation performance was the subject of Chapter 4. Firstly the EOF was monitored as a function of POE 40 stearate concentration in the coating. The DODAB concentration was held constant at 0.1 mM. The EOF was suppressed over the POE 40 stearate concentration range of 0.01% - 0.5% for pH 3.0 and 7.4, and 0.01% - 0.1% for pH 10.0. Above this concentration range, the EOF attains a value not significantly different from that of a bare capillary. A full coating may not be formed on the wall at these higher polymer concentrations. This was hypothesized to be a result of the POE moieties on the outer portion of the vesicles preventing the DODAB from interacting electrostatically with the capillary wall.

Efficiencies ranged from 220 000 – 1 030 000 plates/m over the range of POE 40 stearate concentrations. The EOF was not truly tunable by just varying the POE 40 stearate concentration. However, the POE chain length had a dramatic effect on the EOF. POE 100 stearate suppressed the EOF by an order of magnitude compared to POE 40 stearate. The moderately reversed EOF generated by the DODAB/POE 8 stearate coating enabled the simultaneous separation of acidic and basic proteins within a single run. Migration time RSDs were 1.5 – 4.8% over six runs with efficiencies ranging from 20 000 – 90 000 plates/m for the acidic proteins and 110 000 – 140 000 plates/m for the basic proteins (Foley-Dorsey method).

6.1.3.2 Sequential DODAB/POE Stearate Coating

Another capillary coating method was developed as the mixed method may not have been fully coating the capillary wall. This new method involved first rinsing the capillary with DODAB to form the bilayer. Then a solution of POE stearate was rinsed through the capillary. This method resulted in a much more stable coating compared to

the mixed method. Coatings formed using the mixed method demonstrated protein peak migration time RSDs between 2.4 – 4.6% over 14 runs. The same separation performed on a coating formed using the sequential method resulted in RSDs of 0.4 – 0.5% over 28 consecutive runs. Efficiencies for basic proteins were up to 48% higher on coatings prepared using the sequential method.

The EOF was measured for coatings formed using the sequential method as the POE 40 stearate concentration was varied. The suppressed EOF reached a constant value by 0.01% POE 40 stearate and remained suppressed over the concentration range studied. This suggests a full coating is formed regardless of the polymer concentration, unlike the results from the mixed coating. If the chain length is varied but the concentration is kept constant, the EOF is an order of magnitude more suppressed for POE 100 stearate than POE 8 stearate. The sequentially prepared coatings were used in the separation of histones, which are the major structural proteins of chromatin. The histones were separated with efficiencies as high as 1.2 million plates/m, with nine peaks resolved.

6.1.4 Chapter 5

The high efficiency separations enabled by the DODAB/POE stearate coating allowed the other sources of broadening in protein separations to be studied. In Chapter 5 the effect of various separation conditions including voltage, buffer concentration, buffer co-ion, and protein concentration were studied. An optimum voltage was determined by examining Ohm's plots as well as efficiency *vs.* voltage plots.

Buffer concentration, co-ion and protein concentration all affected peak efficiency in a manner consistent with electromigration dispersion. Increased buffer concentration,

decreased analyte concentration, and a better mobility match between sample and buffer co-ion all enhanced efficiencies on a DODAB/POE 40 stearate coated capillary.

Separations of basic proteins were also performed on a commercially available polyvinyl alcohol (PVA) coating. Efficiencies were significantly lower for all proteins using this coating than with a DODAB/POE 40 stearate coated capillary under similar conditions, except cytochrome c in lithium phosphate buffer, and ribonuclease A, which were comparable. While the separation efficiency was compromised by protein adsorption, the general observations were consistent with electromigration dispersion.

Electromigration dispersion is not commonly considered in analytical scale protein separations by CE. This work illustrates the importance of this phenomenon for such separations. Thus peak efficiencies may not be solely a measure of the effectiveness of a capillary coating. Careful optimization of buffer conditions is necessary to accurately assess the effectiveness of the coating.

6.1.5 Conclusions

In conclusion, the EOF is a fundamental property in CE separations and modification of this property with zwitterions can have interesting results. EOF control is important for protein separations as is the minimization of protein adsorption. DODAB/POE stearate coatings can reduce the negative effects of this phenomenon. Adjusting the coating procedure can result in even better separations. Factors other than adsorption can lead to poor performance and must be controlled to give the best separation possible.

6.2 Future Work

6.2.1 Cellulose Modified DODAB Bilayer Coating

The separation of biomolecules is of great interest in CE. For many of these molecules, adsorption onto the capillary wall is a major concern. As discussed in earlier chapters, coatings are most often employed to combat this phenomenon. A number of non-covalent coatings were assessed in our recent review using a variety of performance measures including stability, efficiency, and migration time reproducibility.¹ Efficiency of protein separations is an important indicator of reversible adsorption on a capillary wall.

In the literature, efficiencies of acidic and basic protein separations are quoted at a variety of pH values.¹ A protein has an overall negative charge if its isoelectric point (pI) is lower than the pH of the buffer solution.² Jorgenson and Lukacs examined the separation of model basic proteins at pH 7 on a bare capillary and noted severe tailing as a result of Coulombic interactions between the proteins and the wall.³ When the pH was increased above the pI of the proteins sharp peaks were obtained initially as the proteins were also negatively charged. The peaks deteriorated in consecutive runs possibly as a result of denaturation at such a high pH (i.e., pH 12). Coating the capillary wall also reduces the problem of adsorption, however; some coatings still perform better for the separation of basic proteins at a low pH rather than a neutral or nearly neutral pH.^{4,5} It was noted in Chapter 3 that efficiencies for basic protein separations performed on the 0.1 mM DODAB/0.1% POE 40 stearate coating were lower at pH 7.4 than at pH 3.0. A neutral pH is often required for biological separations so it is important to have coatings that perform well under these conditions.

One type of coating evaluated in our review paper is the cellulose based coatings. Cellulose acetate exhibited a suppressed EOF.⁶ However, it was unstable as a physically adsorbed coating above pH 7.5. A study of protein separations using capillary isoelectric focusing (CIEF) also found substituted celluloses were not stable under CIEF conditions (i.e., pH 2-12) if only physically adsorbed.⁷ Thermal immobilization of hydroxypropylcellulose (HPC) yielded a very stable coating that could be used for 100 runs with no drop in performance.⁷ This type of HPC coating was also used to separate antibodies by CZE and was stable over a number of days with various buffers.⁸ Stable HPC coatings have also been demonstrated if the HPC was first modified with an epoxyalkyl chain.⁹ Yang and El Rassi examined protein separations using a single chain cationic surfactant covalently bonded to the wall followed by adsorption of epoxyalkyl HPC.

The DODAB forms a semi-permanent coating on the wall,¹⁰ and has been shown in my work to form stable coatings when a diblock copolymer is introduced into the coating solution⁵ (Chapters 3 and 4). The sequential method could be used to add an epoxyalkyl cellulose polymer (Figure 6.1) onto a DODAB bilayer coating. The alkyl portion of the epoxyalkyl cellulose polymer would interact with the C₁₈ chains of the DODAB while the hydrophilic cellulose portion would protrude into solution. No covalent attachment would be required. Protein separations could be run at neutral pH to examine the efficiencies produced. The alkyl chain length of the modified HPC could be adjusted in order to prepare a semi-permanent coating of high stability.

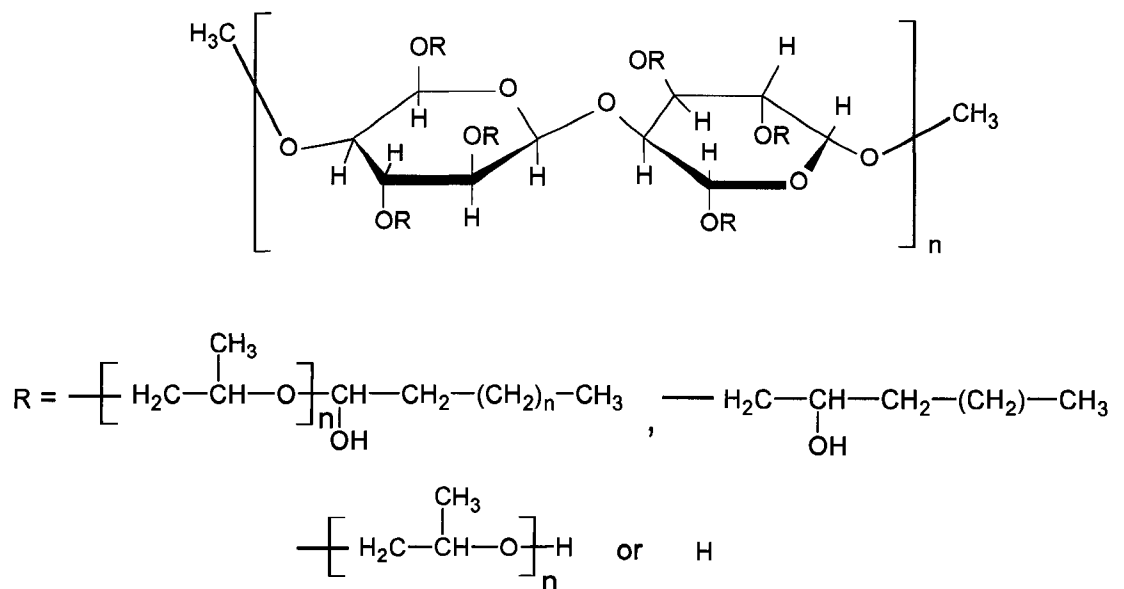


Figure 6.1: Structure of Epoxyalkyl Modified Hydroxypropylcellulose (HPC).

Extending this further to use DODAB as a template for anchoring other diblock polymers could also be tested. The hydrophilicity/hydrophobicity of the coating could then be tailored for specific separations.

6.2.2 Drug Separations

CE is becoming a commonly used technique in pharmaceutical analysis. CE displays a number of advantages over other techniques for this application such as rapidity, low cost of analysis, low solvent consumption, and the possibility for rapid method development.¹¹ A variety of CE modes can be employed for pharmaceutical separations including free zone capillary electrophoresis, non-aqueous capillary

electrophoresis (NACE), and micellar electrokinetic capillary electrophoresis (MEKC). NACE has the advantage of increasing the solubility of organic analytes.¹² However, this mode requires the use of a customized solvent system. MEKC is widely used for the separation of neutral compounds. This technique requires additional additives in the buffer system. These can result in losses in sensitivity, resolution, and mass accuracy when coupled with mass spectrometric detection.^{13,14} pH can be used to control the separation of basic drugs in free zone electrophoresis.^{11,15} However, at low pH the electrophoretic mobilities of some basic drugs can be slow whereas at high pH they will migrate more quickly, but with reduced resolution.¹⁶ At low pH the EOF can be quite variable on a bare capillary,¹⁷ and forensic drug separations often require the resolution of a large number of compounds.^{15,18}

Coatings are one solution to the above mentioned problems. A coating can result in a more reproducible EOF, and if the EOF is suppressed, high resolution can be obtained. Non-covalent coatings have been used for drug separations. The commercially available coating CEofix was used to analyze 73 basic drugs.¹⁹ Reproducibility of the effective mobilities of the drugs was better by a factor of two when the coating was used. More recently, CEofix coated capillaries have been coupled with mass spectrometric detection.²⁰ The RSDs for the migration times of a mixture of basic drugs were $\leq 0.8\%$ (n=7).

The sequential DODAB then POE stearate coating method developed in Chapter 4 could be useful for the separation of drugs. It provides a neutral hydrophilic surface, which reduces interactions of the analytes with the capillary wall. For separations at a low pH the analysis time could be reduced from that on a bare capillary by tuning the

EOF. The tunable EOF would also allow modification of the resolution for separations of a large number of compounds.

6.2.3 Drug Delivery Vehicles

Achieving a desired therapeutic effect through the proper administration of pharmaceutical formulations is an important area of research. The journal *Drug Delivery* publishes research investigating drug delivery and targeting these drugs to specific cells within the body.²¹ Solubilization of hydrophobic drugs can increase their stability as well as the concentration that can be administered in one dose.²² Drug delivery is also important for protein based drugs, which cannot be administered orally as they will lose their therapeutic activity.²³ One mode of entry is controlled release systems, which include microcapsules, vesicles, liposomes, and macromolecular conjugates.²¹ Liposomes are similar to the vesicles formed by DODAB, as discussed in Chapter 3, only they are composed of phospholipids rather than surfactants.²³ Liposomes are often used for drug delivery methods as a result of their low toxicity, biocompatibility, simple preparation, biodegradability, and commercial availability.²⁴ However, the use of liposomes has not been without its challenges. In order for the drug to be effectively delivered to the target cells the liposomes must be able to withstand numerous cell barriers.²⁵ The liposomes must also be able to contain the drug without leakage until the target cell is reached. Therefore, the main issue with liposomes in drug delivery applications is their stability. Polymerization is one method of increasing liposome stability.^{26,27} However, polymerization can result in very rigid membranes, which may lead to drug leakage.²⁸ Grafting polymer chains onto liposomes has been demonstrated to

impart more structural stability.²⁹ POE is often used in drug delivery as a result of its non-toxicity and effectiveness at reducing protein adsorption.³⁰

Carmona-Ribeiro has demonstrated that the drug Amphotericin B, which is used as a fungicide, can be solubilized into DODAB vesicles.³¹ Upon examination of DODAB toxicity, mammalian cells (Normal Balb-c 3T3 (clone A31) mouse fibroblasts and SV40-transformed SVT2 mouse fibroblasts) were shown to remain 100% alive at concentrations where bacteria (*E. coli*, *S. typhimurium*, *P. aeruginosa*, *S. aureus*) and fungi (*C. albicans*) were killed.³¹ The death of the bacterial cells is associated with a positive charge on the cell surface imparted by the DODAB vesicles at DODAB concentrations between 0.01-0.1 mM.³² It was demonstrated that the DODAB vesicles did not rupture upon interaction with *E. coli* or cause disruption of the cell membrane.³³ The occurrence of the positive charge on the cell membrane resulting from the DODAB vesicles appears to have a similar effect on the fungus *C. albicans*, but at a higher DODAB concentration.³⁴ The mammalian cells studied are the most resistant of all studied, showing no toxicity effects below 1 mM DODAB.³⁵

In my work, I have co-adsorbed POE chains onto DODAB vesicles. As a coating, DODAB/POE stearate demonstrated very little interaction with proteins (Chapter 3). The co-adsorption of the POE should impart the same benefits to the DODAB vesicles as the liposome system (i.e., increased vesicle stability, decreased interaction with proteins). DODAB is also a cheaper alternative to phospholipids. For these reasons, the DODAB/POE stearate system warrants investigation for its possible use in drug delivery.

6.2.4 Covalent Coating Comparison

Non-covalent coatings have been the primary focus of this thesis for the reasons discussed in Section 1.5.2. However, covalent coatings do not require regeneration between consecutive runs and typically have greater stability over a longer period of time. Covalent coatings are commonly used for protein separations.³⁶ The performance of the 0.1 mM DODAB/0.1% POE 40 stearate coating was compared to that of a permanently coated PVA capillary in Chapter 5. A comparison between a covalently coated linear polyacrylamide (LPA) coating was also attempted. However, good resolution could not be obtained on the LPA coating.

It has been noted that LPA coatings are not able to completely cover the capillary wall, which results in protein adsorption and a less suppressed EOF.³⁷ Gao and Liu developed a method for crosslinking polyacrylamide within a capillary resulting in a coating capable of reproducible CZE separations of four basic proteins over 240 runs. Efficiencies of the proteins were $\geq 1 \times 10^6$ plates/m at pH 3.25.³⁸ As this coating demonstrates excellent performance for the separation of basic proteins, it would be interesting to investigate how the DODAB/POE stearate coatings compare under the same separation conditions.

6.3 References

- (1) Lucy, C. A.; MacDonald, A. M.; Gulcev, M. D., *J. Chromatogr. A* **2008**, *1184*, 81-105.
- (2) Lauer, H. H.; McManigill, D., *Anal. Chem.* **1986**, *58*, 166-170.
- (3) Jorgenson, J. W.; Lukacs, K. D., *Science* **1983**, *222*, 266-272.
- (4) Graul, T. W.; Schlenoff, J. B., *Anal. Chem.* **1999**, *71*, 4007-4013.
- (5) MacDonald, A. M.; Lucy, C. A., *J. Chromatogr. A* **2006**, *1130*, 265-271.
- (6) Busch, M. H. A.; Kraak, J. C.; Poppe, H., *J. Chromatogr. A* **1995**, *695*, 287-296.
- (7) Shen, Y. F.; Smith, R. D., *J. Microcol. Sep.* **2000**, *12*, 135-141.
- (8) Sanzgiri, R. D.; McKinnon, T. A.; Cooper, B. T., *Analyst* **2006**, *131*, 1034-1043.
- (9) Yang, C. M.; El Rassi, Z., *Electrophoresis* **1998**, *19*, 2278-2284.
- (10) Yassine, M. M.; Lucy, C. A., *Anal. Chem.* **2005**, *77*, 620-625.
- (11) Altria, K.; Marsh, A.; Sanger-van de Griend, C., *Electrophoresis* **2006**, *27*, 2263-2282.
- (12) Porras, S. P.; Riekkola, M. L.; Kenndler, E., *Chromatographia* **2001**, *53*, 290-294.
- (13) Jeannot, M. A.; Zheng, J.; Li, L., *J. Am. Soc. Mass Spectr.* **1999**, *10*, 512-520.
- (14) Schappler, J.; Guillarme, D.; Rudaz, S.; Veuthey, J. L., *Electrophoresis* **2008**, *29*, 11-19.
- (15) Hudson, J. C.; Golin, M.; Malcolm, M.; Whiting, C. F., *Can. Soc. Forensic Sci. J.* **1998**, *31*, 1-29.
- (16) Siren, H.; Hiissa, T.; Min, Y., *Analyst* **2000**, *125*, 1561-1568.
- (17) Ciccone, B., *Am. Lab.* **2001**, *33*, 30-33.
- (18) Hudson, J. C.; Golin, M.; Malcolm, M., *Can. Soc. Forensic Sci. J.* **1995**, *28*, 127-152.
- (19) Boone, C. M.; Jonkers, E. Z.; Franke, J. P.; de Zeeuw, R. A.; Ensing, K., *J. Chromatogr. A* **2001**, *927*, 203-210.

- (20) Vanhoenacker, G.; de l'Escaille, F.; De Keukeleire, D.; Sandra, P., *J. Chromatogr. B* **2004**, *799*, 323-330.
- (21) Stracher, A.; Grainger, D. W., in *Drug Delivery*, Taylor & Francis Group, 2008.
- (22) Palma, S.; Manzo, R. H.; Allemandi, D.; Fratoni, L.; Lo Nostro, P., *J. Pharm. Sci.* **2002**, *91*, 1810-1816.
- (23) Storm, G.; Wilms, H. P.; Crommelin, D. J. A., *Biotherapy* **1991**, *3*, 25-42.
- (24) Jeong, J. M.; Chung, Y. C.; Hwang, J. H., *J. Biotechnol.* **2002**, *94*, 255-263.
- (25) Guo, X.; Szoka, F. C., *Accounts Chem. Res.* **2003**, *36*, 335-341.
- (26) Regen, S. L.; Czech, B.; Singh, A., *J. Am. Chem. Soc.* **1980**, *102*, 6638-6640.
- (27) Liu, S. C.; O'Brien, D. F., *J. Am. Chem. Soc.* **2002**, *124*, 6037-6042.
- (28) Cheng, Z. L.; Aspinwall, C. A., *Analyst* **2006**, *131*, 236-243.
- (29) Lasic, D. D., *Angew. Chem. Int. Edit.* **1994**, *33*, 1685-1698.
- (30) Kwon, G. S.; Kataoka, K., *Adv. Drug Deliver. Rev.* **1995**, *16*, 295-309.
- (31) Carmona-Ribeiro, A. M., *An. Acad. Bras. Cienc.* **2000**, *72*, 39-43.
- (32) Campanha, M. T. N.; Mamizuka, E. M.; Carmona-Ribeiro, A. M., *J. Lipid Res.* **1999**, *40*, 1495-1500.
- (33) Martins, L. M. S.; Mamizuka, E. M.; Carmona-Ribeiro, A. M., *Langmuir* **1997**, *13*, 5583-5587.
- (34) Campanha, M. T. N.; Mamizuka, E. M.; Carmona-Ribeiro, A. M., *J. Phys. Chem. B* **2001**, *105*, 8230-8236.
- (35) Carmona-Ribeiro, A. M.; Ortis, F.; Schumacher, R. I.; Armelin, M. C. S., *Langmuir* **1997**, *13*, 2215-2218.
- (36) Doherty, E. A. S.; Meagher, R. J.; Albarghouthi, M. N.; Barron, A. E., *Electrophoresis* **2003**, *24*, 34-54.
- (37) Gao, L.; Liu, S. R., *Anal. Chem.* **2004**, *76*, 7179-7186.
- (38) Liu, S. R.; Gao, L.; Pu, Q. S.; Lu, J. J.; Wang, X. J., *J. Proteome Res.* **2006**, *5*, 323-329.